PHYLOGENETIC AND PROMOTER ANALYSIS OF THE HUMAN IMMUNODEFICIENCY VIRUS TYPE 1 (HIV-1) LONG TERMINAL REPEAT AND ENVELOPE REGIONS FROM THE TISSUES OF VERTICALLY INFECTED PATIENTS

By

BRANT ROGER BURKHARDT JR.

A DISSERTATION PRESENTED TO THE GRADUATE SCHOOL
OF THE UNIVERSITY OF FLORIDA IN PARTIAL FULFILLMENT
OF THE REQUIREMENTS FOR THE DEGREE OF
DOCTOR OF PHILOSOPHY

UNIVERSITY OF FLORIDA

2001

THIS DISSERTATION IS DEDICATED TO MY WIFE AND PARENTS.

ACKNOWLEDGMENTS

I greatly appreciate all of the training given to me by my mentor, Dr. Maureen Goodenow. She has been extremely influential in my development as a scientist. I also thank Dr. John Sleasman for providing an important clinical relevance to this project, and diligent participation in the collection of numerous autopsy specimens that allowed this study to be possible. I greatly appreciate the contributions by Dr. Ayalew Mergia and Dr. Steven Sugrue for their helpful advice, and constructive criticism throughout this extensive investigation. I would like to acknowledge all of the members of the Goodenow lab past and present for their valuable help with the completion of this project. In addition to providing me with professional guidance, they have also given me remarkable friendships and many good times. These members include Deepa Bhatt, Carter Coberley, James Kohler, Zhong Kou, Feng En Lee, Gina Nykiel, Joseph Oshier, Steven Pomeroy, Adriana Perez, Brian Peyser, Stephanie Rose, Gregory Taylor, and Daniel Tuttle.

My family and my new wife have been so supportive with my academic endeavors. I greatly acknowledge my wonderful wife, Patty, for being so caring and understanding during these stressful times. I also acknowledge my parents, Brant and Louise Burkhardt, for providing me with so many opportunities to accomplish all of my goals and being such giving parents.

TABLE OF CONTENTS

page

ACKNOWLEDGMENTS iii

LIST OF TABLES vi

LIST OF FIGURES vii

ABSTRACT ix

CHAPTERS

1. INTRODUCTION AND BACKGROUND 1

- Specific Aims 1
- Significance 5
- The Human Immunodeficiency Virus 6
- The HIV-1 Long Terminal Repeat (LTR) 7
- Phylogentic Analysis of Tissue Specific LTRs 19
- Cell-Type Expression Determined by LTR of other Retroviruses 20
- Cell-Type Specific Expression of the HIV-1 LTR 20
- HIV-1 Envelope 23
- Phylogenetic Analysis 25
- Specific Aims and Study Design 28

2. PHYLOGENETIC AND PROMOTER ANALYSIS OF THE HIV-1 LTR AND ENVELOPE REGIONS FROM VARIOUS TISSUES OF VERTICALLY INFECTED PEDIATRIC PATIENTS 39

- Introduction 39
- Materials and Methods 41
- Results 47
- Discussion 55

3. THE THYMUS SERVES AS A SOURCE AND SITE OF EVOLUTION OF T-CELL LINE TROPIC (CXCR4) AND DUAL-TROPIC (CXCR4±CCR5) ENV QUASISPECIES........82

Introduction........82
Materials and Methods........85
Results........93
Discussion........100

4. FUNCTIONAL ANALYSIS OF TISSUE SPECIFIC LTRS USING CONGENIC RECOMBINANT LUCIFERASE VIRUSES WITHIN PRIMARY CELLS........121

Introduction........121
Materials and Methods........123
Results........133
Discussion........143

5. CONCLUSIONS........166

REFERENCES........171

BIOGRAPHICAL SKETCH........190

LIST OF TABLES

Table Page

1-1. Overall Patient Cohort and Analysis Performed 38

2-1. Summary of Clinical Data and Tissues Analyzed from all Patients 62

2-2. V3 Alignment with Frequency, Charge, and Predicted Phenotype 64

3-1. Comprehensive Listing of All Patients with Survival Time and Tissues Analyzed by Env V3 Genotype 104

4-1. MAGI Assay Results from LTR-Luc Recombinant Viruses 152

4-2. Luciferase Experession and Gag Copies from Infection of PBMC with LTR-Luc Recombinant X4 Viruses 157

4-3. Luciferase Experession and Gag Copies from Infection of PBMC with LTR-Luc Recombinant R5 Viruses 158

4-4. Luciferase Experession and Gag Copies from Infection of Macrophages with LTR-Luc Recombinant R5 Viruses 159

4-5. Results of LTR-Luc Recombinant Virus Infections 165

LIST OF FIGURES

Figure Page

1-1. HIV-1 proviral genome. 30

1-2. HIV-1 viral lifecycle as demonstrated by an HIV-1 virion infecting a CD4+ T-lymphocyte.. 31

1-3. Generation of the HIV-1 LTRs... 32

1-4. Major regions of the HIV-1 LTR. 33

1-5. Transcriptional elements within the HIV-1 LTR U3 region. 34

1-6. Functional domains in HIV-1 envelope.. 35

1-7. Predicted Folding Pattern of the HIV-1 gp120 36

1-8. Cellular Host Range of HIV-1 as Determined by V3 37

2-1. Phylogenetic analysis of the DNA sequence from the V3 region of envelope and the LTR from representative tissue sequences from each patient. 63

2-2. Nucleotide alignment of LTR sequences. 65

2-3. Parsimony and distance analysis of the V3 region of envelope. 68

2-4. Parsimony and distance analysis of the mid-U3 region of the LTR 72

2-5. Standard curve of bulk luciferase.. 76

2-6. Twenty-four hour time-course of luciferase expression 77

2-7. Three day time-course experiment of luciferase expression. 78

2-8. Transient transfection of Jurkat cells with patient tissue LTR-luciferase constructs. 79

2-9. Transient transfection of Jurkat cells with and without TAT 80

2-10. Transfection of U937 cells without TAT. 81

3-1. Parsimony tree of the V3 DNA sequences. 105

3-2. Parsimony analysis of tissue V3 sequences. 106

3-3. Coreceptor usage and tropism of env recombinant viruses. 110

3-4. Parsimony analysis of the V1 amino acid sequences. 111

3-5 Parsimony analysis of the V2 and C2 amino acid sequences. 115

3-6. Phylogenetic analysis of the V2-V3 DNA sequences. 119

3-7. Model of T-X4 and D-R5X4 emergence within thymus. 120

4-1. Phylogenetic analysis of the tissue LTR and V3 regions from Patient C/S1. 147

4-2. Alignment of LTR sequences. 148

4-3. Methodology of construction and measurement of LTR-Luc Recombinant Viruses. 149

4-4. LTR-Luciferase recombinant virus timecourse experiment in PBMC. 150

4-5. LTR-Luciferase timecourse infection with macrophages. 151

4-6. Representative experiment of PBMC infection with LTR-Luc recombinant viruses. 153

4-7. PBMC infection with LTR-Luc recombinant viruses from all donors. 154

4-8. Representative infection of macrophages with LTR-Luc recombinant viruses. 155

4-9. Macrophage infection with LTR-Luc recombinant viruses from all donors. 156

4-10. Luciferase expression per gag copy of PBMC and macrophages. 160

4-11. Luciferase expression per gag copy of PBMC infected with LTR-Luc recombinant X4 and R5 viruses. 161

4-12. Relative promoter activity within different primary cells. 162

4-13. Representative experiment of PBMC infection with Site-Directed LTR-Luc recombinant viruses. 163

4-14. Representative infection of macrophages with Site-Directed LTR-Luc recombinant viruses. 164

Abstract of Dissertation Presented to the Graduate School
of the University of Florida in Partial Fulfillment of the
Requirements for the Degree of Doctor of Philosophy

PHYLOGENETIC AND PROMOTER ANALYSIS OF THE HUMAN IMMUNODEFICIENCY VIRUS TYPE 1 (HIV-1) LONG TERMINAL REPEAT AND ENVELOPE REGIONS FROM THE TISSUES OF VERTICALLY INFECTED PATIENTS

By

Brant Roger Burkhardt Jr.

December 2001

Chairman: Maureen M. Goodenow
Major Department: Pathology, Immunology, and Laboratory Medicine

The human immunodeficiency virus type 1 (HIV-1), the etiological agent of AIDS, displays significant genotypic and phenotypic diversity between and within patients. This genetic diversity within the virus is dependent on mutation rate of reverse transcriptase, host immune response, and other factors produced in the local environment. HIV-1 infects organs systems that can be either lymphocyte or macrophage dominated; for example peripheral blood and thymus, or brain and lung, respectively. The primary determinant for viral entry is envelope (env), whereas the long terminal repeat (LTR) elements impact gene expression, replication, and integration. HIV has been detected at high frequency in several tissues; however the genotypic and phenotypic quasispecies within these tissues have not been evaluated in the context of both env and LTR. The specific aims of this project were 1) to analyze the env and LTR regions from various tissues of vertically infected patients by phylogenetic analysis, 2) to functionally analyze the tissue specific LTRs by transient transfection in both a T-cell and monocytic cell line, 3) to determine if the thymus is the source of both T-cell line tropic CXCR4-using (T-X4), and dual-tropic CXCR4±CCR5-using (D-X4±R5) quasispecies and 4) to assess the impact of tissue LTRs on gene expression in primary cells such as T-cells and macrophages using congenic recombinant LTR-Luciferase viruses that are identical except for the LTR region.

Env and LTR sequences from brain segregated concordantly from other tissues. Env and LTR segregation was discordant within the thymus and lung. Tissue specific segregation of lung sequences was determined by LTR, whereas the env region was the primary determinant of tissue segregation of thymus sequences. The thymus appears to be the source of both T-X4 and D-X4±R5 quasispecies. Functional analysis by transient transfection and recombinant LTR congenic viruses demonstrated distinct promoter differences among tissue specific LTRs within peripheral blood mononuclear cells (PBMC), macrophages, and a T-cell line. The predominant LTR found in the PBMC had the highest promoter activity in both macrophages and PBMC. All of the LTRs examined by recombinant LTR-Luciferase analysis had a much higher promoter expression in macrophages than PBMC. The lung specific LTR demonstrated a cell type specific promoter expression in macrophages. Regulatory elements within the LTR can impact cell-type specific viral gene expression. Tissue and cell-type specific adaptation of HIV is multifactorial and occurs at the level of entry and gene expression that is impacted by both the env and LTR regions.

CHAPTER 1
INTRODUCTION AND BACKGROUND

Specific Aims

The human immunodeficiency virus type 1 (HIV-1) displays significant heterogeneity in cellular tropism, co-receptor usage, and phenotypic variability (30,39,62,166,186,187). This genetic variability is the result of several factors that include reverse transcriptase, host immune response, and selection (82). During the course of infection, HIV-1 infects most organ systems (26,38,52,116,154,196). These organs systems can either be macrophage or lymphocyte dominated (26,154,179,196). The predominantly infected cell in the brain and lung is the macrophage, in contrast to the lymphocyte in the thymus and peripheral blood. In addition, unique cell-type specific transcriptional factors have been found in both lymphocytes and macrophages (76,77,131). Therefore, when HIV-1 infects different tissues there are two tiers of selection that exert pressure on this pathogen which include cell-type specific pre and post entry factors. The primary determinant for viral entry is envelope (env) (32,45), whereas the long terminal repeat (LTR) elements impact replication, integration, and gene expression (68,70). Differences among tissues in both pre- and post-entry factors would suggest that HIV-1 might adapt to the local milieu by concordant changes in both the LTR and env regions. However, there are currently no studies that examine both the LTR and env regions simultaneously from various tissues and evaluate promoter differences among different tissue specific LTRs. My hypothesis is that tissue specific LTRs will differ phylogenetically and functionally according to regulatory elements located within the LTR that respond to cell type specific transcriptional factors. My dissertation consists of four specific aims that examine this hypothesis.

Specific Aim 1. To Determine If the HIV-1 Env and LTR Regions Phlyogenetically Segregate According to Tissue.

My specific aims will address my hypothesis by first determining whether the HIV-1 env and LTR regions from various tissues segregate phylogenetically according to tissue (Figure 1-1). There are currently no studies that evaluate both the env and LTR regions simultaneously from various tissues. Evaluating only one region of the HIV-1 genome cannot accurately predict whether other regions of HIV-1 will also segregate (129). An analysis of both of these regions is important since they impact separate parts of the viral life cycle. The third hyper-variable loop of the env region, known as V3, impacts cellular tropism and co-receptor usage (85). This region segregates according to tissue and will ideally serve as a positive control for tissue specific clustering of a subgenome of HIV-1. The first aim consisted of a cross-sectional and longitudinal phylogenetic analysis of both the env and LTR regions from various tissues of four vertically infected patients (mother to infant transmission). Genetic sequences were obtained by polymerase chain reaction (PCR) amplification, and subsequently cloned and sequenced. Parsimony analysis was performed on the amino acid sequence of the env V3 region and the nucleotide sequence of the LTR region to evaluate tissue specific segregation of sequences. These tissue specific LTRs were then utilized for functional analysis in both Specific Aims 2 and 4. Results for Specific Aim 1 are discussed in Chapter 2.

The observation of env V3 quasispecies obtained from the thymus that had a predicted phenotype of T-cell line tropic (CXCR4-using) or dual-tropic led to Specific Aim 3 which is discussed in Chapter 3.

Specific Aim 2. To Determine the Impact of Tissue Specific LTRs on Promoter Activity Using a Luciferase Reporter Gene Assay in Both a T-cell and Monocyte Cell Line.

Tissue specific LTRs obtained from Specific Aim 1 were evaluated in a transient transfection luciferase reporter gene assay. Gene expression by these LTRs were evaluated in both a T-cell (Jurkat) and a monocytic (U937) cell line to evaluate promoter differences among tissue specific LTRs in two different cell types. Patient LTRs were ligated into the p-GL3 basic luciferase plasmid, and transiently transfected into both Jurkat (T-cell line) and U937 (monocytic) cell lines to identify functional differences among two different cell types. The luciferase assay served as a primary screen to select which tissue specific LTRs to evaluate in the recombinant LTR assay. Results from Specific Aim 2 are discussed in Chapter 2.

Specific Aim 3. To Determine If the Thymus Serves as a Site of Evolution of T-Cell Line Tropic (CXCR4-using) and Dual-Tropic (CXCR4±CCR5) Env Quasispecies.

Based on the additional observation from Specific Aim 1 that demonstrated T-cell line tropic and dual-tropic quasispecies were typically found in the thymus, I hypothesized that the thymus is the site of evolution for both of these emerging quasispecies. The transmitting populations of HIV-1 are typically macrophage tropic and utilize only CCR5. At later stages of clinical progression, T-cell line tropic and dual-tropic viruses can emerge. These quasispecies are very cytopathic to thymocytes, and have been associated with clinical progression. In addition, the thymus is a vital organ of immunoreconstitution and the emergence of highly cytopathic quasispecies within the thymus may cause the destruction of this organ and induce clinical progression.

Phylogenetic analysis was performed on additional tissues such as the lymph node and spleen that may represent other possible sources of T-cell line tropic and dual-tropic quasispecies. The results from Specific Aim 3 are presented in Chapter 3.

Specific Aim 4. To Evaluate Gene Expression in Primary Cells via Congenic Recombinant LTR Viruses without Variability from other Regions.

Tissue specific LTRs were then evaluated in a recombinant LTR luciferase reporter assay that will determine gene expression by infection of primary cells such as CD4+ T-cells and monocyte derived macrophages. Transient transfections certainly do not mimic the *in-vivo* situation since this method involves the introduction of much higher copy numbers of HIV-1 LTR DNA than that seen during an actual infection of cells. In addition, transfected DNA is not incorporated into the chromatin and therefore may not be regulated in the same manner as an integrated promoter. To accurately determine the impact of tissue specific LTRs on infection in various cell types, congenic single-cycle recombinant LTR viruses expressing luciferase as a reporter gene will be created that can infect primary cells with the only difference residing in the LTR. Promoter expression will be determined by measuring luciferase activity several days post infection. These single-cycle viruses will eliminate the influence of viral spread and enable us to evaluate the impact of the LTR on early post-entry events. This system will allow us to evaluate differences in promoter expression without any variability from other regions of the HIV-1 genome. The final goal of this project is to determine specific sites within the mid-U3 region of the HIV-1 LTR that impact promoter activity in a cell-type specific manner. Specific nucleotide polymorphisms found within tissue derived LTRs will be changed to determine the impact of these sites on cell type promoter activity. Congenic LTR recombinant viruses will be created with these site specific changes created by PCR amplification using a commercial kit. Promoter expression by these viruses will be evaluated by measuring luciferase activity several days post infection in both PBMC and monocyte-derived macrophages (MDMs). Results from Specific Aim 4 are explained in Chapter 4.

Significance

It appears that HIV-1 infects several organ systems early during the course of infection. This presents a major caveat in the effective eradication of this pathogen from the human body. Anti-retroviral therapy is highly effective against virus in actively replicating cells such as CD4+ T cells; however macrophages are terminally differentiated and drugs may not inhibit virus in these cells. Macrophage dominated tissues such as the brain and lung may represent not only a reservoir of virus, but also a possible source of low-level viremia found within patients that are treated with highly-active anti-retroviral therapy (HAART) that have undetectable levels of virus in the blood. Infection of macrophages by HIV-1 is typically considered to be a low-level persistent infection (67). Thus, virus resurging in the presence of anti-virals from these reservoirs represents reactivation rather than a de-novo infection. The LTRs found within these tissues can have profound significance since they contain several transcriptional factor binding sites that would be responsible for viral reactivation. Proper phylogenetic and functional evaluation of the viruses found in these tissues has been somewhat limited mainly due to the difficulty in obtaining HIV-1 by PCR or culturing from tissues. Therefore, a large majority of studies evaluating HIV-1 phylogenetically and functionally have come from studies evaluating the viruses obtained from the PBMC. However, the viruses found in the PBMC most likely represent virus captured in route to other tissues, since the blood is merely a conduit between organ systems rather than representing a true site of active viral replication. In addition, most tissue specific studies of HIV-1 have been monogenomic and therefore can be very misleading since evaluation of one subgenome of HIV-1 cannot be predictive of others. Hence, in order to accurately study HIV-1 in tissues it must be done in the context of two viral subgenomes. Identification of these tissue specific LTRs can then lead to how these promoters regulate cell-type gene expression. Identification of viral sequences found within the LTR may reveal unique post-entry determinants involved in viral activation. Elucidation of how and when HIV infects these compartments may help in the design of therapies to prevent viral infection, and combination strategies to protect these sites from further immune deterioration. This will be the first study to evaluate the env and LTR regions of HIV-1 simultaneously from multiple tissues, and determine if tissue-specific LTRs impact promoter activity in a cell-type manner. The primary focus of these experiments is the LTR region of HIV-1 and how it may impact gene expression in a cell type manner.

The Human Immunodeficiency Virus

The human immunodeficiency virus was first isolated in 1983 by Barre-Sinoussi *et al.* at the Pasteur Institute in Paris (12). The human immunodeficiency virus type 1 (HIV-1) is a ssRNA (positive sense) virus belonging to the Family *Retroviridae*. Virions of HIV-1 contain two copies of the single-stranded RNA that is approximately 9.2 Kb. The genome of HIV-1 is contained in an enveloped virion derived from the plasma membrane of the infected cell with glycoproteins protruding from the surface. The HIV-1 virion is comprised of both structural proteins and enzymes derived from the virus. Uniquely, in the early stages of infection, the viral RNA genome is converted into double-stranded linear DNA and translocated to the nucleus where it is integrated into the host genome (Figure 1-2). The reverse flow of the life-cycle from RNA to DNA gives the family *Retroviridae* their name. The HIV-1 genome contains the major genes of *gag*, *pol*, and *env*, in addition to several accessory genes. The long terminal repeat of HIV-1 flanks the genome. Reverse transcription of the viral RNA genome generates double-stranded viral DNA. Duplications of the U5 and U3 regions are created during reverse transcription so that the viral DNA is longer than the viral RNA at the terminal ends (Figure 1-3). Each LTR is identical in sequence and consists of the U3, R, and U5 regions which are explained in the next section.

The HIV-1 Long Terminal Repeat (LTR)

The HIV-1 long terminal repeats (LTR) impacts several different steps in the post-entry viral life cycle. The LTR region is located at opposite ends of the viral genome and is identical in sequence. The major function of the LTR is to provide binding sites recognized by host cellular transcriptional machinery for expression of the HIV-1 genome but also has other roles including replication and integration (68,70). The LTR for HIV-1 is 633 base pairs (bp) in length and is divided into three regions: U3 (Unique 3'), R (Repeat), and U5 (Unique 5') (Figure 1-4). The LTR is formed during the process of reverse transcription after viral entry into the cell. The U3 region is 454 bp and is derived from the sequence unique to the 3' end of the viral RNA; R is 98 bp in length and is derived from the sequence repeated at both ends of the viral RNA; and U5 is 84 bp in length and is derived from the sequence unique to the 5' end of the viral RNA. The LTR is further divided into several functional regions: the transactivation responsive (TAR) element found in R, the core promoter (nt –78 to –1), the core enhancer (nt -105 to –79), and the modulatory region (nt -454 to –104). The U3 region can be further divided into the mid-U3 region (nt -320 to –120), and the promoter distal (nt –454 to –320).

Both T-cell and macrophage activation result in the induction of multiple genes that impact immune cell function. The regulation of different types of transcription factors is responsible for the activation of these immune cell genes. The HIV-1 LTR architecture is structured to also respond to several immune regulatory transcriptional factors in both macrophages and T-cells. Several tissue specific transcriptional factor binding sites that are linked to immune cell activation are also located within the LTR and may determine cell-type specific expression. The HIV-1 LTR is extremely versatile since it contains several transcriptional factor binding sites, some of which even overlap, that can alter tissue specific expression by simple nucleotide variation which can either create or eliminate a transcriptional factor binding site. To elucidate candidates within the HIV-1 LTR responsible for cell-type specific expression it is necessary to examine the different regulatory regions that are known by sequence or functionally within the LTR. The following review of the LTR examines all of the well characterized transcriptional factors that interact with the HIV-1 LTR with particular attention to any data regarding cell type specific expression impacted by specific transcriptional factors.

Trans-Activation-responsive (TAR) Region (R)

The trans-activator of transcription (TAT) protein of HIV-1 is an 86 amino acid protein encoded by a spliced mRNA derived from two exons within the central region and env gene of the HIV-1 genome (7,177,178). TAT binds to the stem loop structure of TAR RNA at nucleotides +22 to +24 that is present at the 5' end of all HIV-1 RNA's (43,56). The binding of TAT to nascent RNA results in a dramatic increase in HIV-1 gene expression, resulting in a major upregulation of LTR directed transcription by 100 fold. Additional elements have been characterized that bind to the R region which include untranslated binding protein (UBP-1), or leader binding protein (LBP-1), and

CTF/NFI (91). The transcription factor UBP-1 has both a low affinity site encompassing the TATA box (-38 to –16) and a high affinity site located in the sequences surrounding the site of transcription initiation (-16 to +27) (91,197). Binding of UBP-1 to the high affinity site appears to increase transcription, whereas binding of LBP-1 to the low affinity site inhibits transcription as determined by viral RNA synthesis in cell free systems (94). Other cellular factors such as untranslated binding factor-2 (UBP-2) or CTF/NFI also bind to the TAR region; however the exact effect on transcription is unknown (69).

Core Promoter

The TATAA region (-28 to –24) and three Sp1 sites (-78 to –45) make up the core promoter of the LTR. The TATAA region is one of the few elements that are absolutely essential for HIV-1 gene expression (92). Slight nucleotide polymorphisms of this region can be tolerated, although mutations of the TATAA region result in a severe impairment of basal promoter activity and viral replication (15,117). The TATAA region is a binding site for a complex of cellular proteins designated transcription factor IID (TFIID) (57,123,148,189). This complex is composed of TATA binding protein (TBP), TBP-associated factors (TAFS), and the multi-subunit RNA polymerase II. Viral transcripts are initiated 22 bp downstream from the TATAA element. The core promoter of HIV-1 also consists of three GC rich regions extending from –78 to –45 that bind to the cellular transcription factor, Sp1 (75,90). Eliminating the three Sp1 binding sites in the LTR inhibits the ability of the Sp1 protein to stimulate *in-vitro* transcription (90). Transfection of HIV-1 constructs containing one or two mutated Sp1 sites resulted in only moderate decreases in basal and TAT induced gene expression in some but not all cell types (141,155). In contrast, constructs containing mutations of all Sp1 sites exhibited severe decreases in basal and TAT induced gene expression. These results suggest that there is some functional redundancy in the Spl sites. The Spl protein may impact HIV-1 gene expression via several structural elements such as three zinc fingers in its DNA binding domain, dimerization, or multimeriztion motifs, and two glutamine rich domains which are involved in transcriptional activation (46,142). The binding of Spl to its respective binding site within the HIV-1 LTR induces phosphorylation of Spl by an associated DNA-dependant kinase (87). The three Spl binding sites allow for interaction among themselves and other proteins. Overall, the Spl protein behaves as an anchor that recruits other transcriptional factors, and may also serve by itself a critical regulator and initiator of HIV-1 gene expression.

Core Enhancer

The core enhancer of HIV-1 consists of two 10 bp conserved sequences known as Nuclear factor k light-chain of B cells (NF-κB) motiffs which are located between –104 and –81 (131). This transcriptional factor was initially characterized to be important for immunoglobin k light-chain transcription (11,112,127). However, NF-κB has been broadly implicated in several other immunomodulatory genes such as interleukin-2 (IL-2), the IL-2 receptor, tumor necrosis factor alpha (TNF-α), interleukin-6 (IL-6), granulocyte-macrophage colony stimulating factor (GM-CSF), and the class II major histocompatibility complex. This transcriptional factor consisits of two subunits, p50 and p65 which are found in the cytoplasm complexed with its inhibitor, IkB (13). The p50 subunit of NF-κB is the DNA binding domain, whereas the p65 subunit is the activation domain. Cellular activation, as well as cytokines such as TNF-α and IL-2 can induce phosphorylation through protein kinase C and rapid proteolytic degradation of IκB allowing NF-κB to translocate to the nucleus and activate HIV transcription by binding to the NF-κB binding sites within the LTR. Cells treated with mitogens such as phorbol myristic acid (PMA) or phytohemagglutin (PHA) demonstrate increased levels of NF-κB and support high levels of transcription directed by the HIV-1 LTR (95,131,173). Certain cytokines such as IL-1, IL-6, TNF-α, and GM-CSF have been demonstrated to raise levels of NF-κB in cultured T-cells and macrophages and enhance both LTR-directed transcription and viral replication (36,63,136,145). In addition, monocyte differentiation to macrophages can increase levels of NF-κB and induce upregulation of LTR-mediated HIV-1 gene expression (74).

Mutation of the NF-κB sites in HIV-1 reporter gene constructs induced marked decrease in gene expression after transient transfection into T-cell lines in both the presence and absences of TAT (131). In contrast, some investigators have demonstrated that the NF-kB sites are dispensable for viral growth in cell culture because mutations or deletions show only modest effects on gene expression and viral growth kinetics (27,114,155). One report has demonstrated that there is an absolute requirement for NF-κB sites for replication in primary cells (5). Despite the contradictory data, viral isolates cultured from patient peripheral blood mononuclear cells (PBMCs) have been identified with both NF-κB sites deleted (203). Ironically, these NF-κB deleted viruses had a compensatory duplication of another transcriptional factor binding site (TCF-1). This result implies that the NF-κB sites may be dispensable for viral growth due to the abundance of functional redundancy within the HIV-1 LTR.

Modulatory Region

The modulatory region (-454 to –104) is located in the U3 of the HIV-1 LTR and contains several cis-acting transcriptional regulatory elements that impact viral gene expression (Figure 1-5). More than 30 different transcriptional factors could bind to the LTR based on sequence homology with known transcriptional regulatory elements (144). Several transcriptional factors that can bind to the modulatory region have been examined functionally. The wide range of transcriptional factor binding sites within this region enables HIV-1 gene expression in a large variety of cell types and under various cellular conditions. In addition, the modulatory region of the U3 typically has a high degree of genetic variability compared to other regions of the HIV-1 LTR, and represents a strong candidate region for localization of elements that have a potential to impact cell type specific gene expression of HIV-1 (53,60,125,157). In addition, LTR promoter activity typically displays a wide range of variability in various cell types (60,125). Therefore, this wide range of promoter expression may be attributed to the U3 region of the LTR. There are numerous transcriptional factor binding sites within the U3, and several of them have some evidence of impacting gene expression in a cell specific manner. This review of transcriptional factors that bind to the U3 region will address regulatory elements that have been implicated in cell specific expression.

ATF/CREB

The region of the LTR between the T cell factor-1α and the NF-kB sites (-125 to –117) contains a recognition motif for members of the activating transcription factor/cAMP response element binding (ATF/CREB) family of transcription factors (Figure 1-5) (124). ATF/CREB transcription factors isolated from both Jurkat (T-cell) and U-373MG (astroglial) cell lines can bind to the HIV-1 LTR (106,107). In addition, these DNA protein complexes of ATF/CREB and the LTR differed between the U-373MG and Jurkat cell lines in terms of relative abundance and mobility as determined by gel shift analysis. Differences in ATF/CREB binding may be the result of cell type specific differences in the production of ATF/CREB transcriptional factors between these two cell types. One study evaluated the interaction between CCAAT/enhancer binding protein (C/EBP), a known macrophage specific transcription factor, and ATF/CREB. Minor sequence variation within the ATF/CREB binding site affected basal LTR activity as well as LTR function following interleukin-6 (IL-6) stimulation of U937 cells, a treatment that leads to increases in C/EBP activation (156). Mobility shift assays indicated that selected ATF/CREB site variants assisted in the recruitment of C/EBP proteins to the HIV-1 LTR at the C/EBP binding site located at position –110. Both of these results suggest differences in factor recruitment and site occupation, and demonstrate a possible mechanism by which different LTR quasispecies may adapt to the local milieu by changing transriptional capabilities.

T Cell Factor-1α (TCF-1α)

The HIV-1 LTR contains a binding site between –139 and –124 that binds to a transcription factor known as TCF-1α (Figure 1-5). TCF-1α is also known as lymphocyte enhancer-binding protein (LEF-1) (170). This transcriptional factor is T-cell specific and binds to pyrimidine rich sequences. TCF-1α has been demonstrated to be an activator of HIV-1 LTR transcription in Jurkat cells. Golub *et al.* demonstrated that a 24 bp duplication of this region was responsible for a three fold increase in replication and proviral transcription than as compared to of a genetically similar isolate from the same patient that lacked the TCF-1α duplication (73). This TCF-1α duplication has also been isolated from HIV-1 isolates from a patient that contained deletions in the entire NF-kB sites. Duplication of the TCF-1α site in the HIV-1 LTR is not an entirely uncommon finding, because this observation has been found in naturally occuring LTR variants in both asymptomatic as well as symptomatic patients (102,125). Estable *et al.* reported 38% of patient LTRs from a cohort of 478 LTRs from patients with varying clinical progression to contain a duplication around the TCF-1α site (60). Overall, these results suggest that LTR mutations could impact the course of HIV-1 disease, and duplication of important sites within the HIV-1 LTR may compenstate for the loss of other transcriptional factor binding sites.

Upstream Stimulatory Factor (USF)

USF is a member of the basic helix-loop-helix/leucine zipper family of transcription factors and is found in several tissues (Figure 1-5) (160). The data surrounding the effect of USF on HIV-1 LTR activity are somewhat contradictory depending on the cell type used for the evaluation of promoter activity. Several studies have demonstrated both a positive and negative effect of USF on HIV-1 LTR directed transcription. USF can activate the HIV-1 LTR in both T-cells and macrophages (130,174), or can have an inhibitory effect on LTR directed transcription in HeLa (epithelial) cells. Another study has also reported that USF functions as a repressor of LTR gene expression in COS-1 cells (72). In contrast, two *in-vitro* transcription studies performed with nuclear extract from HeLa cells demonstrated that USF is a positive regulator of LTR mediated transcription (55,120). The differences between these two results maybe due to differences in examining transcription *in-vivo* vs *in-vitro*, or differences in the usage of shorter LTR regions. It has been proposed that both LEF and

USF function together to maintain the LTR promoter in an open configuration (92). Overall, these data suggest that USF directs LTR-directed transcription in a cell-specific manner. Further data have implicated USF to be involved in the pathogenesis of AIDS. Rousseau *et al.* demonstrated that a mutation in the USF site which would reduce gene expression may be associated with slow disease progression (157).

Nuclear Factor of Activated T-Cells (NFAT)

The HIV-1 LTR contains two NFAT binding sites between –292 to –255, and the other site between -215 to –203 (Figure 1-5) (88,168). This transcriptional factor is only produced by T-cells. Antigen recognition by the T-cell receptor ultimately increases several transcription factors including NFAT. NFAT will bind to the promoter region of the IL-2 gene and is necessary to activate its transcription (47). The abundance of NFAT is low in unstimulated T-cells, but is dramatically upregulated upon T-cell activation. Several NFAT family members are found sequestered in the cytoplasm of T-cells and translocated to the nucleus upon an increase in intracellular calcium content (149). Two sites of NFAT recognition binding motiffs were found on the HIV-1 LTR through *in-vitro* footprinting with full-length recombinant NFAT protein, and gel shift analysis of nuclear protein obtained from polyclonally activated primary CD4+ T-cells revealed specific binding of NFAT to the NF-kB binding sites of the HIV-1 LTR (48). Other investigators have demonstrated that NFAT was sufficient as a cellular factor to induce a highly permissive state for HIV-1 replication in CD4+ T-cells (97,98). HIV-1 replication was blocked by pharmacological inhibitors (FK 506 and cyclosporin A) of endogenous NFAT. This result suggested that CD4+ T-cells could become permissive for HIV-1 replication by control of regulated host factors such as NFAT.

CCAAT/Enhancer Binding Protein β(C/EBPβ)

C/EBPβ is a strong transcriptional activator that is induced during monocyte/macrophage differentiation (3,132). C/EBPβ is a member of the C/EBP family of transcriptional factors that consists of both transcriptional activators and inhibitors. C/EBP proteins are expressed in different human tissues; however high levels of C/EBP mRNA and protein expression are limited to a few cell types, which include cells of the myeloid lineage. Three C/EBP recognition motiffs have been identified on the HIV-1 LTR by DNA footprinting (Figure 1-5) (188). C/EBPβ is very important in the expression of multiple genes which are expressed in activated monocytes. These include genes encoding IL-1, IL-6, IL-8, TNF-α, and GM-CSF (3). Removal of the C/EBPβ gene from macrophages inhibited normal macrophage bacteriocidal and tumoricidal functions (184). C/EBPβ is the only known C/EBP family member which is increased when the monocytic cell line U937 was activated (78). Inhibition of endogenous C/EBP proteins using either an excess of C/EBP binding sites or a trans-dominant negative inhibitor demonstrated that C/EBP proteins are required for basal and activated levels of HIV-1 in U937 (monocytic cells). HIV-1 with two mutated C/EBP sites was unable to replicate in U937 cells (77). Cell lines overexpressing the C/EBP dominant negative protein LIP were infected with HIV-1 and viral replication occurred in Jurkat T cells but not in U937 monocytes (76). Primary macrophages did not support the replication of HIV-1 harboring mutant C/EBP binding sites in the HIV-1 LTR; however Jurkat, H9, and primary CD4+ T-cells supported replication of both wild type and the C/EBP mutated HIV-1 virus equally well. All of this evidence indicated that the C/EBP sites within the HIV-1 LTR were required for HIV-1 replication in primary macrophages but not CD4+

T-cells. The C/EBP sites within the LTR are considered to be the only macrophage specific transcriptional requirement for HIV-1. HIV-1 has taken advantage of the C/EBP requirement needed not only for monocyte differentiation, but also for bacteriacidal killing by macrophages. In addition, the C/EBPβ transcriptional factor controls a wide variety of cytokines by macrophages (ie. IL-1, IL-6, and TNF-α). Therefore, C/EBP plays a potential pivotal role in an autostimulatory pathway including monocyte/macrophages, cytokines, and HIV-1 infection. Further support for this model has been provided by co-infection studies with Mycobacterium tuberculosis with alveolar macrophages (83). These studies demonstrated that in the uninflamed lung an inhibitory form of C/EBPβ is produced that represses HIV-1 LTR expression, demonstrating that an alternate inhibitory form of C/EBPβ is present in normal lung tissue. In striking contrast, active pulmonary tuberculosis induces stimulatory C/EBPβ expression that enhances HIV-1 viral replication. This mechanism demonstrates the dramatic interplay between the C/EBPβ sites within the HIV-1 LTR, and opportunistic pathogens that may induce dramatic lung involvement found in several patients with AIDS.

Chicken Ovaalbumin Upstream Promoter-Transcriptional Factor (COUP-TF)

A region of the HIV-1 LTR extending from –334 to –371 contains a binding site for COUP-TF (41,135). COUP-TF is a transcriptional factor belonging to the steroid/thyroid hormone receptor superfamily (195). This transcriptional factor is found in high levels in T-lymphocytes, and several brain cell lines. Several studies have indicated that COUP-TF may play a positive or negative role in HIV-1 gene expression depending on the cell context (161,162). Variations within the COUP-TF site may profoundly impact cell type specific expression of the HIV-1 LTR. Initial studies of

COUP-TF by Cooney *et al.* demonstrated that mutation of the COUP-TF site resulted in two to three fold increase in HIV-1 gene expression (41). Co-transfection experiments with COUP-TF and LTR-chloramphenicol transacetylase (CAT) constructs demonstrated that COUP-TF activated LTR directed gene expression by 9-10 fold greater than LTR-CAT alone in human oligodendroglioma cells, but not in neuronal or astrocytoma cells (161). In addition, neuronal cells in the presence of dopamine, a catecholamine neurotransmitter enhancer, increased HIV-1 transcription. COUP-TF has also been found to activate HIV-1 transcription in primary cultured human microglial cells. Overexpression of COUP-TF resulted in the initiation of viral replication in primary HIV-1 infected microglia. It appears that COUP-TF mediated this transcriptional activation by acting on the –68/+29 promoximal promoter site via functional interaction with Sp1 (152). Additional evidence has demonstrated that COUP-TF is able to physically interact and cooperate with TAT (153). All of these results demonstrate that COUP-TF is a pivotal transcriptional factor involved in HIV-1 expression in microglia.

AP-1

There are two putative AP-1 binding sites within the HIV-1 LTR located between –347 to –343 and –333 to –329 (Figure 1-5). However, there are currently no studies that demonstrate a direct interaction of AP-1 with these putative binding sites. AP-1 consists of several protein complexes of the *Jun* family, *c-Jun*, *Jun B*, and *Jun D* combined with members of the *Fos* family (152). Members of the Jun family are expressed in a wide variety of tissues and cells lines, however, the quantitative amounts of Jun vary between cell lines (159). Ironically, despite the presence of AP-1 in several different cell lines including Jurkat (T-cell), HeLa (epithelial), and U373-MG (astroglial), it does not bind to the putative AP-1 sites within the HIV-1 LTR of HIV_{LAI} (T-tropic), $\text{HIV}_{\text{JR-FL}}$, or

$HIV_{JR\text{-}CSF}$ (M-tropic, CNS-derived). AP-1 has been demonstrated to interact with the region between –247 to –222 of both CNS-derived LTRs ($HIV_{JR\text{-}FL}$ and $HIV_{JR\text{-}CSF}$) but not with HIV_{LAI} (23). Mobility shift assays demonstrated that extracts from both glial and HeLa cells but not neuronal or Jurkat cells contained AP-1 that bound to the –247 to –222 region of both $HIV_{JR\text{-}FL}$ and $HIV_{JR\text{-}CSF}$ LTRs. Transient transfection analysis also demonstrated that AP-1 is capable of binding to the region –247 to –222 and stimulating LTR directed gene expression in glial but not neuronal cells. This demonstrates that AP-1 sequence differences in the LTR impact cell type specific expression in microglia.

Phylogentic Analysis of Tissue Specific LTRs

The majority of studies evaluating tissue specific segregation of HIV-1 have been primarily performed with the envelope region. However, the LTR region contains the site of several transcriptional factor binding sites that can impact cell type promoter expression. To date, only one study has evaluated the HIV-1 LTR region from mutiple tissues. Ait-Khaled *et al.* evaluated the LTR regions from the postmortem samples of lymph node, blood, spleen, lung, dorsal root ganglion, and spinal cord of an HIV-1 infected patient (2). HIV-1 LTR quasispecies present in spinal cord and dorsal root ganglion segregated independently from other tissues. Phylogenetic analysis showed that the LTRs from the spinal cord and dorsal root ganglion were genetically distinct from LTR sequences present in other organs and were more closely related to the CNS-derived strain, JR-CSF. In another study evaluating LTRs from brain tissue only, Corboy *et al.* evaluated LTRS obtained from the brains of four HIV-1 infected patients (42). The majority of nucleotide variation within the LTR was observed in regions upstream of the two NF-kb sites. A majority of the LTR sequences from two or more brains shared 11 unique substitutions in transcriptional factor binding sites, of which eight were shared with the CNS-derived clones of JR-CSF and JR-FL. These nucleotide variations found within the brain derived LTRs typically altered the NF-AT and TCF-1α transcriptional factor binding sites.

Cell-Type Expression Determined by LTR of other Retroviruses

Other retroviruses have demonstrated that U3 sequences within the LTR can impact cell type specific regulation. One example comes from the Moloney-murine leukemia virus (Mo-MLV) group. Differences within the U3 region of the LTR impact the ability of the virus to induce tumors, and differences in the specific target cell for infection or transformation (18,24,64,172,183). Minor differences within the U3 region of only a few bases can dramatically alter the specificity of gene expression. Most of the sequence differences within the U3 region of the LTR affect cell specific transcriptional factor binding. Another retrovirus, Mouse mammary tumor virus (MMTV), is strongly dependent on expression of exogenously supplied glucocorticoid hormone (44). This dependance is crucial to the transmission of the virus, from mother to offspring via milk. MMTV expression is limited to lactating mammary glands where glucocorticoid hormone is abundantly expressed. The specificity of this hormone is to the U3 region of the LTR which induces a strong cell specific expression. Overall, there are other examples of retroviruses that contain regulatory elements within the U3 region of the LTR that impact cell type specific viral gene expression.

Cell-Type Specific Expression of the HIV-1 LTR

HIV-1 infects a large multitude of organ systems, and different cell types. HIV-1 infection has been detected in the brain, heart, lung, kidney, gastrointestinal tract, lymph node, spleen, thymus, blood, and bone marrow. It has been firmly established that cell tropism, replication, and cytopathogenecity are linked to the envelope region (32,45).

Several of these organ systems infected with HIV-1 have the macrophage as the predominantly infected cell. Macrophages are an important part of HIV-1 infection since they can be resistant to cytopathic effects of HIV-1 (*in-vitro*) and would serve as sites for viral replication during AIDS when CD4+ T-cells are low or following removal of highly active anti-retroviral therapy (HAART). Also, macrophages serve as a source of several HIV-1 activating cytokines such as IL-1, IL-6, and TNF-α which may result in activation HIV-1 latency and contribute to AIDS related pathogenesis of the lungs, or central nervous system. HIV-1 gene expression is governed by distinct interaction of both viral and host cell transcriptional factors with different regions within the HIV-1 LTR.

A comparison of the sequences within the U3 region of the LTR between the blood derived HIV_{LAI} strain versus the two neurotropic strains of $HIV_{JR\text{-}FL}$ and $HIV_{JR\text{-}CSF}$ demonstrated that the NF-kB and Sp1 sites, in addition to R and U5 were completely conserved (109). In striking contrast, there were approximately 27 base differences upstream of these sites, particularly within the mid-U3 (-320 to –120) region of both $HIV_{JR\text{-}FL}$ and $HIV_{JR\text{-}CSF}$ compared to HIV_{LAI} strain .

Functional analysis of the LTRs from HIV_{LAI}, $HIV_{JR\text{-}FL}$, and $HIV_{JR\text{-}CSF}$ were performed through the use of transgenic mice (109). The LTRs from HIV_{LAI}, $HIV_{JR\text{-}FL}$, and $HIV_{JR\text{-}CSF}$ were linked to a bacterial reporter gene (β-gal), and independent transgenic lines were produced. The CNS LTR ($HIV_{JR\text{-}FL}$, and $HIV_{JR\text{-}CSF)}$ isolates were capable of driving β-gal expression in neurons in the adult CNS, whereas the HIV_{LAI} LTR was not capable of transcriptional activation in the CNS. These data suggested that changes within the U3 region of the LTR, particularly those upstream of the core promoter and enhancer, can determine cell-type specific viral expression.

Additional data regarding cell-type specific expression was demonstrated when Kurth *et al.* detected binding in the region –300 to –260 using an *in-vivo* footprinting analysis with brain extracts of transgenic mice expressing $\mathrm{HIV}_{\mathrm{JR\text{-}CSF}}$ (109). In contrast, binding of this region was not detected from brain extracts of transgenic mice expressing $\mathrm{HIV}_{\mathrm{LAI}}$. Additional footprinting analysis showed brain extracts from nontransgenic mice were able to bind region -296 to –256 of $\mathrm{HIV}_{\mathrm{JR\text{-}CSF}}$ but not $\mathrm{HIV}_{\mathrm{LAI}}$. Studies with linker scanning mutants of the HIV-1 LTR transfected into the NTERA (neuron-like) cell line demonstrated two regions (-219 to –202 and –255 to –238) important for cell specific expression (200). In contrast, a collection of 478 LTRs from 42 patients with varied clinical stages failed to demonstrate any significant cell-type specific promoter expression in either Jurkat (T-cell) or U937 cell lines (60). However, all LTRs tested from the study were obtained from the blood, not from any tissues such as the lung and brain which may account for the lack of cell-type specific promoter expression. HIV-1 LTRs obtained from the PBMCs typically display a wide range of promoter activity both between and within patients. In contrast, several groups have found cell type specific differenences in replication or gene expression in association with nucleotide variations, additions, or deletions within the HIV-1 LTR. One reason for this sharp discrepancy, maybe because there are currently no studies that evaluate tissue-specific LTRs from patients and evaluate them functionally in different cell types. My dissertation attempts to address the question *in-vivo* by obtaining the HIV-1 LTR region from multiple tissues and then perform functional analysis in primary cells to truly evaluate the impact of tissue derived LTRs on cell type gene expression. The focus of my project was on the LTR region but due to exciting data generated from the first specific aim I decided to investigate the tissue specific segregation of the env V3 region within the thymus. The following sections describe the envelope region of HIV-1.

HIV-1 Envelope

The Env glycoprotein (gp) on the surface of HIV-1 virions mediates viral binding to the CD4 receptor located on CD4+ T-lymphocytes, macrophages, and dendritic cells (50,119). After viral attachment, Env gp impacts uptake of virions into cells by fusion of viral and cellular membranes (115). The *env* gene encodes for the heavily glyosylated Env precursor polyprotein, gp160 (6,151). Intracellular cleavage of gp160 yields the surface (gp120) and the transmembrane (gp41) envelope glycoproteins (Figure 1-6). The transmembrane gp41 is approximately 350 amino acids long, hydrophobic, and transverses once through the lipid bilayer of virions and cells (194). Gp120 is heavily glycosylated and located on the surface of the HIV-1 virion, and contains binding sites for both CD4 and the chemokine receptors of either or both CXCR4 and CCR5 (37,105,180). Gp120 consists of five variable domains known as V1-V5, interspersed with five conserved regions designated C1-C5 (Figure 1-7). A disulfide map has been obtained for a secreted form of the gp120 molecule (113). This map showed the existence of 18 cysteine residues that form nine intrachain disulfide bonds. These bonds segregate gp120 that have been further divided by sequence analysis or function. One disulfide loop encompasses V1 and V2 which is segregated by two additional disulfide bonds. In addition the V3 and V4 loops are also divided by disulfide bonds. The C4 region is though to be highly involved with CD4 binding. The majority of data has demonstrated that the V3 region plays an important role in governing multiple biological properties of the HIV virus including tropism and co-receptor usage (33,34,85,167,171). Single amino acid changes within the V3 loop can alter the tropism of HIV-1. As few as three amino acid changes in the V3 domain were demonstrated to confer macrophage tropism on a T-cell line tropic strain (171).

Tropism is defined as the ability of the HIV isolate to replicate in either T-cell lines (MT-2) or macrophages. Co-receptor usage is defined as the ability to utilize the co-receptors of either CCR5 (R5), or CXCR4 (X4), or both. The majority of HIV-1 isolates from patients can replicate in PBMC, however differ in their tropism (MT-2 or macrophages), and co-receptor usage (R5 or X4). The V3 loop contains 35 amino acids arranged in a disulfide loop involving Cys263 to Cys298 (Figure 1-8). Analysis of natural variants of HIV-1, in addition to studies of point mutations in the V3 region have indicated that the V3 is a primary determinant of both co-receptor usage and tropism (33,34). As mentioned before, viruses can be classified based on biological characteristics of viral isolates in culture (Figure 1-8). T-cell line tropic viruses grow in MT-2 (T-cell line) cells, induce synctium, utilize X4, and typically have a V3 charge of 5 or greater. In contrast, macrophage-tropic viruses do not induce synctium, utilize R5, and have a V3 net charge of +3.

Prediction of Tropism by V3 Sequence

The V3 amino acid sequence can predict the viral phenotype (19). Our laboratory has developed a model based on four variables in V3 that can be used as predictors of viral phenotype: (i) number of positively charged amino acid residues (K or R); (ii) number of negatively charged residues (D or E); (iii) net V3 charge [(K+R)-(D+E)]; and (iv) and isoleucine residue at position at 292. The equation to predict viral phenotype based on these variables is shown below:

Predicted phenotype = 0.94 + [1.68x(V3 net charge)] – [1.37x(total positive charges)]+[1.54x(total negative charges)]-[1.19, if aa292=I].

Calculated values for predicted phenotype are rounded arithmetically. Phenotypic definitions are: 1 uses R5 and infects macrophages only (M-R5); 2 uses either R5 and X4 or X4 only, infects macrophages and T cell lines (D-X4±R5); 3 uses X4 and infects T cell lines only (T-X4).

Phylogenetic Analysis

The goal of phylogenetic analysis is to use genetic sequences to obtain or construct a phylogenetic tree that can determine the genetic relationship among a set of given sequences and permit inferences regarding evolutionary relationships. There are two different methods to tree construction. Distance based methods, such as neighbor joining, use only the overall genetic distance between pairs of sequences, disregarding the qualitative information in the specific differences (79,81). This approach maybe rapid, but is imprecise. Character based methods, such as parsimony, look at each variable site and utilize the pattern of variation to elucidate a plausible sequence of changes that relate the sequence to a common ancestor (182).

Neighbor joining method is generally faulted since this analysis does not utilize all of the information available in the sequence. Therefore, the original sequence cannot be reconstructed from the distance matrices derived from the analysis, thereby losing critical information regarding ancestral sequences. However, the neighbor joining method is typically fast and easy to perform which makes this analysis widely used and represents a good starting point for phlyogenetic analysis.

Parsimony analysis takes into account all of the information present in a sequence data set. This method treats all characters as discrete. For example, a particular position in a sequence is a character (ie. G at a specific position); the particular nucleotide or amino acid occupying that position is determined as the character state. Parsimony analysis attempts to interpret shared derived characters. Therefore, parsimony analysis can examine a large amount of sequences and construct multiple possible trees to seek the ancestral sequences and clusters of related sequences. Parsimony analysis can be applied to both nucleotide and amino acid sequences very effectively. My phlyogenetic analysis examined both the nucleotide region of the LTR and the amino acid sequence of envelope. Parsimony analysis represented the most accurate and applicable method to examine my data set for both elucidating ancestral sequences and identifying tissue specific lineages.

Distance analysis can also be used in conjunction with phylogenetic analysis to obtain quantitative estimates of the relative genetic distances between sequences and to use this information to estimate rates of both divergence, and diversity. Divergence is the genetic distance between two distinct groups of sequences. For example, if you were comparing the envelope sequences obtained from the lung versus the sequences obtained from the PBMC that would be considered divergence. Diversity is considered the genetic distance within a specific group of sequences. For example, the genetic distance among all the sequences obtained from the lung would be considered diversity.

The simplest way to calculate a genetic distance between two sequences is to count the number of differences. This measure is often called Hamming distance and contains numerous pitfalls. This method does not take into account back mutation, transition/transversion rates, different base frequencies, and non-uniform substitution rates between sites. Another method that is often used to evaluate genetic distances more accurately is the Kimura two-parameter model. This method assumes that transitions and transversions will occur at unequal rates, specifically that transitions will outnumber transversions. Genetic distance was calculated in my dissertation according to the Kimura two-parameter which is a more accurate method of genetic distance.

Bootstrapping

Bootstrapping, also known as statistical resampling, can be used to evaluate both neighbor joining and parsimony trees. This method reports the level of support for each branch (ie. internal node). This method randomly resamples columns from the alignment of the genetic sequences, so that some positions will not be used and others will be used more than once, and constructs new trees from the dataset. This analysis is performed as many time as specified and is otherwise known as resamplings. The bootstrap value is a count or percentage of how often each branch was present in exactly the same topology in all the resampled trees. For example, when bootstraps are shown on a branch as 65 or 85 this represents the number of times that particular branch segregated from all branches during the resampling process. Bootstrapping is typically a conservative measurement. Therefore, a bootstrap of 95% gives more than 95% confidence in that branch. Bootstraps of 70% or higher may correspond to a 95% confidence level, and is typically considered the approximate cut-off for a significant branch (80). My analysis focuses on all branches that have a bootstrap of 65% or greater in order to identify any tissue specific lineages that are significant.

Specific Aims and Study Design

The experimental design was constructed to address the specific aims of: (1) To determine if the HIV-1 env and LTR regions phylogenetically segregate according to tissue (Chapter 2); (2) To determine the impact of tissue specific LTRs on promoter activity using a luciferase reporter gene assay in both a T-cell and monocytic cell line (Chapter 2); (3) To determine if the thymus serves as a site of evolution of T-cell line tropic (T-X4) and Dual-tropic (D-X4±R5) env quasispecies (Chapter 3); and (4) To evaluate gene expression in primary cells via congenic recombinant LTR viruses without variability from other regions (Chapter 4).

To address Specific Aim 1 four patients that had autopsy specimens of brain, lung, thymus, and longitudinal PBMCs were chosen for this patient cohort (Table 1-1). The LTR and env regions were PCR amplified from these tissues and phylogenetically analysed by parsimony analysis to identify tissue specific quasispecies (Chapter 2). Tissue specific LTRs were functionally analyzed by evaluating promoter activity by transient transfection utilizing a luciferase reporter gene plasmid in a T-cell and monocytic cell line (Chapter 2).

The observation of T-X4 and D-X4±R5 quasispecies in the thymus prompted further investigation to determine if the thymus was the site of evolution for these variants (Chapter 3). Env quasispecies from post-mortem thymus specimens from two other patients were also evaluated , in addition to further analysis of the lymph node, and spleen (Table 1-1). The env populations from the spleen and lymph node was also analyzed from the two patients of our initial four patient cohort that had post-mortem thymus tissue. The lymph node and spleen were evaluated since these tissues represented potential sites for emergence of both T-X4 or D-X4±R5 quasispecies.

Functional analysis of the tissue specific LTRs from patient C/S1 were evaluated by constructing recombinant LTR Luciferase viruses (Chapter 4). Promoter activity among tissue specific LTRs were evaluated in primary cells such as CD4+ T-cells and macrophages to determine if the LTR impacts cell-type specific gene expression.

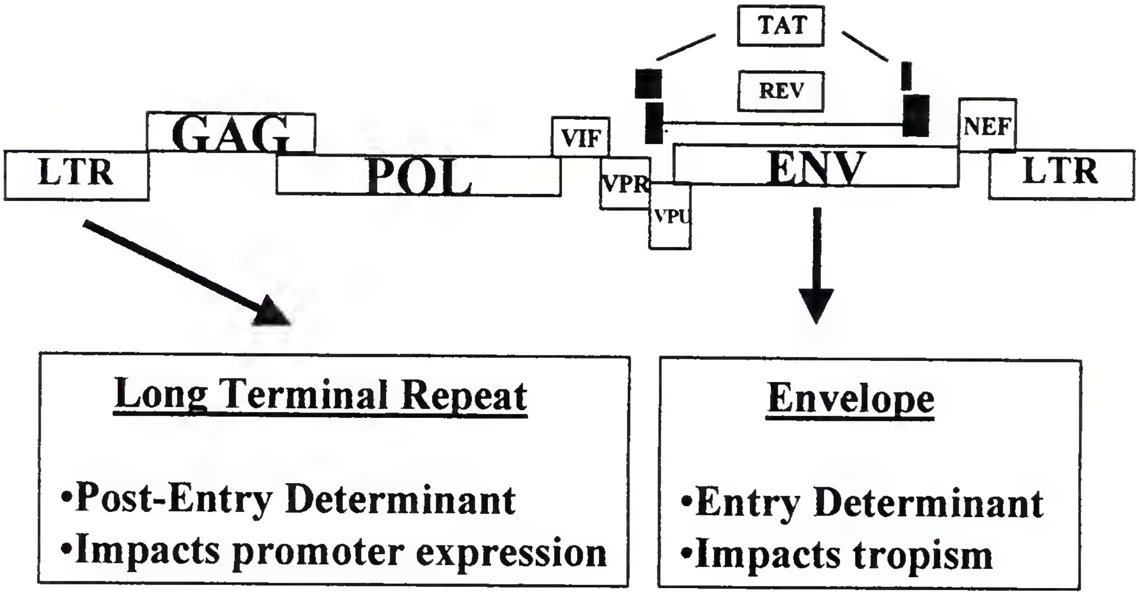

Figure 1-1. HIV-1 proviral genome. The main genes of *gag*, *pol*, and *env* with the accessory genes are shown above. The identical 633 bp long terminal repeats are present at the terminal ends of the HIV-1 genome. The two subgemomic regions of HIV-1 evaluated in this study were the envelope and LTR regions. The env and LTR regions impact two different steps in the viral life cycle as described above.

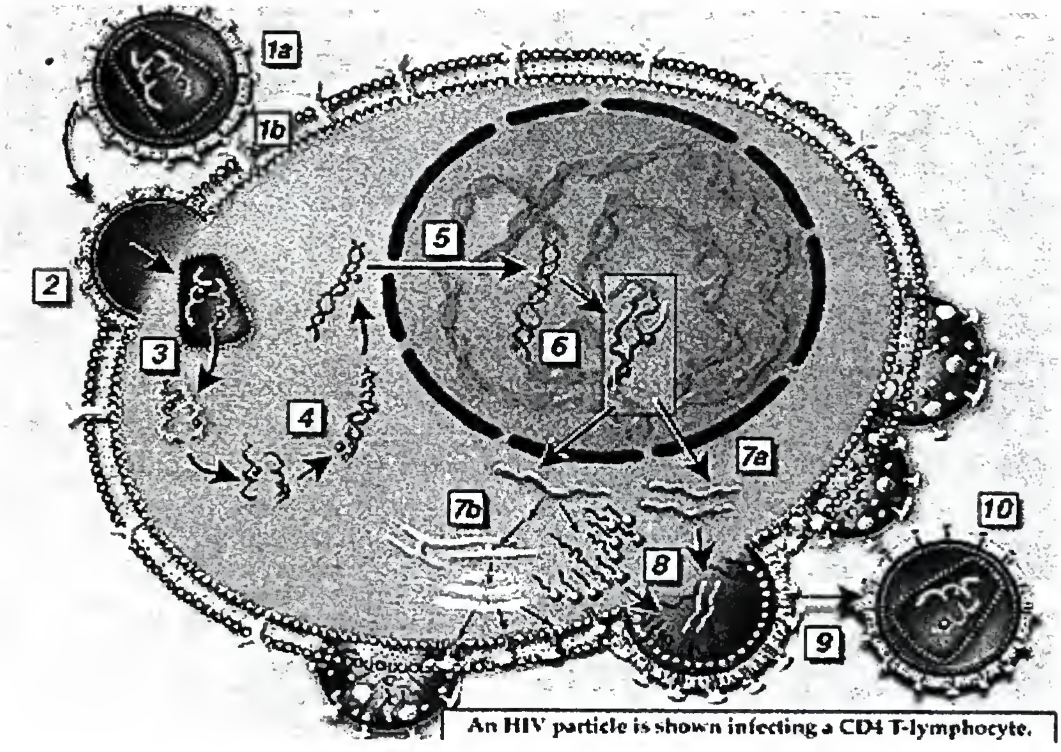

Figure 1-2. HIV-1 viral lifecycle as demonstrated by an HIV-1 virion infecting a CD4+ T-lymphocyte. The HIV-1 lifecycle steps are as follows 1a) Binding of HIV-1 gp120 to CD4, 1b) Binding of HIV-1 gp120 to CCR5 or CXCR4 and subsequent fusion, 2) Release of HIV-1 RNA from protein core into cytoplasm, 3) Uncoating of viral core to expose viral RNA, 4) Reverse transcription of viral RNA into double-stranded DNA, 5) Translocation of viral DNA into the nucleus and integration, 6) Transcription of viral DNA via interaction between HIV-1 LTR and host and viral cellular proteins, 7a) Translation of viral gene products, 7b) Viral envelope processing, 8) Viral assembly at the plasma membrane, 9) Budding of the HIV-1 virion, and 10) Maturation of virions via viral and cellular proteinases to form structural proteins, and viral enzymes (190).

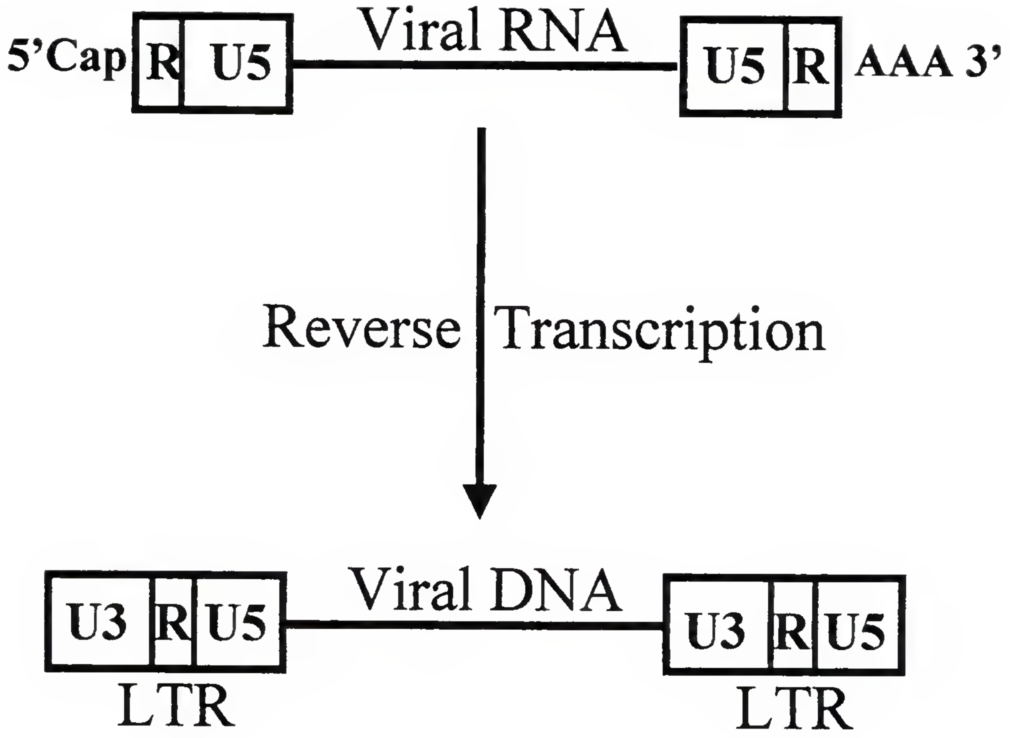

Figure 1-3. Generation of the HIV-1 LTRs. Reverse transcription of the viral RNA genome generates double-stranded viral DNA. Duplications of the U5 and U3 regions are created during reverse transcription so that the viral DNA is longer than the viral RNA at the terminal ends. Each LTR is identical in sequence and consists of the U3, R, and U5 regions.

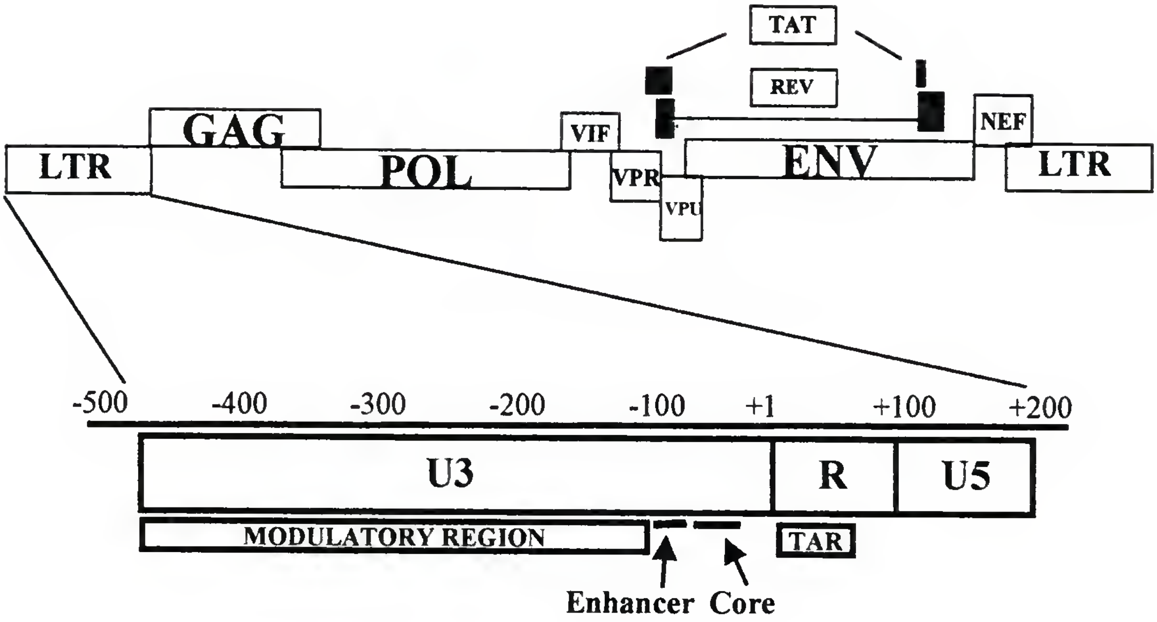

Figure 1-4. Major regions of the HIV-1 LTR. The HIV-1 LTR is expanded from the proviral HIV-1 genome. The major segments of U3, R, and U5 are illustrated above and depicted to relative scale. The HIV-1 LTR is divided into the distinct regions designated U3 (-453 to +1), R (+1 to +98), and U5 (+99 to +185). The modulatory region within the U3 is not genetically conserved and contains several transcriptional factor binding sites. The enhancer region extends from –104 to –81 and contains two NF-kB sites. The core promoter consists of three Sp1 sites (-78 to –45) and a TATAA box (-28 to –24). Both the enhancer and promoter are typically genetically very homogenous among HIV-1 isolates. The R region encodes the sequence which forms the trans-activation response (TAR) element which binds to Tat.

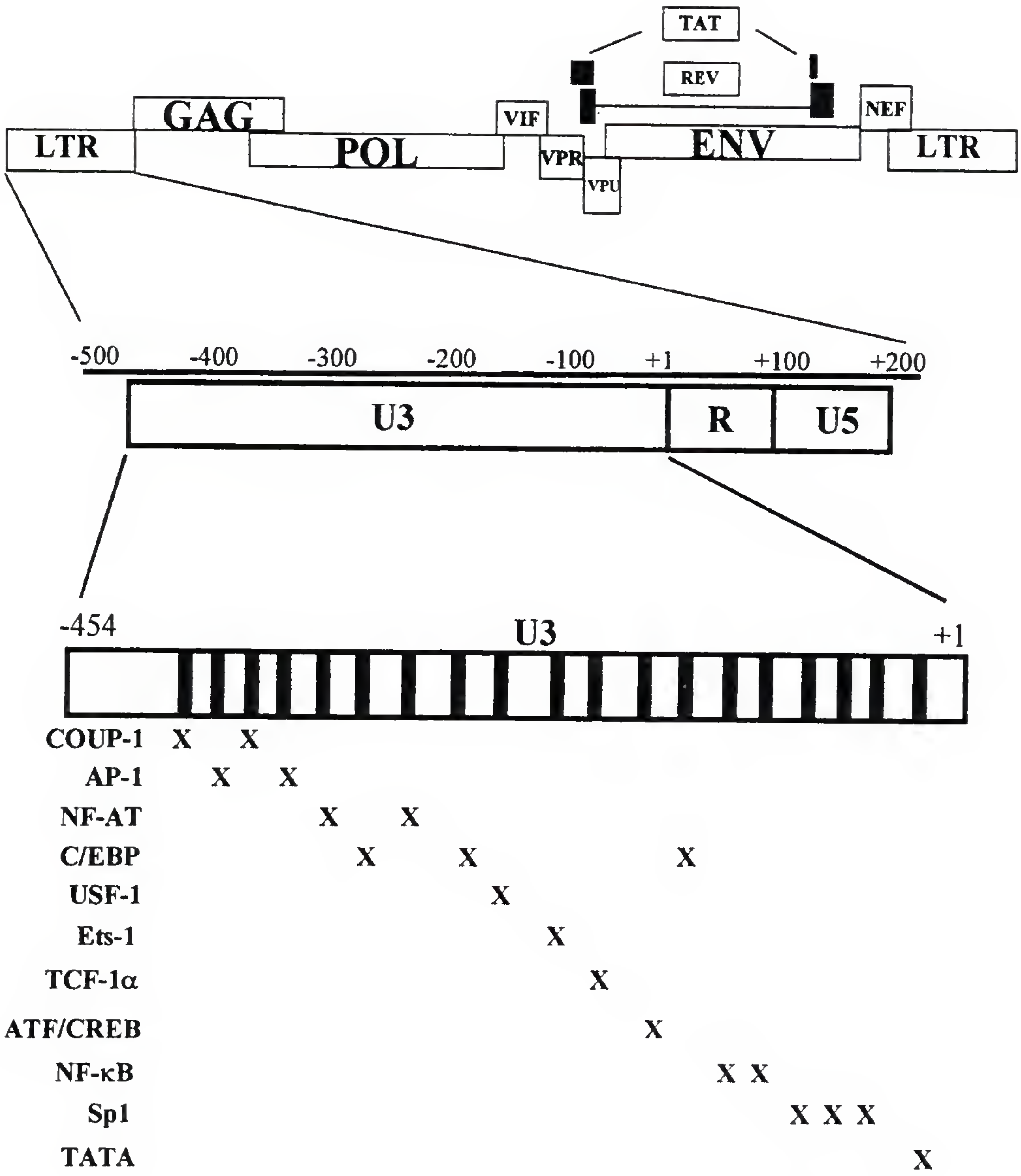

Figure 1-5. Transcriptional elements within the HIV-1 LTR U3 region. The locations within the U3 region of transcriptional factor binding sites are shown in their relative position within the LTR.

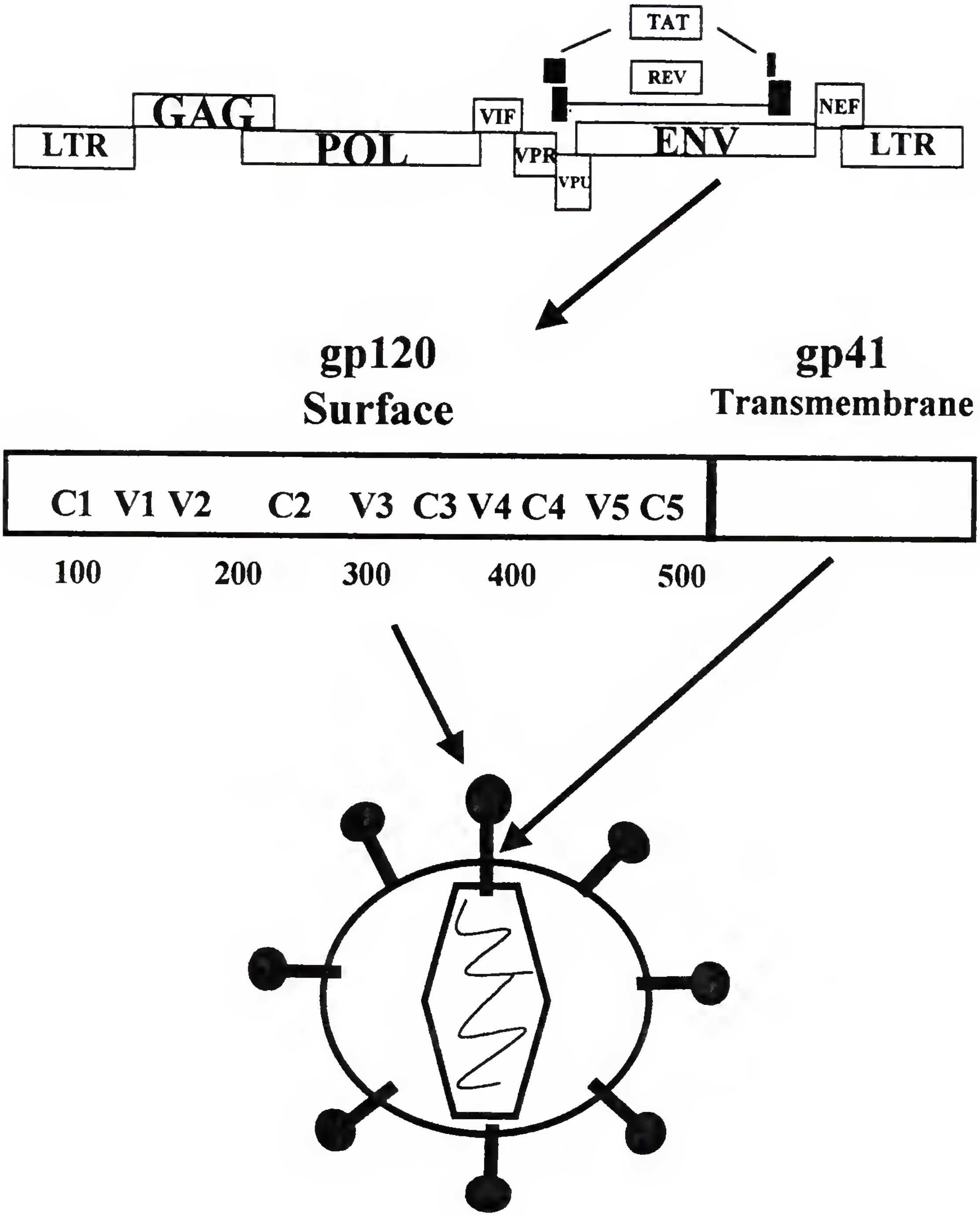

Figure 1-6. Functional domains in HIV-1 envelope. Envelope is cleaved to produce the gp120 surface subunit and the gp41 transmembrane subunit. The gp120 subunit contains five hypervariable regions (V1-V5), and five conserved regions (C1-C5). The amino acid length is shown below gp120. A virion with protruding envelope glycoproteins is represented at bottom of page.

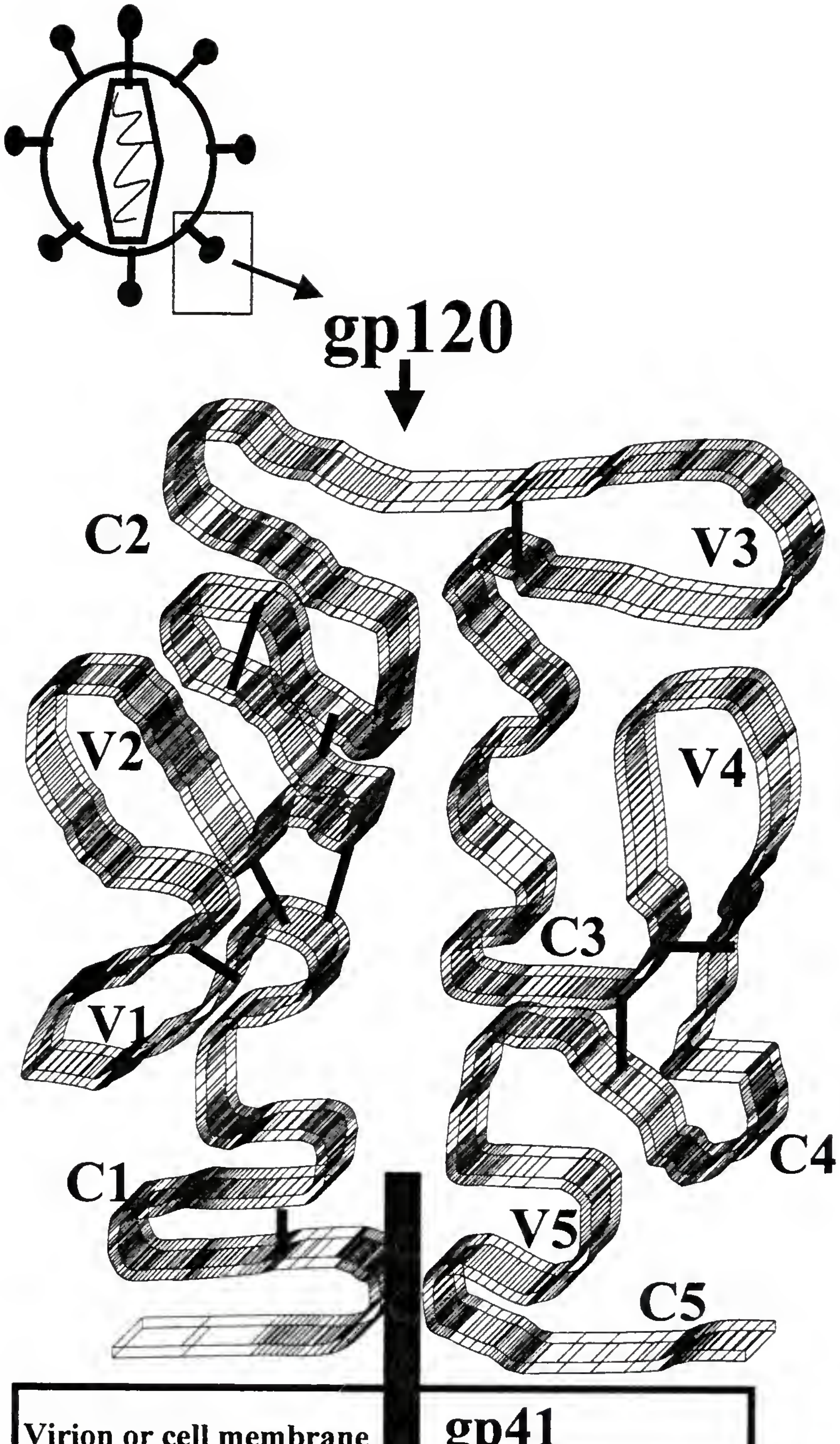

Figure 1-7. Predicted Folding Pattern of the HIV-1 gp120 (113).

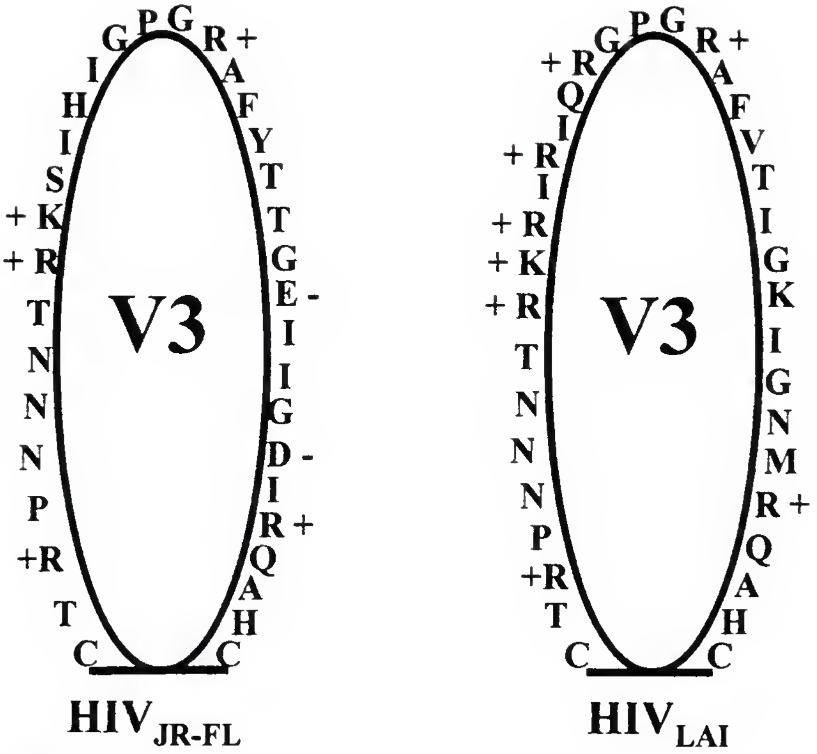
V3
C T +R P N N N T +R +K S I H I G P G R+ A F Y T T G E- I I G D- I R+ Q A H C
HIV
JR-FL
V3
C T +R P N N N T +R +K +R I +R I Q +R G P G R+ A F V T I G K I G N M R+ Q A H C
HIV
LAI

	HIV_{JR-FL}	HIV_{LAI}
V3 Charge	**+3**	**+8**
PBMC	**+**	**+**
Macrophage	**+**	**-**
T-cell Line	**-**	**+**
Coreceptor	**CCR5**	**CXCR4**

Figure 1-8. Cellular Host Range of HIV-1 as Determined by V3. Two different V3 sequences are shown from a M-R5 virus (HIV_{JR-FL}) and a T-X4 virus (HIV_{LAI}). Charged amino acids are designated with a + for positive charge and – for negative charge. Table below V3 sequence indicates viral growth in different cell types and coreceptor usage.

Table 1-1
Overall Patient Cohort and Analysis Performed

Patient	Survival Time (yrs.)	Chapter 2	Chapter 3	Chapter 4	Tissues Analyzed	Patient Code	Phylogenetic Analysis		Transient Transfection		Functional Analysis	
							LTR	Env	Jurkat	U937	PBMC	MDM
1	2	A	R1		Early PBMC	555U	X	X	X	X		
					Late PBMC	1131U	X	X	X	----		
					Lung	1131LU	X	X	X	X		
					Thymus	1131TH	X	X	----	----		
					Lymph Node	1131LY	----	X	----	----		
					Spleen	1131SP	----	X	----	----		
2	2.6	B	------		Early PBMC	187U	X	X	X	X		
					Late PBMC	438U	X	X	X	----		
					Lung	1129LU	X	X	X	X		
					Brain	1129BR	X	----	X	X		
3	7	C	S1	C/S1	Early PBMC	201U	X	X	X	X	----	----
					Late PBMC	1873U	X	X	X	----	X	X
					Lung	1905LU	X	X	X	X	X	X
					Brain	1905BR	X	X	X	X	X	X
					Thymus	1905TH	X	X	----	----	----	----
					Lymph Node	1905LY	----	X	----	----	----	----
					Spleen	1905SP	----	X	----	----	----	----
4	16	D	L1		Early PBMC	263U	X	X	X	X		
					Late PBMC	1276U/1113U[#]	X	X	X	X		
					Lung	1276LU	X	X	X	X		
					Brain	1276BR	X	X	X	X		
					Thymus	1276TH	----	----	----	----		
5	7	-------	S2		Early PBMC	00039U	----	X	----	----		
					Thymus	1126TH	----	X	----	----		
					Lymph Node	1126LY	----	X	----	----		
					Spleen	1126SP	----	X	----	----		
6	0.6	-------	R2		Thymus	1128TH	----	X	----	----		
					Lymph Node	1128LY	----	X	----	----		
					Spleen	1128SP	----	X	----	----		

[#] Timepoint for LTR region was 1276U and envelope region was 1113U

CHAPTER 2
PHYLOGENETIC AND PROMOTER ANALYSIS OF THE HIV-1 LTR AND ENVELOPE REGIONS FROM VARIOUS TISSUES OF VERTICALLY INFECTED PEDIATRIC PATIENTS

Introduction

Human Immunodeficiency Virus Type 1 (HIV-1) entry into target cells is dependent upon binding of the viral glycoprotein (gp120) to CD4 and the chemokine co-receptors of either CCR5 or CXCR4 (14,49,128). There is great heterogeneity between HIV-1 variants in rate of replication, tropism, and co-receptor usage (8,30,62,126,186,187). Cellular tropism and co-receptor usage appears to be primarily determined by the V3 hypervariable region of the gp120 envelope protein (33,34,85,167,171). These differences in viral phenotype maybe the result of different viral reservoirs that are composed of different target cells. The predominant co-receptor expression within these tissues can vary between CCR5 or CXCR4 depending on the local population of cells being either macrophages or CD4+ T cells (9,25,71,158). Several investigators have demonstrated that envelope sequences from the blood are phylogenetically different from those recovered from tissues such as the Central Nervous System (CNS), lung, spleen, bowel, and reproductive tract (10,31,59,84,86,103,137,147,150,169,192,204). Significant phylogenetic segregation within these compartments suggests the existence of viral reservoirs that interact in a limited fashion with the periphery.

Despite the wealth of knowledge demonstrating that env plays an important role in impacting cellular tropism and tissue segregation, there is additional evidence that the Long Terminal Repeat (LTR) may also impact post-entry tissue tropism. The LTR is divided into three compartments; U3, R, and U5 (68,70). Promoter activity is significantly impacted by the genetic heterogeneity found within transcriptional binding sites with the U3 region (60,96,125,130,201-203). The LTR region segregates between the blood and brain by phylogenetic analysis, particularly within the mid-U3 region (2,42). This phylogenetic segregation (as seen with env) suggests that tissues with different cellular reservoirs may be exposed to different transcriptional activators. Other investigators have revealed T-cell and macrophage specific transcriptional factors, therefore tissues that predominantly harbor macrophages as the major HIV-1 infected cell may serve as a compartment of independent replication under both pre and post-entry selection (77,78,131,170,198). Currently, there are no reports that simultaneously evaluate tissue by phylogeny specific tropism according to both the LTR and env regions. Highly active anti-retroviral therapy (HAART) provides a potent yet partially ineffective treatment for HIV-1. Complete elimination of this pathogen from the host has not been completely achieved due to the presence of viral reservoirs that serve as a source of rebound virus. These viral reservoirs are under multiple levels of viral selection that result in separate population of viruses. An understanding of these latent reservoirs is dependent upon identification of both pre and post entry factors responsible for viral selection. Recent evidence has demonstrated that conclusions based on single genomic regions are limited since different parts of the HIV-1 genome may have different evolutionary histories (129). Therefore, true tissue specific tropism needs to be evaluated in the context of multiple regions of the viral genome.

To elucidate whether HIV-1 segregates according to tissue based on two genomic regions, env and LTR, we examined two T-cell dominated tissues (PBMCs and thymus) and two macrophage dominated tissues (lung and brain). The lung and brain are sites where the predominant infected HIV-1 cell is a macrophage. Few studies have examined whether the thymus could serve as a T-cell dominated reservoir. This tissue may provide a source of T-cell line tropic, CXCR4-using viruses and profoundly impact immune reconstitution. HIV-1 env and LTR sequences were obtained from sequential blood samples and several tissues obtained at autopsy from 4 patients with varied clinical progression. All patients were vertically infected, and most received limited anti-retroviral therapy. To evaluate whether different genomic regions determine tissue-specific segregation, phylogenetic analysis was performed in the context of env and LTR, and tissue-specific LTRs were then functionally evaluated by transient transfection in Jurkat (T-cell) and U937 (monocytic) cells.

Materials and Methods

Patient Cohort and Autopsy Processing.

All relevant patient clinical data and total collection of tissues and are listed in Tables 2-1. Peripheral blood mononuclear cells (PBMC) were collected at two timepoints, and tissue specimens from the lung, brain, and thymus were collected at autopsy 24 to 48 hours after death. Blood collection has been described previously (110). Tissues were snap-frozen in 50 ml conical tubes and stored at -80°C until processed for DNA extraction. All protocols were approved by the Institutional Review Board of the University of Florida. Patients A and B were both rapid progressors, whereas Patients C and D were slow and long-term progressors, respectively (Table 1-1, patients 1 to 4). All patients were vertically infected. All patients expired prior to the advent of protease inhibitors. Patient A did not receive anti-retroviral therapy; Patient B received AZT, Patient C received AZT and DDI, and Patient D received ZDV, DDI, and DDC. All patients had both brain and pulmonary complications. Proviral sequences from two PBMC timepoints were obtained from each patient. The early and late PBMC timepoints for each patient were: Patient A (1 yr. and 4 months prior to death); Patient B (1.6 years and 2 weeks prior to death); Patient C (1 yr. and 2 weeks prior to death); and Patient D (4 yr. and 3 months prior to death).

Isolation of DNA from Autopsy Specimens and PBMCs

DNA was extracted from tissue specimens using the SV RNA extraction kit generously supplied by Promega. Extraction was performed with the following modifications. Tissue (10-30 mg.) was removed by punch biopsy from autopsy specimen and placed into a 1.5 ml Eppendorf tube containing 175 ul of SV RNA lysis solution (Promega). The samples were incubated for approximately 2-24 hours with occasional mixing. After incubation period, extraction procedure followed that of manufacturers instructions. DNA was extracted from Peripheral blood mononuclear cells as previously described (110).

PCR Amplification and Cloning

Nested PCR amplifications were performed of long terminal repeat sequences using for the first round, forward primer, NEF9 (5'-GACAGGGCTTGGAAAGGGCTTTGC-3', position 8360-8383, HIV_{LAI}) and the reverse primer, LTR7 (5'-ACCAGAGTCACACAACAGACGGGCACACACTACT-3', position 98-131). The second round LTR amplification used the same reverse primer of LTR7 with a forward primer, NEF11 (5'-CCAGATCTTAGCCACTTTTTAAAAGAAA-3', position 9098-9124). Nested Envelope PCR amplifications used a forward primer, LV15 (5'-GCCACACATGCCTGTGTACCCACA-3', position 6464-6489), and reverse primer, 194G (5'-CTTCTCCAATTGTCCCTCATA, position 7688-7718). Second round amplification of envelope used the same reverse primer with the forward primer, ENV5 (5'CGGGATCCGGTAGAACAGATGCATGAGGAT-3', position 6547-6577).

Approximately 500 ng of DNA extracted from tissue was used for each 50 ul PCR reaction with PCR Buffer (Perkin-Elmer) (50 mM KCl , 20 mM Tris, ph 8.5), 0.05 um each primer, 1.75 mM MgCl2 (Perkin-Elmer), and 0.2 uM each dNTP (Pharmacia). Multiple PCR amplifications were performed on each tissue to prevent PCR bias. The following parameters were used for both LTR and Env PCR amplifications: one cycle of 94°C for 10 min, 35 cycles with each cycle consisting of 94°C for 1 min, 60°C for 1 min, 72°C for 2 min, and final extension of 72°C for 10 min. PCR amplifications were performed in an automated thermal cycler (Perkin-Elmer 9600). Products from the first round reaction were purified with the PCR Purification kit (Qiagen) and 10-20 ul of the purified first round PCR product was used as the template for second round amplifications. The second round LTR amplification produced a product of 650 bp, and the envelope amplification produced an approximate 1.1 kb product. PCR products were ligated into pGEM-T vector (Promega) according to manufacturer's instructions. Fifty µl of Max Efficiency DH5α Competent Cells (Gibco-BRL) were transformed with 4 µl of ligation mix. Transformation procedure was followed according to manufacturers instructions. The transformation was then plated on Luria broth with ampicillian (100 mg/ml), with 50 µl of isopropyl-3-D-thiogalactopyranoside (IPTG; 50 mg/ml), and 50 ul of 5-bromo-4-chloro-3-indoyl-β-D-galactopyranoside (X-Gal; 20 mg/ml) and incubated at 37°C overnight. Approximately 5-15 colonies were picked and grown in Luria Broth with ampicillian (100 ug/ml) at 37°C overnight. Plasmids were extracted using a Miniprep extraction kit (Qiagen) following manufacturer's instructions. Plasmid inserts were confirmed by restriction digestion using *Eco*RI (Gibco-BRL) and analyzed by agarose gel electrophoresis. Correct size LTR products were sequenced with NEF11, while correct inserts for envelope were sequenced with 195C (5'-CTGGGTCCCCTCCTGAGG-3', position 7362-7379). Sequencing was performed using the ABI 373 Prism Dye Terminator Cycle Sequencing Ready Reaction Kit (Perkin-Elmer). The env region was amplified from all tissues except for patient B brain, patient C lung, and patient D thymus. The LTR region was amplified from all tissues except from patient D thymus.

Sequence Data Analysis

Phylogenetic analysis was performed on the nucleotide sequence of the mid-U3 region (-335 to -105), and the amino acid sequence from the V3 region of env. DNA and amino acid sequences from LTR and env respectively were aligned using the ClustalX program version 1.64. Sequences were inserted in regions where insertions or deletions have taken place in order to obtain proper alignment. Parsimony and neighbor-joining trees of the LTR nucleotide region and env amino acid region were constructed using PHYLIP package version 3.5 (61). Distance calculations for intra and inter tissue sequences were performed using the Kumura-2-Parameter algorithm applied in the MEGA software package (108). The bootstrap analysis for nucleotide sequences was carried out with SEQBOOT with 100 resamplings, DNAPARS, and CONSENSE from the PHYLIP package. Bootstrap analysis for amino acids was performed with seqboot with 100 resamplings, PROTPARS, and CONSENSE. All trees were rooted with HIV_{LAI}. To determine the integrity of the dataset, overall phylogenetic trees were constructed from the nucleotide sequence of both the env and LTR regions (Figure 2-1). Representative sequences were chosen from each tissue. Patient sequences were found to segregate from one another and from the outgroup population of HIV_{LAI}. There was no evidence of cross contamination between patient sequences or with HIV_{LAI}.

Determination of Predicted Phenotypes

Viral phenotype was determined according to a previously published equation based on four variables: (i) number of positively charged residues (K or R); (ii) number of negatively charged residues (D or E); (iii) net V3 charge [(K+R)-(D+E)]; and (iv) an isoleucine residue at position 292 (19). The equation used to predict the viral phenotye:

Predicted phenotype= 0.94+[1.68 x (V3 net charge)]-[1.37 x (total positive charges)]+[1.54 x (total negative charges)]-[1.19, if aa292=I]. Calculated values for predicted phenotype are rounded arithmetically. Definitions for the phenotypes are: (1) uses CCR5 only and infects macrophages only (M-R5); (2) uses either CCR5 or CXCR4 or CXCR4 only and infects macrophages and T-cell lines (D-R5/X4 or D-X4); and (3) uses CXCR4 and infects T-cell lines only (T-X4).

Standard Curve of Firefly Luciferase

Firefly luciferase (Sigma) was serially diluted ten-fold in 1X Phosphate Buffered Saline (PBS) with 1 mg/ml Bovine Serum Albumin (BSA). Dilutions of luciferase were from 0.1 pg to 10 μg. Relative light units were measured during a 10 second integration time with a luminometer (Analytical Luminescence Laboratory) in a volume of 100 ul of 1X luciferase assay reagent (Promega).

Construction and Analysis of Patient Luciferase Constructs

Patient LTR sequences were PCR amplified to incorporate complementary restriction sites for subsequent ligation into the upstream region of the luciferase reporter gene in plasmid pGL-3 (Promega). The Kpn I site was introduced at position –455, HIV$_{LAI}$ using the primer LTR27 (5'-GGGGTACCGTTTAAAAGAAAGGGGGG-3') and the reverse primer LTR7 (position 131-98, HIV$_{LAI}$). The predominant LTRs from each tissue were chosen for evaluation in the transient luciferase assay. The Kpn I site was incorporated into the upstream region of the LTR. This introduced Kpn 1 site and the naturally occurring Sst I (position 9619, HIV$_{LAI}$) were used for ligation into the pGL-3 (Promega) luciferase reporter gene. Patient LTR-Luc constructs were prepared using the QIAfilter Maxi-prep kit (Qiagen). The patient constructs were sequenced for confirmation of LTR inserts, and quantitated with absorption spectroscopy. One ug of each construct was transiently transfected into the human acute T-cell leukemia line, Jurkat, or the monocytic cell line, U937, with 12 ug of Superfect transfectin (Qiagen). Approximately 5.25 x 10^5 Jurkat or U937 cells were transfected in a 24 well dish in a total volume of 350 μl of complete RPMI (10% Fetal Bovine Serum, Penicllian/Streptomyocin (100 ug/ml), 0.05% $NaHCO_3$). Twenty four hours post-transfection cells were harvested with the Luciferase Cell Culture Lysis Reagent diluted to 1X (Promega). Twenty ul of the cell lysate was assayed for luciferase expression with a luminometer (Analytical Luminescence Laboratory) according to manufacturer's instructions. Relative light units were measured during a 10 second integration time in a volume of 100 ul of 1X luciferase assay reagent (Promega). The construct LAI-LTR-luc was used in each transfection, and served as a measure of transfection efficiency. All constructs were transfected in triplicate, and results are expressed from two independent transfections. Promoter activity of each construct was determined by dividing the patient LTR promoter activity by the mean LAI-LTR-luc activity.

Results

Envelope V3 Sequences from each Tissue

Table 2-2 shows an alignment of all envelope sequences obtained from various tissues of all patients. Approximately 77% (102/133) of env V3 sequences obtained from all pateints had a charge of ≤ 4 (low-charge) with a predicted phenotype of M-R5. Only 23% (31/133) of V3 sequences had a charge ≥5 (high-charge) with a predicted phenotype of either D-X4±R5, or T-X4. However, minor populations of high charge V3 sequences were detected in all patients. When examining charge distribution according to tissue; the brain, lung, and PBMCs were mostly comprised of low-charge V3 sequences. All V3 sequences from the brain (Table 2-2, Patients C and D) had a low charge with a predicted phenotype of M-R5. The majority of PBMC sequences (62/76) were typically low charge, however 18% of all PBMC sequences had a high V3 charge with a predicted phenotype of D-X4 or D-X4±R5. Approximately 77% (16/21) of V3 sequences obtained from the lung had a low charge, however lung sequences from Patient B had a charge of +5. In contrast, the thymus was the only tissue type from all patients that always contained high charge V3 sequences, and was the only source of V3 sequences with a predicted phenotype of T-X4 or D-X4±R5 (Table 2-2, Patients A and C).

LTR Sequences from each Tissue

The LTR sequences shown in Figure 2-2 are aligned to HIV_{LAI} and represent the major LTR sequences obtained from each tissue. All of the LTR sequences shown in Figure 2-2 were tested by transient transfection in both Jurkat and U937 cells (Figures 2-8, 2-9 and 2-10). If more than one LTR sequence was tested from a certain tissue than the more predominant LTR was the major sequence, while the less predominant LTR sequence was the minor sequence. The majority of nucleotide variations between tissues was found between nucleotides –316 to –105, whereas the promoter distal (-454 to –320), and the R region (+1 to +98) had very few tissue specific nucleotide polymorphisms (data not shown).

–316 to –208 HIV_{LAI}

Tissue specific polymorphisms within this region were found within several tissue LTRs (Figure 2-2 A). For example, the major lung LTRs from Patient A contained two specific nucleotide polymorphisms at positions –250 T→C and -245 C→T, HIV_{LAI} located within the C/EBP site not found in other LTRs from this patient. The majority of lung LTRs from Patient B contained a polymorphism at position –290 T→C and –255 G→C, HIV_{LAI} both located within the NFAT site. Lung LTRs from Patient C contained a unique polymorphism at position –300 G→A, HIV_{LAI} located within a c-myb site. Brain LTRs from Patient B had a polymorphism at position –261 A→G and –255 G→A that occurred within a NFAT and C/EBP site, respectively. LTRs from the brain of Patient C had a polymorphism at position –271 A→C located within the NFAT site. The brain LTRs from Patient D had a polymorphism at position –215 T→A, HIV_{LAI}. No major insertions or deletions were found in any LTRs between –316 to –208, HIV_{LAI}.

-207 to –105

Several brain LTRs from Patient C contained specific polymorphisms found at positions –171 T→G, -156 G→A, -153 A→T, and –132 A→C, HIV_{LAI}. Several insertions were found within the LTRs from Patients A and D within the TCF site located between –139 to –124. Patient A LTRs contained a 5 bp GAACT repeat, and several Patient D LTRs contained a 25 bp imperfect duplication of the TCF site.

-104 to –1

No gross insertions or deletions were observed within the NF-kB or Sp1 sites. Very few tissue specific polymorphisms were observed within this region. However, there was a polymorphism of the TATA box to TAAA found in the majority of LTRs from Patient D. Lung LTRs from Patient B contained two polymorphisms at positions –92 T→C and –91 G→C, HIV_{LAI}. Both PBMC LTRs from Patient C contained a polymorphism at position –60 G→A and –43 G→A, HIV_{LAI}.

Phylogenetic and Distance Analysis of the Env V3 region

Parsimony analysis of the env V3 region revealed strong phylogenetic segregation according to V3 charge in all patients (Figure 2-3). Patient A thymus and PBMC V3 sequences with a +6 V3 charge were found clustered together and were phylogenetically distinct from other V3 sequences that had a charge of +4 and +3 (Figure 2-3, Patient A). Patient B lung and PBMC V3's with a +5 charge were also found to group together yet were independently segregated from early and late PBMC sequences with a charge of +3 (Figure 2-3, Patient B). Thymus V3's with a charge of +5 from Patient C were phylogenetically distinct from brain, PBMC, and other thymus low-charge sequences (Figure 2-3, Patient C). Patient D had a subset of V3 sequences with a +5 charge that segregated from other +3 V3 sequences (Figure 2-3, Patient D). Brain V3's were always found in independent lineages (Figure 2-3, Patients C and D). Patient C brain V3 sequences were phylogenetically distinct from V3 sequences from other tissues (Figure 2-3, Patient C) and brain derived V3 sequences from Patient D were found in two distinct lineages yet segregated from other tissue compartments (Figure 2-3, Patient D). Lung and PBMC V3 sequences were typically intermingled with each other (Figure 2-3, Patients A, C, and D). Certain subsets of PBMC sequences were clustered independently from PBMC V3's grouped with the lung (Figure 2-3, Patients A, C, and D). For example, several lineages of PBMC sequences were found in the phylogenetic analysis of Patients A, C, and D, yet only certain lineages of PBMC sequences were found clustered with the lung. This certainly suggests trafficking between the lung and PBMCs, yet independent lineages can arise in these compartments.

The intra-tissue DNA genetic distance of the V3 region was no greater than 6.3 (+/- 0.8%) for any compartment within all patients (Figure 2-3). The mean genetic diversity within each compartment was approximately 2.4 (+/- 0.4%). The greatest genetic divergence between compartments within each patient was typically found between phylogenetically distinct V3 sequences. For example, thymus sequences from Patient A had a genetic distance of 9.5 (+/- 0.4%) and 8.7 (+/- 1.7%) from the early and late PBMCs, respectively which were phylogenetically distinct from the thymus.

Phylogenetic and Distance Analysis of the LTR

In all patients, populations of lung LTR sequences were found to be phylogenetically distinct from other tissues (Figure 2-4, Patients A, B, C, and D). A certain subset of lung LTRs from Patient A were found to be phylogenetically distinct, and segregate from other tissues (Figure 2-4, Patient A). Lung LTRs from Patient B were found clustered together and represented an entire independent lineage (Figure 2-4, Patient B). LTRs from the lung of Patient C were found in two groups; one lineage grouped with a subset of thymus sequences and another lineage independently segregated from other tissue compartments (Figure 2-4, Patient C). Two lineages of lung LTRs were found with Patient D; one lineage independently segregated from all tissues whereas the second lineage independently segregated from all other tissues (Figure 2-4, Patient D). Brain LTRs were always found in an independent lineage for all patients, and were never found clustered with the lung (Figure 2-4, Patients B, C, and D). Thymus LTR sequences were typically found clustered with other lineages but never found as an independent lineage (Figure 2-4, Patients A and C).

Intra-tissue genetic diversity was generally less than 3% among all tissues, whereas genetic distance between tissues was generally between 2-5%. The greatest genetic divergence between tissues was typically found between brain and all other tissues with a genetic distance of about 5% which was concordant with phylogenetic segregation.

Standard Curve of Bulk Luciferase

The following experiments address the impact of tissue specific LTRs on promoter activity by transient transfection in a T-cell (Jurkat) and monocytic (U937) cell line. Before conducting these experiments it was necessary to evaluate several controls evaluating transient transfections employing the p-GL3 (Promega) luciferase plasmid. These controls included evaluating the linearity and time-course of luciferase expression. The control experiments will ensure that all measurements are taken in the linear range of the luciferase assay. The time-course experiments will evaluate the time post-infection that has the optimum luciferase expression.

To determine the linear range of the luciferase assay, it was necessary to generate a standard curve of relative light unit expression with different concentrations of bulk luciferase. Ten-fold serial dilutions of bulk luciferase (Sigma) were performed in 1X Phoshate Buffered Saline (PBS) with 1 mg/ ml Bovine Serum Albumin (BSA). Twenty μl of the diluted luciferase was measured for light unit expression on a luminometer (Analytical Luminescence Laboratory) according to manufacturer's instructions. Relative light units were measured during a 10 second integration time in a volume of 100 μl of 1X luciferase assay reagent (Promega). The linear range of the assay was between 0.002 pg to 2000 pg of bulk luciferase which had a range of 700 to 8.1×10^6 light units. Figure 2-5 shows the linear range of the assay in Log(RLU) vs. Luciferase. Luciferase expression was linear over seven-orders of magnitude. In addition, this standard curve was repeated in several identical subsequent experiments (data not shown). Therfore, the luciferase assay does appear to be reproducible. All subsequent luciferase readings either from transient transfections or recombinant infections were within the linear range of the assay.

Twenty-four Hour Timecourse of Luciferase Expression

To determine when optimum luciferase expression occurred after tranfection, luciferase readings were taken at 8, 14, and 24 hour timepoints after transient transfection of Jurkat cells with 1 μg of LAI-LTR Luc construct. The highest luciferase expression among the three timepoints was 24 hours post-transfection (Figure 2-6). Minimum luciferase expression was observed 8 hours post-transfection, and luciferase expression for the 14 hour timepoint was 4 fold less than the 24 hour timepoint.

Three Day Time-course of Luciferase Expression

To determine if 24 hours post-transfection is the optimum time for luciferase expression, it was necessary to carry the timecourse experiment beyond 24 hours. Luciferase expression was measured on 24, 48, and 72 hours post-transfection. Transfections of Jurkat cells with LAI-LTR luc construct were performed with and without the plasmid, pRSV-TAT that expresses the TAT protein which upregulates LTR expression. Transfection of Jurkat cells with LAI-LTR luc were performed in duplicate. In both the presence and absence of pRSV-TAT, 24 hours post-transfection has the highest luciferase expression (Figure 2-7). Luciferase expression in the presence of TAT was reduced by 31% at 48 hours, and 62% at 72 hours. Luciferase expression in the absence of TAT remained constant at both 24 and 48 hours post-transfection, but decreased by 25% at 72 hours post-transfection. Therefore 24 hours post-transfection was optimal for luciferase expression for transient transfections and used in subsequent experiments.

Transfection of Jurkat Cells with LTR-Luc Constructs

Jurkat cells were transfected with 1 μg of LTR-Luc patient constructs and harvested for luciferase expression 24 hours post-transfection. Promoter activity is expressed relative to that of the LAI-Luc construct. A wide range of luciferase activity was found among all patient constructs ranging from 0.4 to 2.9 in Jurkat cells (Figure 2-8). Promoter differences among tissue LTR-Luc constructs were compared within a patient, rather than between patients to fully evaluate tissue-LTR promoter differences within an individual. Most promoter differences among the tissue LTR-Luc constructs were found between brain-derived LTRs and other tissue derived LTRs. The PBMC and Lung derived LTRs from most patients had a similar promoter activity in Jurkat cells.

The brain LTR from Patient D had a promoter activity of 2.2 and had the highest promoter activity of all patient D constructs tested including two LTRs from the early and late PBMC's, and the lung (Figure 2-8, Patient D). The mean promoter activity from all non-brain tissue constructs from patient D was 1.0. The brain LTR from Patient C had a promoter activity of 2.31, and had the highest promoter activity among all tissue constructs. In contrast, the major Lung LTR had a promoter activity of 1.4, and the major PBMC LTR had a promoter activitity of 1.9 (Figure 2-8, Patient C). The major brain derived LTR from Patient B had a promoter activity of 1.8 and had the lowest overall promoter activity within that patient (Figure 2-8, Patient B). The PBMC and Lung derived LTRs from most patients had a similar promoter activity in Jurkat cells.

Transfection of Jurkat Cells with and without TAT

To determine if the differences among tissue LTR-Luc constructs would be diminished in the presence of TAT, Jurkat cells were transfected with and without the Tat encoding plasmid, pRSV-TAT (Figure 2-9). Luciferase expression was typically 10-100 fold higher in the presence of TAT for all constructs (data not shown). Relative promoter activity was expressed as light units/HIV_{LAI} light units. For constructs transfected with TAT, the relative promoter activity was expressed as light units/HIV_{LAI} light units with TAT. The relative promoter differences among the tissue LTR-Luc constructs mostly remained constant both in the presence and absence of TAT, however constructs in the presence of TAT were 10-100 fold higher in luciferase expression. For example the brain derived LTR from patients C and D had the highest overall promoter activity both in the presence or absence of TAT (Figure 2-9, Patient C and D).

Transfection of U937 Cells

To evaluated tissue LTR-Luc constructs in another cell type, a monocytic cell line, U937, was evaluated by transient transfection (Figure 2-10). The promoter differences among the different tissue LTR-luc constructs ranged from 0.2 to 15. Tissue specific promoter differences were typically not found among most patients, however the lung LTRs from Patient A had a much higher promoter activity than the EPBMC LTR. The major and minor lung LTR had a promoter activity of 8.7 and 15, respectively, whereas the EPBMC LTR had a promoter activity of 1.

Discussion

My study has evaluated tissue specific segregation of HIV-1 in four patients with tissue pathology in the context of the env and LTR regions. Both of these sub-genomic regions are under selective pressure, but in different parts of the viral life cycle. My results have demonstrated that both the env and LTR regions impact tissue specific segregation. In addition, tissue specific segregation can be discordant among mutliple regions of the viral genome. This suggests that there is varying selective pressures within different tissues on the env and LTR regions. Also, tissue specific LTRs can impact promoter activity in both a T-cell and monocytic cell line.

The majority of research investigating compartmentalization of HIV-1 in different tissues has been examined according to sequence comparisons of single sub-genomic regions, in particular env. HIV-1 may segregate to different tissues according to multiple determinants. Therefore, true tissue segregation needs to be performed in the context of multiple genomes, particularly those that are under selective pressure. For example, tissues where the predominately infected cell is the macrophage may demonstrate monophyletic species present in those tissues according to V3 within env, yet other regions of the genome may not reflect a concordant relationship. Other studies have demonstrated this discordant relationship between different genomic regions among tissues (129). Morris *et al.* demonstrated discordant relationships between p17gag and env V3 sequences between brain and lymphoid tissue. In addition, Cleland *et al.* showed that segregation of HIV quasispecies based upon evolution of env sequences did not result in parallel lineages of quasispecies based on pol sequences (35). Therefore, an important conclusion from multi-genomic studies is that different parts of the HIV-1 genome can have different evolutionary histories which would limit the conclusions drawn from monogenomic studies. This incongruent relationship between multiple sub-genomes of HIV-1 may be the result of different degrees and types of selective pressures within various host tissues. This variable selection on different viral subgenomes of HIV would explain why divergent quasispecies would be propagated in the local environment of either lung, brain, or thymus. These selection pressures would include local immune system, HIV target cells, and availability and type of post-entry transcriptional factors. All of these variables would induce a constraint on the viral sub-genomes of env and LTR. Our study evaluated multiple tissues, and temporal PBMCs, according to the env and LTR regions. Phylogenetic analysis revealed both concordant and discordant relationships between genomes and among tissues. The strongest concordant relationship between env and LTR tissue specific segregation was found within the brain. Both brain env and LTR sequences were typically clustered together and segregated from all other tissue compartments with significant bootstrap values. Based on lung sequences, env PBMC and lung clones were found clustered together. In contrast certain lung LTR sequences were found segregated from all other tissue compartments. In addition, these lung LTR sequences were found to be functionally different from most other LTR sequences, particularly those from the brain. The thymus represented a reverse scenario, where tissue-specific segregation is due to env rather than LTR.

The predominant HIV-1 infected target cell is the microglial cell in the brain, and the alveolar macrophage in the lung (101,193,196). Both of these cells are in the myeloid lineage and low charge, M-R5 genotype env V3 genotypes preferentially infect macrophage cell lines (33,34). All brain env sequences from our study had a low charge M-R5 V3 genotype that was phylogenetically distinct from all other tissues. Both the lung and brain appear to be infected early during the course of infection, however these myeloid cells are latently infected *in-vivo*, and at resting conditions are not a site for viral replication. Therefore, active viral replication in a certain cell type is dependant upon cellular factors that interact with HIV involved in transcriptional regulation. Our phylogenetic analysis demonstrated a strong concordance between env and LTR segregation among the brain, lung and PBMCs however this concordant segregation was not found according to thymus sequences. Tissue specific segregation within the thymus was determined by env rather than LTR. Therefore, it appears that LTR segregation is not a mere reflection of tissue tropism determined by env. In addition, lung LTR sequences were always phylogenetically distinct from brain derived LTRs indicating independent lineages within both of these tissues.

Thymus Segregation Determined by Env

Tissue specific segregation of HIV thymus sequences was determined by env. Several thymus sequences had a high charge T-X4 genotype, whereas PBMC sequences were mainly comprised of low charge M-R5 genotype. Functional analysis of these thymus specific V3 sequences demonstrated sole usage of CXCR4, rather than CCR5 (19). As demonstrated with the LTR region, phylogenetic differences are consistent with functional differences. The milieu of the thymus may provide an environment for a strong pre-entry selective pressure. More than 95% of the cells in the thymus express CD4, and therefore expression of chemokine co-receptors would be a strong selective pre-entry determinant of tropism (99). Surface expression of CXCR4 is widely expressed on fetal thymocytes (143). Another study showed the majority of freshly isolated postnatal thymocytes from uninfected children express moderate to high levels of CXCR4 in comparison to CCR5 expression, which was present at low levels on 0.1 to 0.2% of the thymocyte population. Also, this preferential distribution of CXCR4 expression was a major determinant for NL4-3 and JR-CSF tropisms and determines replication kinetics of these two isolates (143). The onset of CXCR4 tropism has been implicated in rapid progression (163). High charge V3 sequences were found within the thymus in patients A and C, with either no or low numbers of high charge V3 sequences within the PBMCs. No high charge +6 V3 sequences were found within the lung or brain of any patients, although Patient B did have some +5 V3 sequences found within the lung. Our data suggests that the thymus is the sole source of CXCR4 viruses, and viral trafficking between the thymus and blood can occur although somewhat limited. Despite the lack of dissemination of the CXCR4 tropic viruses throughout the body, this does not detract from the biological implication of infection of the thymus. Proper formation of a T-cell repertoire during ontogeny requires the existence of a functional thymus. Thymic HIV-1 infection, particularly in infants has been consistent with progression to AIDS (104). Also, thymic architecture in AIDS patients is severely disrupted in adults and children (58,138,139). Therefore, thymic infection appears to eliminate the ability for T-cell reconstitution, which is necessary for successful control of the virus.

Lung Segregation Determined by LTR

Lung specific LTR segregation was found among all four patients even in the abscence of env segregation. The milieu of the lung is very different from the brain. Despite both the lung and brain containing macrophages as the predominantly infected cell, the lung is not an immunologically privileged site. The lung is the most common site of disease for AIDS-associated processes, and is affected in 90% of AIDS patients (100,133). Several opportunistic infections such as *Mycobacterium tuberculosis*, and *Pneumocystis carinni* have been demonstrated to enhance HIV-1 replication. The CCAAT/enhancer binding proteins (C/EBP) are required for HIV-1 replication in primary macrophages, and monocytic cell lines but not CD4+ T cells (76-78). Honda *et al.* demonstrated that coinfection of THP-1 macrophages with HIV-1 and M. tuberculosis induced a novel C/EBP binding protein that resulted in increased HIV-1 replication (83). These results demonstrated that the milieu of the lung with an opportunistic infection can alter C/EBP expression and alter viral replication which may result in cellular tropism being impacted by LTR. This strong post-entry selective pressure may drive LTR tissue specific segregation within the lung.

Our LTR phylogenetic analysis found tissue specific polymorphisms present in both lung and brain LTRs. Our functional analysis correlated with published functional studies demonstrating differences brain-derived and lymphocytic LTRs (21,42,109). However, other investigators have indicated that the LTR is not a determinant of tropism (146,185). Our LTR analysis revealed several tissue specific polymorphisms were found within transcriptional binding sites, although there were several nucleotide changes within undefined binding sites. Phylogenetic segregation of the LTR region was found to be concordant with functional segregation. For example, brain LTR sequences from Patient D were found to cluster together and segregate from all other tissue compartments which was concordant with functional differences in the luciferase reporter assay. Although the promoter differences between certain tissue specific LTRs, particularly between brain and lung LTRs, were statistically different, these functional differences are not more than 2 fold greater from each other . However, these tissue specific LTRs were tested in the context of a mature T-cell line, and may not truly represent an accurate cell model. These tissue specific brain and lung LTRs most likely came from HIV-1 infected infected macrophages. Promoter analysis in macrophages would probably be a more accurate model, but most macrophage cell lines (ie THP-1, U937) are not fully matured macrophages and would also have their limitations. HL-60 cells can be fully differentiated into macrophages. Functional analysis of these tissue specific LTRs were attempted in matured HL-60 cells but failed due to unsuccessful transfections (Data not shown). Additional experiments using congenic recombinant viruses with tissue specific LTRs to assess expression in primary cells are currently in progress. Kim *et al.* showed that although transfection analysis offer an adequate approximation of the promoter effects of mid-U3 deletions, the analysis of viral replication using a recombinant system offered a more accurate picture (96). Several mutants had effects on viral replication that were much more severe than predicted in transient transfections. Therefore, our promoter differences may have been more dramatic if tested in a recombinant system using fully differentiated macrophages. Results presented in Chapter 4 evaluate promoter differences between the tissue LTRs of patient C in PBMC and macrophages using congenic recombinant viruses.

Our data shows that tissue specific segregation of HIV-1 among the lung, brain, thymus, and blood is a multifactorial process that involves both pre- and post-entry factors along with the local milieu of the host tissue. Both phylogenetic and functional analysis of the LTR region revealed tissue specific promoter differences. Anti-retroviral therapy does not result in complete eradication of the virus that may be due to these reservoirs which appear to be infected early during the course of infection. Pathological destruction within these sites is due to viral reactivation rather than de-novo infection. Therefore, an understanding of these pre and post-entry cellular factors may allow the development of drugs that may prevent and control HIV-1 infection within these protected tissues.

TABLE 2-1
Summary of Clinical Data and Tissues Analyzed from all Patients

Patient	**Progression**	**Initial Timepoint (yr.)**		**Patient Survival (yr.)**	**Time of Study (yr.)**	**Therapy**	**HIV/AIDS Pathology**	**Tissues Analyzed**
		Patient Age	**CDC Stage**[*]					
A	Rapid	1	B2	2	1	None	Cardiomegaly L.I.P[‡] Pneumonia	Early PBMCs Late PMBCs Lung Thymus
B	Rapid	1	A2	2.6	1.6	AZT	Cardiomyopathy Encephalopathy M.A.I.[†] Pneumonia	Early PBMCs Late PBMCs Lung Brain
C	Slow	1	B2	7	6	ZDV DDI	Encephalopathy L.I.P[‡] Pneumonia	Early PBMCs Late PBMCs Lung Brain Thymus
D	Long-term	12	B3	16	4	ZDV DDI DDC	Cardiomyopathy Encephalopathy M.A.I[†] Pneumonia	Early PBMCs Late PBMCs Lung Brain

[‡] Lymphoid interstitial pneumonitis

[*] All patients were C3 at time of death

[†] *Mycobacterium avium intracellulare*

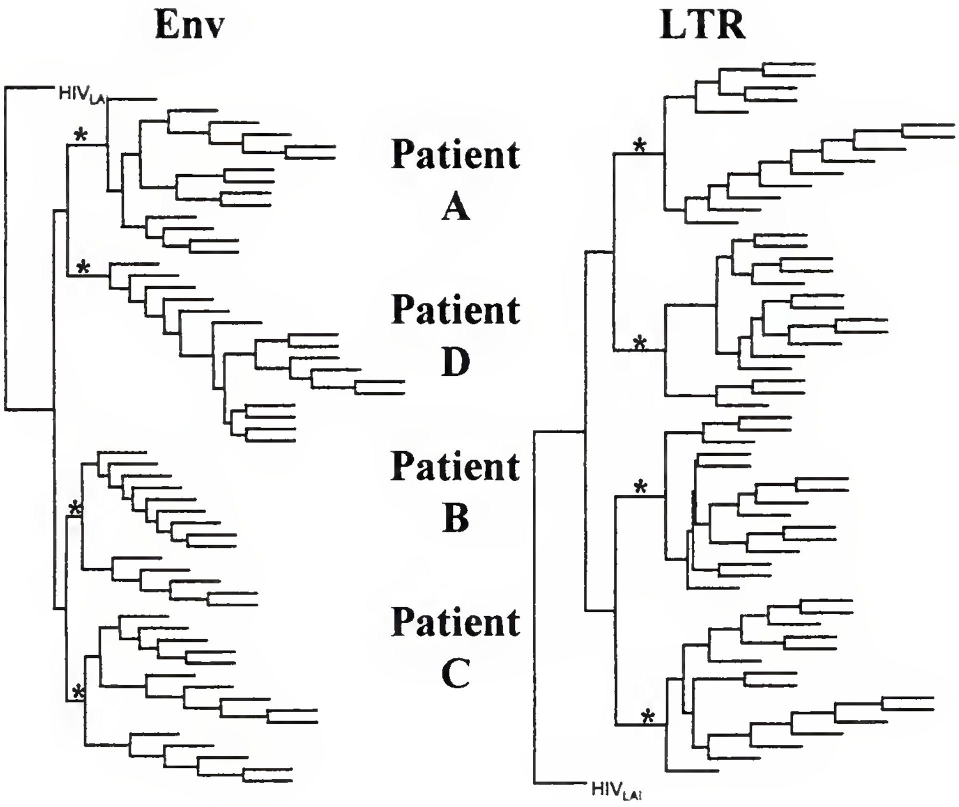

Figure 2-1. Phylogenetic analysis of the DNA sequence from the V3 region of envelope and the LTR from representative tissue sequences from each patient. The left and right trees are envelope and LTR, respectively. * denotes a bootstrap value of ≥ 64 based on 100 replicate trees.

TABLE 2-2
V3 Alignment with Frequency, Charge, and Predicted Phenotype

Patient A

TISSUE	N[A]	JR-FL CTRPNNNTRKSIHIGPGRAFYTTGEIIGDIRQAHC	#[B]	CHARGE[C]	Predicted Phenotype[D]
Early PBMC	13	----ss----r------------rqv---------	2	+6	2
		----smk-kqr------------rqvt--------	1	+6	2
		----s-------------------qv---------	3	+4	1
		----s-------p-----------qv---------	2	+4	1
		----s--------------s----qv---------	2	+4	1
		----s----r-------s------qv---------	2	+3	1
		----s-------p----s------qv---------	1	+3	1
Late PBMC	8	----skk--qr------------rqve--------	2	+6	2
		----s----r-------s------qv---------	6	+4	1
Lung	10	----s-------p-----------qv---------	6	+4	1
		----s-------p----k------qv---------	3	+4	1
		----ss------p----k------qv---------	1	+4	1
Thymus	10	----skk--qr------------rqve--m-----	10	+6	3

Patient B

TISSUE	N	CTRPNNNTRKSIHIGPGRAFYTTGEIIGDIRQAHC	#	CHARGE	Predicted Phenotype
Early PBMC	5	-i-------r-------------------------	4	+3	1
		-i-------r------------------n------	1	+3	1
Late PBMC	6	-i-------r--r----------....--------	3	+5	2
		-i---------------------------------	3	+3	1
Lung	6	-i-------r--r----------....--------	5	+5	2
		-is------r--r----------....--------	1	+4	1

Patient C

TISSUE	N	CTRPNNNTRKSIHIGPGRAFYTTGEIIGDIRQAHC	#	CHARGE	Predicted Phenotype
Early PBMC	14	-l-------r--n----------r-----------	1	+4	1
		-l-------r--n----------------------	12	+3	1
		-l-----i-r--n----------------------	1	+3	1
Late PBMC	6	-q----------t-------f--------------	5	+3	1
		-q--------g-t-------f--------------	1	+3	1
Brain	10	-q-------r---m-----l---------------	10	+3	1
Thymus	10	-q----h---r-tms---vv-----v-----r---	1	+5	2
		-q----h---r-tms---vv-----v----kr---	1	+5	2
		-q----------t-------f--------------	7	+3	1
		-q---------vt-------f--------------	1	+3	1

Patient D

TISSUE	N	CTRPNNNTRKSIHIGPGRAFYTTGEIIGDIRQAHC	#	CHARGE	Predicted Phenotype
Early PBMC	12	----s----r-mr-----v--aa....--------	5	+5	2
		----s----r-mr----kv--aa....--------	1	+5	2
		---------------------aa------------	6	+3	1
Late PBMC	12	---------------------aa--------l---	3	+3	1
		-----------------k---aa--------l---	5	+3	1
		-i-------------------aa--------l---	1	+3	1
		---------------------aa------------	3	+3	1
Brain	6	-----------l-----k---aa--------l---	2	+4	1
		-----------------k---aa--m-----l---	4	+3	1
Lung	5	---------------------aa--------l---	5	+3	1

[A] Total number of clones produced for that timepoint.

[B] Number of clones with identical amino acid sequence.

[C] Total V3 net charge calculated by [K+R]-[D+E].

[D] Phenotype Definitions: 1 = uses R5 only, infects macrophages only; 2 = uses either R5 and X4 or X4 only, infects Macrophages and T cell lines; 3 = uses X4 only, infects T cell lines only.

A.

```
          -316    c myb                       NFAT                           C/EBP                              NFAT -208
HIVLAI LTR  TACAAGCTAGTACCAGTTGAGCCAGATAAGGTAGAAGAGGCCAATAAAGGAGAGAACACCAGCTTGTTACACCCTGTGAGCCTGCATGGAATGGATGACCCTGAGAGAG      N

Patient A
EPBMC        t             c          gc        a        g            a  c             a             g ca  g     g           8/9
LPBMC        t             c          gc        a        g            a  c             a             g ca  g     g         11/11
Lung M       t             c          gc        a        g            a  c    c    t   a             g ca  g     g           4/7
Lung m       t             c          gc        a        g            a  c             a             g ca  g     g           3/7
Thymus       t             c          gc        a        g            a  t             a             g ca  g     g          9/10

Patient B
EPBMC        t             a g                           g        g   a  aac           a                         a    a     4/10
LPBMC        t             a g                           g            a  cac  c        a                         a    ag     3/5
Lung         t             a g        c                  g            a  cac           a                         a    a      7/7
Brain M      t             a g                           g         g  a  aac           a                         a    a      8/9
Brain m      t             a g                           g            a  cac  c        a                         a    a      1/9

Patient C
EPBMC        t               g  t                 a                   a    c    g      a             g         a a    at   10/15
LPBMC M      t    t          g  t                 a      g            a    c    g                    g         a a           5/7
LPBMC m      t               g  t                 a      g            a    c    g                    g         a a           2/7
Lung M       t             a g  t                 a      g            a    c    g                    g         a a           7/9
Lung m       t               g  t                 a      g            a    c  c g      a             g         a a    a      2/9
Brain        t               g  t                 a       c           a    c    g      a             g         a a           6/7
Thymus       t    t          g  t                 a      g            a    c    g      a             g         a a    a      7/8

Patient D
EPBMC M      t               c  t     gc       ga        g            a t     c        a             g         t g   g       6/9
EPBMC m      t                  t     gc        a        g            a t     c        a             g         t g   g       3/9
LPBMC M      t                  t     gc        a        g            a t     c        a       a   a g         t g   g       4/6
LPBMC m      t                  t     gc        a        g            a t     c        a             g         t g   g       2/6
Lung         t                  t     gc        a        g            a t     c        a       a     g         t g   g       3/5
Brain        t                  t     gc        a        g            a t     c        a             g         t a   g       6/8
```

Figure 2-2. Nucleotide alignment of LTR sequences. A) Nucleotide alignment from –316 to –208, HIV_{LAI}; B) Nucleotide alignment from –207 to –105, HIV_{LAI} for Patients A, B, and C and –196 to –105 for Patient D; C) Nucleotide alignment from –104 to –1, HIV_{LAI}. N refers to frequency of LTR sequence to total number of LTR sequences obtained from that tissue. LTR sequences are aligned relative to HIV_{LAI} including transcriptional factor binding sites. A space indicates an identical sequence to the reference; a letter indicates a sequence different than the reference. Tissues followed by M or m refers to the major or minor sequence, respectively, that were evaluated by transient transfection shown in Figures 2-8 through 2-10.

B.

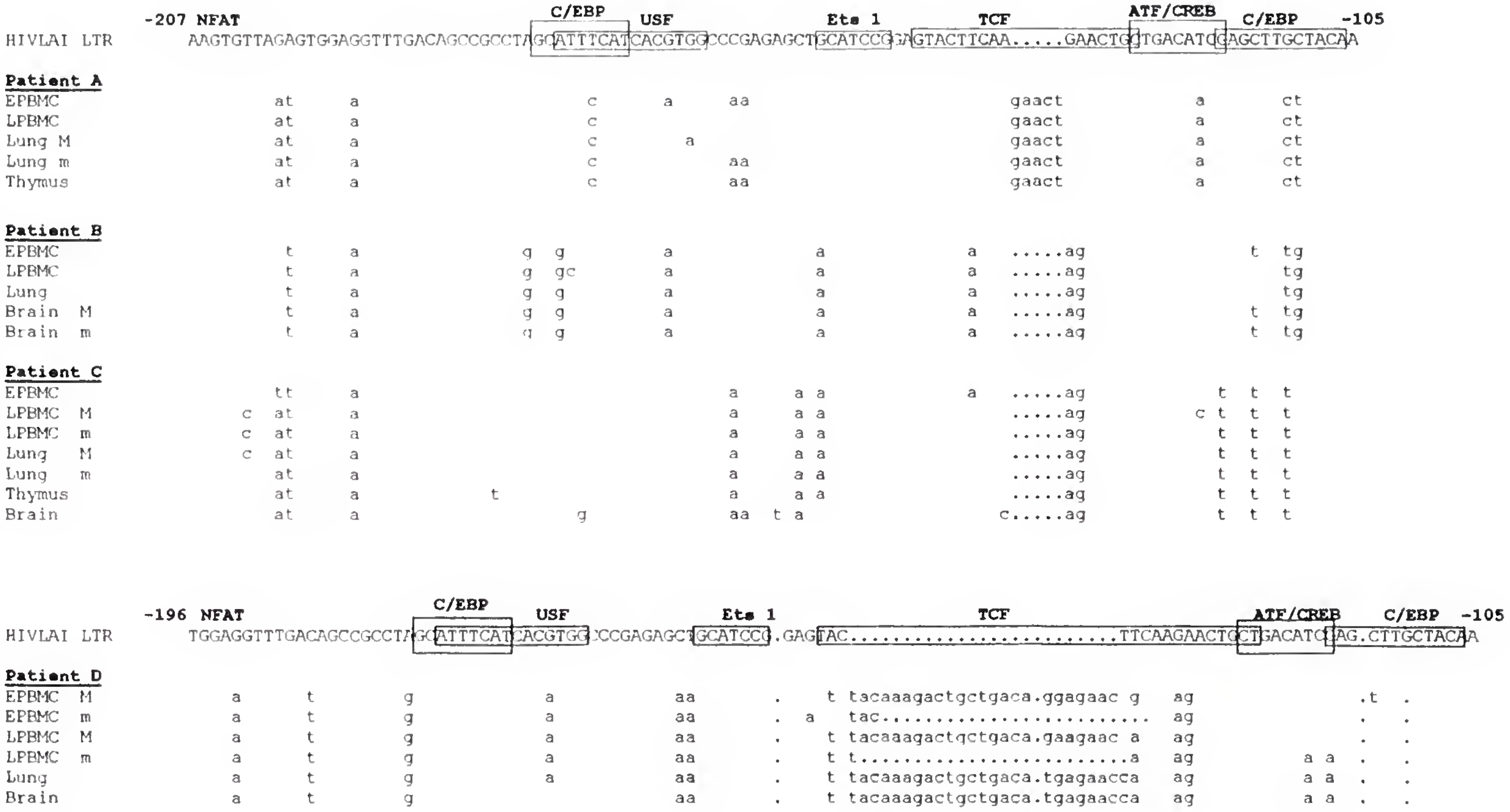

```
             -207 NFAT                             C/EBP    USF               Ets 1       TCF             ATF/CREB   C/EBP    -105
HIVLAI LTR       AAGTGTTAGAGTGGAGGTTTGACAGCCGCCTAGCATTTCATCACGTGGCCCGAGAGCTGCATCCGGAGTACTTCAA.....GAACTGCTGACATCGAGCTTGCTACAA

Patient A
EPBMC                    at     a                     c      a     aa                        gaact            a       ct
LPBMC                    at     a                     c                                      gaact            a       ct
Lung M                   at     a                     c        a                             gaact            a       ct
Lung m                   at     a                     c            aa                        gaact            a       ct
Thymus                   at     a                     c            aa                        gaact            a       ct

Patient B
EPBMC                     t     a               g  g         a             a             a   .....ag               t  tg
LPBMC                     t     a               g  gc        a             a             a   .....ag                  tg
Lung                      t     a               g  g         a             a             a   .....ag                  tg
Brain  M                  t     a               g  g         a             a             a   .....ag               t  tg
Brain  m                  t     a               g  g         a             a             a   .....ag               t  tg

Patient C
EPBMC                    tt     a                                  a     a a             a   .....ag            t  t  t
LPBMC  M              c  at     a                                  a     a a                 .....ag          c t  t  t
LPBMC  m              c  at     a                                  a     a a                 .....ag            t  t  t
Lung   M              c  at     a                                  a     a a                 .....ag            t  t  t
Lung   m                 at     a                                  a     a a                 .....ag            t  t  t
Thymus                   at     a            t                     a     a a                 .....ag            t  t  t
Brain                    at     a                    g             aa  t a                  c.....ag            t  t  t


             -196 NFAT                  C/EBP     USF               Ets 1                   TCF                       ATF/CREB    C/EBP  -105
HIVLAI LTR       TGGAGGTTTGACAGCCGCCTAGCATTTCATCACGTGGCCCGAGAGCTGCATCCG.GAGTAC........................TTCAAGAACTGCTGACATCGAG.CTTGCTACAA

Patient D
EPBMC  M              a      t        g            a            aa       .    t tacaaagactgctgaca.ggagaac g   ag                .t  .
EPBMC  m              a      t        g            a            aa       .  a   tac........................   ag                .   .
LPBMC  M              a      t        g            a            aa       .    t tacaaagactgctgaca.gaagaac a   ag                .   .
LPBMC  m              a      t        g            a            aa       .    t t.........................a   ag           a a  .   .
Lung                  a      t        g            a            aa       .    t tacaaagactgctgaca.tgagaacca   ag           a a  .   .
Brain                 a      t        g                         aa       .    t tacaaagactgctgaca.tgagaacca   ag           a a  .   .
```

Figure 2-2.--continued.

C.

```
              -104 NF-kB         NF-kB        Sp1 (3)     Sp1 (2)    Sp1 (1)                 TATA Box                    -1
HIVLAI LTR       GGGACTTTCCGCTGGGGACTTTCCA.GGGAGGCGTGGCCTGGGCGGGACTGGGGAGTGGCGAGCCCTCAGATGCTGCATATAAGCAGCTGCTTTTTGCCTGTACT

Patient A
EPBMC                                     .      t                c    t                                       c
LPBMC                                     .      t                c    t                                       c
Lung   M                                  .      t                c    t                                       c
Lung   m                                  .      t                c    t                                       c
Thymus                                    .      t                c    t                                       c

Patient B
EPBMC                                     g          a
LPBMC                                     g          a
Lung                         cc           g          a
Brain  M                                  g          a
Brain  m                                  g          a

Patient C
EPBMC                                     g          a  g
LPBMC  M                                  t          a  g      a  a            a                         c   .
LPBMC  m                                  t          a  g      a  a            a                         c   .
Lung   M                                  t          a  g         a                                      c   .
Lung   m                                  t          a  g         a                                          .
Brain                                     t          a  g         a                                          .

Patient D
EPBMC  M                                  g      t                c    .                         a
EPBMC  m                                  g      t                c    .                         a
LPBMC  M                                  g      t                c   .                          a           c
LPBMC  m                                  g      t       a   a    ca   .          t              a           c
Lung                             a        g      t                c    .                         a           c
Brain                                     g      t                c    .                         a       c   .
```

Figure 2-2.--continued.

A. Patient A

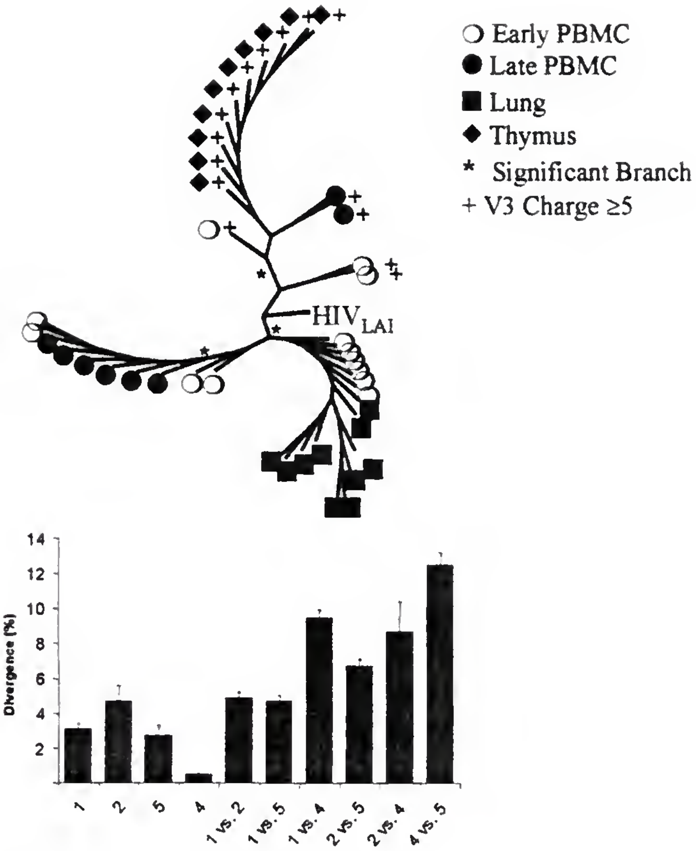

	1	2	5	4	1 vs. 2	1 vs. 5	1 vs. 4	2 vs. 5	2 vs. 4	4 vs. 5
EP	X				X	X	X			
LP		X			X			X	X	
Lu			X			X		X		X
Th				X			X		X	X

Figure 2-3. Parsimony and distance analysis of the V3 region of envelope. A) Patient A; B) Patient B; C) Patient C; D) Patient D. Phylogenetic analysis was performed on the amino acid sequence of the V3 loop of envelope. Branches with a bootstrap value greater than 60% are shown with an *. Symbols for each tissue are shown in the key. Each symbol represents one clone. + denotes a V3 net charge of 5 or greater. Distance calculations for intra and inter tissue sequences were performed using the Kimura-2-Parameter algorithm applied in the MEGA software package. The numbers on the x-axis of the distance graph represent the following tissues: 1-EPBMC (EP); 2-LPBMC (LP); 3-Brain (Br); 4-Thymus (Th); and 5-Lung (Lu). A single number represents the diversity within a tissue, whereas vs. represents divergence between tissues.

B. Patient B

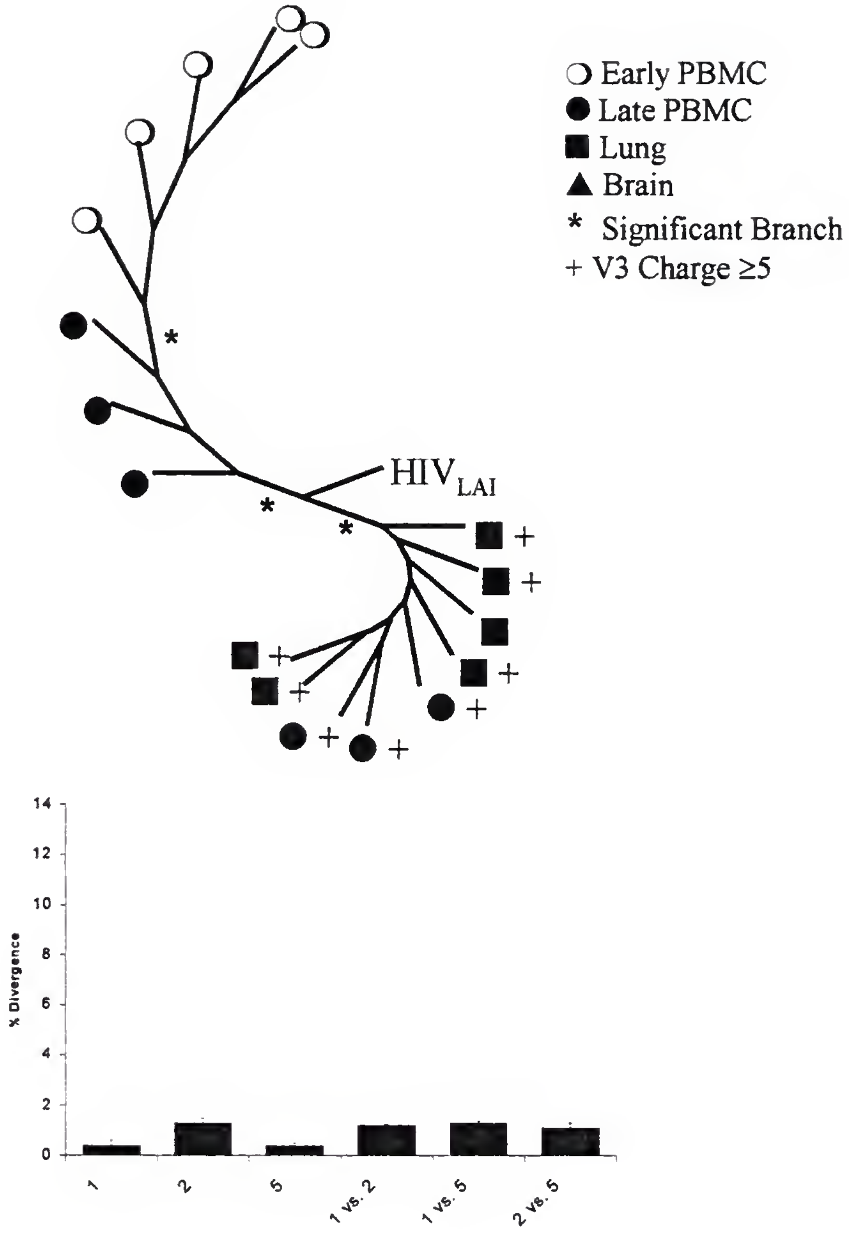

	1	2	5	1 vs. 2	1 vs. 5	2 vs. 5
EP	X			X	X	
LP		X		X		X
Lu			X		X	X

Figure 2-3.--continued.

C. Patient C

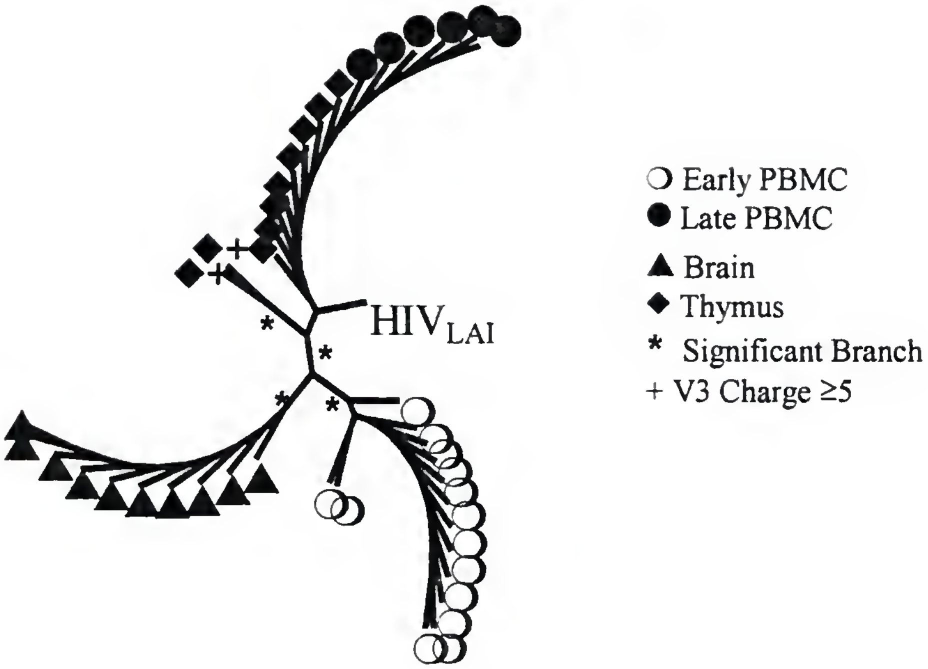

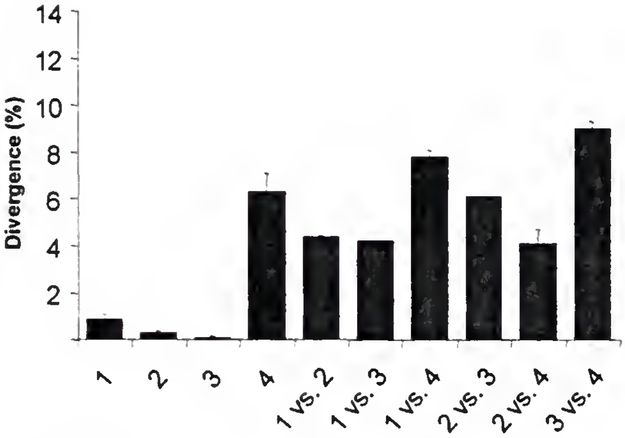

	1	2	3	4	1 vs. 2	1 vs. 3	1 vs. 4	2 vs. 3	2 vs. 4	3 vs. 4
EP	X				X	X	X			
LP		X			X			X	X	
Br			X			X		X		X
Th				X			X		X	X

Figure 2-3.--continued.

D. Patient D

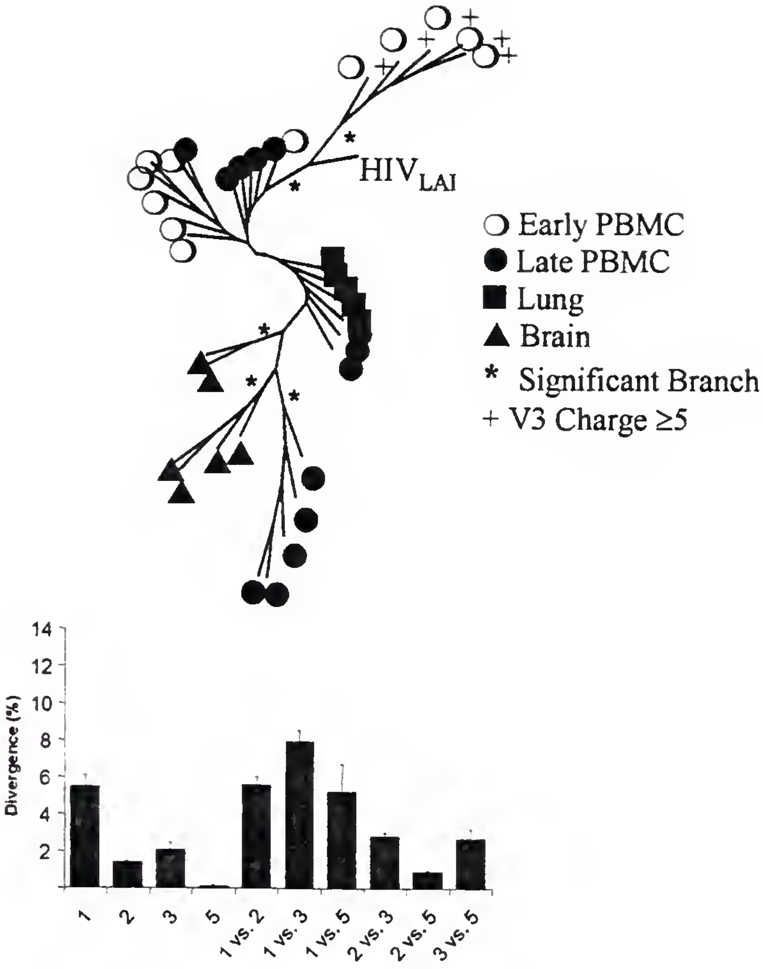

	1	2	3	5	1 vs. 2	1 vs. 3	1 vs. 5	2 vs. 3	2 vs. 5	3 vs. 5
EP	X				X	X	X			
LP		X			X			X	X	
Br			X			X				X
Lu				X			X		X	X

Figure 2-3.--continued.

A. Patient A

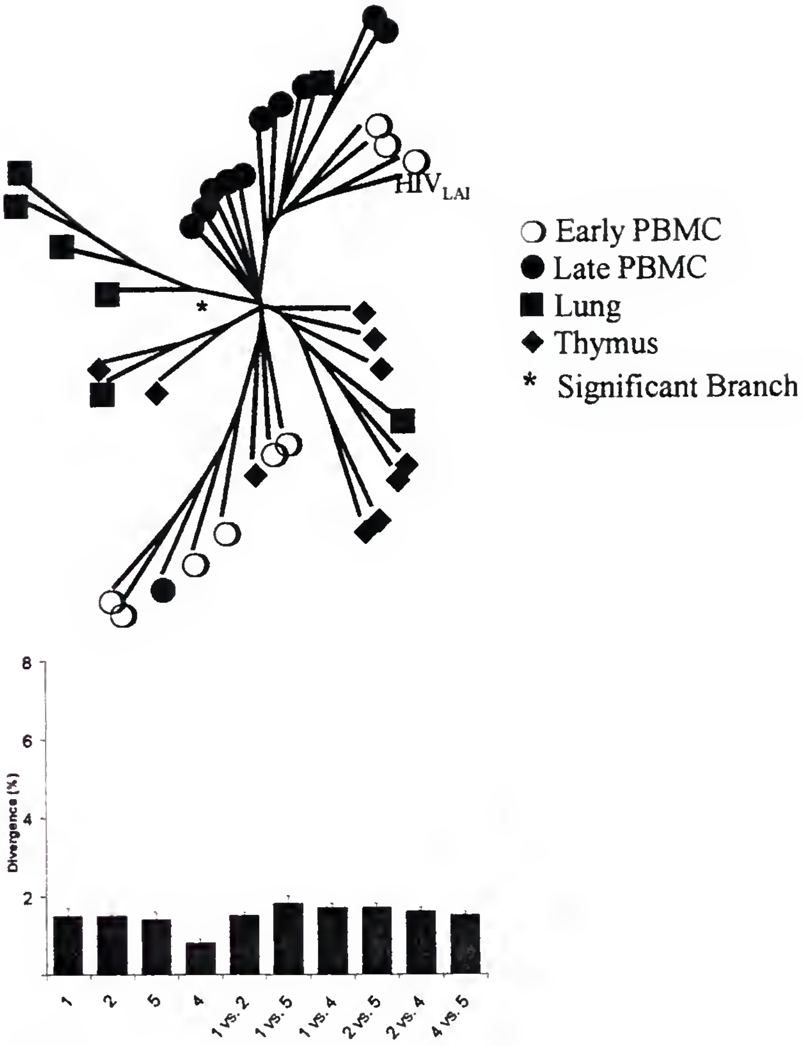

EP	X				X	X	X			
LP		X			X			X	X	
Lu			X			X		X		X
Th				X			X		X	X

Figure 2-4. Parsimony and distance analysis of the mid-U3 region of the LTR. A) Patient A; B) Patient B; C) Patient C; D) Patient D. Phylogenetic analysis was performed on the mid-U3 region located between –335 to –105, HIV$_{LAI}$. Branches with a bootstrap value greater than 60% are shown with an *. Symbols for each tissue are shown in the key. Each symbol represents one clone. Distance calculations for intra and inter tissue DNA sequences were performed using the Kimura-2-Parameter algorithm applied in the MEGA software package. The numbers on the x-axis of the distance graph represent the following tissues: 1-EPBMC (EP); 2-LPBMC (LP); 3-Brain (Br); 4-Thymus (Th); and 5-Lung (Lu). A single number represents the divergence within a tissue, whereas vs. represents divergence between tissues.

B. Patient B

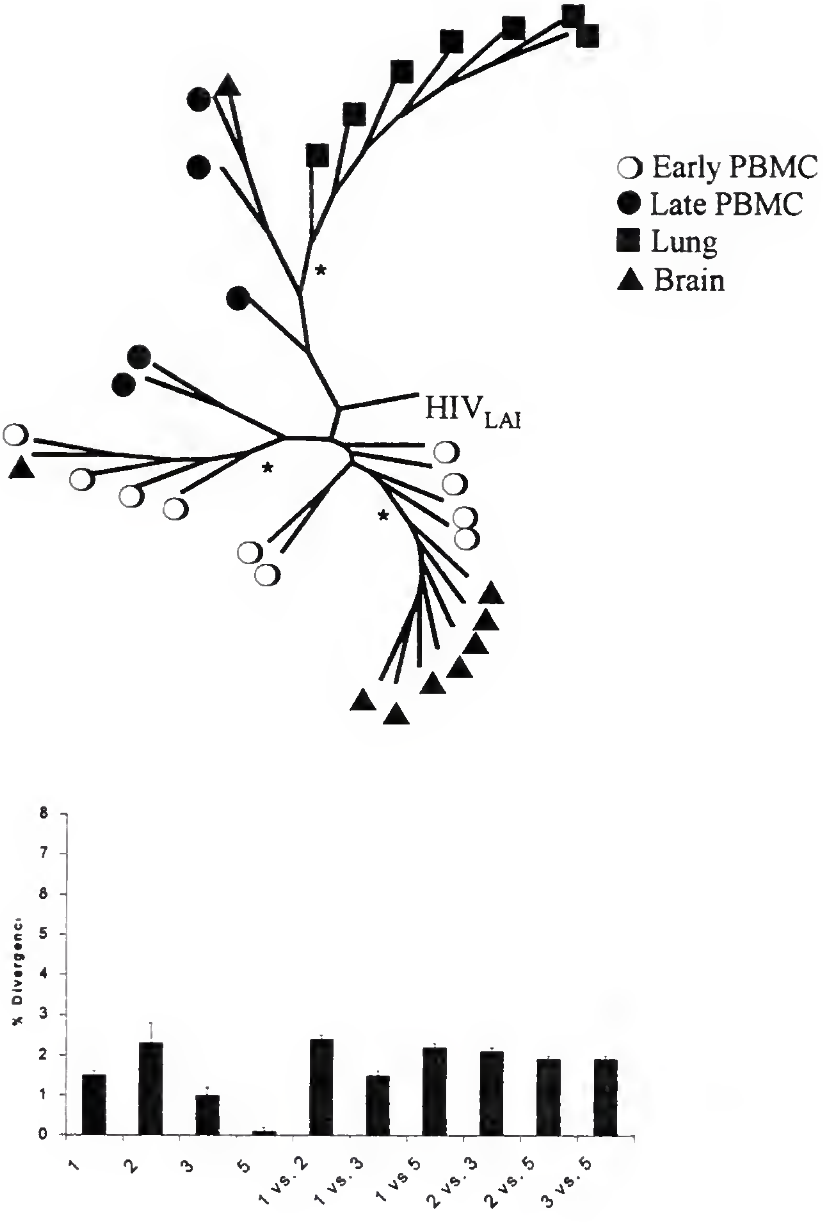

EP	X				X	X	X			
LP		X			X			X	X	
Br			X			X		X		X
Lu				X			X		X	X

Figure 2-4.--continued.

C. Patient C

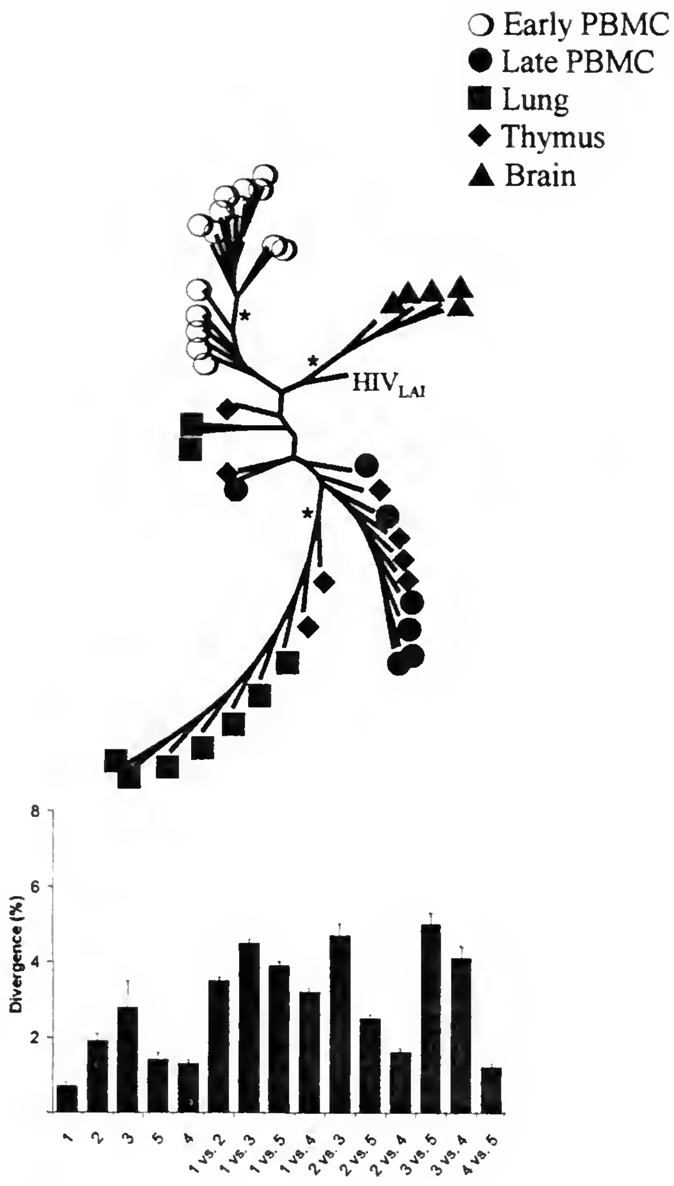

EP	X					X	X	X	X						
LP		X				X				X	X	X			
Br			X				X			X			X	X	
Th					X				X			X		X	X
Lu				X				X			X		X		X

Figure 2-4.--continued.

D. Patient D

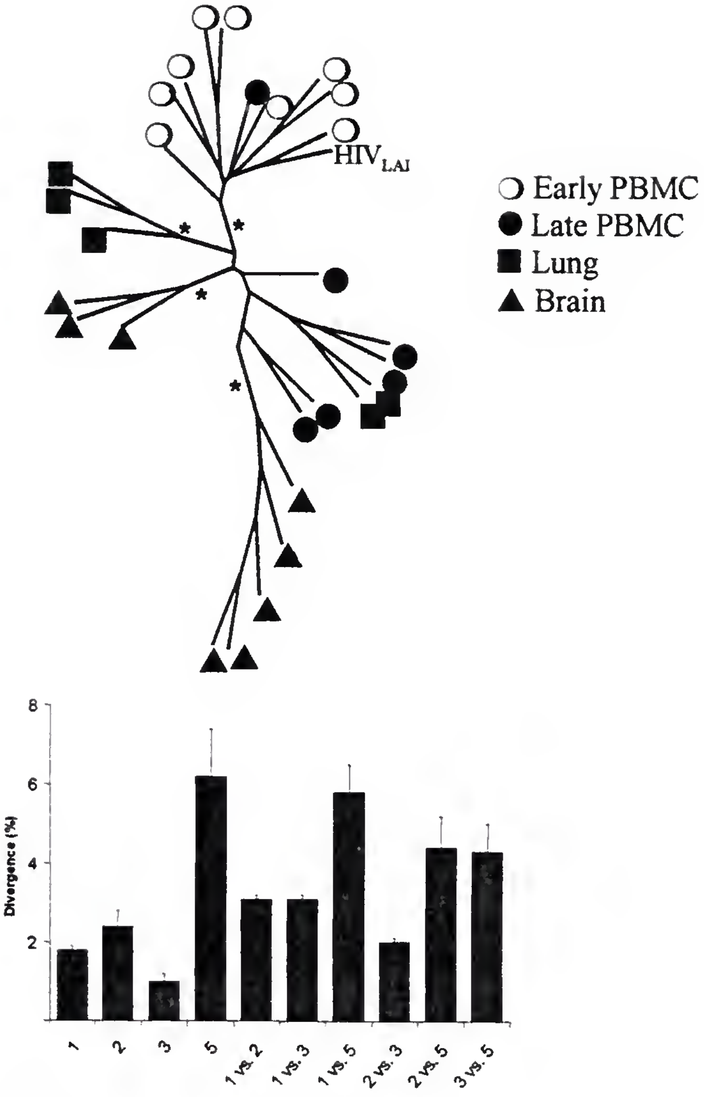

	1	2	3	5	1 vs. 2	1 vs. 3	1 vs. 5	2 vs. 3	2 vs. 5	3 vs. 5
EP	X				X	X	X			
LP		X			X			X	X	X
Br			X			X		X		X
Lu				X			X		X	X

Figure 2-4.--continued.

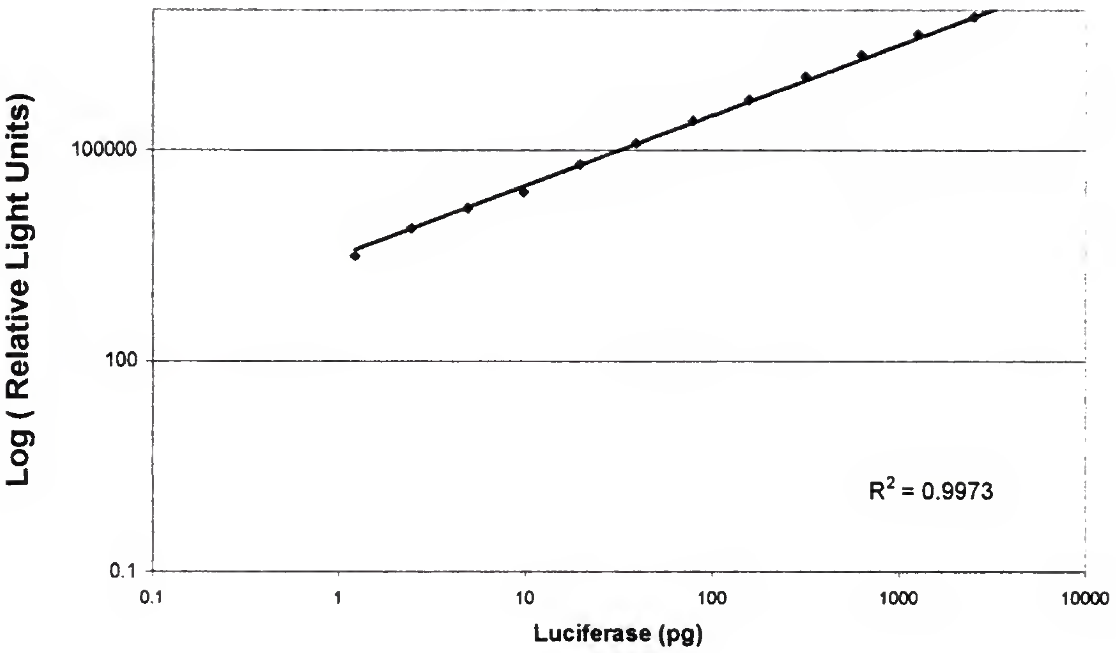

Figure 2-5. Standard curve of bulk luciferase. Luciferase was diluted ten-fold in 1X PBS with 1mg/ml BSA and measured for luciferase expression. Luciferase expression was linear over seven-orders of magnitude with an R^2 value of 0.9973.

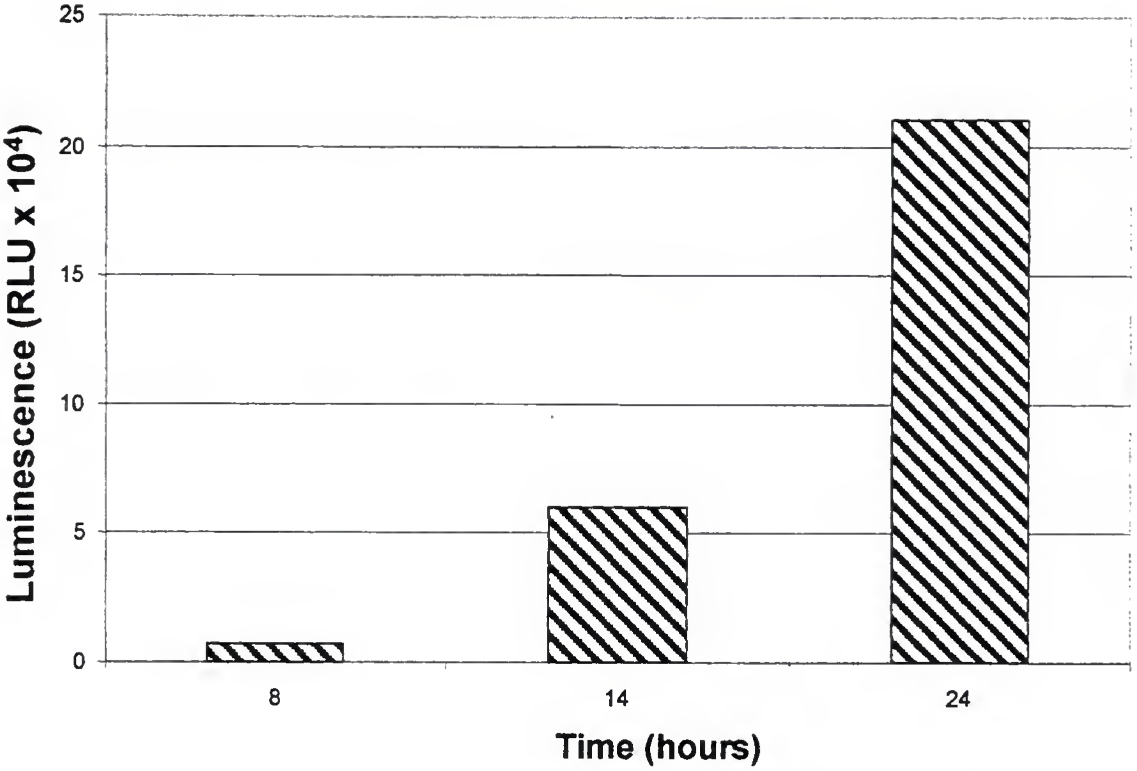

Figure 2-6. Twenty-four hour time-course of luciferase expression. Jurkat cells were transfected with one ug of the LAI-LTR luc construct. The cells were harvested at timepoints 8, 14, and 24 hours post-transfection. The highest luciferase expression was 24 hours post transfection.

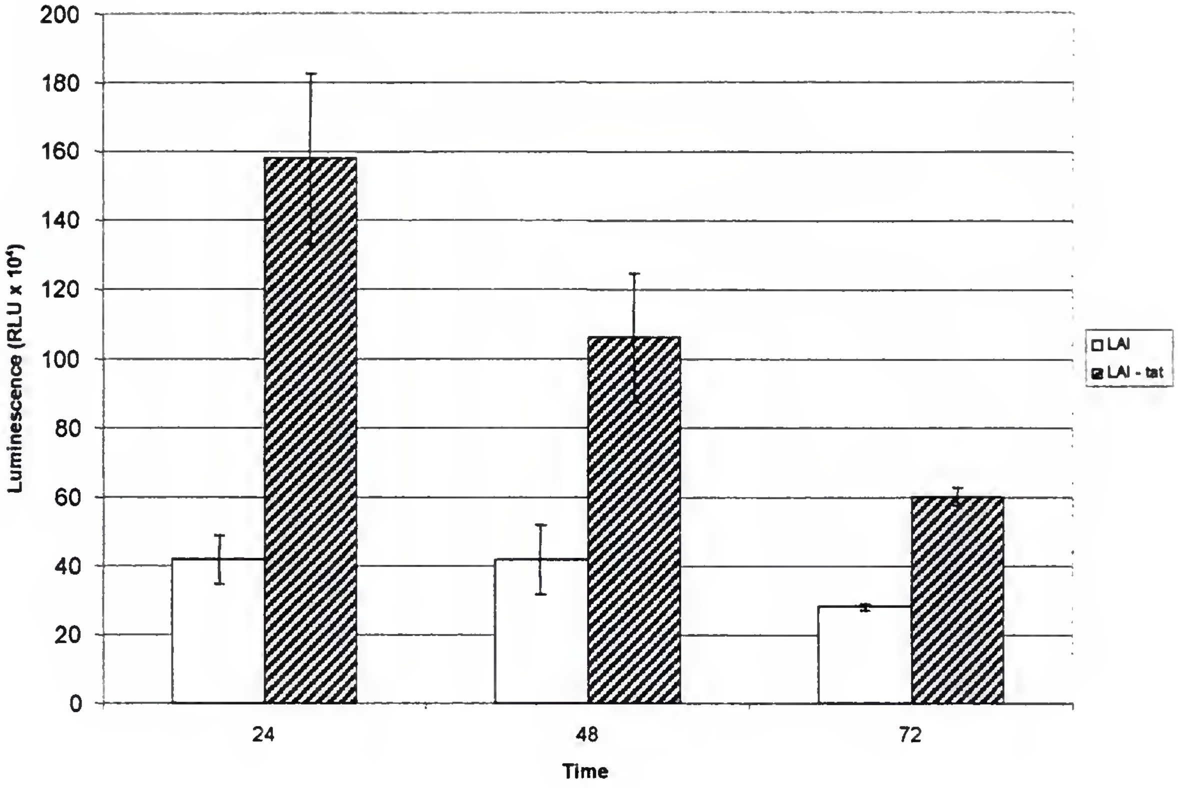

Figure 2-7. Three day time-course experiment of luciferase expression. Jurkat cells were Transfected with LAI-LTR luc construct in the absence and presence of pRSV-TAT. Luciferase expression was measured 24, 48, and 72 hours post transfection.

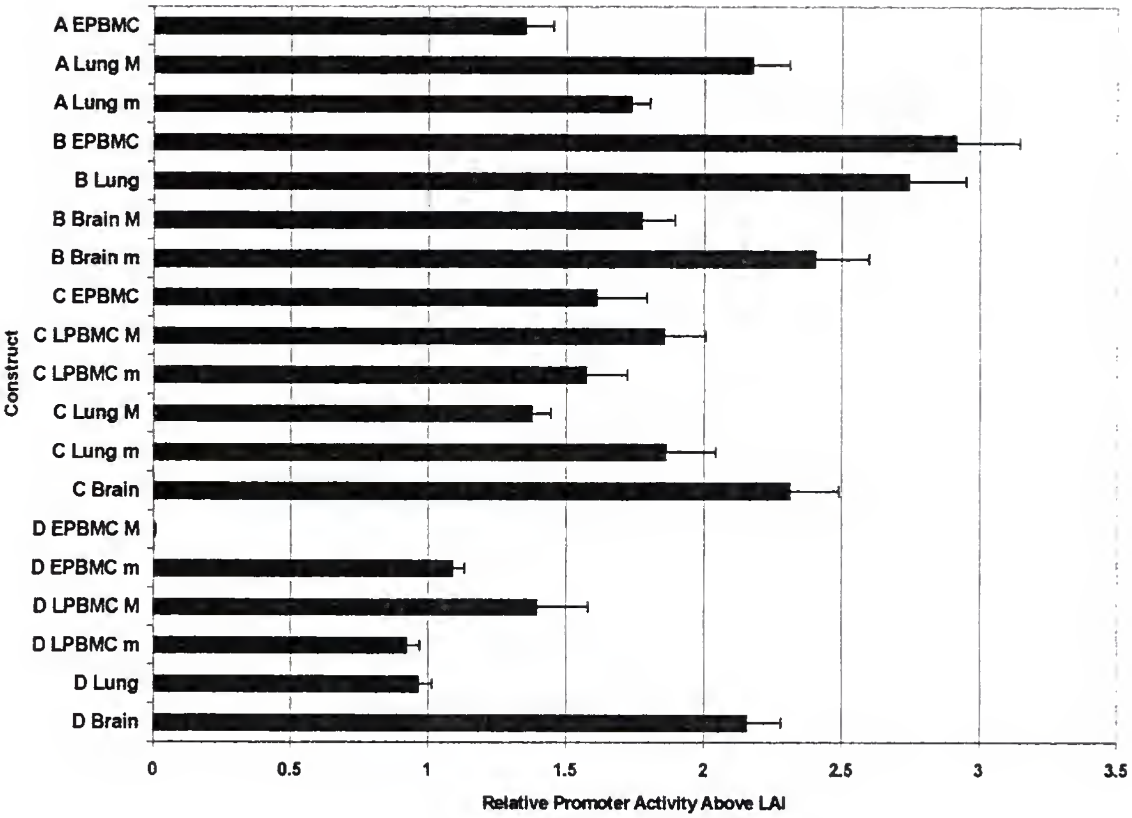

Figure 2-8. Transient transfection of Jurkat cells with patient tissue LTR-luciferase constructs. Jurkat cells were transfected with 1 ug of LTR-Luc constructs without TAT and harvested for luciferase expression 24 hours post-transfection. Each construct is indicated by patient; tissue; and whether the LTR sequence was a major or minor variant. Relative promoter activity was calculated as the promoter activity relative to that of HIV_{LAI}. Each promoter activity is the mean of two separate transfections with each construct tested in triplicate. The error bar represents the standard error of the mean.

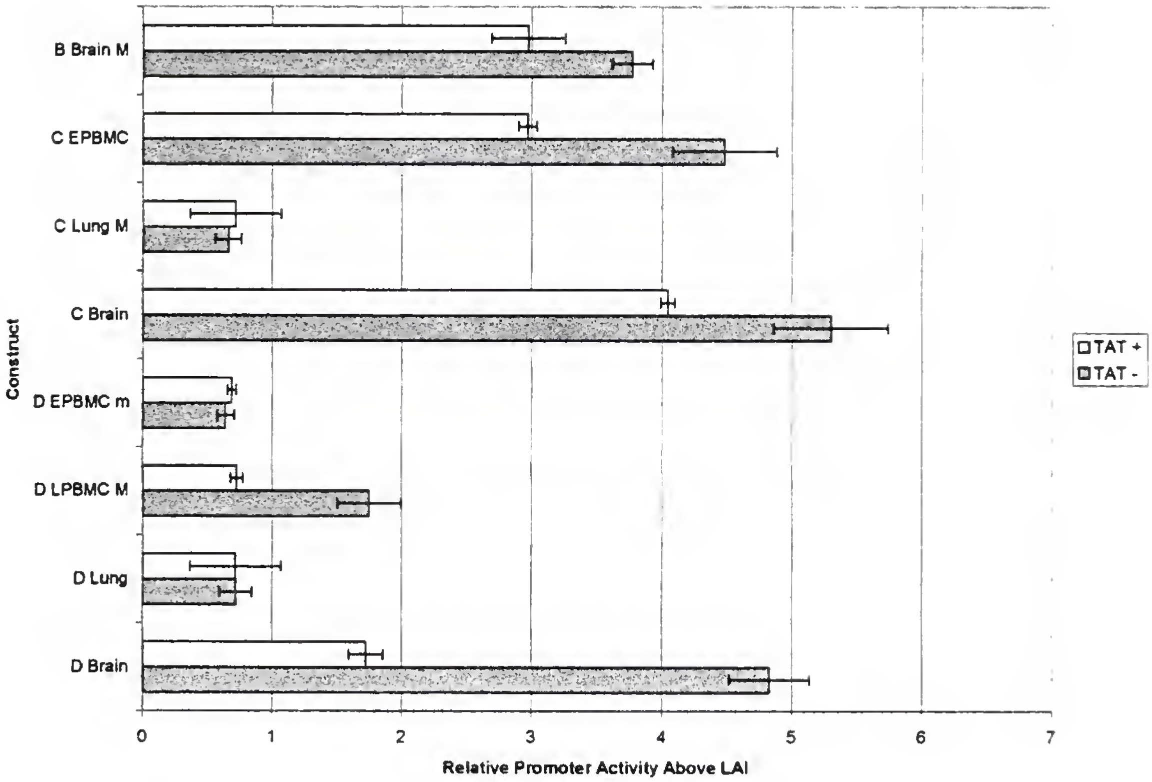

Figure 2-9. Transient transfection of Jurkat cells with and without Tat. Jurkat cells were transfected with 1 μg of LTR-Luc constructs both with and without the Tat expressing plasmid, pRSV-Tat and harvested for luciferase expression 24 hours post-transfection. Each construct is indicated by patient; tissue; and whether the LTR sequence was a major or minor variant. Relative promoter activity were calculated as the promoter activity relative to that of HIV_{LAI}. Each promoter activity is the mean of two separate transfections with each construct tested in triplicate. The error bar represents the standard error of the mean.

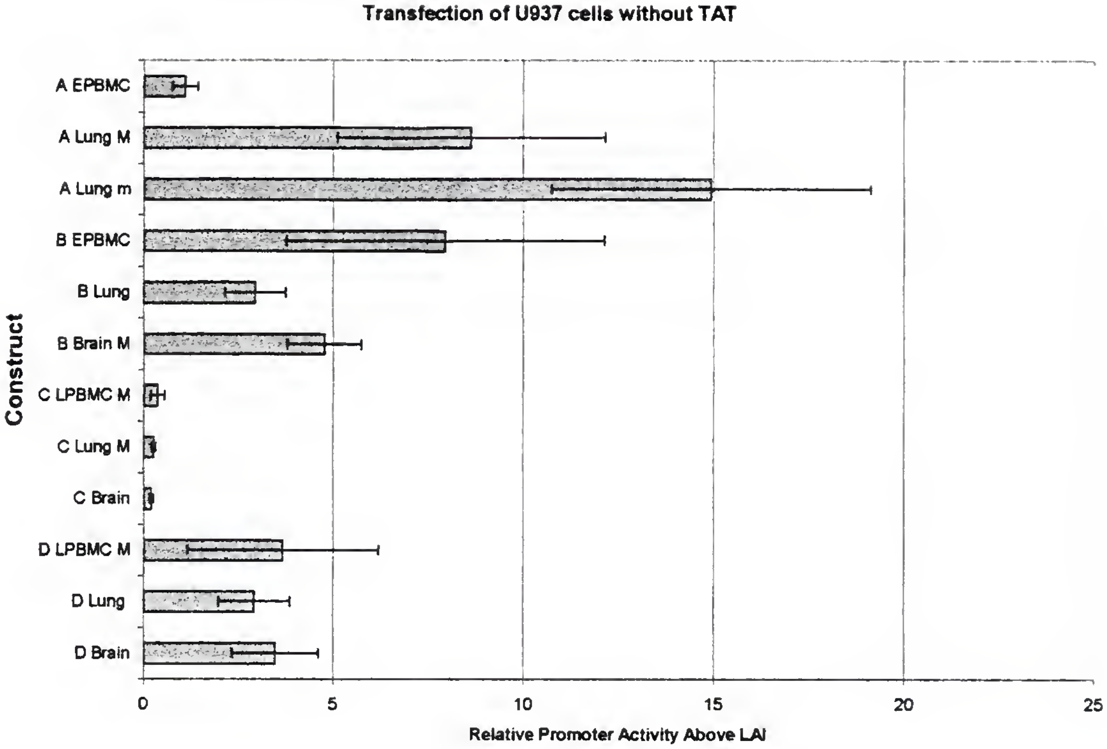

Figure 2-10. Transfection of U937 cells without Tat. U937 cells were transfected with 1 μg of LTR-Luc constructs without Tat and harvested 24 hours post-transfection. Each construct is indicated by patient; tissue; and whether the LTR sequence was a major or minor variant. Relative promoter activity was calculated as the promoter activity relative to that of HIV_{LAI}. Each promoter activity is the mean of two separate transfections with each construct tested in triplicate. The error bar represents the standard error of the mean.

CHAPTER 3

THE THYMUS SERVES AS A SOURCE AND SITE OF EVOLUTION OF T-CELL LINE TROPIC (CXCR4) AND DUAL-TROPIC (CXCR4±CCR5) ENV QUASISPECIES

Introduction

Despite the importance of the human thymus in the pathogenesis of the human immunodeficiency virus type 1 (HIV-1) in both children and adults, there are no studies that concurrently evaluate the *in-vivo* viral quasispecies present within the thymus and multiple tissues of HIV-1 infected patients. The difficulty in obtaining thymic tissue for viral analysis has resulted in the paucity of information regarding *in-vivo* viral populations found in the thymus at late stages of HIV-1 infection in children. The thymus can serve as an extremely susceptible site and productive source of HIV-1 infection. Thymocytes express the necessary cellular receptors for HIV-1 entry, such as CD4, CXCR4, and CCR5 (16,17,99,143). CXCR4 is highly expressed on all immature thymoctyes but is reduced on the maturest single-positive subset (99). In contrast, CCR5 is expressed at low levels on the majority of thymocytes (199). In addition the thymic microenvironment is rich in several HIV-1 promoting cytokines necessary for T-cell education and development such as tumor necrosis factor (TNF), and interleukin-7 (IL-7) (28,29).

HIV-1 does infect the thymus of both fetuses and children (28,93,111,154). Infection of thymocytes is common particularly in fetuses (140). Pediatric HIV-1 infected patients have a bimodal pattern in the progression to AIDS with 50% of patients progressing to AIDS within 24 months (65,66,121). Early progression of HIV-1 infected infants has been associated with thymus dysfunction (104). Macrophage-tropic, CCR5-using (M-R5), nonsyncytium strains have been demonstrated to be the transmitting quasispecies of HIV-1 in both sexual and vertical transmission (51,134,191). Clinical progression to AIDS in both children and adults is correlated with the emergence of T-cell line tropic, CXCR4-using (T-X4), strains (40,51,164,166). HIV-1 can infect multiple cell types within the thymus, however not all HIV-1 strains have the same effect on thymoctyes. In particular, T-X4 strains (NL4-3) can infect CXCR4+ immature thymocytes, replicate extenively, and induce severe thymocyte depletion rapidly (16,17,89). Infection of thymocytes with an M-tropic, R5 strain (Ba-L) have shown slow viral spread within cortical thymoctyes with modest cytopathic effects. Where and how these T-X4 strains that are highly destructive to the thymus emerge is currently unknown. The loss of CD4+ T cells within some patients maybe due to the infection of the thymus with a T-tropic variant that causes rapid destruction of immature T-cells and inhibits immunoreconstitution. Therefore, the site and source of these T-tropic, X4-using variants is of the utmost importance since early prevention with critical antiviral therapies would prevent further irreversible immune deterioration and further clinical progression.

The V3 loop of the HIV-1 envelope (env) impacts chemokine receptor usage, and tropism of the virus (33,34,85,167,171). Several studies have demonstrated that most V3 quasispecies from tissues such as the lung, brain, colon, or gastrointestinal tract typically are M-R5 and therefore it is highly unlikely that T-X4 variants emerge in these tissues (25,31,175,176). Other tissues such as the peripheral blood mononuclear cells (PBMCs), and lymph node have been comprised of both M-R5 and T-X4 variants (166,175). However, the PBMCs are a mere conduit between tissues and are another unlikely site of

T-X4 evolution. Lymphocyte trafficking would suggest the T-X4 HIV-1 variants found in the thymus would most likely migrate to the lymph node . Since there is such high X4 expression within the thymus and T-X4 strains such as $\text{HIV}_{\text{NL4-3}}$ have been found to be very cytopathic in thymocytes, the thymus would represent the strongest candidate for a source and site of emergence for T-X4 HIV-1 variants.

To properly evaluate where T-X4 HIV-1 variants emerge, a study would have to determine the HIV-1 env quasispecies from multiple tissues over time from infected patients. However, obtaining longitudinal samples from tissues such as the thymus would subject the patient to needless and uncomfortable surgical procedures and would be unethical. Nevertheless, tissues obtained at autopsy and longitudinal PBMCs would provide a suitable data set to elucidate where T-X4 or Dual-tropic (D-X4±R5) variants emerge. As mentioned before, inclusion of thymic tissue would provide the most likely candidate for a possible source and site of propagation of T-X4 HIV-1 quasispecies. If T-X4 or D-X4±R5 viruses emerge in the thymus and migrate to other tissues, such as the lymph node via the blood, then most of these strains would be found in the thymus with minor populations within the blood and lymph node.

Our study evaluated the HIV-1 env quasispecies, and predicted phenotype present from the autopsy specimens of the thymus, lymph node, spleen, brain, lung, plasma, and longitudinal PBMCs from HIV-1 infected children that varied in clinical progression. In addition, we have functionally characterized thymic env quasispecies for co-receptor usage and tropism. Our results suggest that the thymus is a source of both T-X4 and D-X4±R5 quasispecies, and may be the potential site of evolution for the R5 to X4 evolutionary transition associated with the progression to AIDS in children and adults.

Materials and Methods

Patients and Tissue Collection

A list of patients with survival time, tissues collected, and polymerase chain reaction (PCR) results are shown in Table 3-1. Patients R1 and S1 overlap with the initial patient cohort described in Chapter 1 and correspond to patients A and C presented in Chapter 2 (Table 1-1). PBMCs were longitudinally collected at two timepoints for patients R1 and S1 and one PBMC timepoint for patient S2. For patient R1, the early and late PBMC timepoints were collected one year and four months prior to death, respectively. PBMCs were not available for analysis for patient R2. For patient S1, the early and late PBMC timepoints were collected 6 years and 2 weeks prior to death. The PBMC timepoint for patient S2 was collected 2 years prior to death. The early and late PBMC collection for patient L1 was 4 years and six months prior to death, respectively. Tissues were collected at autopsy 24 to 48 hours after death. The dates of collection for tissues were between 1991 to 1997. Blood and plasma collection has been previously described (110). Tissues were fresh frozen in 50 ml conical tubes and stored at -80°C until processed for DNA extraction. All patients received limited anti-retroviral therapy such as AZT, ZDV, DDI, or DDC. No patients received protease inhibitors since all expired prior to the advent of protease inhibitors. All protocols were approved by the Institutional Review Board of the University of Florida College of Medicine.

DNA Isolation From Tissue Specimens

DNA was extracted from the lung, and brain using the SV RNA extraction kit (Promega). DNA extractions of the lung and brain were performed with the following modifications. Multiple tissue biopsies (10-30 mg of tissue/biopsy) were taken from different parts of the brain and lung tissue and placed into a 1.5 ml Eppendorf tube containing 175 ul of SV RNA lysis solution (Promega). The sample was then incubated for 24 hours with occasional mixing. After the incubation period, extraction procedure followed that of manufacturer's instructions. DNA was extracted from the lymph node, spleen, and thymus using the Dneasy tissue extraction kit (Qiagen). Multiple biopsies were taken from each tissue and DNA was extracted according to manufacturer's instructions. DNA was extracted from PBMC samples as previously described (110). Extracted tissue DNA was analyzed by agarose gel electrophoresis and quantitated by A_{260}/A_{280} spectroscopy. Several DNA extractions from each tissue were pooled together, and multiple PCR amplifications were performed on the combined DNA extraction. This was done to ensure an accurate representation of all viral sequences present within a tissue.

PCR Amplification and Cloning

The entire V1-V5 region of envelope was PCR amplified from various tissues. Nested Envelope PCR amplifications were performed using a forward primer, LV15 (5'-GCCACACATGCCTGTGTACCCACA-3', position 6464-6489), and reverse primer, 194G (5'-CTTCTCCAATTGTCCCTCATA, position 7688-7718). Second round amplification of envelope used the same reverse primer with the forward primer, ENV5 (5'CGGGATCCGGTAGAACAGATGCATGAGGAT-3', position 6547-6577).

Approximately 500 ng of DNA extracted from each tissue was used for each 50 ul PCR reaction with PCR Buffer (Perkin-Elmer) (50 mM KCl , 20 mM Tris, ph 8.5), 0.05 μm each primer, 1.75 mM $MgCl_2$ (Perkin-Elmer), and 0.2 μM each dNTP (Pharmacia). Multiple PCR amplifications were performed on each combined tissue

DNA extraction. The following parameters were used for the env PCR amplifications: one cycle of 94°C for 10 min, 35 cycles with each cycle consisting of 94°C for 1 min, 60°C for 1 min, 72°C for 2 min, and final extension of 72°C for 10 min. PCR amplifications were performed in an automated thermal cycler (Perkin-Elmer 9600). Products of 1.1 kb from the first round reaction were purified with the PCR Purification kit (Qiagen) and 10-20 μl of the purified first round PCR product was used as the template for second round amplifications. PCR products were ligated into pGEM-T vector (Promega), which was used to transform 50 μl of Max Efficiency DH5α Competent Cells (Gibco-BRL). Approximately 5-15 ampicillian resistant colonies were picked and grown in Luria Broth with ampicillian (100 ug/ml) at 37°C overnight. Plasmids were extracted using a Miniprep extraction kit (Qiagen) following manufacturer's instructions. Plasmid inserts were confirmed by restriction digestion using *Eco*RI (Gibco-BRL) and analyzed by agarose gel electrophoresis. The 1.1 kb correct size envelope products were sequenced with 195C (5'-CTGGGTCCCCTCCTGAGG-3', position 7362-7379). Sequencing was performed using the ABI 373 Prism Dye Terminator Cycle Sequencing Ready Reaction Kit (Perkin-Elmer). The median number of clones obtained from each tissue was 9 (Range 2-15).

PCR Amplification and Cloning from Plasma

Plasma viral RNA was isolated from the plasma of Patient R2 at 4 months prior to death which was concordant with the late PBMC timepoint for this patient. Plasma samples were not available for Patients R2 and S2. Several unsuccessful attempts were made at extracting viral RNA from plasma samples from Patient S1. Plasma Viral RNA was extracted using QIAGEN RNA extraction kit (Qiagen) according to manufacturer's instructions. Reverse transcription was carried out using 1 µg of total RNA mixed with 4 µl of random hexamer (500ng/ul) (Gibco-BRL) in a DEPC treated microfuge tube, this was heated to 95°C for 5 minutes followed by 10 minutes incubation at 65°C . The tubes was then quenched on ice and then the following was added: 5ul of 0.1 M DTT, 2.5 ul of 10mM dNTPs solution, 10ul of 5X transcription buffer (Gibco BRL, 250 mM Tris-HCl , pH 8.0, 375 mM KCl, 15mM $MgCl_2$), 3 µl (500 U) of M-MLV transcriptase (Gibco BRL) then the volume was made up to 50 ul using DEPC treated water and incubated at 42°C for 60 minutes. Reverse transcriptase was inactivated by heating at 95°C for 5 minutes. The reverse transcripted mixture was subjected to two consecutive PCRs. 10 ul of the reverse transcripted mixture was used as the template for the first PCR amplification.The first PCR amplification was carried out at 94°C for 5 minutes for one cycle followed by 35 cycles at 94°C for 30 second, 60°C for one minute, 72°C for 2 minutes followed by a final extension at 72°C for 7 minutes, using an the primer pairs of LV15 (described above) and 194G (described above). Ten µl of the first round PCR product was used as a template for the second PCR amplification using the forward primer, ENV6565F (5'-AGCAGAAGAAGAGGTAGTAAT-3', position 7066-7086), and the reverse primer, ENV6883R (5'-ACAATTAAAACTGTGCGTTACA-3', position 7384-7405). Second round PCR amplifications were under the following conditions; 94°C for 5 minutes for one cycle followed by 35 cycles at 94°C for 30 seconds, 58°C for 30 seconds, 72°C for 30 seconds followed by a final extension at 72°C for 10 minutes. The PCR products were excised from agarose gel and then subjected to purification using QIAquick Gel Extraction Kit (Qiagen) and sequenced as described above.

Sequence Data Analysis and Phenotype Prediction

Phylogenetic analysis was performed on both the nucleotide and amino acid sequence between the V1 and V3 regions of HIV-1 env obtained from various patient tissues. Env amino acid and nucleotide sequences were aligned using the ClustalX program version 1.64. Sequences were inserted in regions where insertions or deletions have taken place in order to obtain proper alignment. Parsimony trees of the env amino acid and nucleotides were constructed using PHYLIP package version 3.5 (61). The bootstrap analysis for nucleotide sequences was carried out with SEQBOOT with 100 resamplings, DNAPARS, and CONSENSE from the PHYLIP package for the nucleotides. Bootstrap analysis for amino acids was performed with SEQBOOT with 100 resamplings, PROTPARS, and CONSENSE. All trees were drawn with HIV_{LAI} as the outgroup. Parsimony trees of env based on amino acids were typically concordant with nucleotide trees.

Determination of Predicted Viral Phenotye Based on V3 Genotype

Viral phenotype was determined according to a previously published equation based on four variables: (i) number of positively charged residues (K or R); (ii) number of negatively charged residues (D or E); (iii) net V3 charge [(K+R)-(D+E)]; and (iv) an isoleucine residue at position 292 (19). The equation used to predict the viral phenotye:

Predicted phenotype= 0.94+[1.68 x (V3 net charge)]-[1.37 x (total positive charges)]+[1.54 x (total negative charges)]-[1.19, if aa292=I]. Calculated values for predicted phenotype are rounded arithmetically. Definitions for the phenotypes are: (1) uses CCR5 only and infects macrophages only (M-R5); (2) uses CXCR4 either alone or in combination with CCR5 and infects macrophages and T-cell lines (D-R5X4/X4); and (3) uses CXCR4 and infects T-cell lines only (T-X4).

Construction of Envelope Recombinant Viruses

Envelope V1-V5 and V3 regions were amplified from envelope sequences previously ligated into p-GEM T-easy cloning vector (Promega). The following primer sets were used for PCR amplification of V1-V5, D1 (5'-CACAGTCTATTATGGGGTACCTGTGTGGAA-3') and 194G (previously described). For amplification of the V3 region only the following primers were used FSTUC2 (5'-CACAGGCCTGTCCAAAGATATCCTT-3') and 195C (previously described). Amplification was performed in the presence of 1.5 mM $MgCl_2$ with the following parameters: 5 minutes at 94°C, then 35 cycles of 95°C for 30 seconds, 60°C for one minute, and 72°C for two minutes, followed by a final extension of 72°C for 10 minutes. The resulting approximate 1400 bp and 500 bp products were purified with a PCR purification kit (Qiagen). The V1-V5 products were digested serially with *Kpn*I and *Mfe*I (NEB) for 1.5 hrs. each and were gel purified with a Gel Extraction Kit (Qiagen). The V1-V5 inserts were then ligated with T4 DNA Ligase (Promega) into an expression vector (pcDNA3.1+, Invitrogen) containing the entire HIV-$1_{\text{JR-FL}}$ env reading frame according to manufacturer's instructions. V3 inserts were digested serially with *Stu*I and *Bsu*36I (NEB) for 1.5 hrs. at 37°C and gel isolated as described above. The low charge (<5) V3 inserts were ligated into the HIV-$1_{\text{JR-FL}}$ env expression vector and the high charge (≥5) V3 inserts were ligated into an expression vector containing a chimera of HIV-$1_{\text{JR-FL}}$ *env* in which the V1-V5 region was replaced with HIV-1_{LAI} (HIV-$1_{\text{JR-FL}\Delta\text{LAIV1-}}$

v5). For all constructs, 50 µl of STBL2 Competent Cells (Gibco-BRL) were transformed with 5 µl of ligation mix according to manufacturer's protocol. The transformants were plated on Luria broth agar with ampicillian (100 mg/ml) and incubated overnight at 30°C. Colonies were isolated and grown for Miniprep plasmid isolation (Qiagen). Plasmid V1-V5 and V3 inserts were confirmed by restriction digestion with *KpnI/Mfe*I and *StuI/Bsu*36I, respectively. Sequencing was performed as described above.

Envelope recombinant viruses were produced by co-transfecting the env expression constructs and pNL4.3.Luc.E- (AIDS Reagent Program) into HEK 293 cells. The day before transfection, 1.3 x 10^6 cells were seeded in duplicate into T25 flasks. Cells were incubated overnight at 37°C to produce approximately 40-80% confluency. On the day of transfection, cells were washed with DPBS (Gibco-BRL) and 2 ml of complete media was applied to the cells. Into 500 µl was of DMEM (Gibco) was combined 8.6 µg of pNL4.3.Luc.E-, 2.86 µg of the envelope expression construct, and 57.2 µl Superfect (Qiagen). The resulting solution was vortexed for 10 seconds and allowed to incubate at room temperature for 10 minutes. To each T25 flask was added 260 µl of the transfection complex solution and the cells were allowed to incubate at 37°C. After 3 hours, the medium was removed and the cells were washed once with 2 ml of DMEM. Two ml of fresh complete media was added to the cells and incubated for 48 hours at 37°C. The supernatants were then removed, combined from duplicate transfections, and filtered (0.45 µm), aliquoted, assayed by ELISA for p24 (Coulter) and stored at -80°C.

Coreceptor Usage Determinations

To determine the coreceptor specificity of thymic quasispecies, NIH 3T3-CD4+ cells coexpressing either CCR5 or CXCR4 (AIDS Reagent Program) were infected in triplicate with 60 ng of p24 of V3 envelope recombinant viruses. The day after infection, cells were washed once with DPBS (Gibco) and fresh media was applied to the indicator cells. On day four post-infection, cells were harvested with the Luciferase Cell Culture Lysis Reagent (Promega) diluted 1X according to manufacturer's instructions. Forty μl of the cell lysates were assayed for luciferase expression with Luciferase Assay Substrate (Promega) using a Monolight 2010 Luminometer (Analytical Luminescence Laboratory).

Monoctye Derived Macrophages and MT-2 Cell Infections

Monoctye derived macrophages were prepared as previously described. MT-2 cells were generously provided by the AIDS Reagent Program. MDM's were seeded into a 48 well dish at 1 x 10^6 cells/well and allowed to differentiate in the presence of GM-CSF (1 ng/ml) (Gibco-BRL). Five to six days after plating the cells were washed three times with DPBS (Gibco) and infected in triplicate with 20 ng of p24 of the V1-V5 recombinant viruses. The day after infection, the cells were washed and fresh media was applied. On day four post-infection cells were lysed and assayed for luciferase activity as described before.

MT-2 cells were plated at 5 x 10^4 per well in a 96-well round bottom plate and infected in triplicate with 20 ng p24 of the V1-V5 envelope recombinant viruses. Four days post infection the cells were lysed and assayed for luciferase activity as described before.

Results

Phylogenetic Analysis and Predicted Phenotype of Tissue V3 Sequences

To ensure the integrity of the data, parismony analysis was performed on the nucleotides from the V3 region of env from a representative sequence from each tissue from all patients examined in this cohort. Patient sequences were found to segregate from one another and from the outgroup population of $\mathrm{HIV}_{\mathrm{LAI}}$ (Figure 3-1). Several multiple lineages were found within each patient. In addition, signature amino acid sequences observed from the patients of this cohort have not been identified in any of the previous sequences analyzed by our laboratory (data not shown).

Phylogenetic analysis of the amino acids from the V3 region of envelope from various tissues revealed genetic segregation according to V3 genotype and net charge (Figure 3-2). In three of four patients (Figure 3-2, Parts A, B, and C), mixed populations of viral env sequences with low (V3 charge <5) and high charged (V3 charge ≥ 5) V3's were identified. V3 sequences from Patient R1 phylogenetically segregated according to V3 charge into two distinct groups (Figure 3-2A). One cluster of V3 sequences obtained from the early and late PBMC, lung, spleen, lymph node, and plasma had a low V3 charge with a predicted phenotype of M-R5. In contrast, the second population containing V3 sequences from the thymus and PBMC all had a high V3 charge with a predicted phenotype of T-X4 or D-X4±R5, respectively. High charge V3s were only found in the thymus, and a minor subset of both early and late PBMC. All V3 sequences obtained from the lung, brain, plasma, and spleen had a low V3 charge.

Phylogenetic segregation according to V3 charge and phenotype was also found with both patients S1 and S2 (Figures 3-2B and 3-2C). One lineage contained all low-charge V3 sequences, whereas the other lineage contained all high charge V3 sequences with a predicted phenotype of D-X4±R5. All V3 sequences obtained from the PBMC, spleen, and brain of patient S1 had a low V3 charge with a predicted phenotype of M-R5 (Figure 3-2C). High charge V3 sequences were localized to both the thymus and lymph node with a predicted phenotype of D-X4±R5. Similar phylogenetic segregation was observed with patient S2. All PBMC and spleen sequences from patient S2 had a low V3 charge with a predicted phenotype of M-R5. As observed with the phylogenetic analysis of patient S1, high charge V3 sequences were localized to the thymus and lymph node and not found in any other tissues.

All V3 sequences obtained from patient R2 had a low charge with a predicted phenotype of M-R5 (Figure 3-2B). No high charge V3 sequences were found within any tissue. The absence of high charge V3 sequences within the thymus was concordant with the lack of detecting any high charge V3 sequences in other tissues. V3 sequences obtained from the lung, brain, and late PBMC of patient L1 all had a low V3 charge with a predicted phenotype of M-R5 (Table 2-2, Patient D). HIV-1 envelope was not detected in the thymus of this patient despite repeated attempts (data not shown). High charge V3 sequences were detected 4 years prior to death, yet not found within any tissue at death. This may suggest that the intact thymus is necessary to evolution of both T-X4 or D-X4±R5 viruses. Therefore if the thymus is completely destroyed then high charge V3 variants are not propagated and cannot be disseminated to other tissues. Nevertheless, high charge V3 sequences were always detected in the thymus when found in other tissues. Furthermore, the detection of low charge V3 populations within the thymus was always concordant with low charge V3 populations in other tissues.

Patients R1, S1, and S2 clearly had distinct independent lineage's comprised of either M-R5 and T-X4 lineages but never both. High charge V3 sequences with a predicted phenotype of either D-X4±R5 or T-X4 were typically identified in the thymus and lymph node, whereas most other V3 sequences from other tissues were M-R5. The thymus was the only tissue to contain only T-X4 V3s and detection of high charge V3s within the thymus was always concordant with the presence of T-X4 or D-X4±R5 V3s in other tissues. In addition, the lack of high charge V3s in the thymus was concordant with the absence of high charge V3s in other tissues. Both of these results suggested the thymus as the source of both T-X4 and D-X4±R5 strains.

Co-Receptor Determination and Tropism of Tissue Derived Envelopes

Phylogenetic analysis revealed a charge specific segregation of V3 sequences, particularly with env sequences obtained from the thymus. All high charged V3 sequences had a predicted phenotype of either D-R5X4/X4 or T-X4. NIH 3T3-CD4+ cells expressing either CCR5 or CXCR4 were utilized to determine co-receptor usage of tissue env sequences. All high charged V3 sequences used X4 with greater or the same efficiency as LAI (Figure 3-3, Part A). Most high charged V3 sequences did not utilize R5 to any detectable level. The exception was the V3 sequence S2TH1 which used both R5 and X4, although this was concordant with the predicted phenotype of D-R5X4/X4. A dramatic difference was found between the high charge V3's of R1TH1 and R1LP1. R1TH1 and R1LP1 were obtained from the same patient, but from the thymus and late PBMC's respectively. R1TH1 had a methionine at position 292, whereas R1LP1 contained an isoleucine. R1TH1 utilized X4 to approximately 15x the efficiency of LAI whereas R1LP1 had a 3x fold greater difference than LAI. Both S1TH2 and S1TH3 employed X4 to approximately 20x LAI relative entry, without any detectable R5 usage. All low charged V3 sequences with a predicted M-R5 phenotype used R5 with no detectable X4 usage.

Monocyte-derived macrophages (MDM's) and MT-2 cells were infected with the V1-V5 recombinants from the high charged V3 species from the thymus to determine tropism (Figure 3-3, Part B). In all cases, the predicted phenotype was concordant with the actual phenotype. Both LAI and R1TH1 had a T-X4 predicted phenotype and both infected MT-2 cells only, and did not infect MDM's to any detectable level. JR-FL had a predicted phenotype of M-R5, only infected MDM's and not MT-2 cells. S1TH2 and S2TH1 had a D-R5X4/X4 predicted phenotype and both infected MDM's and MT-2 cells.

Parsimony Analysis of V1, V2, and C2 Regions

To examine regions outside of V3 for charge specific segregation, we examined the amino acids from the V1, V2, and C2 regions of env. This analysis focused on the V1, V2, and C2 regions in relation to V3 charge and tissue specific segregation. This was done to identify any determinants outside of V3 that may impact coreceptor usage and tropism of the virus. For example, the V3 impacts coreceptor usage and tropism, but other determinants outside of V3 (ie. V1 or V2) may enhance or diminish the biological phenotype of the virus. In all patients, there was never a complete concordance between number of high charge containing lineages found according to V3 in either V1, V2 and in some cases C2 (Figures 3-4 and 3-5). High charge V3's were typically clustered in one lineage (Patients R1, S1, and S2). High charge V3's were not found from Patient R2, yet a phylogenetically distinct group of V3's with a different charge of +4 was examined for charge specific segregation according to V2, and C2. A high charge containing or linked lineage was determined if a high charge V3 was found on a branch that segregated from any or all other sequences. A linked high charge lineage was determined if the V1, V2, or C2 sequence was linked to a high charge V3 and found on a branch that segregated from any or all other sequences.

Analysis of the V1 amino acid sequence from the tissues of all patients did not segregate in tissue specific lineages concordant with V3 (Figure 3-4). Most V1 sequences from all patients clustered in one lineage and failed to segregate by tissue or charge. Most V1 sequences from Patient R1 clustered in one lineage linked with mixed V3 charges (Figure 3-4, Part A). The second group of V1 sequences segregated from other branches with a low bootstrap value. V1 sequences from patient R2 segregated in two lineages each contained mixed populations of V3 charges and tissues (Figure 3-4, Part B). V1 sequences obtained from both Patients S1 and S2 were found in one lineage linked to both high and low V3 charge sequences (Figure 3-4, Parts C and D).

Parsimony analysis of env sequences from Patient R1 revealed highly concordant tissue specific segregation between V2, C2, and V3 (Figure 3-5, Part A). Typically, the majority of lung, spleen, and lymph node sequences clustered together by parsimony analysis by V2, C2, and V3. In contrast, V2 and C2 sequences linked to high charge V3's from the thymus clustered together and segregated from other tissues. According to V3 analysis, only one high charge lineage was found containing thymus, and PBMC sequences (Figure 3-2, Part A). In contrast, two high charge linked lineages were found according to C2, whereas only one linked high charge lineage was found according to V2.

According to V3 analysis from the sequences of Patient R2, only one lineage of +4 V3 sequences were identified (Figure 3-2, Part B). Two linked high charge (+4) lineages were shown according to V2 and C2 (Figure 3-5, Part B). Tissue segregation was discordant between various tissues. By V2 analysis, thymus sequences clustered together and segregated from both spleen and lymph node sequences. By C2 and V3 analysis, thymus, lymph node, and spleen sequences were intermingled and clustered together.

For patient S1, according to V3 analysis, independent tissue specific segregation was found among the brain, EPBMC, low charge lymph node and LPBMC, and thymus sequences (Figure 3-2, Part C). Tissues specific segregation according to V3 was concordant to both V2 and C2. Thymus and lymph node sequences having a high charge segregated into one lineage according to V3. High charge V3's did not have distinguishable C2 regions and according to C2 were found clustered with LPBMC, thymus, and lymph node sequences. Early PBMC's segregated from all other tissues by C2. Three lineages were found containing V2 sequences linked to high charge V3's. Most V2 sequences linked to high charge V3's were grouped together and segregated from other tissues. In contrast, there were two V2 sequences linked to a high charge V3 that clustered with different tissues. One high charge linked V2 was clustered with the EPBMC's and brain. The other high charge linked V2 clustered with a low charge V3 linked lineage containing LPBMC's, spleen , lymph node, and thymus.

For Patient S2, all high charge V3's were found in one group (Figure 3-2, Part D). C2 and V2 sequences linked to high charge V3s were found in two lineages (Figure 3-5, Part D). Most high charge linked V2's were found clustered on one branch, whereas high charge linked C2's were clustered with several different tissues.

Parsimony Analysis of V2-V3 of Env

In general, trees generated from translated amino acids may be less accurate than those generated from nucleotide sequences when determining ancestreal sequences. Therefore, we chose to utilize the V2-V3 DNA sequence of env by parsimony analysis to determine the ancestral sequences of those found in the thymus. We selected several representative sequences from each tissue to deduce which early PBMC sequences were ancestors to env populations found in various tissues (Figure 3-6). From the phylogenetic analysis of Patient R1, it appears that for each major lineage there was an ancestral early PBMC sequence that gave rise to either late PBMC or various tissue quasispecies (Figure 3-6, Part A). Within the lineage that contains thymus sequences, there are early PBMC sequences that have a dual-tropic R5X4 predicted genotype that gave rise to late PBMC variants with a similar predicted phenotype. The only descendants of these dual-tropic env variants are only found in the thymus and no other tissues. These late PBMC dual-tropic sequences appear to have evolved into thymic sequences with a T-tropic X4 genotype. In particular, these late PBMC sequences evolved into thymus sequences by a single amino acid change (Isoleucine→Methionine) at position 292. Interestingly, there is a minor cluster of early PBMC sequences (dual-tropic) that do not appear to evolve into any envelope sequences found in any other tissues obtained later which indicates multiple dual-tropic lineages concurrently evolving with strict selection for particular quasispecies for T-tropic, X4 emergence.

Concordant with Patient R1, parsimony analysis of the V2-V3 region of env from Patients S1 and S2 revealed two independent lineages that segregated according to V3 net charge and predicted phenotype (Figure 3-5, Parts B and C). The M-R5 and D-X4±R5 lineages were always found on two independent lineages and were never found clustered together. Each lineage comprised of either M-R5 or D-X4±R5 envelope sequences but never both. Phylogenetic analysis of all patients revealed two lineages segregating according to V3 charge without a common progenitor and ancestreal sequence. There was no evidence of an M-R5 to D-X4±R5 to T-X4 continuam, which suggests that the intermediate is unstable and very transient.

Discussion

The thymus plays a crucial role in the establishment of T-cell immunity in children. Damage to the thymic architecture or infection of thymocytes by HIV-1 would have a devastating effect on immunoreconstitution. Evolution of a T-X4 quasispecies would require two essential factors: 1) Expression of high levels of CXCR4 and, 2) Transcriptionally active environment that promotes viral turnover. The thymus satisfies both of these requirements since thymocytes express high levels of CD4 and CXCR4 and produce several cytokines that sustain a high level of HIV transcription (29,99). Our study has demonstrated that the thymus serves as a privileged source of both T-X4 and D-X4±R5 quasispecies. High charge V3 T-X4 quasispecies were never found as the major sequence in any patient (Figure 3-2). The only tissues to consistently contain either T-X4 or D-X4±R5 quasispecies were the thymus, lymph node, and PBMC's. The thymus was the only tissue to contain a homogenous population of T-X4 quasispecies (Figure 3-2, Part A). In addition, these T-X4 populations only utilized CXCR4 and infected MT-2 cells. The fact that the all other tissues such as the lung, lymph node, spleen, and plasma from Pateint R1 contained only low charge, M-R5 variants suggests that T-X4 quasispecies replicate in a highly localized manner. Dual-tropic predicted phenotypes were found concordantly in the thymus and lymph node in Patients S1 and S2 (Figures 3-2, Parts C and D) . In both patients S1 and S2, the dual-tropic quasispecies comprised a minor subset of the total V3 sequences found within the thymus and the lymph node. High charge V3 sequences were never detected only outside the thymus. The thymus was the only tissue that consistently contained a high charge V3 sequence when other high charge V3 sequences were found outside the thymus. All of the env variants found in one patient which was a rapid progressor were low-charge with a predicted phenotype of M-R5 (Patient R2). Other investigators have also reported that some rapid progressors only have only M-R5 viruses. However, a group of phylogenetically distinct thymus V3's with a charge of +4 that segregated from other sequences suggested the initial emergence of an independent lineage within the thymus. All of these data together suggest a localized, independent evolution of T-X4 and D-X4±R5 quasispecies that arise in the thymus with extremely limited trafficking to other tissues.

In both patients S1 and S2, the dual-tropic quasispecies comprised a minor subset of the total V3 sequences found within the thymus and the lymph node. This result suggests that minor populations of phenotypically distinct HIV-1 quasispecies can co-exist in the thymus, and these minor populations have limited trafficking within the periphery. These minor populations may represent recently evolved dual-tropic variants, whereas the major population of M-tropic, R5-using quasispecies may represent the founder virus that initially infected the thymus. Another possibility is the differences observed between the occurrence of M-tropic and Dual-tropic predicted phenotypes seen in patient S1 and S2 is merely due to sampling error. This outcome is extremely unlikely since several steps were taken to ensure adequate sampling of the HIV-1 V3 quasispecies present in the thymus. These steps included: DNA extracted from multiple biopsies from each tissue, multiple PCRs, several ligations, and multiple colonies sequenced from each patient thymus. Based on this data both T-tropic and Dual-tropic viruses appear to develop within the thymus and not in other tissues. In our tissue V3 analysis, we could not find any cases of either T-tropic (X4) or Dual-tropic (R5) quasispecies present only outside of the thymus.

Our data suggests a model of T-tropic or D-tropic emergence occuring within the thymus (Figure 3-7). It is possible that M-tropic viruses may infect the thymus, and establish infection through either dendritic cells or mature thymocytes. Both of these cell populations have been demonstrated to be the major target for M-tropic infection, and dendritic cells are capable of transmitting M-tropic viruses to mature CD4+ thymocytes. The high expression of CXCR4 on immature thymocytes would select for either T-X4 or Dual-tropic variants that can now replicate in a large population of immature thymocytes found in infant thymuses. The highly cytopathic, T-tropic variants could then rapidly deplete the thymus of immature thymoctyes, and eliminate the export of naïve T-cells to the periphery. The emergence of either a T-tropic or dual-tropic variant in the thymus may completely inhibit T-cell renewal particularly in pediatric patients.

These T-tropic or Dual-tropic variants that emerge in the thymus could then migrate to colonize peripheral lymphoid organs such as the lymph node or spleen via the blood. Therefore, according to the thymic T-tropic/Dual-tropic emergence model, both of these variants should be detected within the thymus, lymph node, and PBMC's. Our data completely supports this model thymic T-tropic emergence. For example, phylogenetic analysis of Patients S1 and S2 showed high-charge D-X4±R5 quasispecies in both the lymph node and thymus, whereas other tissues only contained low-charge M-R5 genotypes. The thymus appears to be an active source of highly pathogenic strains of HIV-1 that are capable of eliminating immunoreconstitution.

Evolution of T-X4 and D-X4±R5 quasispecies may have even further implications besides destruction of the thymus. Infection of the thymus appears to be pivotal in the generation of HIV-1 infected T-cells that are initially quiescent upon leaving the thymus and may lead to the source of latent HIV in humans. Brooks *et al.* has demonstrated in the SCID-hu model that activation inducible HIV can be generated during thymopoiesis (20). Single positive CD4 thymoctyes were infected with HIV_{NL4-3} (T-tropic) or HIV_{JR-CSF} (M-tropic) and could be exported to the periphery and can be activated upon T-cell receptor stimulation. Therefore, T-X4 or D-tropic variants may not only eliminate immunoreconstitution but also establish a viral reservoir. It is possible that T-X4 variants that have been reported to infect the immature subset of thymoctyes may establish a reservoir, that can become activated and induce clinical progression. The thymus appears to have a multi-factorial role in the pathogenesis of HIV-1 particularly in children. Future studies need to address how T-X4 viruses emerge and how effective antiviral therapy can eliminate HIV-1 from this critical organ.

TABLE 3-1
Comprehensive Listing of All Patients with Survival Time and Tissues Analyzed by Env V3 Genotype

Patient	Survival	Thymus	Lymph Node	Spleen	PBMCs[A]	Lung	Brain	Plasma
R1	2 yrs.	+	+	+	+	+	NA[B]	+
R2	8 mo.	+	+	+	U[C]	NA	ND[D]	NA
S1	7 yrs.	+	+	+	+	+	+	U
S2	7 yrs.	+	+	+	+[E]	NA	ND	NA
L1	16 yrs.	U	ND	ND	+	+	+	NA

[A] Peripheral Blood Mononuclear Cells
[B] Tissue not available
[C] Envelope not detected by PCR
[D] Tissue not analysed by PCR
[E] Early PBMC env sequences only
+ Envelope sequences obtained by PCR

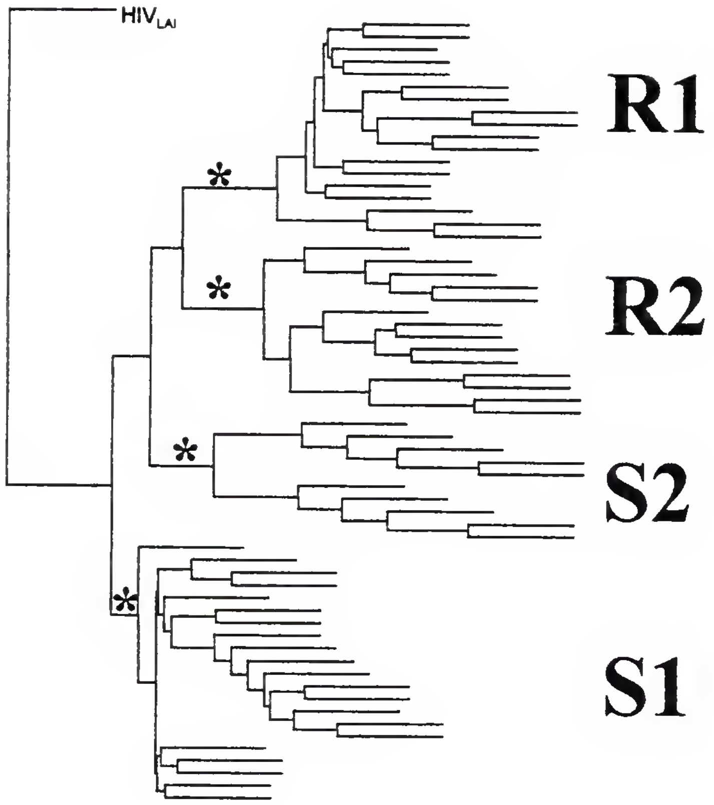

Figure 3-1. Parsimony tree of the V3 DNA sequences. Represenative V3 sequences from each patient are designated by letters (R1, R2, S1, and S2). * denotes a bootstrap greater than 65%.

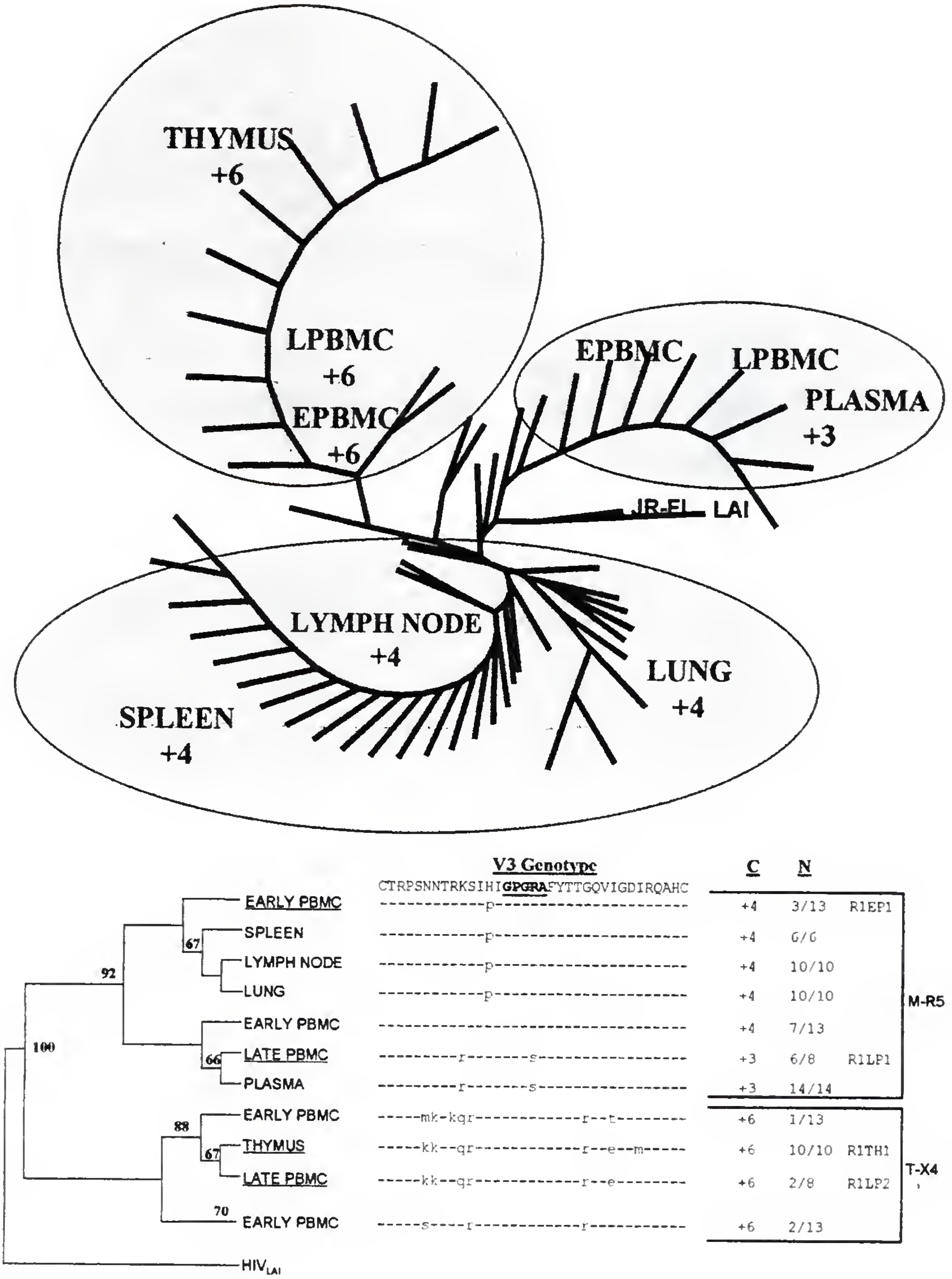
THYMUS
+6
LPBMC
+6
EPBMC
+6
EPBMC
LPBMC
PLASMA
+3
JR-FL
LAI
LYMPH NODE
+4
LUNG
+4
SPLEEN
+4
V3 Genotype
C
N
CTRPSNNTRKSIHIGPGRAFYTTGQVIGDIRQAHC
EARLY PBMC ------------p---------------------- +4 3/13 R1EP1
SPLEEN ------------p---------------------- +4 6/6
LYMPH NODE ------------p---------------------- +4 10/10
LUNG ------------p---------------------- +4 10/10
EARLY PBMC ----------------------------------- +4 7/13
LATE PBMC ---------r-------s----------------- +3 6/8 R1LP1
PLASMA ---------r-------s----------------- +3 14/14
EARLY PBMC -----mk-kqr------------r--t-------- +6 1/13
THYMUS -----kk--qr------------r--e--m----- +6 10/10 R1TH1
LATE PBMC -----kk--qr------------r--e-------- +6 2/8 R1LP2
EARLY PBMC -----s----r-------------r---------- +6 2/13
M-R5
T-X4
HIV$_{LAI}$
100
92
67
66
88
67
70

Figure 3-2. Parsimony analysis of tissue V3 sequences. Top tree is a radiagram of all patient V3 sequences. Tissue groupings are designated by a gray circle denoted by tissue and V3 charge. Bottom tree is a phylogram of representative V3 sequences. Numbers on tree branches refer to bootstrap values from 100 trees. Patient V3 sequences are aligned to an EPBMC sequence, except for Patient R2 which was aligned to spleen sequence. C refers to V3 amino acid net charge, and N denotes frequency of specific sequence out of total sequences obtained from that tissue. A- Patient R1, B- Patient R2, C- Patient S1, and D- Patient S2. Underlined tissues denote V3 sequence was functionally tested for co-receptor usage (Figure 3-3A). Patient code for sequences functionally tested is shown to right of clonal frequency.

B. Patient R2

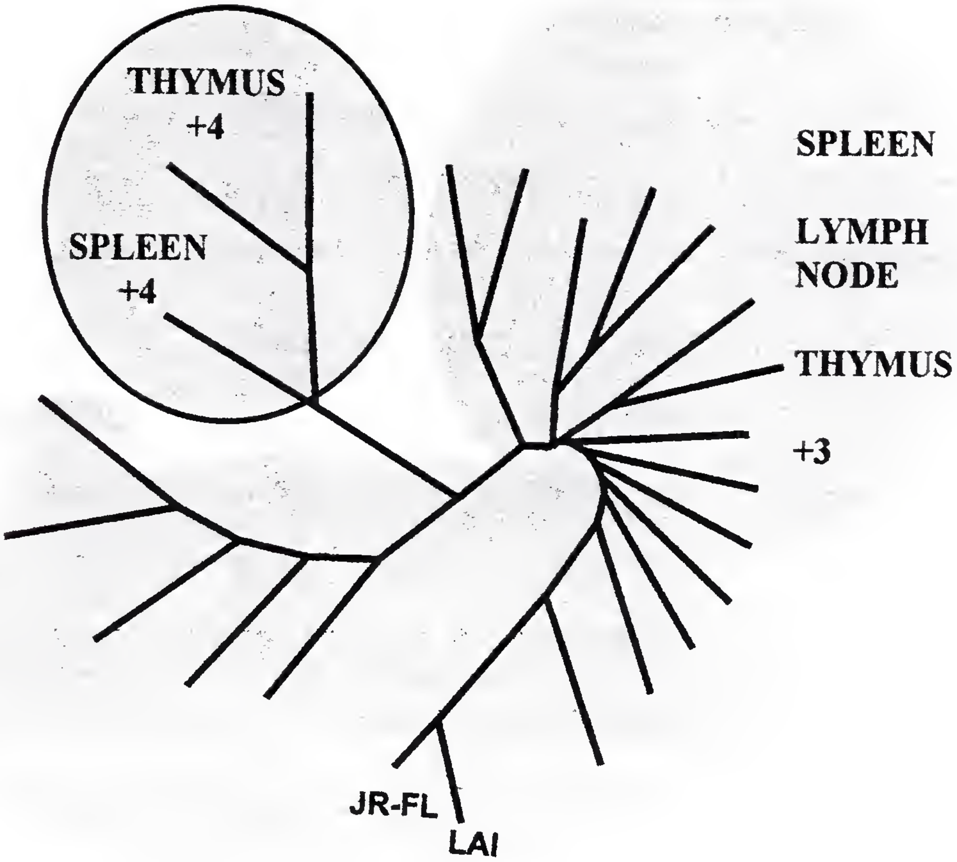

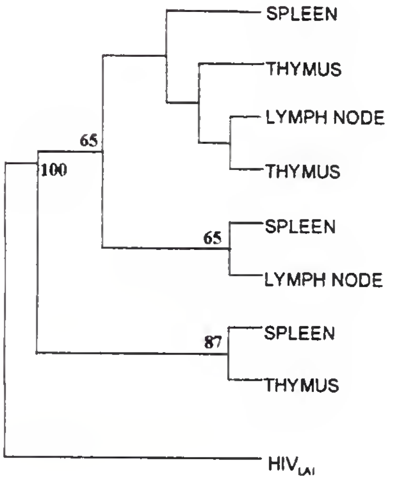

	V3 Genotype	**C**	**N**	
	CTRPNNNTRRSIHMNN**GPGRA**LYTGEVIGDIRQAYC			
SPLEEN	------------------------------------	+3	5/10	M-R5
THYMUS	------------------------------------	+3	3/8	
LYMPH NODE	------------------------------------	+3	3/5	
THYMUS	---------k--------------------------	+3	3/8	
SPLEEN	--------------------s--------e------	+3	4/10	
LYMPH NODE	-----------v-----------------e------	+3	2/5	
SPLEEN	-----------v-i-------------l-n------	+4	1/10	
THYMUS	-----------v-i-------------l-n------	+4	2/8	
HIV_LAI				

Figure 3-2.--continued.

C. Patient S1

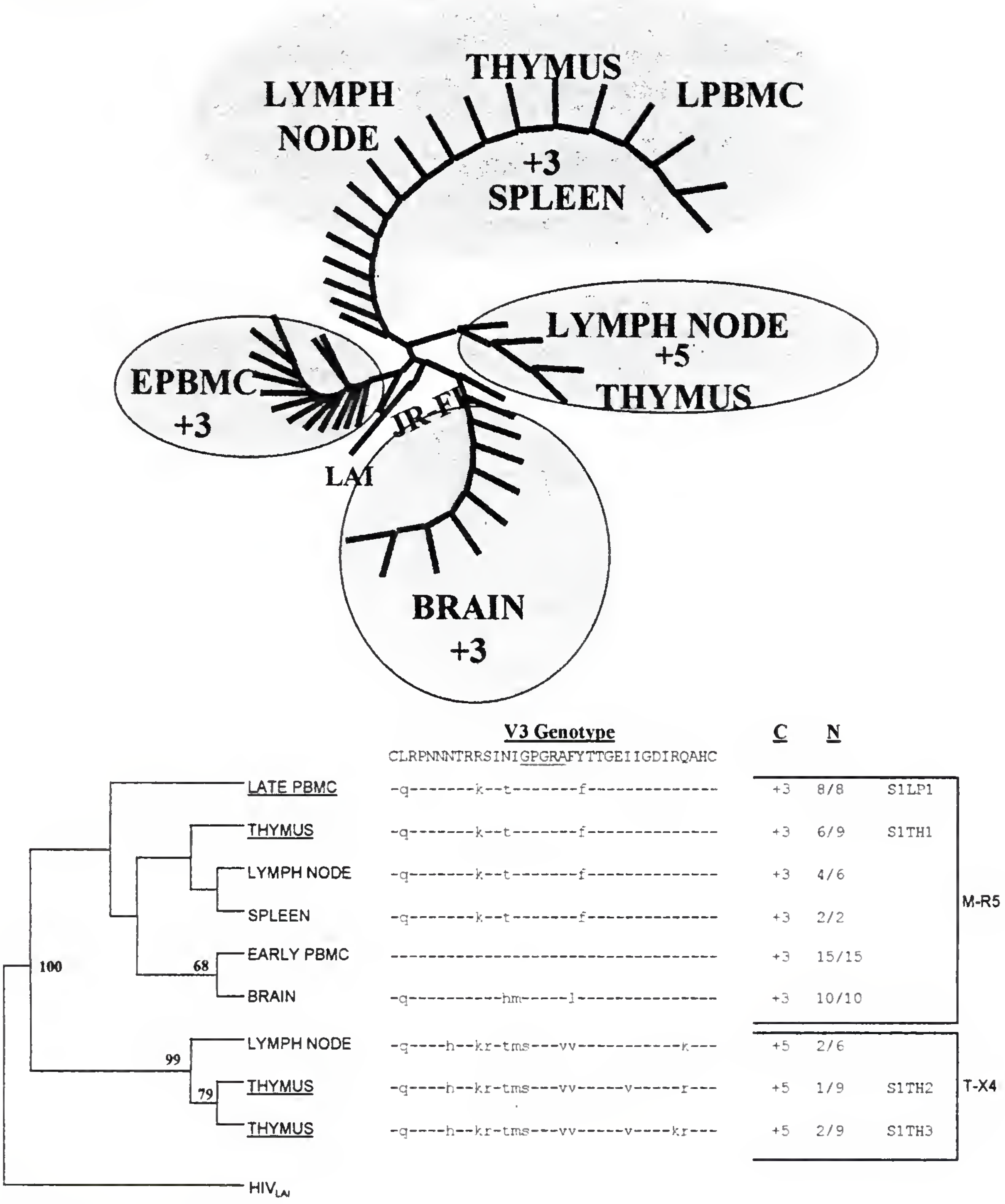

	V3 Genotype	C	N		
	CLRPNNNTRRSINIGPGRAFYTTGEIIGDIRQAHC				
LATE PBMC	-q-------k--t-------f--------------	+3	8/8	S1LP1	M-R5
THYMUS	-q-------k--t-------f--------------	+3	6/9	S1TH1	
LYMPH NODE	-q-------k--t-------f--------------	+3	4/6		
SPLEEN	-q-------k--t-------f--------------	+3	2/2		
EARLY PBMC	-----------------------------------	+3	15/15		
BRAIN	-q----------hm-----l---------------	+3	10/10		
LYMPH NODE	-q----h--kr-tms---vv-----------k---	+5	2/6		T-X4
THYMUS	-q----h--kr-tms---vv-----v-----r---	+5	1/9	S1TH2	
THYMUS	-q----h--kr-tms---vv-----v----kr---	+5	2/9	S1TH3	

Figure 3-2.--continued.

D. Patient S2

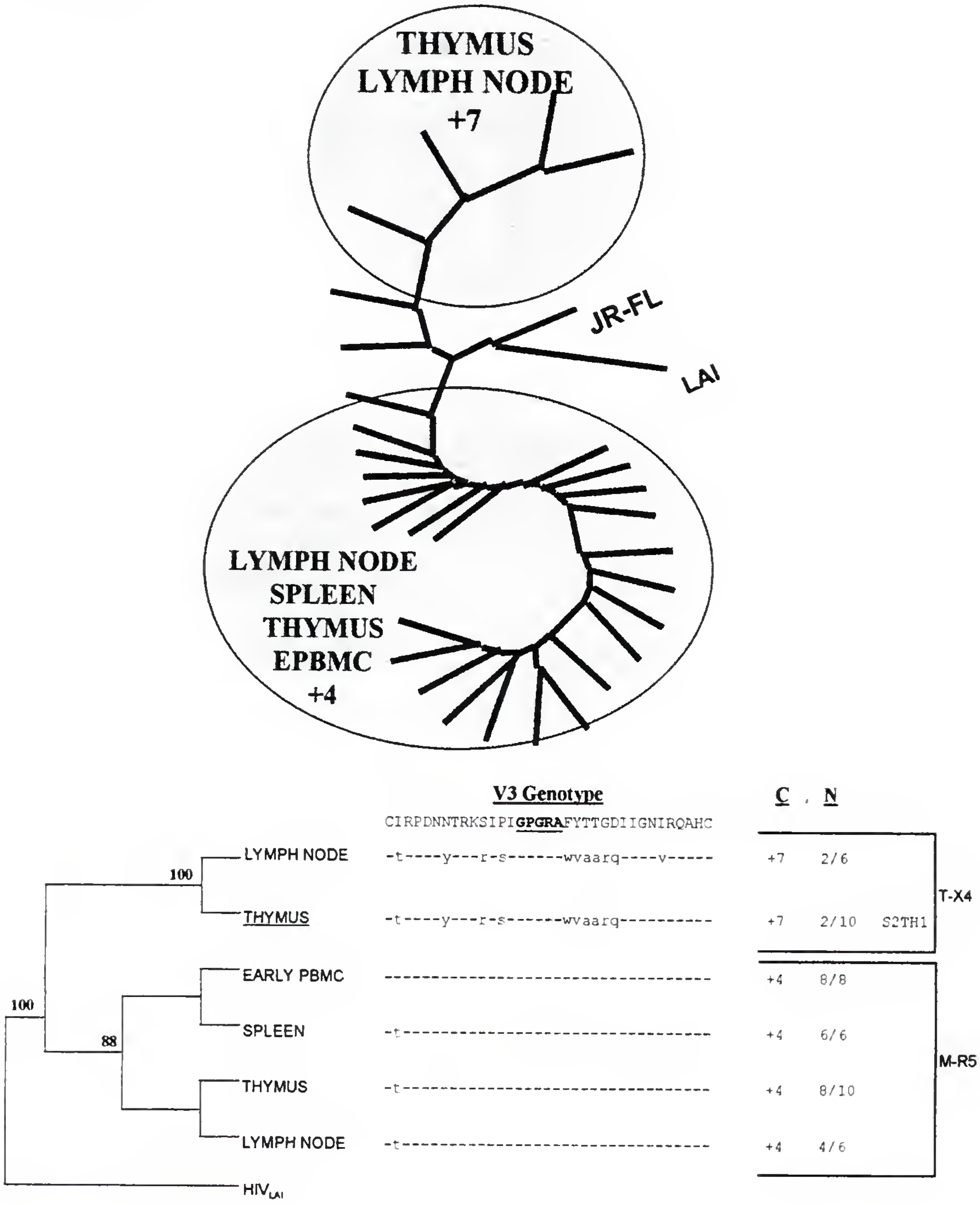

Figure 3-2. --continued.

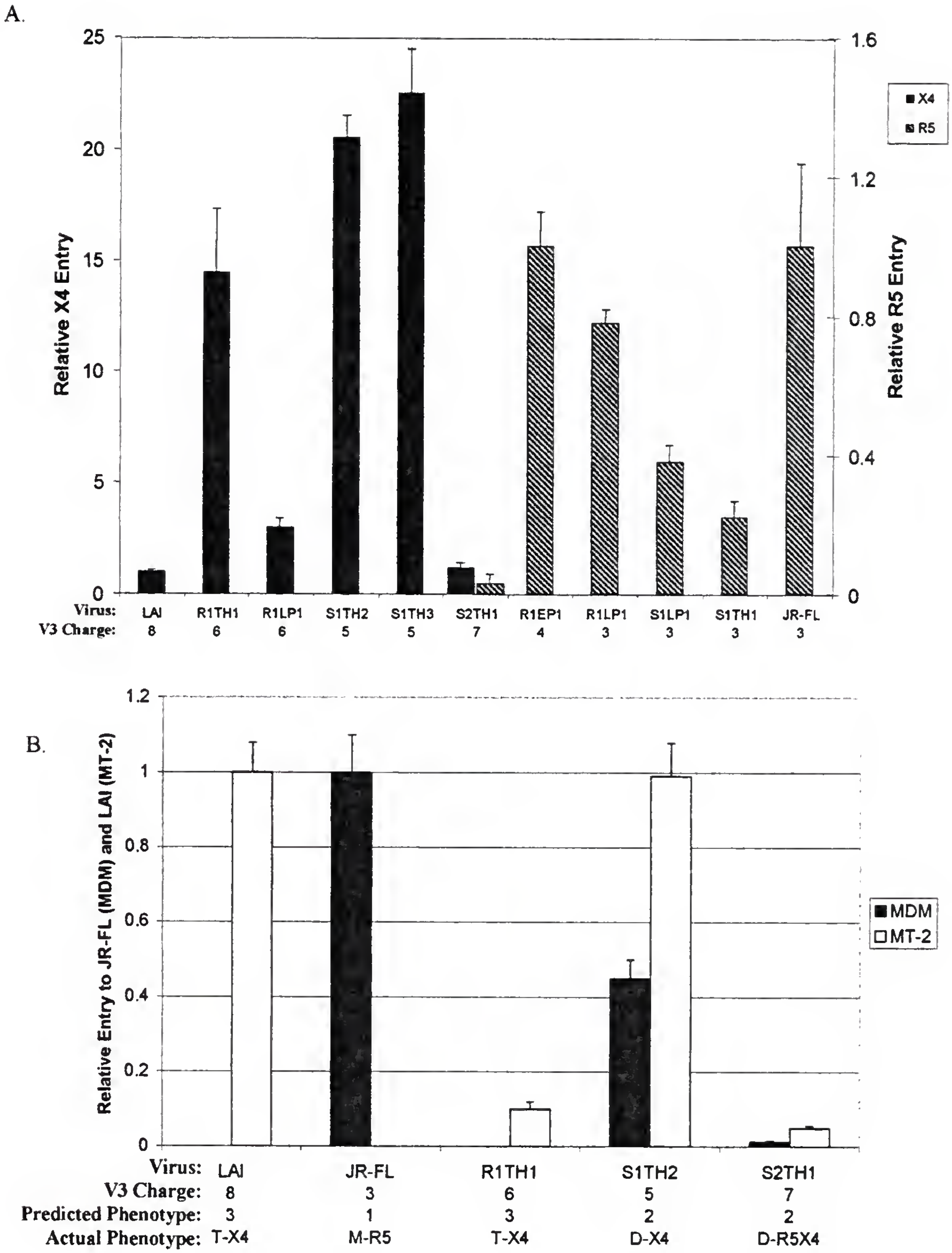

Figure 3-3. Coreceptor usage and tropism of env recombinant viruses. A) Coreceptor usage of V3 recombinant viruses as determined by infection of NIH 3T3-CD4+ cells; B) Tropism of V1-V5 recombinant viruses as determined by MT-2 cells or MDM.

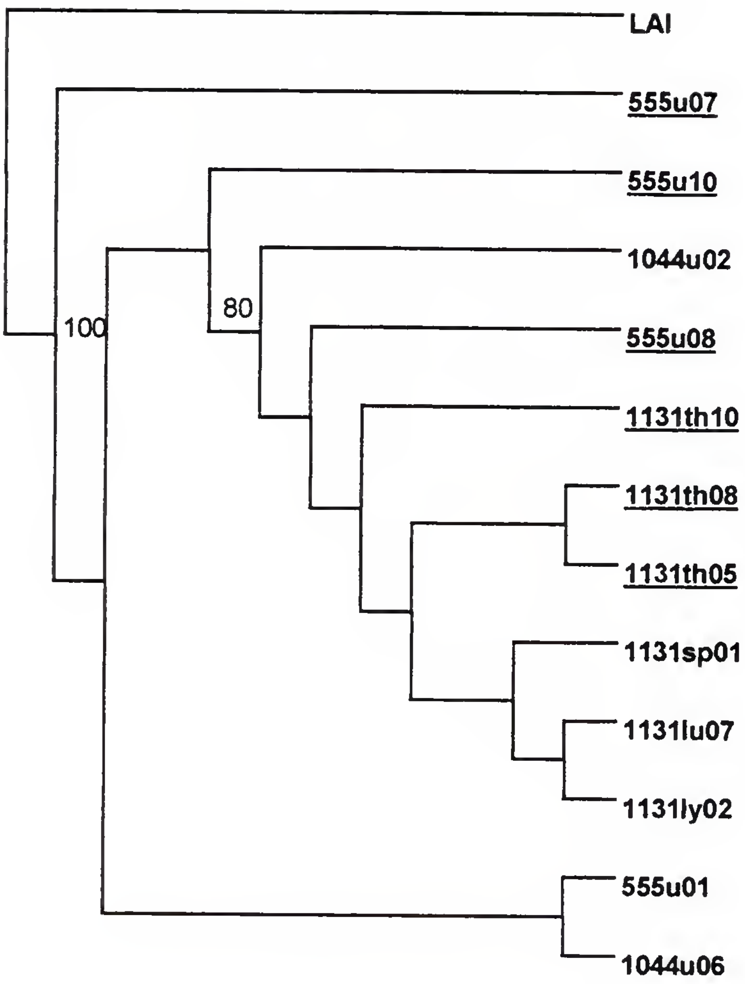

Figure 3-4. Parsimony analysis of the V1 amino acid sequences. Sequences are designated according to patient code, tissue from which the sequence was obtained, and clone number. Representative sequences were chosen from each tissue. After patient code, the following designations are used, U=PBMC, LU=Lung, LY= Lymph Node, Th= Thymus, Sp=Spleen, and Br=Brain. Bootstraps are shown on branches greater than 65%. * denotes branch containing sequence linked to high charged V3. Underlined sequences denote linked to high high charge V3. Patient R2 did not contain high charge V3 sequences therefore +4 charge sequences were highlighted. A-Patient R1, B-Patient R2, C-Patient S1, and D-Patient S2.

B. Patient R2

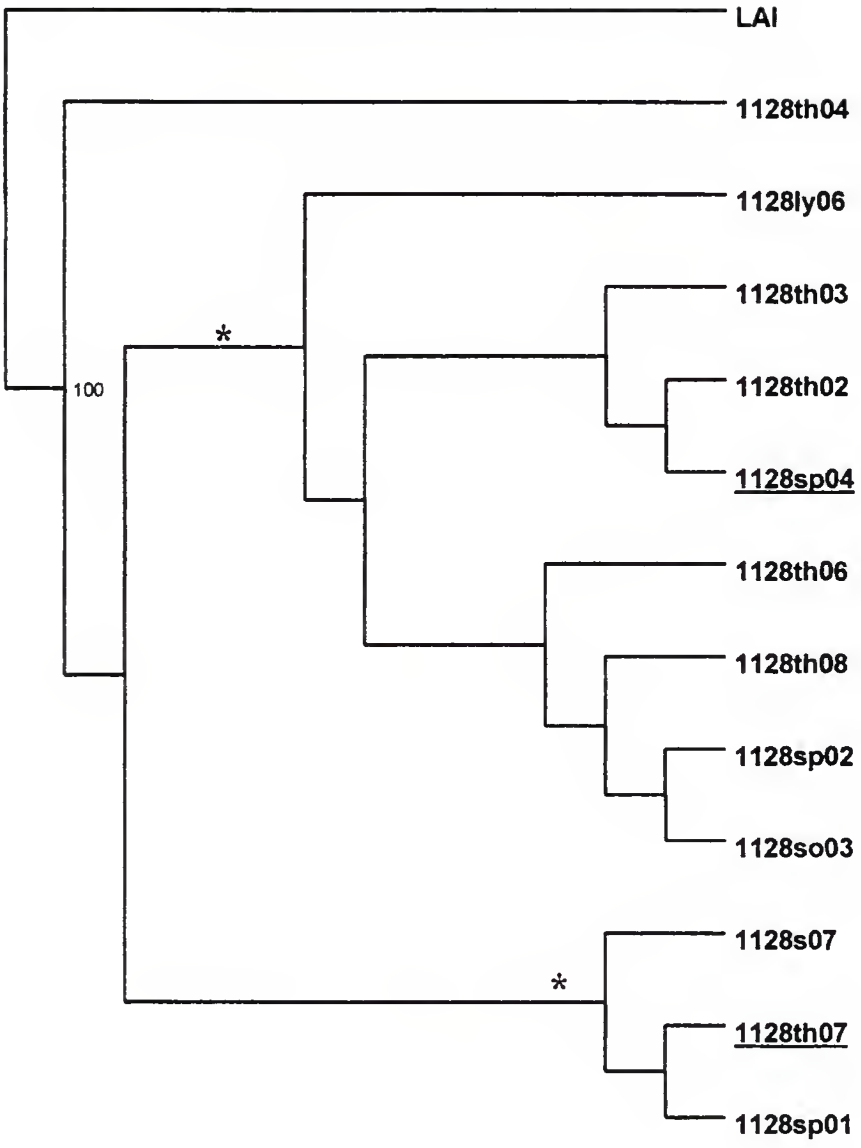

Figure 3-4.--continued.

C. Patient S1

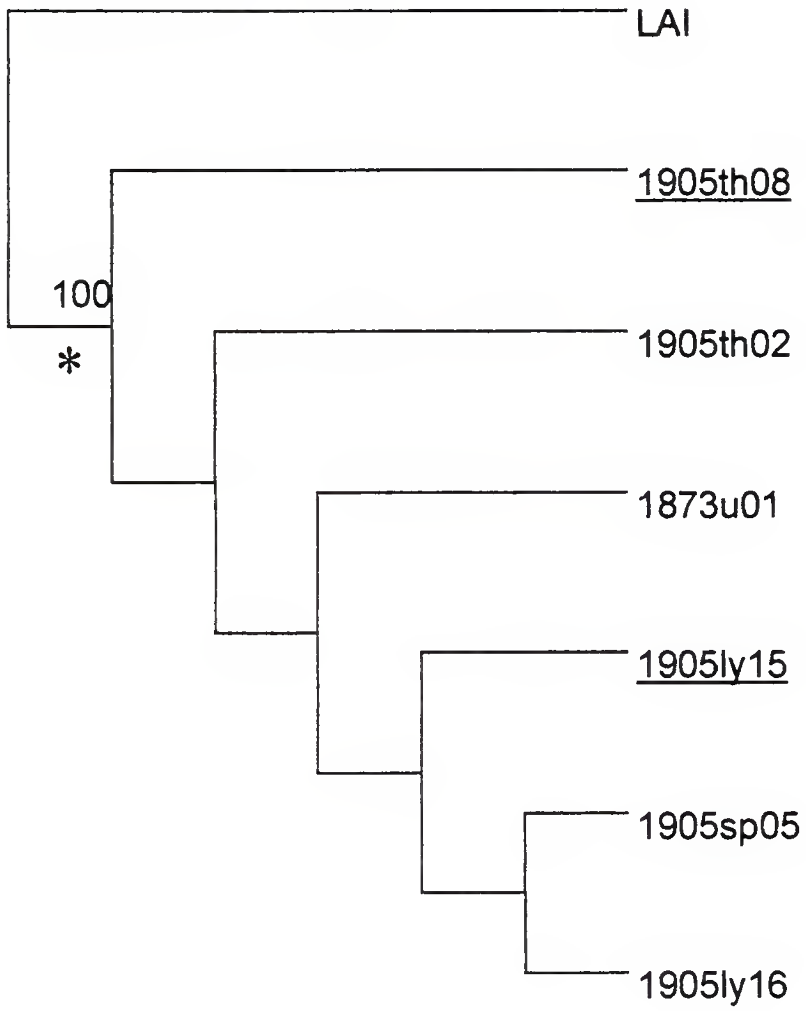

Figure 3-4.--continued.

D. Patient S2

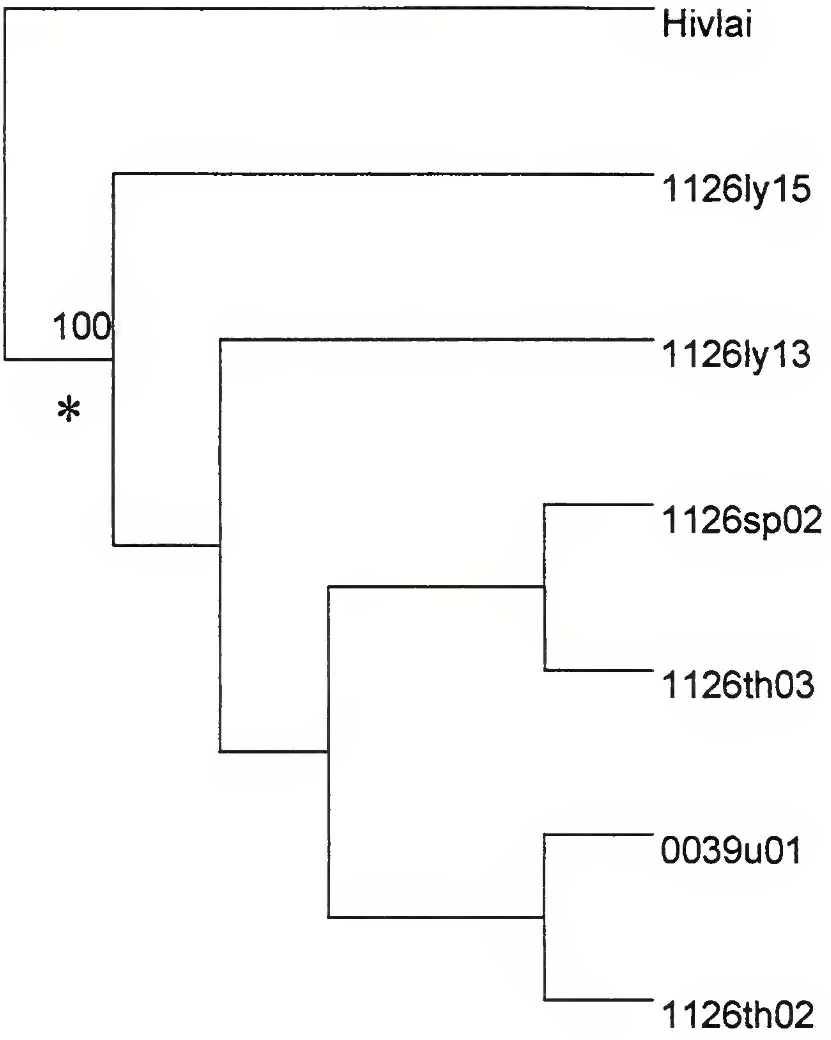

Figure 3-4.--continued.

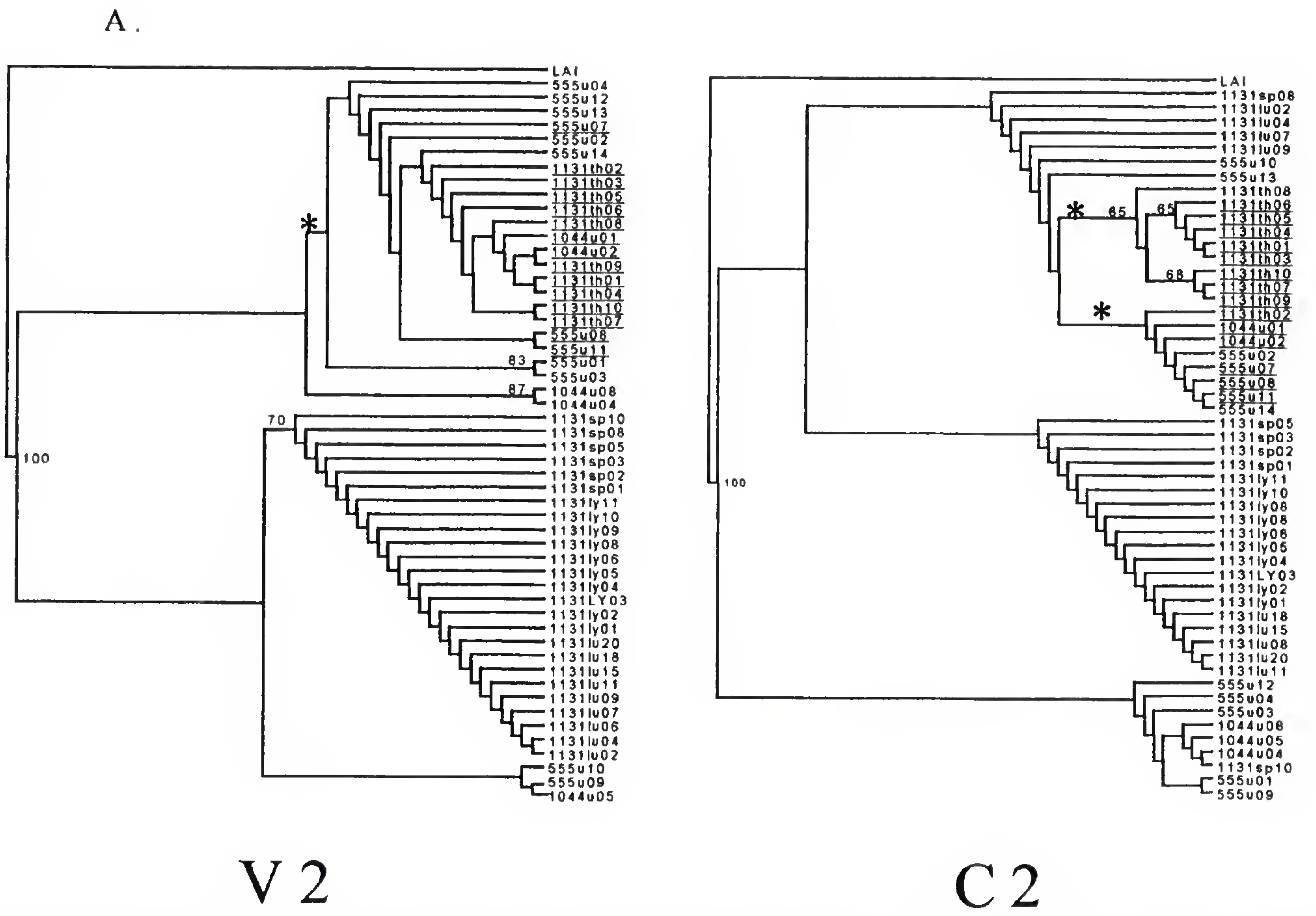

Figure 3-5 Parsimony analysis of the V2 and C2 amino acid sequences. Sequences are designated according to patient code, tissue from which sequence was obtained, and clone number. After letter code, the following designations are used, U=PBMC's, LU=Lung, LY=Lymph Node, Th=Thymus, Sp=Spleen, and Br=Brain. Bootstraps are shown on branches. * denotes branch containing sequence linked to high charged V3. Underlined sequences denote linked to high charge V3. A- Patient R1, B- Patient R2, C- Patient S1, and D-Patient S2.

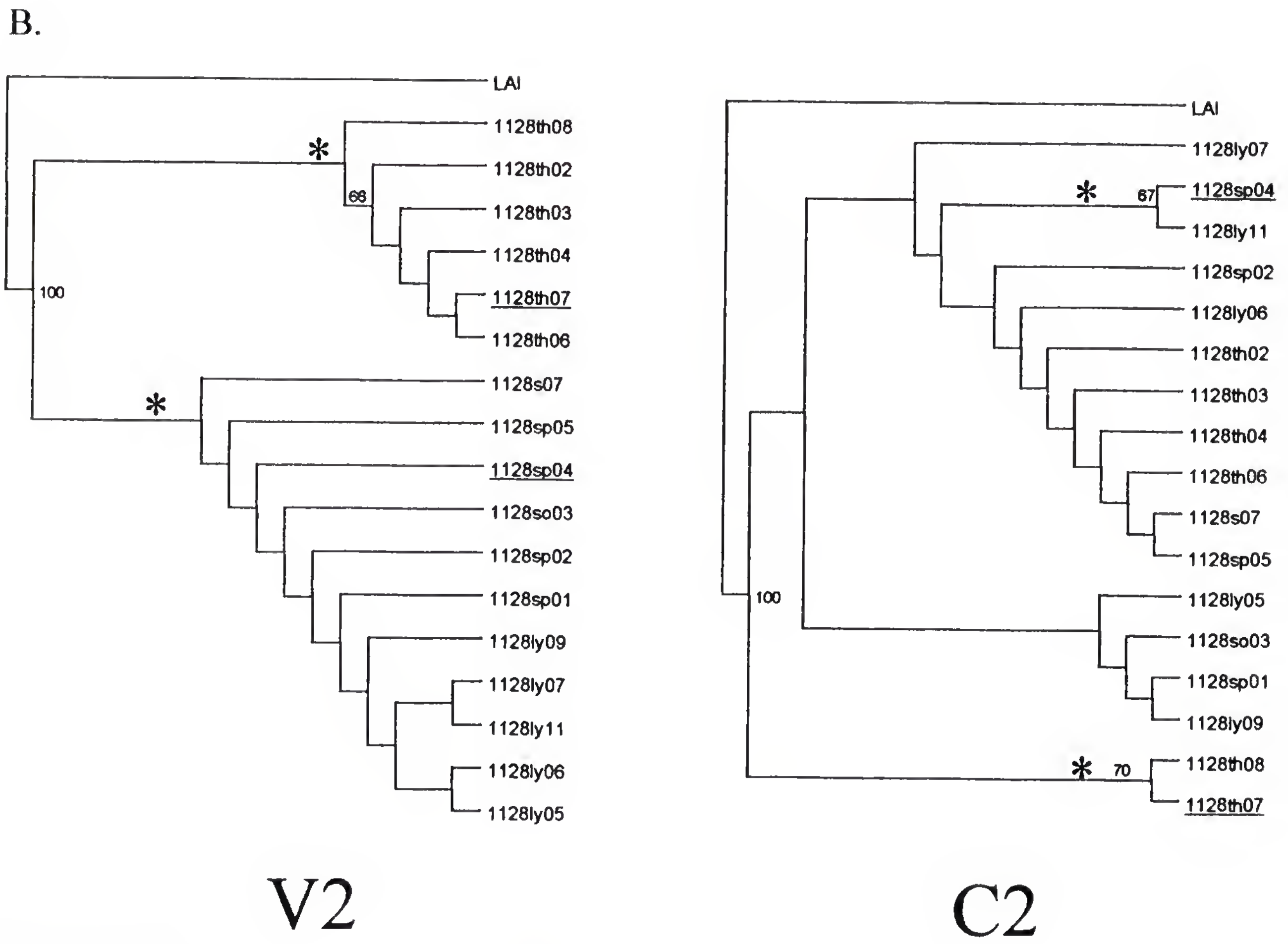

Figure 3-5.-- contnued. (Patient R2)

C.

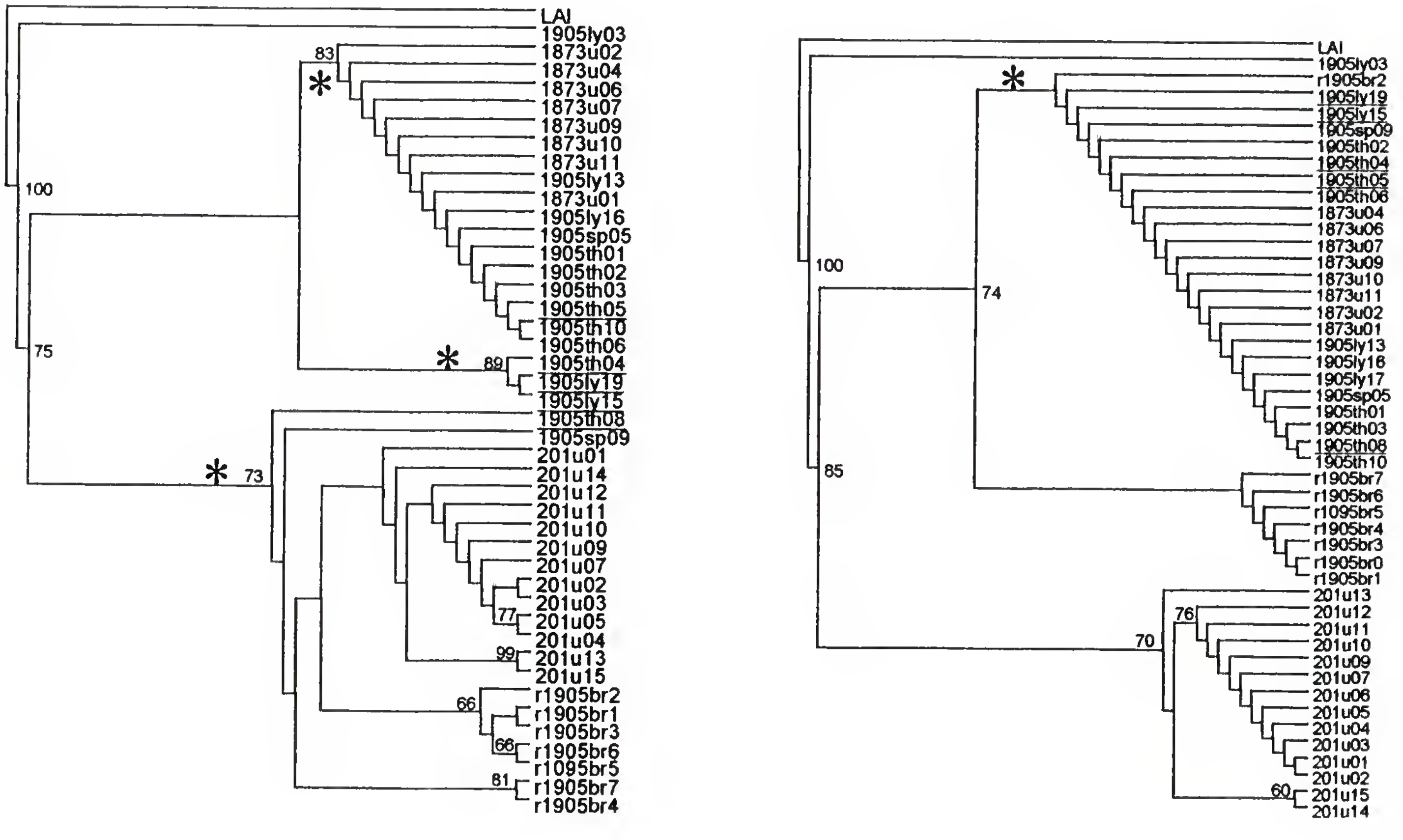

V2 **C2**

Figure 3-5.--continued. (Patient S1)

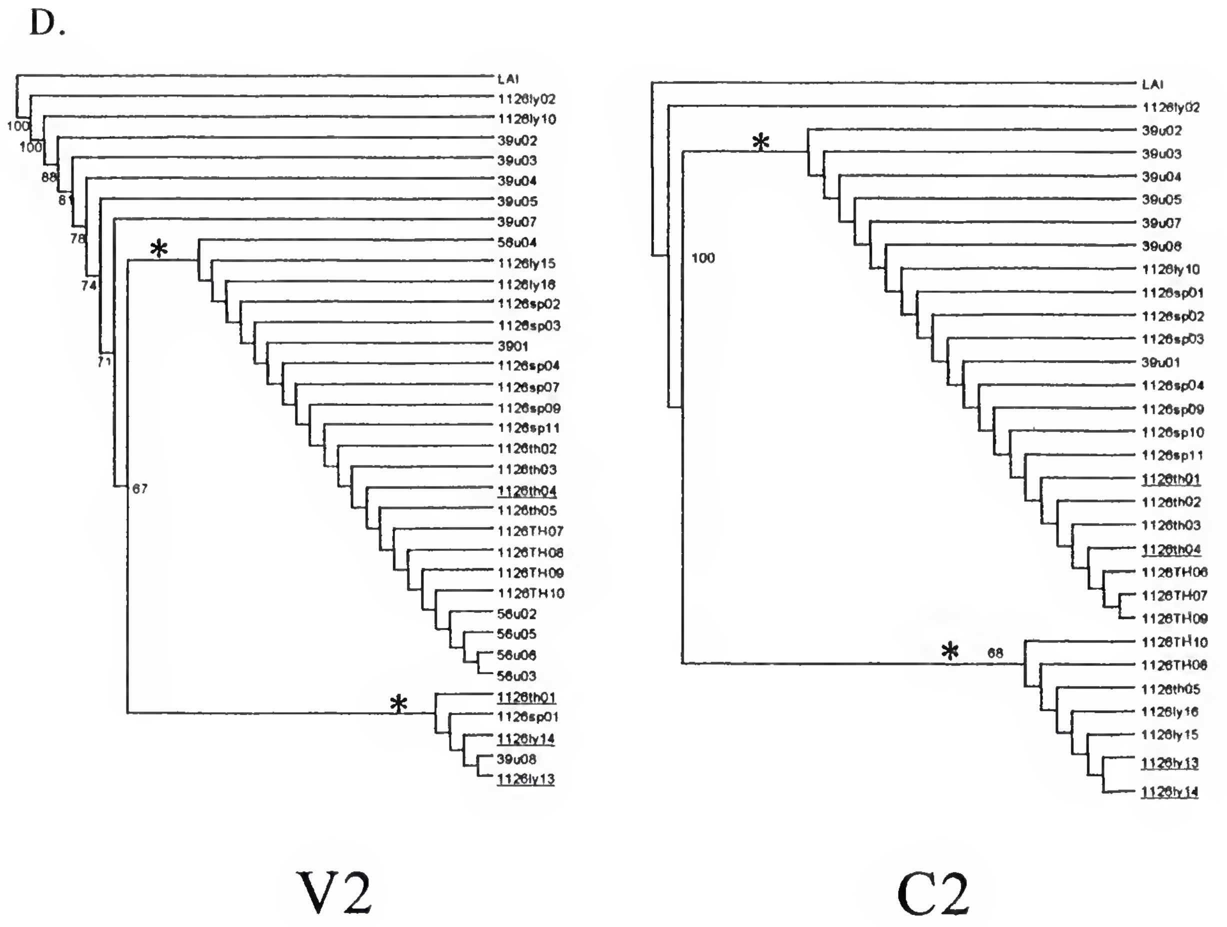

Figure 3-5.--continued. (Patient R2)

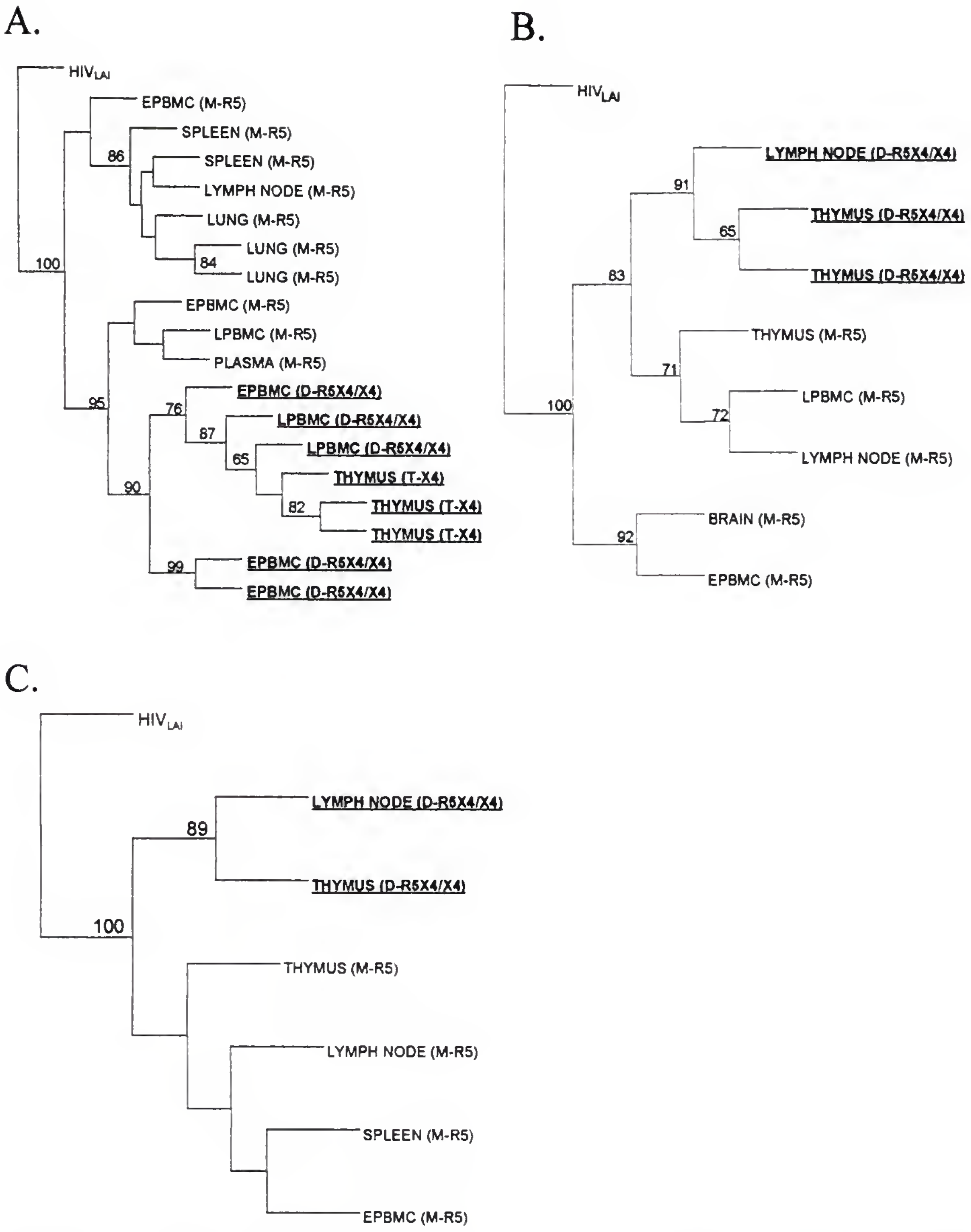

Figure 3-6. Phylogenetic analysis of the V2-V3 DNA sequences. Parismony analysis was performed on the V2-V3 DNA sequences. Numbers on tree branches are bootstrap values from 100 replicate analysis. Only bootstrap values greater than 65% are shown on trees. Each branch is designated according to tissue sequence. Tissue sequences with a V3 charge ≥ 5 are underlined and bolded. The letters in parenthesis following the tissue designation are predicted phenotype based on V3 net charge as described before. A.- Patient R1, B- Patient S1, and C- Patient S2.

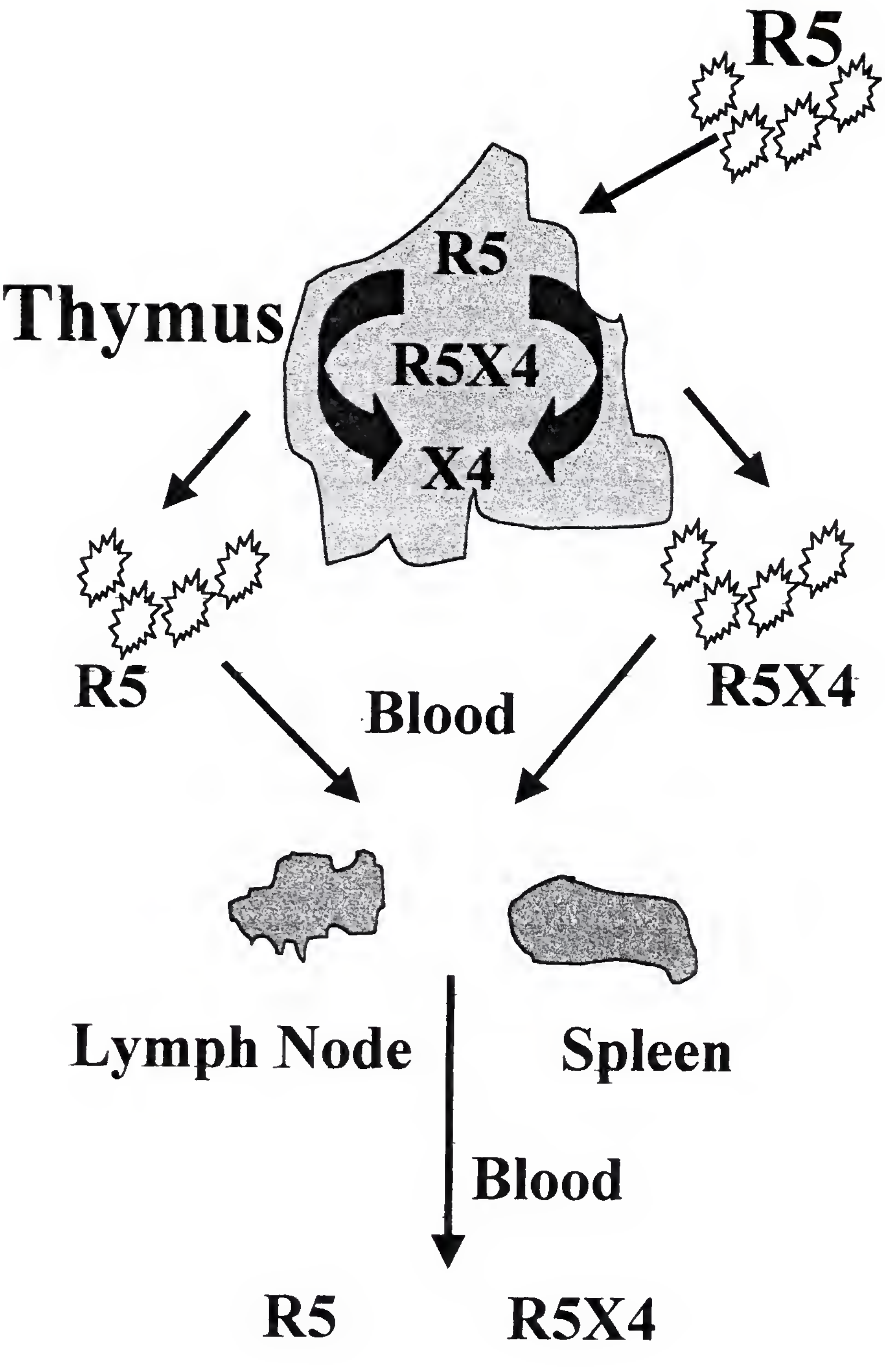

Figure 3-7. Model of T-X4 and D-R5X4 emergence within thymus. This model presents the initial infection of the thymus with an M-R5 variant. High X4 expression coupled with a highly permissive environment for replication induces evolution to a D-R5X4 variant that may evolve to a T-X4. Both M-R5 and D-R5X4 quasispecies may emigrate from the thymus via the blood, and infect lymphatic organs such as the lymph node and spleen.

CHAPTER 4

FUNCTIONAL ANALYSIS OF TISSUE SPECIFIC LTRS USING CONGENIC RECOMBINANT LUCIFERASE VIRUSES WITHIN PRIMARY CELLS

Introduction

The human immunodeficiency virus type 1 (HIV-1) long terminal repeat (LTR) impacts pathogenesis predominantly at the level of gene expression. Other retroviruses, such as murine-moloney leukemia virus and mouse mammary tumor virus have demonstrated that subtle differences within the LTR impact viral gene expression in a cell-type manner which have a profound effect on the course of disease (44,64). Typically the genetic differences among the HIV-1 LTRs between and within patients resides in the U3 region (60,125). The well characterized T-tropic, HIV_{LAI} and M-tropic, $HIV_{JR\text{-}FL}$ differ between their LTRs by 27 bp located within the U3 region (42). The U3 region of the HIV-1 LTR contains several transcriptional factor binding sites such as NF-kB, Sp1, AP-1, TCF-1, USF, C/EBP, NFAT, and COUP-1 (All defined in Chapter 1) (70). In addition, the study to elucidate additional transcriptional factors that interact with the HIV-1 LTR is continually ongoing. Specific transcriptional factors such as NFAT and C/EBP are specifically expressed expressed in either CD4+ T cells or macrophages, respectively (76,98). Minor nucleotide differences among HIV-1 LTRs may alter binding sites of cell type specific transriptional factors and therefore impact gene expression in a cell type manner. For example, intact C/EBP sites are essential for HIV-1 expression in macrophages and macrophage cell lines, but not in CD+ T cells (76). The M-tropic strains of $HIV_{JR\text{-}FL}$ and $HIV_{JR\text{-}CSF}$ were shown to direct expression in the neurons of transgenic mice, whereas the T-tropic strain HIV_{LAI} failed to express in the central nervous system (42). Phylogenetic analysis of nervous tissue derived LTRs has revealed distinct lineages within the brain that segregate from LTRs derived from other tissues such as the lung or lymph node (2). Our data has also shown that the LTR can segregate among several different tissues including the lung, brain, thymus, and blood.

Very few studies have evaluated the impact of tissue specific LTRs on cell type gene expression. In addition, most studies evaluating HIV-1 LTR expression have utilized transient transfection into cell lines. This model although widely used and informative does not offer an adequate representation of an HIV-1 infection. First, copious amounts of DNA are used in the transient transfections that far exceed the quantity observed for an *in-vivo* infection. Second, transient transfections are typically performed in cell lines which do not always represent primary cells. Most cell lines are transformed, and therefore the cellular milieu may be rich in several transcriptional factors that are not found in the same abundance as in primary cells. Also, many cell lines that are used as a model for primary cells, many are not even at the correct stage of differentiation. For example, the U937 and THP-1 monocytic cell lines are typically used in HIV-1 infection studies as a model for macrophages. However, both of these cell lines are both either monocytic or even premonocytic, and therefore at best represent a poor cell line to choose to represent macrophages. Particularly since HIV-1 infection has been demonstrated to be quite different between monocytes and macrophages (130). Through the use of congenic LTR viruses with either an X4 or R5 envelope we can infect peripheral blood mononuclear cells (PBMCs) and macrophages. This allows us to test the effects of tissue specific LTRS on promoter activity within primary cells. Third, transient transfections skip over a vital part of the viral lifecycle. During a transient transfection, the DNA is essentially inserted into the cell, and therefore there is no interaction between HIV-1 env and the necessary receptors of CD4 and CXCR4 and CCR5. The interaction of virus and the cell would certainly change the intracellular milieu and therefore to evaluate promoter activity it must be done in the presence of an actual infection. Fourth, transfected DNAs are not incorporated into the chromatin and therefore may not be regulated in the same manner as an integrated LTR promoter.

To test the effects of tissue specific LTRs on promoter activity within primary cells, we have utilized a system the employs single-cycle congenic LTR luciferase viruses. The 5' U3 region controls transcription, but only the 3' U3 region of HIV is transcribed into genomic viral RNA. This 3' U3 sequence is copied during reverse transcription, providing the template for the 5' U3 region in progeny provirus. Therefore, transfection of 3' mutant proviral constructs that are envelope deleted, with a complementary envelope should yield single-cycle viral progeny with two mutated LTRs. Our system allows us to infect different primary cells through the use of complementing with either a X4-using (LAI) or R5-using (JR-FL) envlope. Our novel approach has demonstrated that tissue specific LTRs have functional differences within PBMCs and macrophages.

Materials and Methods

Patient Clinical Data and Tissue Collection

The LTRs examined by functional analysis in this Chapter are from patient #3 in Table 1-1. This patient was also described in Chapter 2 (Table 2-1, patient C) and Chapter 3 (Table 3-1, patient S1). In brief, this patient was vertically infected and survivived for 7 years. Early and late PBMC's were collected at 6 yrs. and 2 weeks prior to death, respectively. Tissue specimens were collected from the lung, brain, lymph node, spleen, and thymus at autopsy 24 to 48 hours after death.

Isolation of DNA from Autopsy Specimens and PBMCs

Described previously in Chapters 2 and 3 Materials and Methods

PCR Amplification and Cloning

Described previously in Chapters 2 and 3 Materials and Methods. Env and LTR was successfully amplified from the PBMC's, brain, and thymus. The env region was not successfully amplified from the lung. Also, amplification of the HIV-1 LTR was not performed on the lymph node and spleen.

Sequence Data Analysis

Described previously in Chapters 2 and 2 Materials and Methods

Construction of the LTR-Luc Recombinant

Recombinant viruses were constructed from the molecular clone of HIV_{LAI}, pLAI.2. pLAI.2 was kindly provided by Keith Peden (NIH). A diagram of the construction of the LTR-Luc recombinant viruses is shown in Figure 4-3. The following modifications were made for insertion of the luciferase gene and creation of an env V3-V5 deletion within pLAI.2. To generate the deletion of V3-V5 within env, pLAI.2 was digested with *Sal*I (position 5837, pLAI.2) and *Xba* I (position 8980, pLAI.2) and ligated into pBluescript SK+ vector (pBSSK+) using T4 DNA ligase (Gibco). To remove the V3-V5 region of pLAI.2, pBSSK+ containing the *SalI*/*Xba*I fragment was digested with *Bgl*II (positions 7134 and 7734, pLAI.2) and subsequently self re-ligated with T4 DNA ligase (Gibco). To create compatible ends for insertion of the luciferase gene, pBSSK+Δenv was digested with *Mlu*I and *Xba*I. To remove the luciferase gene from the p-GL3 basic plasmid, p-GL3 was digested with *Mlu*I and *Xba*I (positions 15 and 1742, p-

GL3 basic). The luciferase gene was then ligated into pBSSK+Δenv, and then digested with *Sal*I and *Xba*I to remove the fragment containing the env deletion (V3-V5) and luciferase gene. This 4.1 kb fragment was ligated into the *SalI/Xba*I digested pLAI.2 (positions 5867 and 8980, HIVLAI) to create the pLAI.2Δenvluc+ construct. Further modifications were performed to create compatibles restriction sites for insertion of patient LTR's into the 3' LTR of pLAI.2Δenvluc+ construct. The *Xho*I site located within the luciferase gene was removed by introducing a point mutation using the Quick Change Site Directed Mutagenesis Kit (Stratagene) and manufacturer's instructions were followed accordingly. The point mutation was introduced using the primer pair, LTRLUCXHOIKOF (5'-GCTAGCCCGGGCGCGAGTCTGCGATCTAAG-3'), and, LTRLUCXHOIKOR (5'-CTTAGATCGCAGACTCGCGCCCGGGCTAGC-3'). The *Xho*I and *Bgl*I sites were utilized to cassette patient LTRs from the shuttle vector described below into the LTR-Luc recombinant (pLAI.2Δenvluc+ construct.).

Construction of Patient LTR Recombinants

To subclone patient LTRs into the 3' LTR of the LTR-Luc recombinant, it was necessary to create a shuttle vector. The shuttle vector was created by incorporating PstI (position 8990, pLAI.2) and XbaI (position 10724, pLAI.2) sites surrounding the 3' LTR of pLAI.2. This fragment was digested with PstI and XbaI and ligated into a previously digested plasmid of p-GEM 3z (Promega). The resultant plasmid was utilized as the shuttle vector to facilitate ligation of patient LTRs into the Recombinant LTR-Luc vector. Patient LTRs that were previously ligated into pGEM T-easy (Promega) were amplified with LTR31 (previously described) to incorporate an *Xho*I site at the 5' end of the LTR. Patient LTRs were then digested with *Xho*I and *Afl*II, and ligated into the *Xho*I and *Afl*II digested shuttle vector. The shuttle vector was digested with *Xho*I and *Bgl*I to remove the approximate 1.7 kb fragment and ligated into the LTR-Luc Recombinant vector. The sequence of the 3' LTR of the LTR-Luc recombinant was confirmed using the ABI 373 Prism Dye Terminator Cycle Sequencing Ready Reaction Kit (Perkin-Elmer) using the primer LTRRecSeq (5'-CCT CAT AAA GGC CAA GAA GGG CGG AAA-3').

Construction of Site-Directed LTR-Luc Recombinants

To produce point mutations into the LTR-Luc recombinant vector, Brain LTR, the Quickchange Site directed mutagenesis kit (Stratagene) was used following manufacturer's instructions. To introduce the C→A change at position –270, HIV_{LAI}, the following primer pair was used, forward primer, 1905BR03-270CtoAF (5'-GGT AGA AGA AGC CAA TAA AGG AGA GAA CAA CAG CC- 3'), and the reverse primer, 1905BR03-270CtoAR (5'GGC TGT TGT TCT CTC CTT TAT TGG CTT CTT CTA CC-3'). For the G →T change at position –171, the forward primer, 1905BR03-171GtoTF (5'- GAC AGC CGC CTT AGC ATT TCA TCA CGT GGC CAA AGT GAT G –3'), and the reverse primer, 1905BR03-171GtoTR (5'- CAT CAC TTT GGC CAC GTG ATG AAA TGC TAA GGC GGC TGT C –3'). For the change at position –156, the forward primer, 1905BR03-156AtoGF (5'- GCA TGT CAT CAC GTG GCC AGA GTG ATG CAT CCG GAG –3'), and the reverse primer, 1905BRO3-156AtoGR (5'- CTC CGG ATG CAT CAC TCT GGC CAC GTG ATG ACA TGC –3'). To introduce these site-directed changes, PCR amplification was performed on the shuttle vector containing the Brain LTR insert and LTR recombinant viruses were produced as described below.

Production of LTR-Luc Recombinants

As mentioned above, the 3' LTR of the recombinant vector was replaced with the patient LTR. LTR luciferase recombinant viruses were produced by co-transfecting the LTR-Luc Recombinant vector with either the LAI (X4) or JR-FL (R5) expression vector. The envelope expression vector was either pcDNA3.1+ containing the entire HIV-1_{JR-FL} or HIV-1_{LAI} reading frame. The day before transfection, $6x10^6$ HEK 293 cells were seeded in complete DMEM (Gibco) supplemented with 10% FBS, penicillian (100U/ml), and streptomycin (100 µg/ml) into T75 flasks. The cells were incubated at 37°C, 5% CO_2 for 24 hours to produce approximately 50% confluency. On the day of transfection, 13.6 µg of the LTR-Luc Recombinant vector and 9 µg of the envelope expression construct were diluted into 700 µl of incomplete DMEM (Gibco) with 90 µl of Superfect transfection reagent (Qiagen). The resulting mixture was vortexed for 10 seconds and incubated at room temperature for 10 min. During the room temperature incubation, media was removed from the T75 flasks, and cells were washed with 15 ml of 1X PBS. After washing, 6 ml. of complete DMEM was added to each T75 flask. After the 10 min. incubation period, the transfection mixture (790 µl) was added dropwise directly onto the cells in the T75 flask. The cells were incubated with the transfection complex for 3 hours at 37°C, 5% CO_2. After 3 hours, the complete DMEM was removed from the T75 flask and the cells were washed twice with 15 ml. of 1X PBS. Six ml. of complete DMEM was added to each T75 flask, and incubated at 37°C, 5% CO_2. After 24 hours, the DMEM was removed and fresh DMEM was added to the T75 flask and incubated at 37°C, 5% CO_2. After another 24 hours, the supernatants were collected and filtered through a 0.45 μm syringe filter (Acrodisc). Two hundred μl aliquots were stored at –80 C, and assayed for p24 (Coulter).

Infection of Donor PBMC's and Macrophages

From each leukopak (Civitan), blood was divided into two conicals. Fifteen ml. of blood was aliqoted into one conical, and 25 ml. into another conical. Peripheral blood mononuclear cells (PBMC's) were isolated from the conical containing 15 ml. Monocyte-derived macrophages (MDM's) were isolated from the other conical containing 25 ml of blood.

PBMC's were isolated from the 15 ml. of blood by centrifugation over a Ficoll gradient and incubated in complete RPMI medium (10% FBS, Penicillian (100 U/ml), Streptomycin (100 μg/ml), and IL-2 (30 U/ml), and 0.05% $NaHCO_3$). Approximately $60x10^6$ PBMC's were stimulated for 15 min. with phytohemagglutin (PHA) (Sigma) at 5 ug/ml and incubated at 37°C, 5% CO_2. After 15 minutes, the PHA concentration was diluted to 2 μg/ml by adding 12 ml. of complete RPMI containing IL-2 (30 U/ml) and incubated for 24 hours at 37°C, 5% CO_2. After 24 hours, the cells were washed and 20 ml of fresh complete RPMI containing IL-2 (30 U/ml) was added and cells were incubated at 37°C, 5% CO_2 for 3 days. On the day of infection, 2×10^5 cells were plated in a 96-well plate with complete RPMI containing IL-2 (30 U/ml). PBMC's were infected in triplicate with 40 ng of p24 with LTR-Luc recombinant viruses. The day after infection, 150 μl of complete RPMI was removed and fresh complete RPMI with IL-2 was added. Three days post-infection cells were harvested, and lysed with 200 μl of 1X Cell Culture Lysis Reagent (Promega). Forty μl of the cell lysates were assayed for luciferase expression with a 10 s. integration time using a Monolight 2010 Luminometer (Analytical Luminescence Laboratory).

From the 25 ml. of blood, monocytes were isolated using the RosetteSep Antibody Cocktail (Stemcells Technologies). MDM's were plated at 1 x 10^6 cells/ml in a 48-well plate with RPMI containing 15% Human AB Serum (Sigma), penicillian (100 U/ml), streptomycin (100 ug/ml), Hepes (2.5 mM) and GM-CSF (1 ng/ml) (macrophage media). MDM's were incubated at 37°C, 5% CO_2 for 5 days. On the day of infection, MDM's were checked for macrophage morphology and washed twice with 1X DPBS (Gibco) and fresh macrophage media without GM-CSF was added. Macrophages were infected in triplicate with 40 ng of p24 of the LTR-Luc recombinant viruses. Four days post-infection, the cells were harvested for luciferase expression and assayed for luciferase activity as described above.

MAGI-CCR5 Assay

The MAGI-CCR5 (Multi-nuclear activation of galactosidase indicator) cell line was received from the AIDS reagent program. Protocol for maintenance and infection of MAGI-CCR5 cell line followed manufacturer's instructions. The day before infection, MAGI-CCR5 cells were plated at 4 x 10^4 cells/ml in complete DMEM containing 10% FBS, penicillian (100 U/ml), streptomycin (100 μg/ml), fungizone (0.25 μg/ml), L-glutamine (300 μg/ml), G418 (1 μg/ml), and hygromycin (50 U/ml). The cells were incubated for 24 hours at 37° C, 5% CO_2. The next day, cells were at approximately 40% confluency and media was removed from cells. Dilutions of Recombinant LTR-Luc viruses were made at 30, 60, and 90 ng of p24 and added to each well in a total of volume of 150 μl of complete DMEM without G418 and hygromycin with 20 μg/ml of DEAE-

Dextran. Cells were incubated at 37°C, 5% CO_2 for 2 hours. After the 2 hour incubation, 1 ml of complete DMEM without G418 and hygromycin was added to each well and incubated for two days at 37° C, 5% CO_2. After the 2 day incubation, one ml of fixing solution (1X PBS, 1% formaldehyde, 0.2% glutaraldehyde) was added to each well, and incubated at room temperature for 5 minutes. Fixing solution was removed and cells were washed twice in 1X PBS. After washing, 400 μl of staining solution (Potassium ferrocyanide (4 mM), Potassium ferricyanide (4 mM), $MgCl_2$ (2 mM), and 1X PBS) was added to each well and cells were incubated at room temperature for 50 min. at 37° C, 5% CO_2. Cells were then washed twice with 1X PBS, and 1 ml. of 1X PBS was added to each well for storage. The total number of blue stained nuclei was counted for each well under both 10x and 20x magnification with a light microscope.

Quantification of HIV DNA Copy Number by Real-time PCR

PBMC and macarophages were isolated from the same donor as described before. These primary cells were evaluated for both number of HIV infected cells and luciferase expression. Luciferase expression experiments were performed as described before, except infections were performed in duplicate. For the quantitation experiments, all LTR-Luc recombinant viruses were treated with 50U/ml of Deoxyribonuclease (Gibco-BRL) for 1 hour at room temperature prior to infection. PBMCs and macrophages were infected with 40 ng of p24 LTR-Luc recombinant virus in duplicate. In addition, one well of PBMC and macrophages were infected in the presence of AZT to serve as a negative control. PBMC and macrophages were both washed 24 hours post-infection to remove virus. For PBMC, cells were harvested on day 3 post-infection, and pelleted at 400 x g for 5 minutes in a 0.5 ml microcentrifuge tube. PBMC were then washed 2X with 1X DPBS (Gibco), and lysed by incubation at 50°C for 24-48 hrs. in 100 μl of K buffer containing 50 mM KCl, 10 mM Tris-HCl (ph 8.3), 2.5 mM MgCl2, 0.5% Tween 20, and 100 μg/ml Proteinase K (Gibco). After the incubation period, the lysed cells were incubated at 95°C for 5 min. to denature the proteinase K. On day 4 post-infection, macrophages were washed 2X with 1X DPBS (Gibco), and lysed with 200 μl of K buffer as described above.

The quantitation of HIV-1 copy number was based on the "real-time" quantitative PCR method. In brief, proviral copy number is determined by the cleavage of fluorescent dye labelled probe by the 5'-3' exonuclease activity of Taq DNA polymerase during PCR and measuring the fluorescence by the ABI Prism 7700 Sequence Detector System (PE Applied Biosytems). First, a standard curve was generated of the synthetic target of apo (5'-CTG GAA TTG CGA TTT CTG GTA AAC GGA AGT CTG GCA GGG TGA TTC TCG TAG G-3') and gag (5'-ATC TGG CCT GGT GCA ACT GGT CTA TCC CAT TCT GCA GCT TCC TCA TTG ATG ATT TGC ATG GCT GCT TGA TGT-3') to evaluate number of infected cells, and HIV proviral copies, respectively. The standard curve of the apo and gag target sequences was used to quantitate actual number of gag to apo copies. To evaluate the number of gag and apo copies within each infection, a standard curve was generated using serial dilutions of the chronically HIV-infected ACH-2 T-cell line which contains one proviral copy per cell. The following primer pair and probe spanning gag were: for gag primer 5'-ACA TCA AGC AGC CAT GCA AAT-3'; rev gag primer 5'-ATC TGG CCT GGT GCA ATA GG-3'; and gag probe sequence 5'-6-FAM-CAT CAA TGA GGA AGC TGC AGA CTG GGA TAG A-TAMRA-3'. The following primer pair and probe spanning apo were: for apo primer 5'-TGA AGG TGG

AGG ACA TTC CTC TA-3'; rev apo primer 5'-CTG GAA TTG CGA TTT CTG GTA A-3'; and apo probe sequence 5'-VIC-CGA GAA TCA CCC TGC CAG ACT TCC GT-TAMRA-3'. Amplification reactions (25 µl) contained 1X buffer A, 2.5 mM $MgCl_2$, 200 µm dATP, dCTP, and dGTP, 400 µM dUTP, 0.625 U of AmpliTaq Gold, 0.25 U of AmpErase UNG (PE Applied Biosystems), 0.25 µM of each primer, and 75 nM of probe. The thermal cycling conditions were 95°C for 10 min., and 40 cycles of 95°C for 15 sec., and 62°C for 1 min.

Calculations from Proviral Gag Copy Number

Tables 4-1, 4-2, and 4-3 show the raw data and calculations for number of gag copies and luciferase expression for the PBMC and macrophage infections with the LTR-Luc recombinant viruses of LAI, JR-FL, Brain, Lung, and PBMC. Gag copies were calculated by performing real-time PCR on all cell lysates in both macrophages and PBMCs isolated from the same donor. Evaluation of gag copies and measurement of luciferase expression were performed in duplicate for each LTR-Luc recombinant virus. Since gag copies were measured from 20 µl of lysate from both PBMCs (out of 50 µl total) and macrophages (out of 100 µl total), a correction factor of 2.5x for PBMC and 5x were used to calculate the number of gag copies detected in the total amount of cells from each well. A correction factor of 2.5X was used to correct for the total amount of luciferase expression within each well. To determine the gag per total number of cells for both PBMC and macrophages the following calculation was performed:

(Gag per 20 µl/cells per 20 µl) X 2.5 (correction factor for total well) X (Averge number of cells) = corrected gag per total cells. To determine the relative light unit (RLU) per corrected gag: RLU per total well/corrected gag per total cells. The calulation of relative promoter activity was: RLU per corrected gag/RLU per corrected gag of LAI X4 (for PBMC) and LAI R5 (for PBMC infected with LTR-luc R5 viruses and macrophages).The % of infected cells was determined by dividing the gag per total cells by the average cell number among each well.

Results

Parsimony analysis of both the nucleotides of the LTR region (-335 to –105) and the amino acids of the V3 region of env was performed to elucidate tissue specific lineages (Figure 4-1). Two major lineages were found according to the parsimony analysis of both the LTR and V3 regions. One lineage consisted of brain sequences, and the other lineage was comprised of sequences from all other tissues. Similar topography was observed with both the LTR and env regions.

Concordance between tissue specific segregation of both the LTR and env regions was found with sequences obtained from the brain, PBMC's, and thymus. Brain LTR and env sequences were always found clustered together and independently segregated from the sequences obtained from other tissues (Figure 4-1). Early PBMC LTR and env sequences concordantly segregated from other tissues. Lung LTR sequences all grouped on the same branch, and were found clustered with two thymus LTR's. Unfortunately, lung env sequences were not available for comparison. Late PBMC, and thymus LTR sequences were clustered together which was concordant with Late PBMC and thymus env sequences that were also grouped on the same branch. A subset of env sequences obtained from the thymus with a high V3 charge clustered with other high charge V3 sequences from the lymph node that segregated from other tissues. Discordantly, thymus LTR sequences segregated on the same branch as Late PBMC's, lung, and thymus.

LTR Sequences from Each Tissue

The alignment of tissue LTRs revealed several tissue specific polymorphisms that occurred within known transcriptional factor binding sites (Figure 4-2). The majority of LTR's obtained from the brain had 8 site-specific polymorphisms that occurred at positions –270 (NFAT), -203, -171 (C/EBP), -156, -153, -149 (Ets-1), and –132 (TCF). Lung LTRs had 2 site-specific polymorphisms at positions –334 (COUP-1), and –301. The dominant thymus and late PBMC LTR's were identical and shared a unique nucleotide polymorphism at position –310.

LTR-Luc Recombinant Virus PBMC Timecourse Infection

To determine the time post-infection in PBMC with optimum luciferase expression, 2×10^5 PBMC were infected in duplicate with 40 ng of p24 per LTR-Luc recombinant virus. The construction of the LTR-Luc recombinant viruses is outlined in Figure 4-3. Cells were harvested at 24 hour timepoints from 0-4 days post-infection and assayed for luciferase activity (Figure 4-4). Three different LTR-Luc recombinant viruses were evaluated including LAI, MB01, and MB03. MB01 and MB03 are previously characterized LTRs that have consistently demonstrated a promoter activity of LAI-like, and 3-5x greater activity than LAI, respectively (Data not shown). On Days 0 and 1 post-infection there was little to no luciferase expression. Day 2 was the earliest timepoint that had detectable luciferase expression for all LTR-Luc recombinant viruses tested. Day 3 had the highest luciferase expression for all LTR-Luc recombinant viruses tested. On average there was a 2 to 5-fold difference in luciferase expression between days 2 and 3. Luciferase expression decreased by Day 4. Therefore, day 3 post-infection was optimal and used in subsequent PBMC infections.

LTR-Luc Recombinant Virus Macrophage Timecourse Infection

To determine the optimum luciferase expression in macrophages after infection, 1×10^6 macrophages were infected in duplicate with 40 ng p24 of the JR-FL R5 LTR-Luc recombinant virus (Figure 4-5). Macrophages were harvested at 24 hour timepoints on days 0, 1, 2, 3, 4, 5, and 6 post-infection and assayed for luciferase activity. Minimal luciferase activity was detected from days 0-3. Day 4 post-infection had the highest luciferase expression with a 10-fold increase in luciferase expression between days 3 and 4. Luciferase expression on days 5 and 6 was lower than day 4. Therefore, day 4 post-infection of macrophages with the LTR-Luc recombinant virus was optimal for luciferase expression and utilized in all macrophage infection experiments.

MAGI-CCR5 assay

Promoter differences among LTRs may be due to variability in quantity of infectious virions between viral preparations. Therefore it was necessary to measure the number of infectious particles per LTR-luciferase recombinant virus. Since these LTR-luc recombinant viruses are single-cycle and replication defective, standard methods for measuring infectious dose such as $TCID_{50}$ cannot be utilized. Therefore, the MAGI-CCR5 assay was performed to determine the number of infectious virions per LTR-Luc recombinant viral stock. The MAGI-CCR5 cell line contains one integrated copy of the HIV-1 LTR linked to the β-galactosidase gene. This indicator cell line can detect both X4 and R5 using viral strains after one round of infection and can be used to titer viral isolates including those that are replication defective. Different concentrations of p24 were applied to the MAGI cells and number of blue nuclei were counted after 2 days (Table 4-1). The infectivity ratio (I.R.) (# of blue cells/ng of p24) were calculated for 3 different concentrations of p24. The average infectivity ratio was the average of the 3 infectivity ratios ± standard error of the mean.

The average infectivity among the LTR-Luc recombinant viruses ± standard error of the mean was LAI X4 0.67 ±(0.14), JR-FL X4 0.50 ±(0.11), Brain X4 0.43 ±(0.09), Lung X4 1.02 ±(0.47), LAI R5 0.64 ±(0.02), JR-FL R5 0.29 ±(0.006), Brain R5 0.26 ±(0.09), and Lung R5 ±(0.052) (Table 4-1). The range of the infectivity ratios was 0.26-1.02 with a mean of 0.5. There was no statistical difference among the average infectivity for all LTR-Luc recombinant viruses (p=0.25, ANOVA). Therefore, there was no difference in the infectious units per ng of p24 among the constructs, and amount of p24 used for infection of the MAGI cells was concordant with number of infected cells in most cases. Therefore, primary cells such as PBMCs and macrophages were infected with equivalent amounts of p24, and any differences in luciferase expression can be attributed to true LTR promoter differences rather than variability in infectious virions in viral stocks.

PBMC Infection with LTR-Luc Recombinant Viruses

PBMC ($2x10^5$) were infected in triplicate from 3 independent donors with 40 ng of p24 of the LTR-luc recombinant viruses. PBMC were harvested 3 days post-infection and assayed for luciferase activity (Figure 4-6). A representative experiment from the primary cells of Donor 1 is shown in Figure 4-6. The results from the PBMC infection from all donors is shown in Figure 4-7. From the representative experiment, for the LTR-luc recombinant viruses using X4 the order from highest to lowest with regard to relative promoter activity was: JR-FL X4 (5.3) > PBMC X4 (3.7) > Brain X4 (2.9) > Lung X4 (2.3) > LAI X4 (1.0). The order from highest to lowest relative promoter activity for those recombinants using R5 was: PBMC R5 (7.1) > JR-FL R5 (4.2) > Brain R5 (3.4) > Lung R5 (2.7) > LAI R5 (1.0). The JR-FL X4 recombinant had the highest promoter activity in the X4 subset, whereas the PBMC R5 recombinant had the highest promoter activity in the R5 subset. The LAI recombinant had the lowest promoter activity in both subsets. Among the lung, brain, and PBMC recombinant viruses the lung recombinant was always the lowest or LAI-like, whereas the PBMC recombinant consistently had the highest promoter activity.

Macrophage Infection with LTR-Luc Recombinant Viruses

Macrophages (1 x 10^6) obtained from the same three donors from which the PBMC were received were infected in triplicate with 40 ng of p24 of LTR-Luc recombinant viruses. Macrophages were harvested 4 days post-infection, and assayed for luciferase activity. Figure 4-8 shows a representative experiment from donor 1, and figure 4-9 shows the results from all donors. Results were typically consistent among all donors with regard to relative promoter activity. The results from highest to lowest with regard to relative promoter activity from donor 1 were: PBMC R5 (17) > JR-FL R5 (8.9) > Brain R5 (6.0) > Lung R5 (3.3) > LAI (1.0). As observed with the promoter activity in PBMC, LAI LTR had the lowest promoter activity. Among the lung, brain, and PBMC LTR R5 viruses, the PBMC had the highest promoter activity, while the Lung LTR had the lowest promoter activity. The magnitude of promoter differences between LTRs was much greater in macrophages than PBMC. For example, in PBMC the differences among LTR-Luc recombinant X4 viruses ranged from 2.3 (Lung X4) to 3.7 (PBMC X4). In contrast, the difference among LTR-Luc recombinant R5 viruses tested in macrophages ranged from 3.3 (Lung R5) to 17 (PBMC R5).

Percentage of Infected Cells for PBMC and Macrophages

To rule out the possibility that promoter differences were due to the number of infected cells we had to measure how many PBMC and macrophages were infected. I performed this by measuring the number of proviral gag copies present during an infection to estimate number of cells infected. This assay allowed us to measure several aspects: number of infected cells, luciferase units per infected cell, and relative promoter activity corrected for number of infected cells. This data is presented in the following sections. Approximately 0.2% of PBMC were infected (range 0.1 to 0.2) with a range of gag copies per total cells from 579 to 2439 per approximately 8 x 10^5 cells with either the LTR-Luc recombinant X4 or R5 viruses (Table 4-2 and 4-3). However, the % of total PBMC infected with the LTR-Luc recombinant R5 viruses may be misleading since not all PBMC are equally susceptible to infection with an R5 virus. Only about 10% of PBMCs will be expressing CCR5 with the majority of those R5 expressing cells being CD45RO. Therefore, assuming that only 10% of the PBMC were susceptible to infection with a LTR-Luc recombinant R5 virus that would increase the number of infected cells to 1.6% (range 0.6 to 2.6) since now the PBMC population that can be infected is decreased (Table 4-3). Therefore, the PBMC expressing R5 are significantly more infected than PBMC expressing X4. About 0.4% (range 0.2 to 0.8) of macrophages were infected per well, by the LTR-Luc recombinant virus with a range of 434 to 1983 gag copies per 2 x 10^5 macrophages (Table 4-4).

Luciferase Expression per Gag Copy

The luciferase units per gag copy corrected for number of cells was significantly higher in macrophages than PBMC (Figure 4-10). The average luciferase unit per corrected gag was 190 LU/gag in macrophages versus 16.6 LU/gag and 3.6 LU/gag in

PBMC infected with X4 or R5 LTR-Luc recombinant viruses respectively (Figures 4-10 and 4-11). This result clearly demonstrated that gene expression in macrophages is high PBMCs infected with LTR-Luc R5 viruses expressed the lowest amount of luciferase units per gag copy.

Relative Promoter Differences among the LTR-Luc Recombinant Viruses

To evaluate promoter differences among the LTR-Luc recombinant viruses, the LU/gag copy were compared to that of LAI LU/gag copy (Figure 4-12). The relative promoter differences among the LTR-Luc X4 recombinant viruses in PBMCs were from highest to lowest: PBMC X4 (7.5) > Brain X4 (5.2) > JR-FL X4 (3.7) > Lung X4 (1.9) > LAI X4. The promoter differences among the LTR-Luc R5 recombinant viruses in PBMCs were: PBMC R5 (2.2) > Brain R5 (1.5) > LAI R5 (1.0) > JR-FL R5 (0.7) > Lung R5 (0.6). For macrophages infected with the LTR-Luc recombinant R5 viruses the relative promoter differences were: PBMC R5 (4.4) > Lung (4.2) > Brain (2.1) > JR-FL (1.2) > LAI (1.0). Therefore, the relative promoter differences among the tissue LTR constructs remained constant when accounting for number of infected cells. This result demonstrates that the promoter differences are due to the LTR and not number of infected cells.

The PBMC LTR-Luc recombinant virus had the highest promoter activity in both PBMCs and macrophages. The brain, PBMC, and lung LTR-Luc recombinant viruses always had different relative promoter activities from each other in both PBMCs and macrophages. The lung LTR-Luc recombinant demonstrated cell-type specific promoter expression. The lung LTR-Luc virus had the lowest relative promoter activity in PBMC, yet had one the highest relative promoter activities in macrophages. This result demonstrated a cell-type specific gene expression impacted by the LTR.

Site-Directed Mutagenesis of the Brain LTR

Specific nucleotide changes within LTR sequences obtained from various tissues may have a profound impact on cell-type specific gene expression. Therefore, I focused a site-specific investigation of the LTR obtained from the brain. The brain LTR was most likely obtained from a microglial cell since this cell type is the predominantly infected cell in the brain (196) . Multiple site-specific polymorphisms were found within the brain LTR that were not identified from the LTR sequences from other tissues. The majority of LTRs obtained from the brain had 7 site-specific polymorphisms that occurred at positions –270 (NFAT), -203, -171 (C/EBP), -156, -153, -149 (Ets-1), and –132 (TCF). Three of these unique brain polymorphisms were further investigated based on their potential role in cell type specific expression particularly in macrophages. The unique polymorphisms at position –270, -171, and –156 were examined by changing these positions to match the sequence found in the other tissue LTRs (Figure 4-2). The polymorphism within the brain LTR at position –270 was further investigated since the region surrounding this position (-256 to –296) of the $\mathrm{HIV}_{\mathrm{JR\text{-}CSF}}$ LTR but not of the $\mathrm{HIV}_{\mathrm{LAI}}$ LTR specifically bound protein in nuclear extracts of newborn brain from mice tested in electrophoretic mobility shift assays. No specific protein binding was observed to this region in liver or HeLa cell nuclear extracts. In addition, additional phylogenetic studies of brain derived LTRs have suggested considerable genetic variability within this region implying some potential role in cell type specific gene expression (42). The polymorphism at position –171 was further investigated since it occurred within a macrophage specific transcriptional factor binding site known as C/EBP (76-78). In addition $\mathrm{HIV}_{\mathrm{JR\text{-}CSF}}$ and $\mathrm{HIV}_{\mathrm{JR\text{-}FL}}$ which have been derived from nervous tissue from the same patient do not have similar phenotypes. $\mathrm{HIV}_{\mathrm{JR\text{-}CSF}}$ grows in brain glioma explant cultures whereas HIV_{JR-FL} fails to replicate to detectable levels in these tissue cultures. One of the genetic differences between these sequences occurs within the C/EBP site at the position of -170. The polymorphism at position –156 was further investigated since this change introduced a novel ATF/CREB binding site based on the TFSEARCH program for the identification of transcription factor binding sites (4). ATF/CREB transcription factors isolated from both Jurkat (T-cell line) and U373MG (astroglial) cell lines can bind to the HIV-1 LTR (106,107). In addition, these DNA protein complexes of ATF/CREB and the LTR differed between the U-373MG and Jurkat cell lines in terms of relative abundance and mobility (106,107). Another study has demonstrated that ATF/CREB and C/EBP can affect basal LTR activity and LTR function following IL-6 stimulation of U937 (monocytic) cells (156).

PBMC Infection with Site-Directed LTR-Luc Recombinant Viruses

PBMC ($2x10^5$) were infected in triplicate from 3 independent donors with 40 ng of p24 of the LTR-luc recombinant viruses. PBMC were harvested 3 days post-infection and assayed for luciferase activity (Figure 4-13). A representative experiment from the primary cells of Donor 1 is shown in Figure 4-13. The results from the PBMC and macrophage infection from all donors are summarized in Table 4-5. From the representative experiment, for the LTR-luc recombinant viruses using X4 the order from highest to lowest with regard to relative promoter activity was: C270A X4 (6.5) > JR-FL X4 (5.3) > G171T X4 (5.1) > PBMC X4 (3.7) > Brain X4 (2.9) > A156G X4 (2.8) > Lung X4 (2.3) > LAI X4 (1.0). The order from highest to lowest relative promoter activity for those recombinants using R5 was: C270A R5 (8.9)> G171T R5 (7.6) > PBMC R5 (7.1) > A156G R5 (5.4) > JR-FL R5 (4.2) > Brain R5 (3.4) > Lung R5 (2.7) > LAI R5 (1.0). The recombinant 270 X4 and R5 had the highest promoter activity in both

---

the X4 and R5 subsets and LAI had the lowest promoter activity in both subsets. Among the lung, brain, and PBMC recombinant viruses the lung recombinant was always the lowest or LAI-like, whereas the PBMC recombinant consistently had the highest promoter activity. All site-directed recombinants. (C270A X4, C270A R5, G171T X4, G171T R5, and A156G R5) with the exception of A156G X4 resulted in an increase of relative promoter activity compared to the brain LTR.

Macrophage Infection with Site-Directed LTR-Luc Recombinant Viruses

Macrophages (1 x 10^6) obtained from the same three donors from which the PBMC were received were infected in triplicate with 40 ng of p24 of LTR-Luc recombinant viruses. Macrophages were harvested 4 days post-infection, and assaayed for luciferase activity. Figure 4-14 shows a representative experiment from donor 1, and Table 4-5 shows the results from all donors. Results were typically consistent among all donors with regard to relative promoter activity. The results from highest to lowest with regard to relative promoter activity from donor 1 were: G171T R5 (24.8) > PBMC R5 (17) > C270A R5 (8.9) > A156G R5 (10.6) > JR-FL R5 (8.9) > Brain R5 (6.0) > Lung R5 (3.3) > LAI (1.0). As observed with the promoter activity in PBMC, LAI LTR had the lowest promoter activity. Among the lung, brain, and PBMC LTR R5 viruses, the PBMC had the highest promoter activity, while the Lung LTR had the lowest promoter activity. The magnitude of promoter differences between LTRs was much greater in macrophages than PBMC. For example, in PBMC the differences among LTR X4 viruses ranged from 2.3 (Lung X4) to 6.5 (C270A X4). In contrast, the difference among LTR R5 viruses ranged from 3.3 (Lung R5) to 25 (G171T R5). All site directed LTR-Luc recombinants (C270A, G171T, and A156G R5) had a promoter activity greater than the Brain LTR.

Discussion

Phylogenetic analysis of LTR's obtained from various tissues revealed independent lineages among the lung, PBMC, and brain. Independent segregation between brain and non-brain LTRs has been reported before in one other previous study (2). However, results from Ait Khaled *et al.* concluded there was no segregation between lung and PBMC LTRs. Although, segregation between lung and other tissue LTRs was identified in the previous study, the bootstrap value as not considered significant. Independent genetic segregation between the lung and PBMC has been found according to the V3 region of env, but our report is the first to identify independent lineages evolving through both the LTR and env regions (86).

LTR sequences obtained from the brain had the most significant independent clustering of sequences with most unique nucleotide polymorphisms occuring in transcriptional binding sites upstream from the NF-kB sites. Our finding was in agreement with a previous report that demonstrated considerable variation seen in regions upstream of the NF-kB sites and several nucleotide variations found within the transcriptional binding sites of NFAT and USF (42). The core promoter and enhancer sites were conserved among all tissue LTRs (data shown in Chapter 2). Overall, these results suggest a mandatory requirement for specific sites within the LTR particularly the core promoter and enhancer, whereas transcriptional factor binding sites located upstream may be more pliable and undergo a selection for specific tissue transcriptional factors.

The predominant bran, lung, and PBMC LTR had distinct promoter differences in both macrophages and PBMCs. The PBMC LTR-Luc virus had the highest promoter activity in both the macrophages and PBMCs. The brain and lung LTR-Luc viruses had similar promoter activities in both PBMCs and macrophages when examining the relative promoter activity without evaluation of LU per gag copy. The predominant LTR from the blood may represent a lineage that has evolved to express in both PBMC and macrophages. This is the first study to evaluate tissue specific LTRs from within a patient. Most of the LTR studies to date have demonstrated that promoter activities from within and between patients have a wide range of transcriptional activity without any correlation to clinical progression (53,54,102,125). Most of the previous studies have only evaluated PBMC-derived LTRs, and typically utilized transient transfections. This approach, although fruitful, may have been biased since LTRs were not obtained from various tissues, and were not tested in primary cells such as macrophages and PBMCs. The brain and lung represent sites where the predominantly infected cell is the macrophage and PBMC. This may explain why the brain and lung LTR-Luc viruses may have had similar relative promoter activities, since both were probably macrophage derived. The lung and brain had different LTR sequences, yet similar promoter activities in both macrophages and PBMCs which suggests indpendent mechanisms for determining promoter expression.

The mutational analysis of the brain LTR revealed several unique sites that appear to have an overall repressive effect. Several unique polymorphisms were found within the brain LTR at positions –270, -171, and –156 that were not found in any other tissues. Our mutational analysis changed those specific sites back to the nucleotide sequence found in other tissues. The 270, and 171 LTR-Luc recombinant viruses had a greater promoter activity than the brain LTR-Luc virus in both macrophages and PBMC. In contrast, the 156 LTR-Luc virus did not show any significant change from the brain LTR in both PBMC and macrophages. The position at –270 and –171 encompasses the

NFAT, and C/EBP sites, respectively. Several studies examining the regions encompassing these sites have revealed that there are both potential activator and repressor functions in this region (96,118,201). In particular, many brain-derived LTR sequences share many polymorphisms within the NFAT site between –292 and –255 (1,2,42). Kurth *et al.* showed that the region between –296 to –256 of JR-FL was able to bind to brain-derived proteins, whereas the LAI LTR was not. Kim *et al.* demonstrated that DNA substitutions within the region between –201 to –130 significantly lowered transcriptional activity in T cells.

Evaluation of the luciferase units (LU) per gag revealed distinct differences between different primary cells with regard to infectivity and promoter expression. CD45RA cells are immunologically naïve, express CXCR4, and comprise the majority of PBMCs. CD45R0 cells have immunological memory function, express CCR5 (some CXCR4), and are typically about 10% of the PBMCs after PHA stimulation. Our ability to utilized both a X4 (LAI) and R5 (JR-FL) envelope allowed us to target our LTR-Luc viruses to these specific cell subsets of CD45RA, CD45RO, and macrophages Based on % of infected cells and RLU per gag copy, CD45RA cells and macrophages appear to be equally permissive for infection, yet macrophages are extremely optimal for promoter function of the LTR. In striking contrast, CD45RO cells are highly permissive for infection, yet are the least optimal for promoter function of the LTR. These results are not concordant with previous published reports that demonstrate that CD45RO cells are more permissive for HIV replication than CD45RA cells when cells where stimulated through CD3 activation (122,181) . When cells are stimulated by PHA, both CD45RA and CD45RO cells produce similar amounts of virus (122,165). All of our experiments were conducted with PHA stimulated PBMCs, which may in part account for the similarities between CD45RA and CD45RO promoter function.

The use of single-cycle recombinant LTR-Luc recombinant viruses allowed the evaluation of promoter activity in the context of primary cells. In addition the promoter differences observed among the tissue LTRS were entirely due to promoter function since these LTR-Luc recombinant viruses were congenic. Therefore, all LTR-Luc recombinant viruses were identical except for their 3' LTR. In addition, the results from our MAGI assay demonstrated similar numbers of infectious units per ng of p24. Also, our viral construction method avoid the use of prolonged virus cultivation therefore minimizing the occurrence of introducing polymorphisms within the genome.

The findings from this study demonstrate the adaptibility of HIV to infect different types of cells. In particular, it is possible that HIV promoter activity is inversely correlated to the proliferation capability of the target cell. For example, macrophages are terminally differentiated cells that may not undergo stimulation unless upon exposure to cytokines such as TNF or IL-6, therefore basal promoter activity is required to be high in a transcriptionally non-permissive environment. In contrast, CD45RO cells can undergo several cycles of expansion in response to other antigens, therefore viral progeny can be duplicated upon cell cycle and which negates the need for high basal LTR promoter activity.

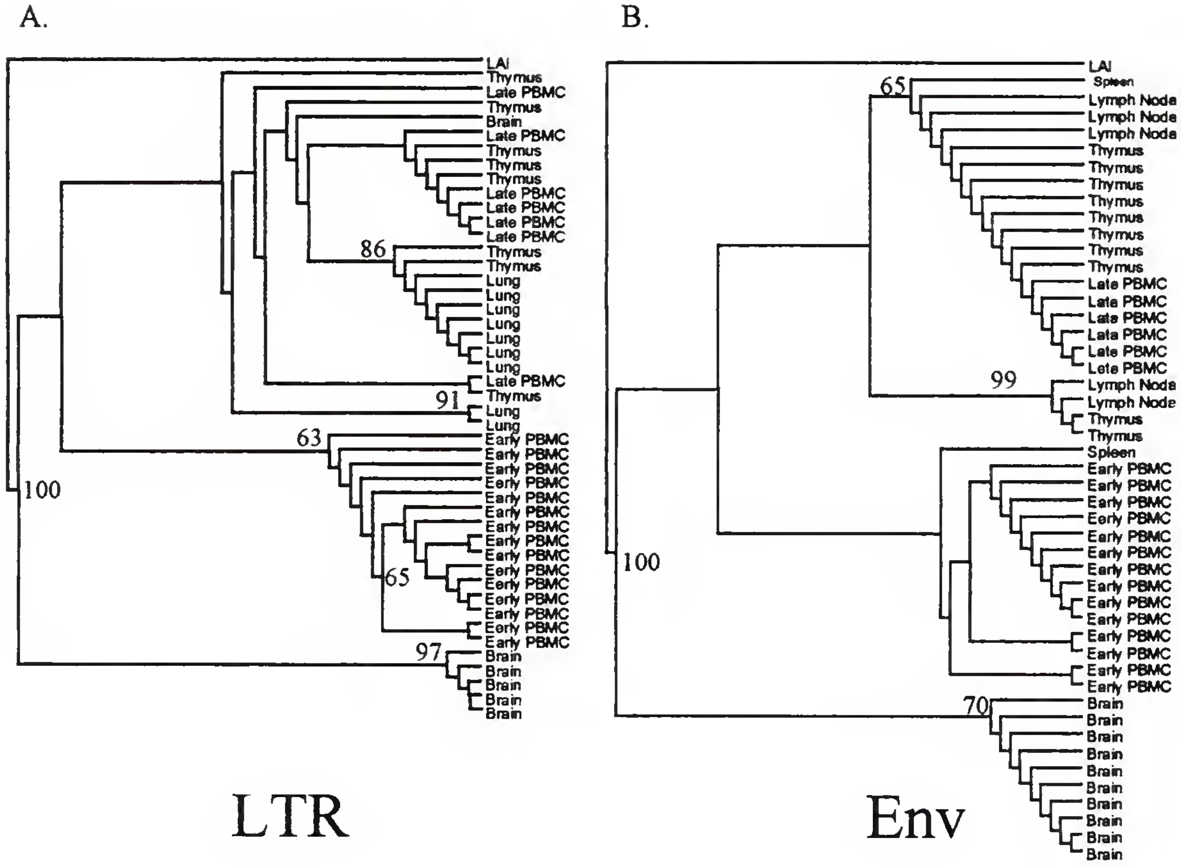

Figure 4-1. Phylogenetic analysis of the tissue LTR and V3 regions from Patient C/S1. Parsimony analysis was performed on the nucleotides of the LTR between –335 to –105, and the amino acid sequence of the V3 region. A) LTR, B) Env V3.

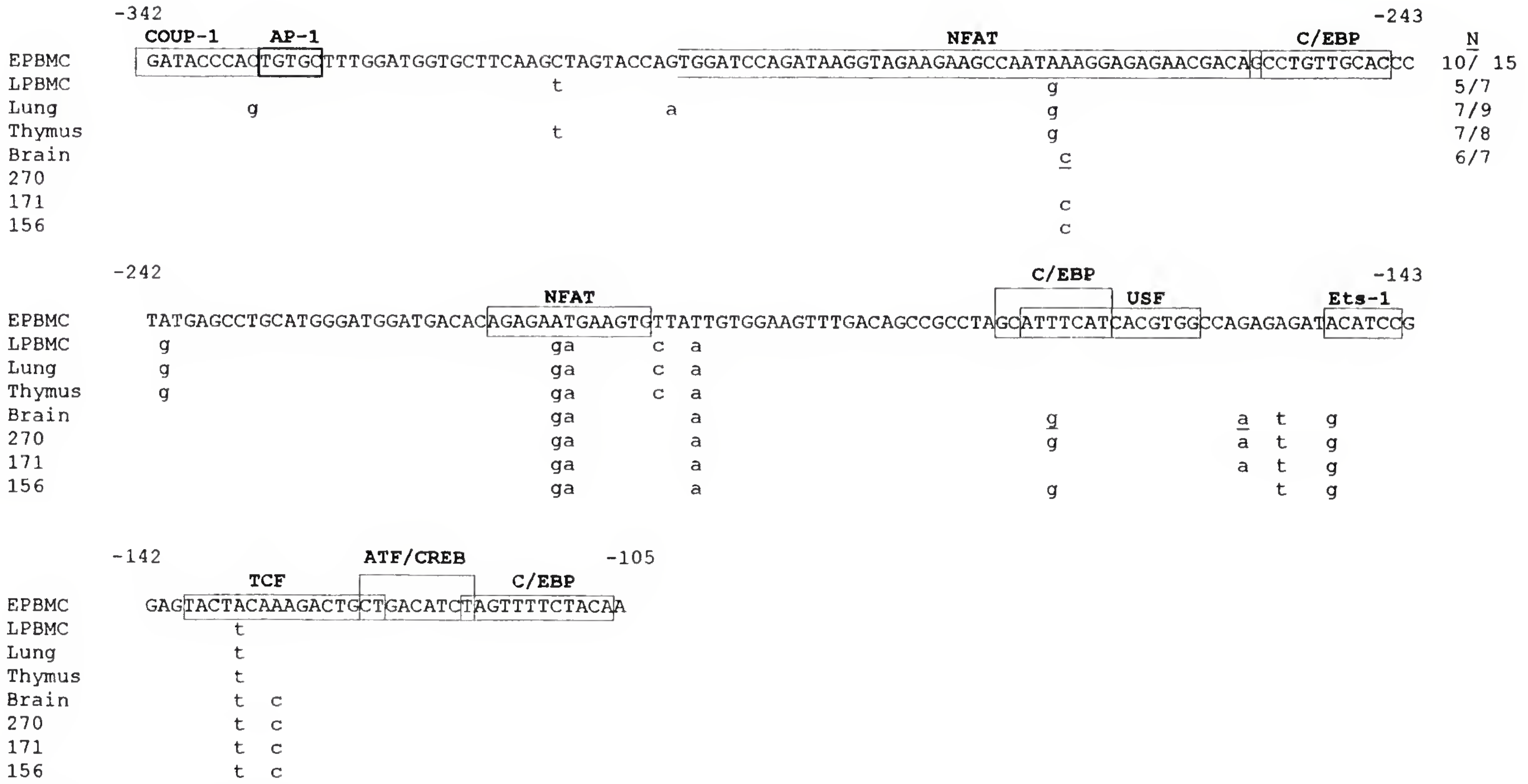

Figure 4-2. Alignment of LTR sequences. The major tissue specific LTRs from –342 to –105 are aligned to the EPBMC LTR. N refers to frequency to frequency of LTR sequence to total number of LTR sequences obtained from that tissue. Transcriptional factor binding sites are highlighted. A space indicates identical sequence to reference, and a letter indicates a difference. The nucleotides that were changed in the brain LTR to the EPBMC LTR are underlined.

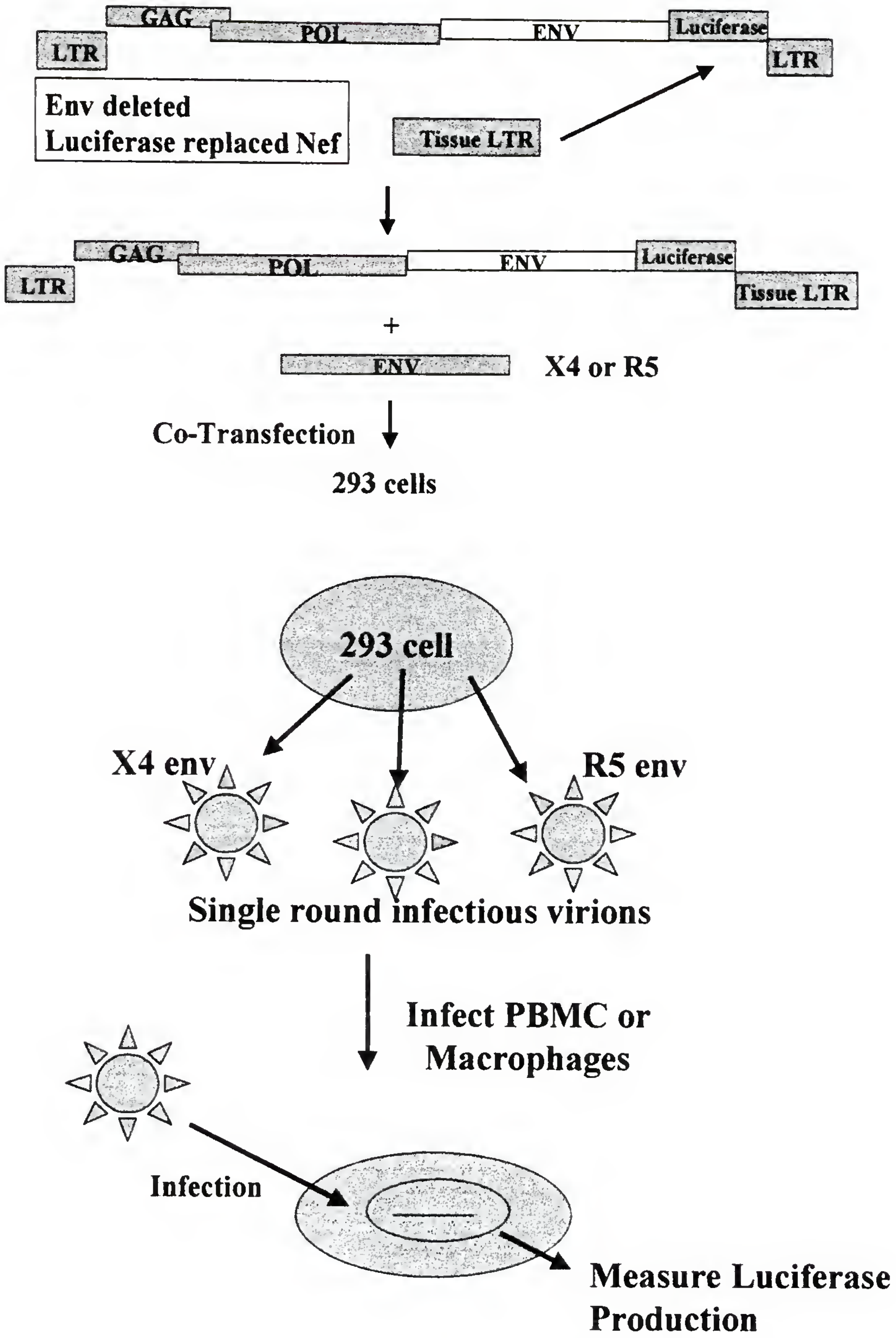

Figure 4-3. Methodology of construction and measurement of LTR-Luc Recombinant Viruses.

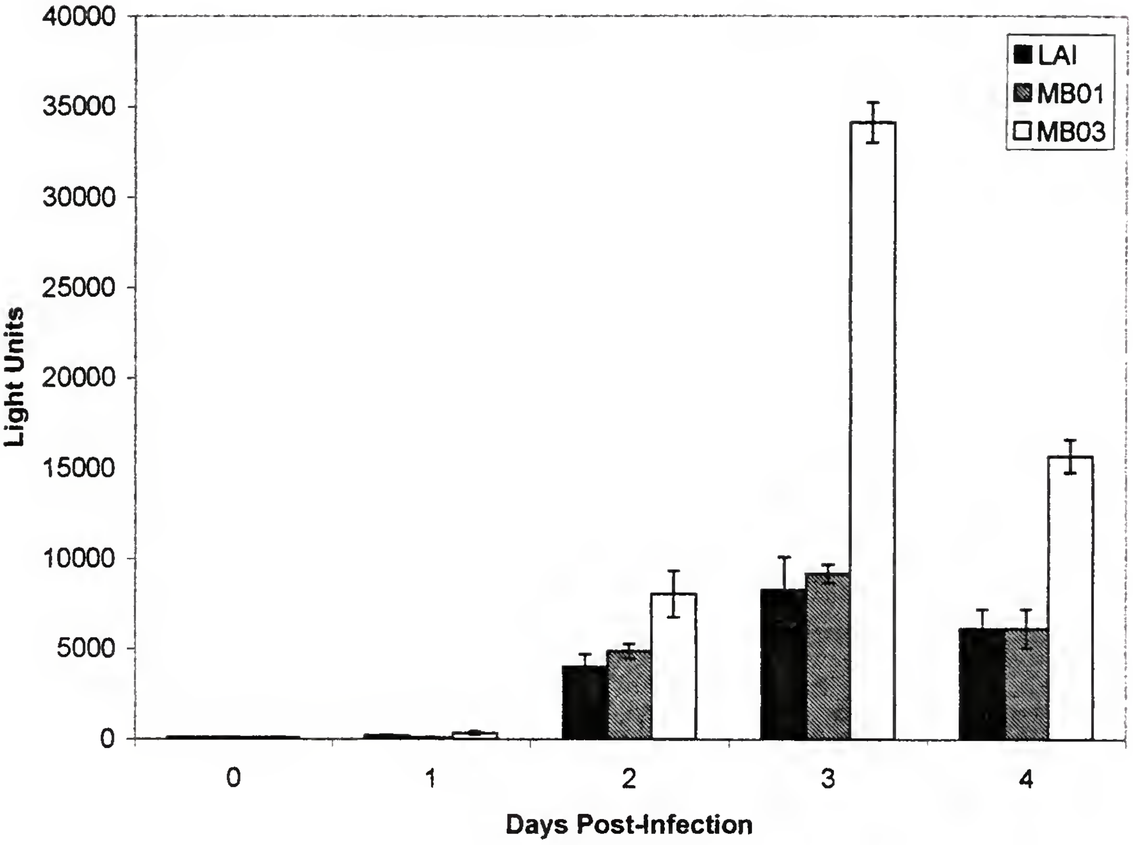

Figure 4-4. LTR-Luciferase recombinant virus timecourse experiment in PBMC. PBMC were infected with 20 ng of p24 of LAI, MB01, and MB01 X4 LTR-Luc recombinant viruses. At timepoints, 0, 1, 2, 3, and 4 days post-infection PBMC's were harvested and assayed for luciferase expression.

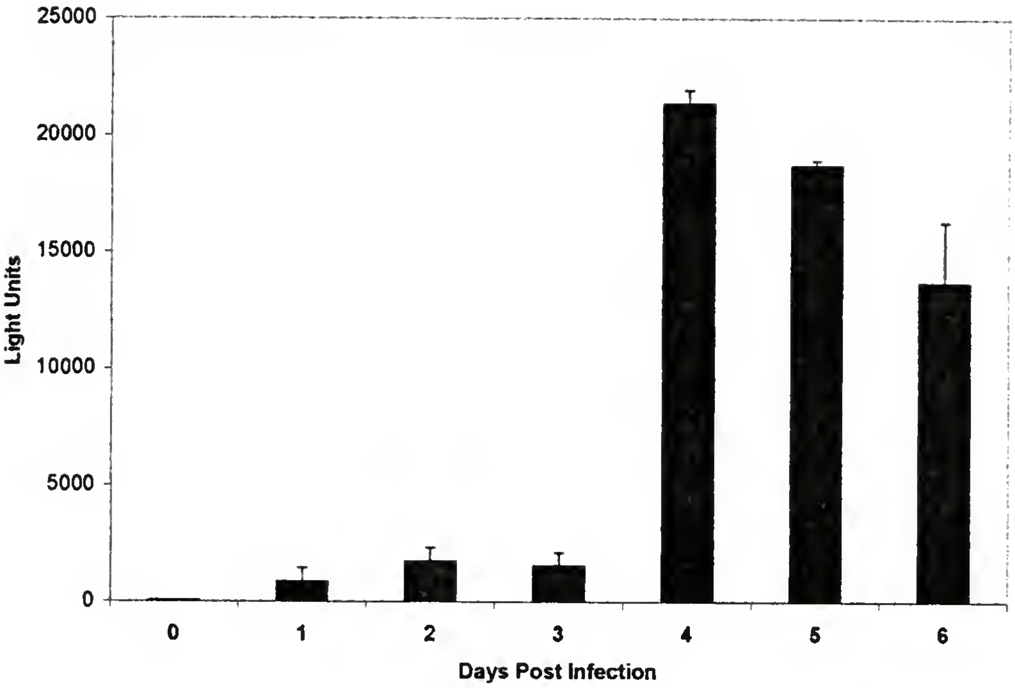

Figure 4-5. LTR-Luciferase timecourse infection with macrophages. Macrophages were infected with 40 ng of the JR-Fl R5 LTR-Luc recombinant virus. Macrophages were harvested at days, 0, 1, 2, 3, 4, 5, and 6 post-infection and assayed for lucifersase activity.

TABLE 4-1
MAGI Assay Results from LTR-Luc Recombinant Viruses

		X4 Envelope			R5 Envelope		
Virus LTR	p24 (ng)	Blue Cells	I.R.[A]	Mean I.R.±SEM[B]	Blue Cells	I.R.	Mean I.R.±SEM
LAI	30	28	0.9	0.7 (0.1)	20	0.7	0.6 (0.02)
	60	37	0.6		39	0.7	
	90	42	0.5		53	0.6	
JR-FL	30	21	0.7	0.5 (0.1)	9	0.3	0.3 (0.006)
	60	29	0.5		17	0.3	
	90	28	0.3		25	0.3	
Brain	30	10	0.3	0.4 (0.1)	17	0.6	0.6(0.1)
	60	21	0.4		42	0.7	
	90	55	0.6		35	0.4	
Lung	30	10	0.3	1 (0.5)	13	0.4	0.4 (0.05)
	60	47	0.8		22	0.4	
	90	175	1.9		36	0.4	

[A] Infectivity ratio is # of blue cells/ng p24 (# of infectious virions per ng of p24)

[B] Average infectivity is the average of all infectivity ratios with the standard error of the mean

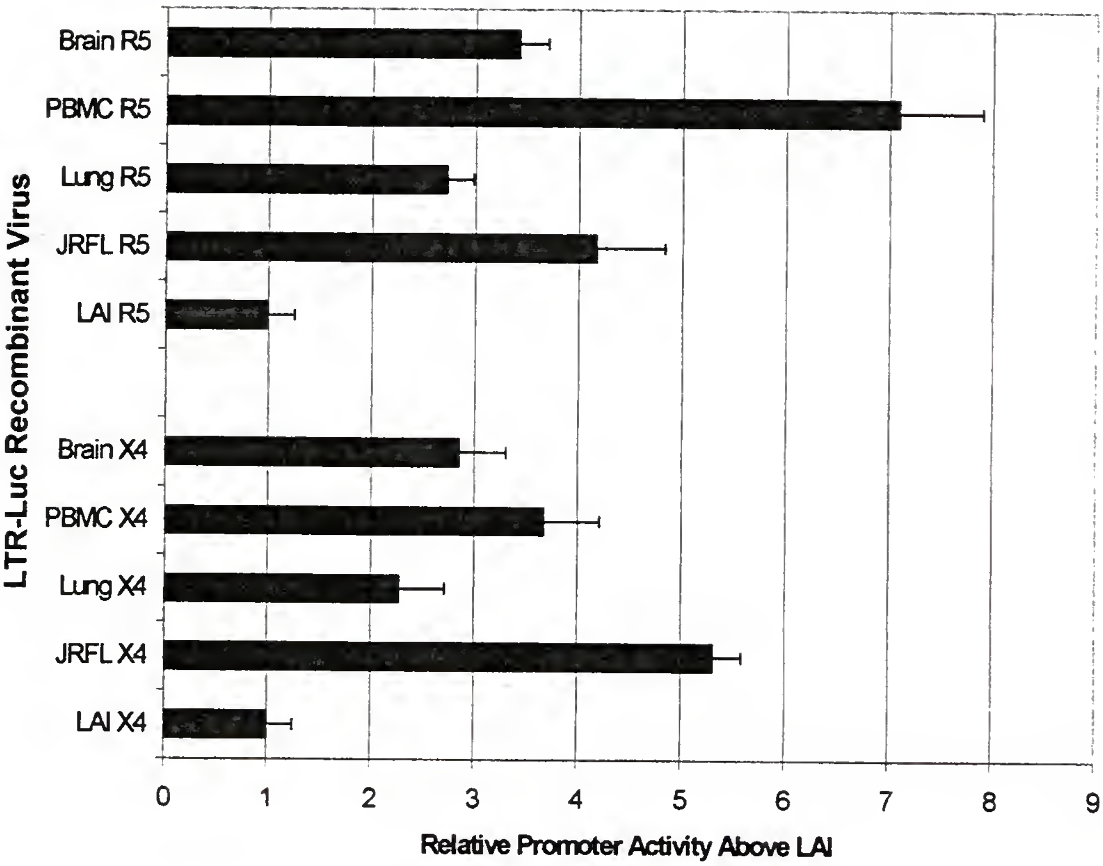

Figure 4-6. Representative experiment of PBMC infection with LTR-Luc recombinant viruses. PBMC's were plated at 2 x 10^5 cells in a 96-well plate and infected in triplicate with 40 ng of p24 of recombinant viruses. PBMC's were infected with either X4 or R5 viruses. PBMC's were collected 3 days post-infection, lysed, and assayed for luciferase activity. Error bars represent standard error of the mean.

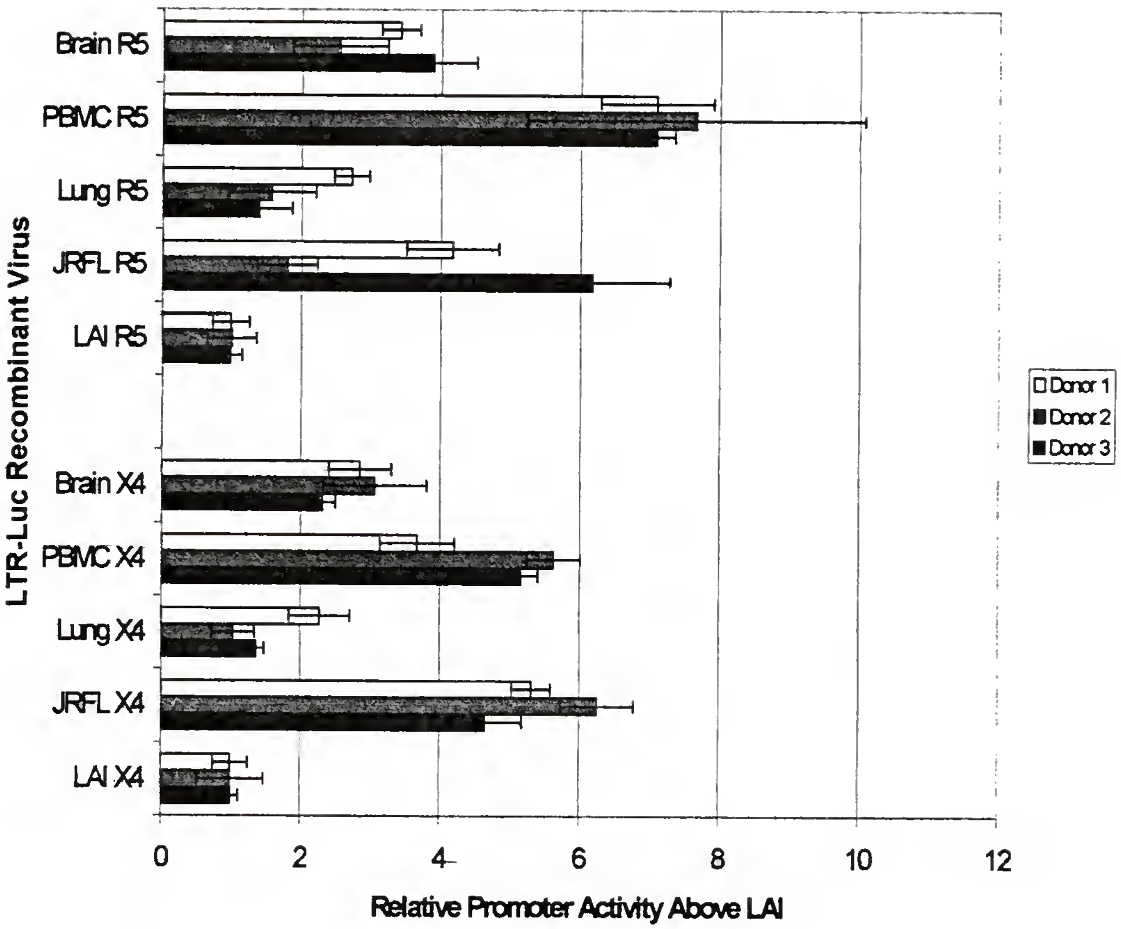

Figure 4-7. PBMC infection with LTR-Luc recombinant viruses from all donors. PBMC's were infected with LTR-Luc recombinant viruses as described before in Figure 4-6. Error bars represent standard error of the mean.

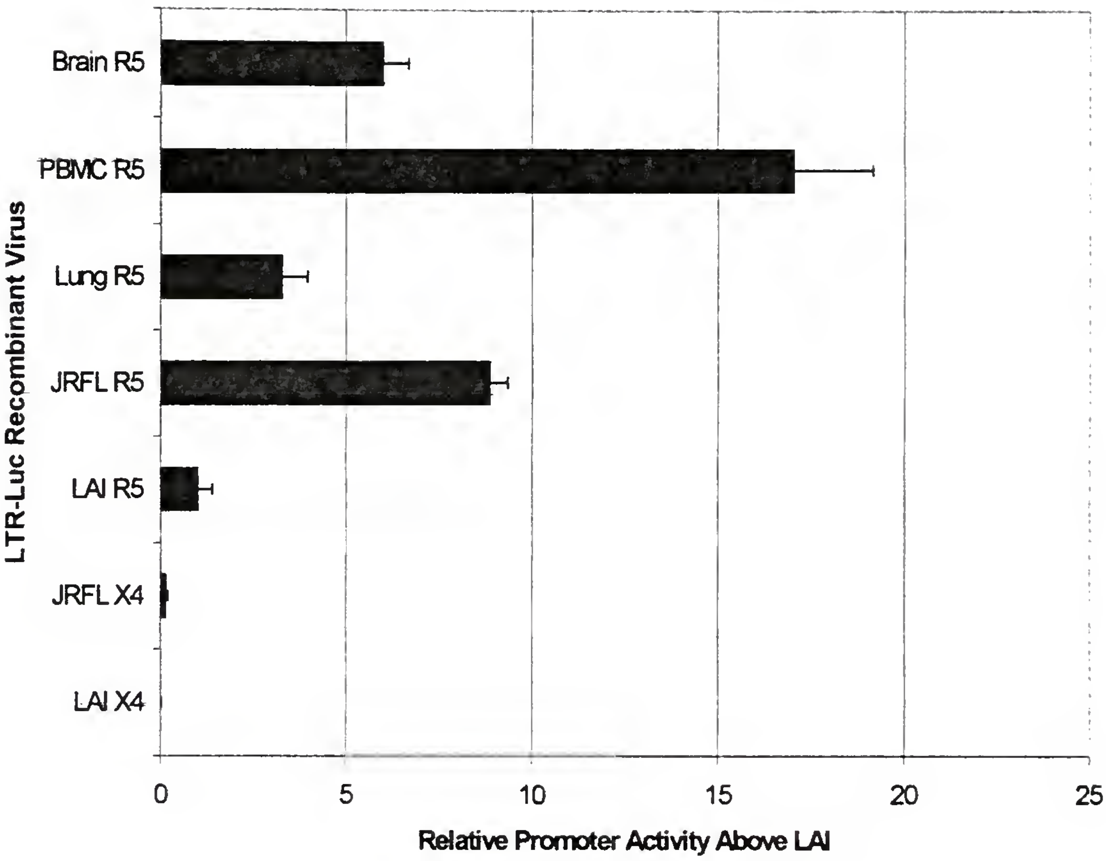

Figure 4-8. Representative infection of macrophages with LTR-Luc recombinant viruses. Monocytes were plated at 1×10^6 cells/ml in a 48-well dish and allowed to differentiate for 5 days in the presence of GM-CSF. Macrophages were infected in triplicate with 40 ng of p24 of the LTR-Luc recombinant R5 viruses. LAI and JR-FL X4 viruses were also tested to serve as negative controls for entry. Four days post-infection, macrophages were lysed and assayed for luciferase activity. Error bars represent standard error of the mean.

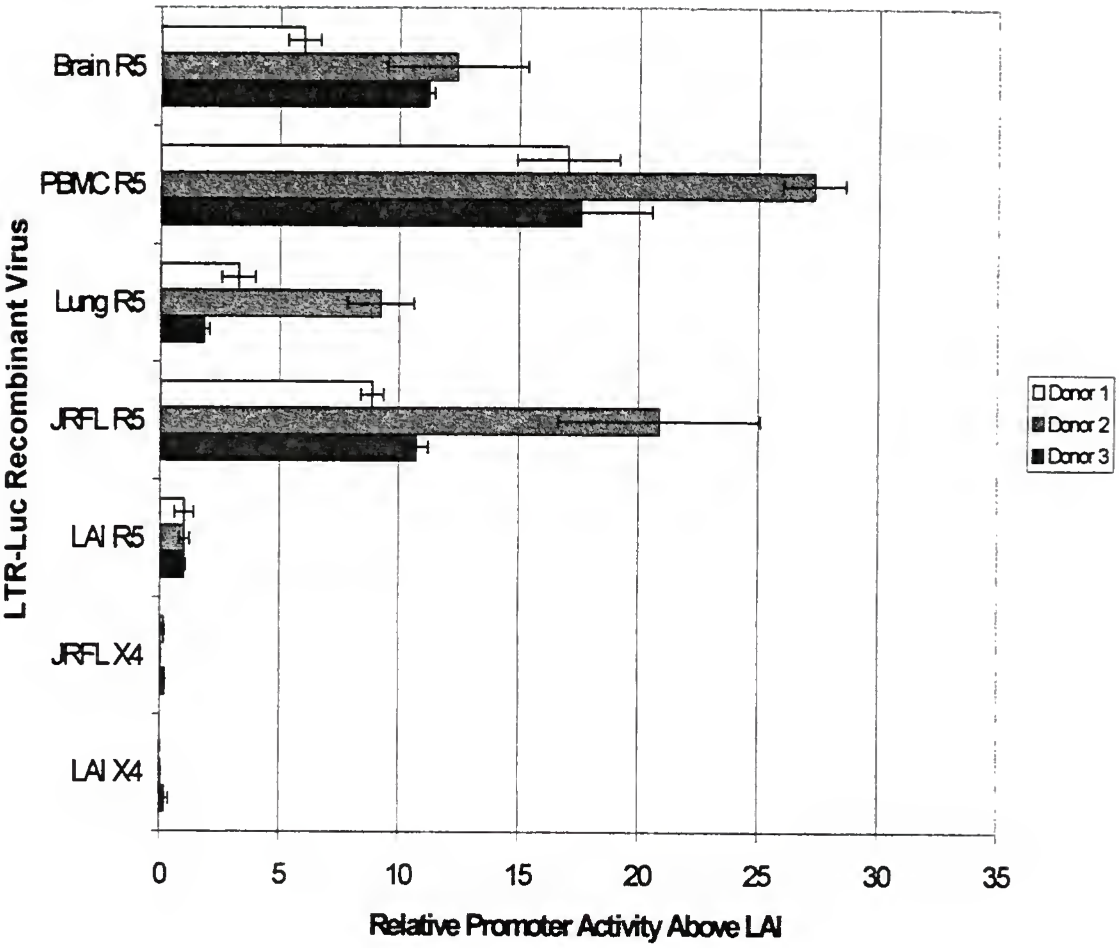

Figure 4-9. Macrophage infection with LTR-Luc recombinant viruses from all donors. Macrophages were infected as described before in Figure 4-8. Error bars represent standard error of the mean.

TABLE 4-2
Luciferase Experession and Gag Copies from Infection of PBMC with LTR-Luc Recombinant X4 Viruses

X4 Virus in PBMC	LAI X4	JR-FL X4	Brain X4	Lung X4	PBMC X4	Average
Gag per 20 µl of 50 µl	679	480	262	380	707	
Cells	757834	556243	679431	629428	750182	674624
Gag per total cells	1510	1456	650	1017	1589	
RLU[A] per 40 µl of 100 ul	2602	9279	5816	3424	20489	
RLU per total well	6505	23198	14540	8560	51223	
Gag per total cells	1510	1456	650	1017	1589	
RLU per corrected gag	4.3	16	22.4	8.4	32.2	16.6
Relative to LAI X4	1	3.7	5.2	2	7.5	
Gag per total cells	1510	1456	650	1017	1589	
Average cell number	674624	674624	674624	674624	674624	
% cells infected	0.2%	0.3%	0.1%	0.2%	0.2%	0.2%

[A] Relative light units

TABLE 4-3
Luciferase Experession and Gag Copies from Infection of PBMC with LTR-Luc Recombinant R5 Viruses

R5 Virus in PBMC	LAI R5	JR-FL R5	Brain R5	Lung R5	PBMC R5	Average
Gag per 20 µl of 50 µl	292	658	331	407	984	
Cells	1187602	1058341	662086	856193	951362	943117
Gag per total cells	580	1466	1179	1121	4439	
RLU[A] per 40 µl of 100 ul	696	1247	2181	752	6401	
RLU per total well	1740	3118	5453	1880	16003	
Gag per total cells	580	1466	1179	1121	4439	
RLU per corrected gag	3.0	2.1	4.6	1.7	6.6	3.6
Relative to LAI X4	1	0.7	1.5	0.6	2.2	
Gag per total cells	580	1466	1179	1121	4439	
Average cell number	943117	943117	943117	943117	943117	
% cells infected	0.1%	0.2	0.1	0.1	0.3	0.2%
Average cells expressing R5 (estimate)	94311	94311	94311	94311	94311	
% R5 cells infected	0.6%	1.6%	1.3%	1.2%	4.7%	1.9%

[A] Relative light units

TABLE 4-4

Luciferase Experession and Gag Copies from Infection of Macrophages with LTR-Luc Recombinant R5 Viruses

R5 Virus in PBMC	LAI R5	JR-FL R5	Brain R5	Lung R5	PBMC R5	Average
Gag per 20 µl of 100 µl	45	212	221	96	570	
Cells	113576	213791	287807	277056	360017	250449
Gag per total cells	496	1252	962	434	1983	
RLU[A] per 40 µl of 100 ul	14667	43626	59509	53908	257979	
RLU per total well	36668	109065	148773	134770	644948	
Gag per total cells	496	1252	962	434	1983	
RLU per corrected gag	3.0	2.1	4.6	1.7	6.6	190
Relative to LAI X4	1	1.2	2.1	4.2	4.4	
Gag per total cells	496	1252	962	434	1983	
Average cell number	250449	250449	250449	250449	250449	
% cells infected	0.2%	0.5%	0.4%	0.2%	0.8%	0.4%

[A] Relative light units

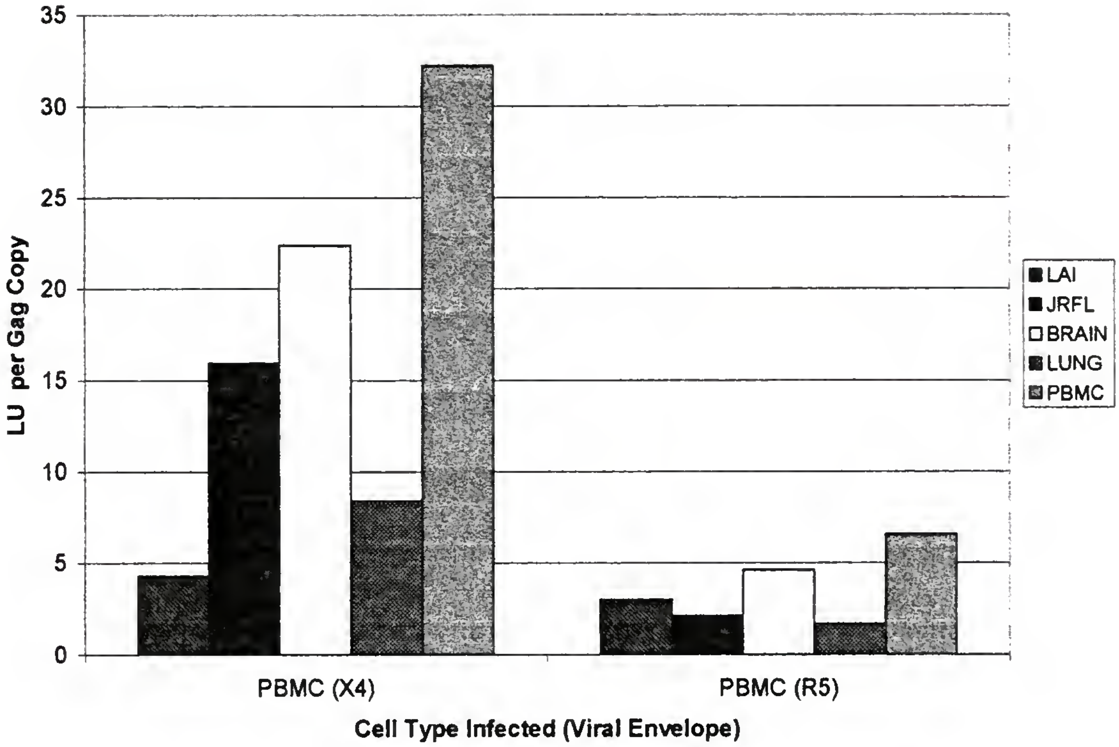

Figure 4-10. Luciferase expression per gag copy of PBMC infected with LTR-Luc recombinant X4 and R5 viruses. PBMC were infected with 40 ng of p24 of LTR-Luc recombinant viruses and harvested 3 days post-infected. Cells were measured for luciferase expression and proviral gag copies.

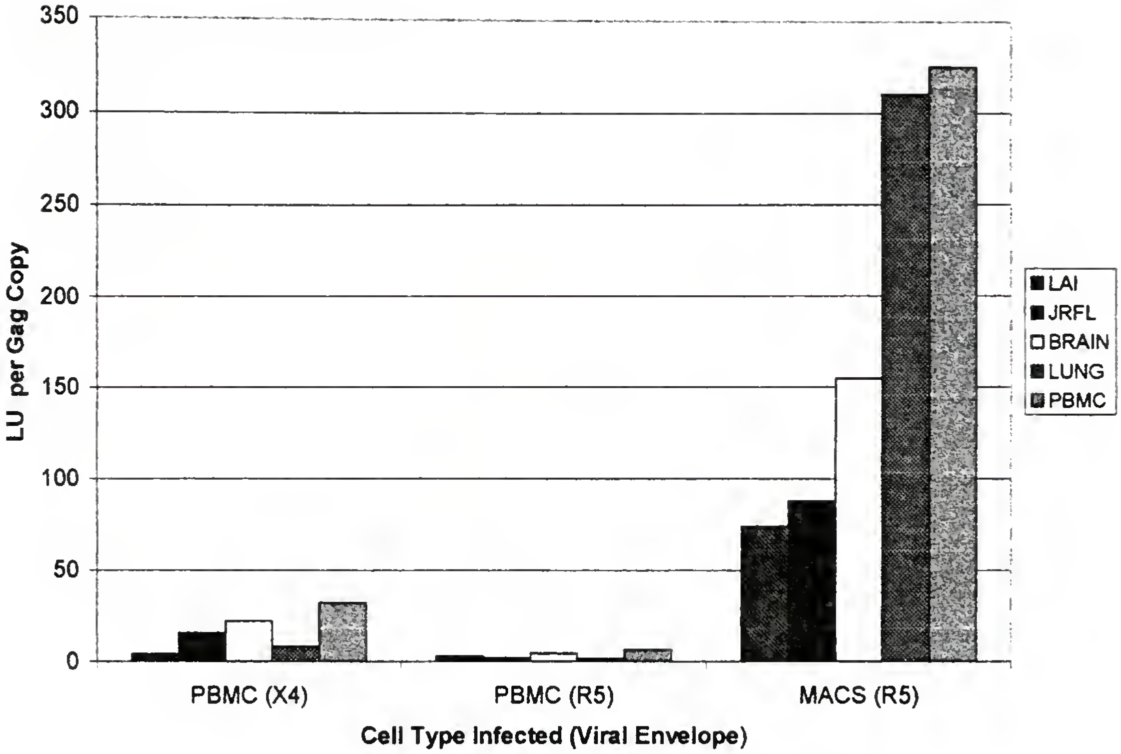

Figure 4-11. Luciferase expression per gag copy of PBMC and macrophages. PBMC and macrophages were infected with 40 ng of p24 of LTR-Luc recombinant viruses. PBMC and macrophages were harvested 3 and 4 days post-infection, respectively. Cells were measured for luciferase expression and proviral gag copies.

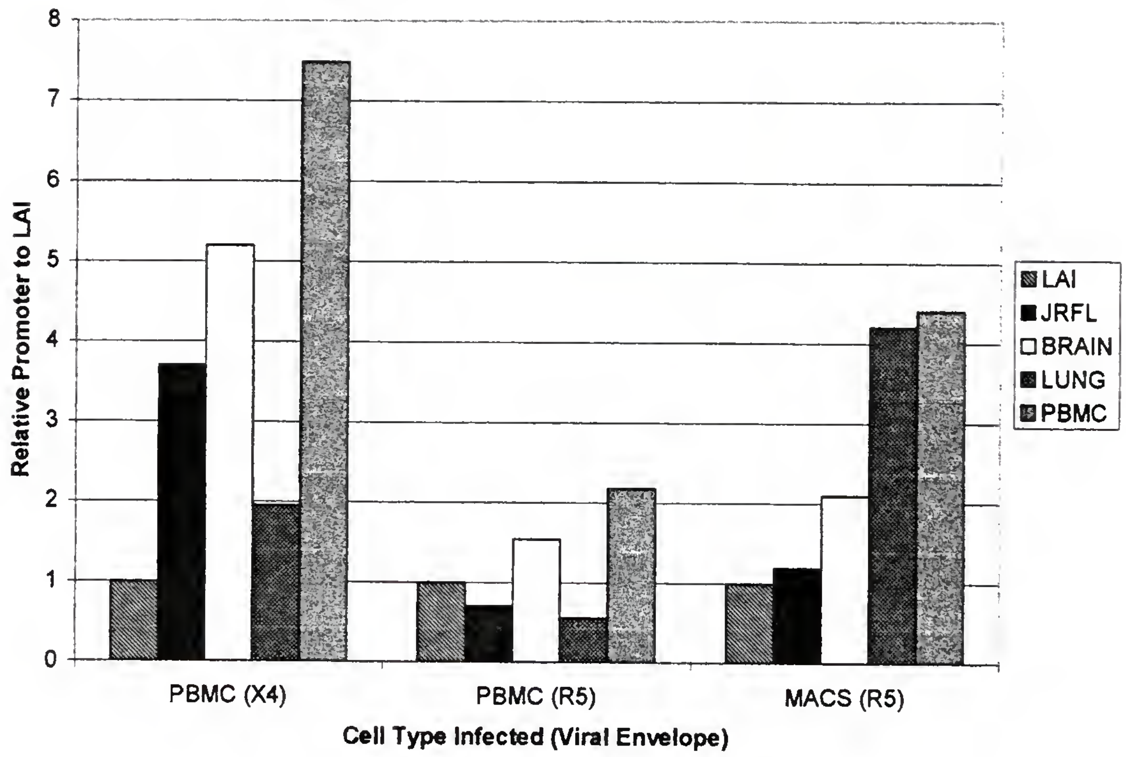

Figure 4-12. Relative promoter activity within different primary cells. Relative promoter activity is expressed as luciferase units per gag copy of LTR-Luc recombinant divided by LAI luciferase units per gag copy.

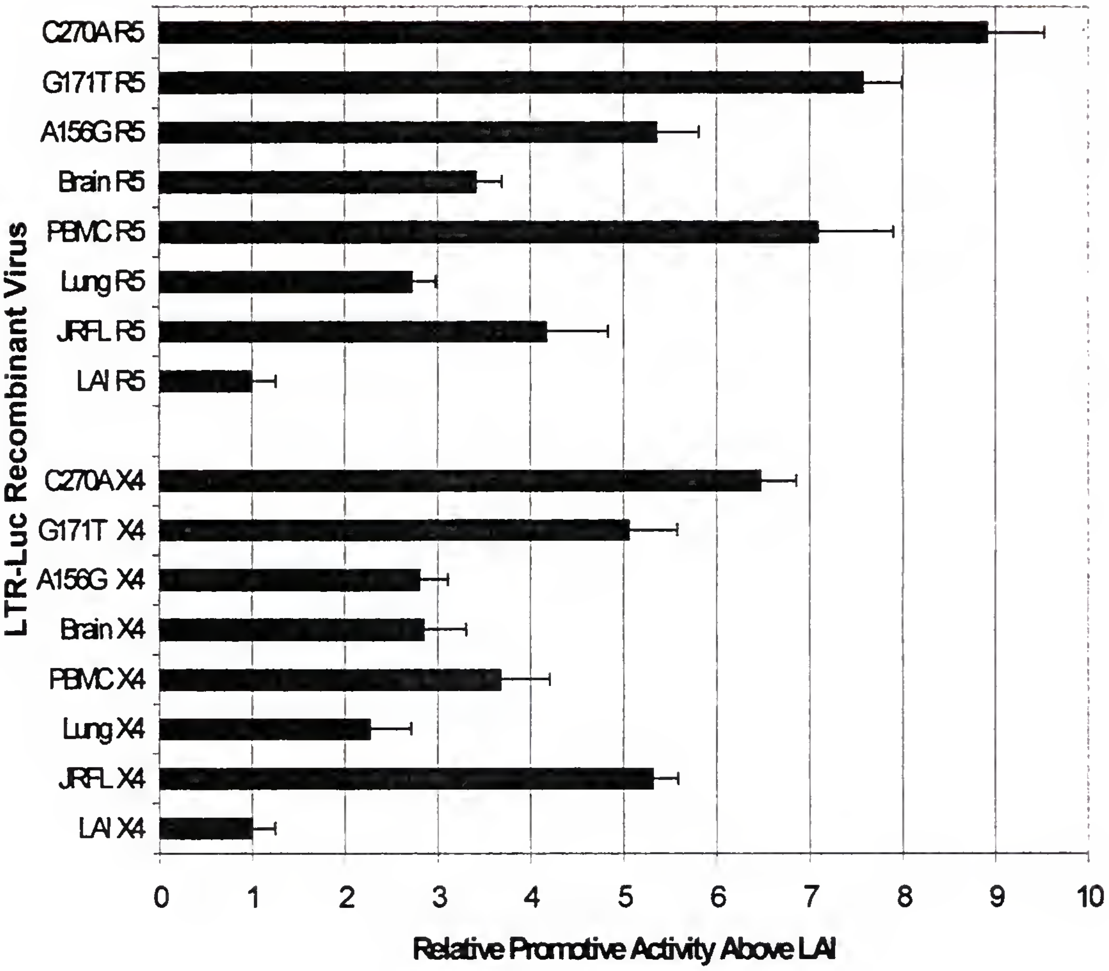

Figure 4-13. Representative experiment of PBMC infection with Site-Directed LTR-Luc recombinant viruses. PBMC's were plated at 2 x 10^5 cells in a 96-well plate and infected in triplicate with 40 ng of p24 of recombinant viruses. PBMC's were infected with either X4 or R5 viruses. PBMC's were collected 3 days post-infection, lysed, and assayed for luciferase activity. Error bars represent standard error of the mean.

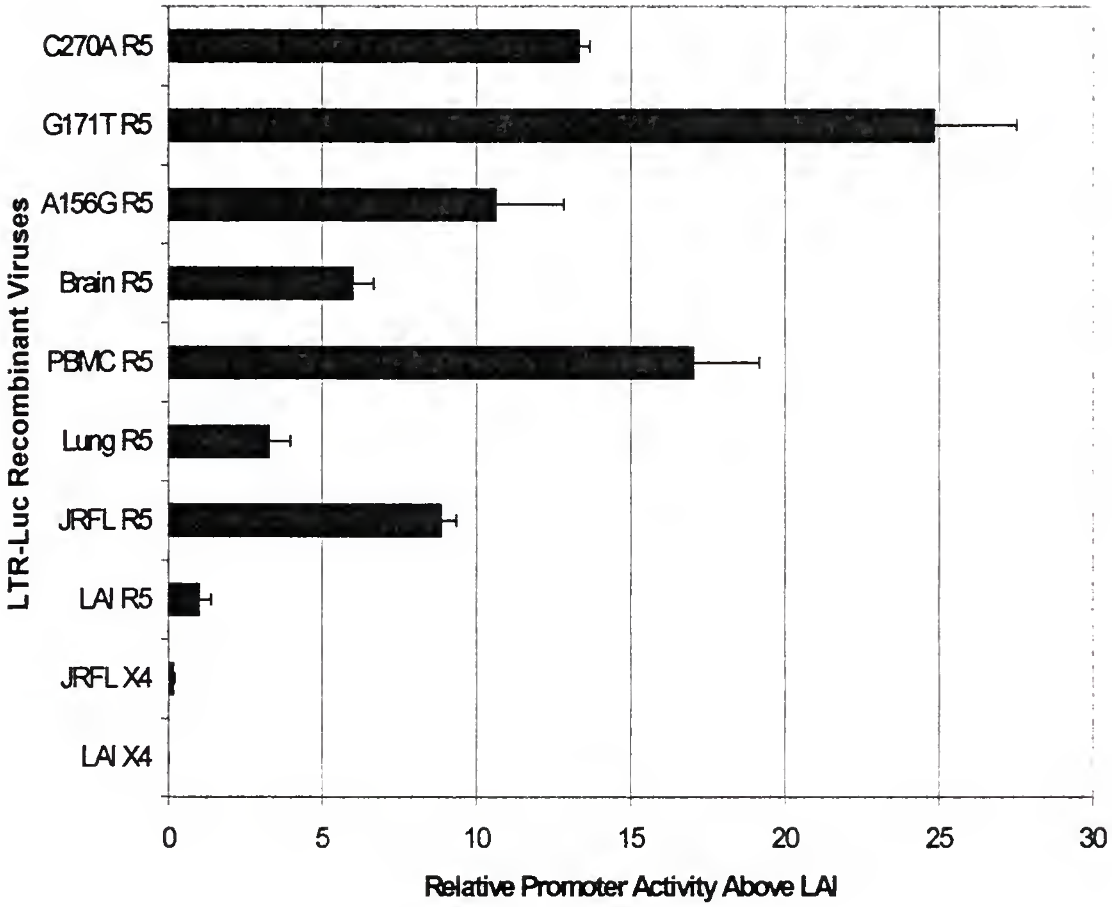

Figure 4-14. Representative infection of macrophages with Site-Directed LTR-Luc recombinant viruses. Monocytes were plated at 1×10^6 cells/ml in a 48-well dish and allowed to differentiate for 5 days in the presence of GM-CSF. Macrophages were infected in triplicate with 40 ng of p24 of the LTR-Luc recombinant R5 viruses. LAI and JR-FL X4 viruses were also tested to serve as negative controls for entry. Four days post-infection, macrophages were lysed and assayed for luciferase activity. Error bars represent standard error of the mean.

TABLE 4-5
Results of LTR-Luc Recombinant Virus Infections

Virus	Donor 1			Donor 2			Donor 3		
	PBMC		Macrophages	PBMC		Macrophages	PBMC		Macrophages
	X4	**R5**	**R5**	**X4**	**R5**	**R5**	**X4**	**R5**	**R5**
LAI	1.0 (0.2)	1.0 (0.3)	1.0 (0.4)	1.0 (0.5)	1.0 (0.4)	1.0 (0.2)	1.0 (0.1)	1.0 (0.2)	1.0 (0.07)
JR-FL	5.3 (0.3)	4.2 (0.7)	8.9 (0.47)	6.3 (0.5)	1.8 (0.4)	21 (4.2)	4.6 (0.5)	6.2 (1.1)	10.7 (0.5)
Lung	2.3 (0.4)	2.7 (0.25)	3.3 (0.7)	1.0 (0.3)	1.6 (0.6)	9.2 (1.4)	1.4 (0.1)	1.4 (0.5)	1.8 (0.2)
PBMC	3.7 (0.5)	7.1 (0.8)	17 (2.1)	5.6 (0.4)	7.6 (2.4)	27.3 (1.3)	5.2 (0.2)	7.1 (0.3)	17.6 (3.0)
Brain	2.9 (0.5)	3.4 (0.3)	6.0 (0.68)	3.1 (0.7)	2.5 (0.7)	12.4 (2.9)	2.3 (0.2)	3.9 (0.6)	11.2 (0.2)
A156G	2.8 (0.3)	5.4 (0.5)	10.6 (2.2)	3.1 (0.2)	2.2 (0.9)	15 (3.7)	4.4 (0.4)	5.9 (0.4)	8.3 (0.4)
G171T	5.1 (0.5)	7.6 (0.4)	25 (2.67)	4.4 (0.3)	2.3 (0.2)	22.4 (7.4)	3.8 (0.7)	14.5 (0.5)	24.4 (3.5)
C270A	6.5 (0.4)	8.9 (0.6)	13.3 (0.3)	5.6 (1.0)	4.3 (0.4)	22.3 (5.3)	4.9 (0.5)	9.1 (2.2)	27.7 (1.3)

Note: Values are presented as relative promoter activity above LAI. Numbers in parenthesis refer to standard error of the mean for triplicate measurements of relative promoter activity.

CHAPTER 5
CONCLUSIONS

HIV-1 can infect a multitude of tissues and cell types during the course of infection. The ability of HIV-1 to accomplish this is dependant on mutliple regions of the viral genome. Each subgenome can impact different parts of the viral lifecycle, and determine pathogenesis. HIV-1 is truly a mutant swarm of quasispecies with genetic variability found in several parts of the viral genome. To fully understand how HIV-1 infects and adapts to different tissues and cell types, it is necessary to study multiple subgenomic regions that affect different parts of the viral life cycle. In addition, viral sequences from longitudinal PBMC and various tissues must be examined to determine evolutionary patterns over time and between different host tissues. Functional analysis of different tissue env and LTR sequences would determine the impact of tissue specific adaptation on viral entry and gene expression. My dissertation work is the first study to phylogenetically and functionally evaluate the LTR and env regions from multiple tissues, and longitudinal PBMC from vertically infected children. This study simultaneously examines the env and LTR regions of the HIV-1 genome from the lung, brain, PBMC, spleen, lymph node, plasma, and thymus from six patients with varied clinical progression. My study was the first to genetically and functionally examine the *in-vivo* viral quasispecies present in the thymus. This dissertation is also novel in that I have functionally examined tissue specific LTRs for promoter activity in primary cells such as PBMC and macrophages. I also have examined sequences within the mid-U3 region of the LTR for cell-type specific regulation.

Evolution of Independent Viral Lineages within Tissues is Determined by Env and LTR

Phylogenetic analysis of the env and LTR HIV-1 sequences from various tissues revealed different evolutionary histories for both subgenomic regions depending on the tissue origin. One very important result was the fact that brain and lung env or LTR sequences were never found clustered together, and were always segregated from one another. This strongly suggested multiple independent lingeages evolving in separate compartments. However, phylogenetic analysis indicated some viral trafficking between the lung, thymus, and PBMC. The brain always contained a separate compartment of viruses by both the env and LTR regions. The lung typically contained two populations of LTR sequences. This result indicates that different cell types such as macrophages or CD4+ T cells within particular tissues such as the lung may create two populations within a tissue. Each tissue imposes a different form of either pre- or post-entry selective pressure on the virus which induces discordant relationships among different parts of the viral genome. Distinct thymus env sequences were found segregated from all other tissue compartments whereas thymus LTR sequences were always clustered with other tissue LTR sequences. This indicates a strong pre-entry selective pressure in thymus, whereas post-entry selective pressure appears to be limited. Within the thymus, this pre-entry selection maybe from CXCR4 expression (pre-entry factor), and the lack of post-entry selective pressure is due to a highly permissive transcriptional environment owed to the high production of cytokines. The selective force behind variable evolutionary histories is determined by factors in the local milieu of the host tissue, and the various subgenomic regions that regulate both pre- (env) and post-entry (LTR) determinants. The importance of tissue specific HIV-1 quasispecies should not be underestimated since they represent a constant reservoir of independent evolving viral populations, which may represent a source of virus that cannot be reached with current antiviral therapies. Further studies need to evaluate other regions of the HIV-1 genome with regard to tissue specific segregation and how these regions may lead to further viral adaptation and pathogenesis.

Thymus is the Source of T-X4 and D-R5X4 Quasispecies

One of the most novel findings of my research was to demonstrate that the thymus is the source of T-cell line tropic, CXCR4-using (T-X4), and dual-tropic (D-X4±R5) quasispecies. The thymus was the only tissue to consistently contain T-X4 and D-X4±R5 quasispecies. The only other tissues containing T-X4 and D-X4±R5 quasispecies were the lymph node or PBMC at low frequency. Our data suggests a model in which M-R5 viruses initially infect the thymus, and establish infection through either dendritic cells, thymic epithelial cells, or mature thymocytes which predominantly express R5. Both of these cell populations have been demonstrated to be the major target for M-tropic infection, and dendritic cells are capable of transmitting M-tropic viruses to mature CD4+ thymocytes (22,199). The high expression of CXCR4 on immature thymocytes would select for either T-X4 or Dual-tropic variants that can now replicate in a large population of immature thymocytes found in infant thymuses. The highly cytopathic, T-X4 variants could then rapidly deplete the thymus of immature thymoctyes, and eliminate the export of naïve T-cells to the periphery. This would then eliminate the ability of the host for CD4+ T cell renewal, and induce a rapid clinical progression. These T-X4 or D-X4±R5 variants that emerge in the thymus would then migrate to colonize peripheral lymphoid organs such as the lymph node or spleen via the blood. The emergence of either a T-tropic or dual-tropic variant in the thymus may completely inhibit T-cell renewal particularly in pediatric patients.

Tissue Specific LTRs have Distinct Promoter and Cell-Type Differences

My study was the first to functionally evaluate tissue specific LTRs from multiple tissues. Transient transfection and functional analysis using congenic LTR-Luc recombinant viruses revealed distinct promoter differences among tissue specific LTRs. These measurable and consistent promoter differences among tissue specific LTRs indicated a restricted local post-entry LTR adaptation. The PBMC LTR had the highest promoter activity in both PBMC and macrophages. The brain and lung LTR Post-entry LTR adaptation of HIV-1 occurs not only within specific tissues, but also within T-cell subsets (CD45RA and CD45R0). There was no evidence of an LTR expressing only in macrophages and not PBMC or visa-versa. Since HIV-1 has such a restricted lineage of cells to infect such as CD4+ T-cells and macrophages, there maybe a strong selective pressure to maintain the ability for gene expression in both cell types. However, all LTRs studied by recombinant analysis had higher promoter activity in macrophages than PBMC. In addition, the lung LTR had the lowest promoter activity among all constructs in PBMC yet had one of the highest promoter activities in macrophages. This result suggests that although there are no cell-type restricted LTR's, there are LTR's that have adapted within a local milieu to have higher promoter expression in certain cell types (ie. macrophages). In addition, LTR adaptation may be more crucial for expression in macrophages rather than PBMC. In contrast, low promoter expression may be tolerated in PBMC without the need for adaptation since the HIV LTR maybe designed more toward T-lymphocyte activation. One important observation is that the virus that is transmitted and found in the reproductive tract is typically M-R5 (191). This may result in the transmission of viruses that are more adaptated toward replication in macrophages rather than PBMC.

Further studies need to address these tissue specific LTR's in their natural milieu. For example, the brain and lung LTR need to be evaluated in the context of the predominantly infected cell found within the tissue. Functional analysis of the brain and lung LTR should be performed in the microglial and alveolar macrophages, respectively. These tissue LTRs have been selected within a particular environment and are responsive to cell-type specific transcriptional factors. Therefore, mimicking the cellular environment from which these LTRs have adapted to will allow proper evaluation of true *in-vivo* differences via recombinant studies. Overall, both tissue and cell-type tropism of HIV-1 is multifactorial and impacted by multiple regions of the HIV-1 genome coupled with host cellular factors that induce viral adaptation at multiple levels.

REFERENCES

1. Ait-Khaled, M. and V. C. Emery. 1994. Phylogenetic relationship between human immunodeficiency virus type 1 (HIV-1) long terminal repeat natural variants present in the lymph node and peripheral blood of three HIV-1-infected individuals. J.Gen.Virol. 75 (Pt 7):1615-1621.

2. Ait-Khaled, M., J. E. McLaughlin, M. A. Johnson, and V. C. Emery. 1995. Distinct HIV-1 long terminal repeat quasispecies present in nervous tissues compared to that in lung, blood and lymphoid tissues of an AIDS patient. AIDS 9:675-683.

3. Akira, S., H. Isshiki, T. Nakajima, S. Kinoshita, Y. Nishio, S. Natsuka, and T. Kishimoto. 1992. Regulation of expression of the interleukin 6 gene: structure and function of the transcription factor NF-IL6. Ciba Found.Symp. 167:47-62.

4. Akiyama, Y. 1998. TFSEARCH Program. http://www.rwcp.or.jp/papia.

5. Alcami, J., d. L. Lain, L. Folgueira, M. A. Pedraza, J. M. Jacque, F. Bachelerie, A. R. Noriega, R. T. Hay, D. Harrich, R. B. Gaynor, and . 1995. Absolute dependence on kappa B responsive elements for initiation and Tat-mediated amplification of HIV transcription in blood CD4 T lymphocytes. EMBO J. 14:1552-1560.

6. Allan, J. S., J. E. Coligan, F. Barin, M. F. McLane, J. G. Sodroski, C. A. Rosen, W. A. Haseltine, T. H. Lee, and M. Essex. 1985. Major glycoprotein antigens that induce antibodies in AIDS patients are encoded by HTLV-III. Science 228:1091-1094.

7. Arya, S. K., C. Guo, S. F. Josephs, and F. Wong-Staal. 1985. Trans-activator gene of human T-lymphotropic virus type III (HTLV-III). Science 229:69-73.

8. Asjo, B., L. Morfeldt-Manson, J. Albert, G. Biberfeld, A. Karlsson, K. Lidman, and E. M. Fenyo. 1986. Replicative capacity of human immunodeficiency virus from patients with varying severity of HIV infection. Lancet 2:660-662.

9. Bagasra, O., E. Lavi, L. Bobroski, K. Khalili, J. P. Pestaner, R. Tawadros, and R. J. Pomerantz. 1996. Cellular reservoirs of HIV-1 in the central nervous system of infected individuals: identification by the combination of in situ polymerase chain reaction and immunohistochemistry. AIDS 10:573-585.

10. Ball, J. K., E. C. Holmes, H. Whitwell, and U. Desselberger. 1994. Genomic variation of human immunodeficiency virus type 1 (HIV-1): molecular analyses of HIV-1 in sequential blood samples and various organs obtained at autopsy. J.Gen.Virol. 75 (Pt 4):67-79.

11. Ballard, D. W., W. H. Walker, S. Doerre, P. Sista, J. A. Molitor, E. P. Dixon, N. J. Peffer, M. Hannink, and W. C. Greene. 1990. The v-rel oncogene encodes a kappa B enhancer binding protein that inhibits NF-kappa B function. Cell 63:803-814.

12. Barre-Sinoussi, F., J. C. Chermann, F. Rey, M. T. Nugeyre, S. Chamaret, J. Gruest, C. Dauguet, C. Axler-Blin, F. Vezinet-Brun, C. Rouzioux, W. Rozenbaum, and L. Montagnier. 1983. Isolation of a T-lymphotropic retrovirus from a patient at risk for acquired immune deficiency syndrome (AIDS). Science 220:868-871.

13. Beg, A. A. and A. S. Baldwin, Jr. 1993. The I kappa B proteins: multifunctional regulators of Rel/NF-kappa B transcription factors. Genes Dev. 7:2064-2070.

14. Berger, E. A. 1997. HIV entry and tropism: the chemokine receptor connection. AIDS 11 Suppl A:S3-16.

15. Berkhout, B. and K. T. Jeang. 1992. Functional roles for the TATA promoter and enhancers in basal and Tat- induced expression of the human immunodeficiency virus type 1 long terminal repeat. J.Virol. 66:139-149.

16. Berkowitz, R. D., S. Alexander, C. Bare, V. Linquist-Stepps, M. Bogan, M. E. Moreno, L. Gibson, E. D. Wieder, J. Kosek, C. A. Stoddart, and J. M. McCune. 1998. CCR5- and CXCR4-utilizing strains of human immunodeficiency virus type 1 exhibit differential tropism and pathogenesis in vivo. J.Virol. 72:10108-10117.

17. Berkowitz, R. D., S. Alexander, and J. M. McCune. 2000. Causal relationships between HIV-1 coreceptor utilization, tropism, and pathogenesis in human thymus. AIDS Res.Hum.Retroviruses 16:1039-1045.

18. Bosze, Z., H. J. Thiesen, and P. Charnay. 1986. A transcriptional enhancer with specificity for erythroid cells is located in the long terminal repeat of the Friend murine leukemia virus. EMBO J. 5:1615-1623.

19. Briggs, D. R., D. L. Tuttle, J. W. Sleasman, and M. M. Goodenow. 2000. Envelope V3 amino acid sequence predicts HIV-1 phenotype (co-receptor usage and tropism for macrophages). AIDS 14:2937-2939.

20. Brooks, D. G., S. G. Kitchen, C. M. Kitchen, D. D. Scripture-Adams, and J. A. Zack. 2001. Generation of HIV latency during thymopoiesis. Nat.Med. 7:459-464.

21. Buzy, J. M., L. M. Lindstrom, M. C. Zink, and J. E. Clements. 1995. HIV-1 in the developing CNS: developmental differences in gene expression. Virology 210:361-371.

22. Cameron, P. U., M. G. Lowe, F. Sotzik, A. F. Coughlan, S. M. Crowe, and K. Shortman. 1996. The interaction of macrophage and non-macrophage tropic isolates of HIV- 1 with thymic and tonsillar dendritic cells in vitro. J.Exp.Med. 183:1851-1856.

23. Canonne-Hergaux, F., D. Aunis, and E. Schaeffer. 1995. Interactions of the transcription factor AP-1 with the long terminal repeat of different human immunodeficiency virus type 1 strains in Jurkat, glial, and neuronal cells. J.Virol. 69:6634-6642.

24. Celander, D., B. L. Hsu, and W. A. Haseltine. 1988. Regulatory elements within the murine leukemia virus enhancer regions mediate glucocorticoid responsiveness. J.Virol. 62:1314-1322.

25. Chan, S. Y., R. F. Speck, C. Power, S. L. Gaffen, B. Chesebro, and M. A. Goldsmith. 1999. V3 recombinants indicate a central role for CCR5 as a coreceptor in tissue infection by human immunodeficiency virus type 1. J.Virol. 73:2350-2358.

26. Chayt, K. J., M. E. Harper, L. M. Marselle, E. B. Lewin, R. M. Rose, J. M. Oleske, L. G. Epstein, F. Wong-Staal, and R. C. Gallo. 1986. Detection of HTLV-III RNA in lungs of patients with AIDS and pulmonary involvement. JAMA 256:2356-2359.

27. Chen, B. K., M. B. Feinberg, and D. Baltimore. 1997. The kappaB sites in the human immunodeficiency virus type 1 long terminal repeat enhance virus replication yet are not absolutely required for viral growth. J.Virol. 71:5495-5504.

28. Chene, L., M. T. Nugeyre, F. Barre-Sinoussi, and N. Israel. 1999. High-level replication of human immunodeficiency virus in thymocytes requires NF-kappaB activation through interaction with thymic epithelial cells. J.Virol. 73:2064-2073.

29. Chene, L., M. T. Nugeyre, E. Guillemard, N. Moulian, F. Barre-Sinoussi, and N. Israel. 1999. Thymocyte-thymic epithelial cell interaction leads to high-level replication of human immunodeficiency virus exclusively in mature CD4(+) CD8(-) CD3(+) thymocytes: a critical role for tumor necrosis factor and interleukin-7. J.Virol. 73:7533-7542.

30. Cheng-Mayer, C., D. Seto, M. Tateno, and J. A. Levy. 1988. Biologic features of HIV-1 that correlate with virulence in the host. Science 240:80-82.

31. Cheng-Mayer, C., C. Weiss, D. Seto, and J. A. Levy. 1989. Isolates of human immunodeficiency virus type 1 from the brain may constitute a special group of the AIDS virus. Proc.Natl.Acad.Sci.U.S.A 86:8575-8579.

32. Chesebro, B., J. Nishio, S. Perryman, A. Cann, W. O'Brien, I. S. Chen, and K. Wehrly. 1991. Identification of human immunodeficiency virus envelope gene sequences influencing viral entry into CD4-positive HeLa cells, T-leukemia cells, and macrophages. J.Virol. 65:5782-5789.

33. Chesebro, B., K. Wehrly, J. Nishio, and S. Perryman. 1992. Macrophage-tropic human immunodeficiency virus isolates from different patients exhibit unusual V3 envelope sequence homogeneity in comparison with T-cell-tropic isolates: definition of critical amino acids involved in cell tropism. J.Virol. 66:6547-6554.

34. Chesebro, B., K. Wehrly, J. Nishio, and S. Perryman. 1996. Mapping of independent V3 envelope determinants of human immunodeficiency virus type 1 macrophage tropism and syncytium formation in lymphocytes. J.Virol. 70:9055-9059.

35. Cleland, A., H. G. Watson, P. Robertson, C. A. Ludlam, and A. J. Brown. 1996. Evolution of zidovudine resistance-associated genotypes in human immunodeficiency virus type 1-infected patients. J.Acquir.Immune.Defic.Syndr.Hum.Retrovirol. 12:6-18.

36. Clouse, K. A., D. Powell, I. Washington, G. Poli, K. Strebel, W. Farrar, P. Barstad, J. Kovacs, A. S. Fauci, and T. M. Folks. 1989. Monokine regulation of human immunodeficiency virus-1 expression in a chronically infected human T cell clone. J.Immunol. 142:431-438.

37. Cocchi, F., A. L. Devico, A. Garzino-Demo, A. Cara, R. C. Gallo, and P. Lusso. 1996. The V3 domain of the HIV-1 gp120 envelope glycoprotein is critical for chemokine-mediated blockade of infection. Nat.Med. 2:1244-1247.

38. Cohen, A. H., N. C. Sun, P. Shapshak, and D. T. Imagawa. 1989. Demonstration of human immunodeficiency virus in renal epithelium in HIV-associated nephropathy. Mod.Pathol. 2:125-128.

39. Connor, R. I. and D. D. Ho. 1994. Human immunodeficiency virus type 1 variants with increased replicative capacity develop during the asymptomatic stage before disease progression. J.Virol. 68:4400-4408.

40. Connor, R. I., K. E. Sheridan, D. Ceradini, S. Choe, and N. R. Landau. 1997. Change in coreceptor use coreceptor use correlates with disease progression in HIV-1--infected individuals. J.Exp.Med. 185:621-628.

41. Cooney, A. J., S. Y. Tsai, B. W. O'Malley, and M. J. Tsai. 1991. Chicken ovalbumin upstream promoter transcription factor binds to a negative regulatory region in the human immunodeficiency virus type 1 long terminal repeat. J.Virol. 65:2853-2860.

42. Corboy, J. R. and P. J. Garl. 1997. HIV-1 LTR DNA sequence variation in brain-derived isolates. J.Neurovirol. 3:331-341.

43. Cordingley, M. G., R. L. LaFemina, P. L. Callahan, J. H. Condra, V. V. Sardana, D. J. Graham, T. M. Nguyen, K. LeGrow, L. Gotlib, A. J. Schlabach, and . 1990. Sequence-specific interaction of Tat protein and Tat peptides with the transactivation-responsive sequence element of human immunodeficiency virus type 1 in vitro. Proc.Natl.Acad.Sci.U.S.A 87:8985-8989.

44. Cordingley, M. G., A. T. Riegel, and G. L. Hager. 1987. Steroid-dependent interaction of transcription factors with the inducible promoter of mouse mammary tumor virus in vivo. Cell 48:261-270.

45. Cordonnier, A., L. Montagnier, and M. Emerman. 1989. Single amino-acid changes in HIV envelope affect viral tropism and receptor binding. Nature 340:571-574.

46. Courey, A. J., D. A. Holtzman, S. P. Jackson, and R. Tjian. 1989. Synergistic activation by the glutamine-rich domains of human transcription factor Sp1. Cell 59:827-836.

47. Crabtree, G. R. 1989. Contingent genetic regulatory events in T lymphocyte activation. Science 243:355-361.

48. Cron, R. Q., S. R. Bartz, A. Clausell, S. J. Bort, S. J. Klebanoff, and D. B. Lews. 2000. NFAT1 enhances HIV-1 gene expression in primary human CD4 T cells. Clin.Immunol. 94:179-191.

49. D'Souza, M. P. and V. A. Harden. 1996. Chemokines and HIV-1 second receptors. Confluence of two fields generates optimism in AIDS research. Nat.Med. 2:1293-1300.

50. Dalgleish, A. G., P. C. Beverley, P. R. Clapham, D. H. Crawford, M. F. Greaves, and R. A. Weiss. 1984. The CD4 (T4) antigen is an essential component of the receptor for the AIDS retrovirus. Nature 312:763-767.

51. De Rossi, A., L. Ometto, S. Masiero, M. Zanchetta, and L. Chieco-Bianchi. 1997. Viral phenotype in mother-to-child HIV-1 transmission and disease progression of vertically acquired HIV-1 infection. Acta Paediatr.Suppl 421:22-28.

52. Dean, N. C., J. A. Golden, L. A. Evans, M. L. Warnock, T. E. Addison, P. C. Hopewell, and J. A. Levy. 1988. Human immunodeficiency virus recovery from bronchoalveolar lavage fluid in patients with AIDS. Chest 93:1176-1179.

53. Delassus, S., R. Cheynier, and S. Wain-Hobson. 1991. Evolution of human immunodeficiency virus type 1 nef and long terminal repeat sequences over 4 years in vivo and in vitro. J.Virol. 65:225-231.

54. Delassus, S., A. Meyerhans, R. Cheynier, and S. Wain-Hobson. 1992. Absence of selection of HIV-1 variants in vivo based on transcription/transactivation during progression to AIDS. Virology 188:811-818.

55. Di Fagagna, F. D., G. Marzio, M. I. Gutierrez, L. Y. Kang, A. Falaschi, and M. Giacca. 1995. Molecular and functional interactions of transcription factor USF with the long terminal repeat of human immunodeficiency virus type 1. J.Virol. 69:2765-2775.

56. Dingwall, C., I. Ernberg, M. J. Gait, S. M. Green, S. Heaphy, J. Karn, A. D. Lowe, M. Singh, M. A. Skinner, and R. Valerio. 1989. Human immunodeficiency virus 1 tat

protein binds trans-activation- responsive region (TAR) RNA in vitro. Proc.Natl.Acad.Sci.U.S.A 86:6925-6929.

57. Dynlacht, B. D., T. Hoey, and R. Tjian. 1991. Isolation of coactivators associated with the TATA-binding protein that mediate transcriptional activation. Cell 66:563-576.

58. Embretson, J., M. Zupancic, J. L. Ribas, A. Burke, P. Racz, K. Tenner-Racz, and A. T. Haase. 1993. Massive covert infection of helper T lymphocytes and macrophages by HIV during the incubation period of AIDS [see comments]. Nature 362:359-362.

59. Epstein, L. G., C. Kuiken, B. M. Blumberg, S. Hartman, L. R. Sharer, M. Clement, and J. Goudsmit. 1991. HIV-1 V3 domain variation in brain and spleen of children with AIDS: tissue-specific evolution within host-determined quasispecies. Virology 180:583-590.

60. Estable, M. C., B. Bell, A. Merzouki, J. S. Montaner, M. V. O'Shaughnessy, and I. J. Sadowski. 1996. Human immunodeficiency virus type 1 long terminal repeat variants from 42 patients representing all stages of infection display a wide range of sequence polymorphism and transcription activity. J.Virol. 70:4053-4062.

61. Felsenstein J. 1993. PHYLIP manual version 3.5.

62. Fenyo, E. M., L. Morfeldt-Manson, F. Chiodi, B. Lind, A. von Gegerfelt, J. Albert, E. Olausson, and B. Asjo. 1988. Distinct replicative and cytopathic characteristics of human immunodeficiency virus isolates. J.Virol. 62:4414-4419.

63. Folks, T. M., J. Justement, A. Kinter, C. A. Dinarello, and A. S. Fauci. 1987. Cytokine-induced expression of HIV-1 in a chronically infected promonocyte cell line. Science 238:800-802.

64. Franz, T., F. Hilberg, B. Seliger, C. Stocking, and W. Ostertag. 1986. Retroviral mutants efficiently expressed in embryonal carcinoma cells. Proc.Natl.Acad.Sci.U.S.A 83:3292-3296.

65. Frederick, T., L. Mascola, A. Eller, L. O'Neil, and B. Byers. 1994. Progression of human immunodeficiency virus disease among infants and children infected perinatally with human immunodeficiency virus or through neonatal blood transfusion. Los Angeles County Pediatric AIDS Consortium and the Los Angeles County-University of Southern California Medical Center and the University of Southern California School of Medicine. Pediatr.Infect.Dis.J. 13:1091-1097.

66. Galli, L., M. de Martino, P. A. Tovo, C. Gabiano, M. Zappa, C. Giaquinto, S. Tulisso, A. Vierucci, M. Guerra, P. Marchisio, and . 1995. Onset of clinical signs in children with HIV-1 perinatal infection. Italian Register for HIV Infection in Children. AIDS 9:455-461.

67. Garcia-Blanco, M. A. and B. R. Cullen. 1991. Molecular basis of latency in pathogenic human viruses. Science 254:815-820.

68. Garcia, J. A. and R. B. Gaynor . 1994. The human immunodeficiency virus type-1 long terminal repeat and its role in gene expression. Prog.Nucleic Acid Res.Mol.Biol. 49:157-196.

69. Garcia, J. A., D. Harrich, E. Soultanakis, F. Wu, R. Mitsuyasu, and R. B. Gaynor. 1989. Human immunodeficiency virus type 1 LTR TATA and TAR region sequences required for transcriptional regulation. EMBO J. 8:765-778.

70. Gaynor, R. 1992. Cellular transcription factors involved in the regulation of HIV-1 gene expression [published erratum appears in AIDS 1992 Jun;6(6):following 606]. AIDS 6:347-363.

71. Ghorpade, A., M. Q. Xia, B. T. Hyman, Y. Persidsky, A. Nukuna, P. Bock, M. Che, J. Limoges, H. E. Gendelman, and C. R. Mackay. 1998. Role of the beta-chemokine receptors CCR3 and CCR5 in human immunodeficiency virus type 1 infection of monocytes and microglia. J.Virol. 72:3351-3361.

72. Giacca, M., M. I. Gutierrez, S. Menzo, F. D. Di Fagagna, and A. Falaschi. 1992. A human binding site for transcription factor USF/MLTF mimics the negative regulatory element of human immunodeficiency virus type 1. Virology 186:133-147.

73. Golub, E. I., G. G. Li, and D. J. Volsky. 1990. Differences in the basal activity of the long terminal repeat determine different replicative capacities of two closely related human immunodeficiency virus type 1 isolates. J.Virol. 64:3654-3660.

74. Griffin, G. E., K. Leung, T. M. Folks, S. Kunkel, and G. J. Nabel. 1989. Activation of HIV gene expression during monocyte differentiation by induction of NF-kappa B. Nature 339:70-73.

75. Harrich, D., J. Garcia, F. Wu, R. Mitsuyasu, J. Gonazalez, and R. Gaynor. 1989. Role of SP1-binding domains in in vivo transcriptional regulation of the human immunodeficiency virus type 1 long terminal repeat. J.Virol. 63:2585-2591.

76. Henderson, A. J. and K. L. Calame. 1997. CCAAT/enhancer binding protein (C/EBP) sites are required for HIV-1 replication in primary macrophages but not CD4(+) T cells. Proc.Natl.Acad.Sci.U.S.A 94:8714-8719.

77. Henderson, A. J., R. I. Connor, and K. L. Calame. 1996. C/EBP activators are required for HIV-1 replication and proviral induction in monocytic cell lines. Immunity. 5:91-101.

78. Henderson, A. J., X. Zou, and K. L. Calame. 1995. C/EBP proteins activate transcription from the human immunodeficiency virus type 1 long terminal repeat in macrophages/monocytes. J.Virol. 69:5337-5344.

79. Hillis, D. M., M. W. Allard, and M. M. Miyamoto. 1993. Analysis of DNA sequence data: phylogenetic inference. Methods Enzymol. 224:456-487.

80. Hillis, D. M. and Bull J.J. 1993. An empirical test of bootstrapping as a method for assesing confidence in phylogenetic analysis. Syst.Biol. □□:182-192.

81. Hillis, D. M., J. P. Huelsenbeck, and C. W. Cunningham. 1994. Application and accuracy of molecular phylogenies. Science 264:671-677.

82. Ho, D. D., A. U. Neumann, A. S. Perelson, W. Chen, J. M. Leonard, and M. Markowitz. 1995. Rapid turnover of plasma virions and CD4 lymphocytes in HIV-1 infection. Nature 373:123-126.

83. Honda, Y., L. Rogers, K. Nakata, B. Y. Zhao, R. Pine, Y. Nakai, K. Kurosu, W. N. Rom, and M. Weiden. 1998. Type I interferon induces inhibitory 16-kD CCAAT/ enhancer binding protein (C/EBP)beta, repressing the HIV-1 long terminal repeat in macrophages: pulmonary tuberculosis alters C/EBP expression, enhancing HIV-1 replication. J.Exp.Med. 188:1255-1265.

84. Hughes, E. S., J. E. Bell, and P. Simmonds. 1997. Investigation of the dynamics of the spread of human immunodeficiency virus to brain and other tissues by evolutionary analysis of sequences from the p17gag and env genes. J.Virol. 71:1272-1280.

85. Hwang, S. S., T. J. Boyle, H. K. Lyerly, and B. R. Cullen. 1991. Identification of the envelope V3 loop as the primary determinant of cell tropism in HIV-1. Science 253:71-74.

86. Itescu, S., P. F. Simonelli, R. J. Winchester, and H. S. Ginsberg. 1994. Human immunodeficiency virus type 1 strains in the lungs of infected individuals evolve independently from those in peripheral blood and are highly conserved in the C-terminal region of the envelope V3 loop. Proc.Natl.Acad.Sci.U.S.A 91:11378-11382.

87. Jackson, S. P., J. J. MacDonald, S. Lees-Miller, and R. Tjian. 1990. GC box binding induces phosphorylation of Sp1 by a DNA-dependent protein kinase. Cell 63:155-165.

88. Jain, J., Z. Miner, and A. Rao . 1993. Analysis of the preexisting and nuclear forms of nuclear factor of activated T cells. J.Immunol. 151:837-848.

89. Jenkins, M., M. B. Hanley, M. B. Moreno, E. Wieder, and J. M. McCune. 1998. Human immunodeficiency virus-1 infection interrupts thymopoiesis and multilineage hematopoiesis in vivo. Blood 91:2672-2678.

90. Jones, K. A., J. T. Kadonaga, P. A. Luciw, and R. Tjian. 1986. Activation of the AIDS retrovirus promoter by the cellular transcription factor, Sp1. Science 232:755-759.

91. Jones, K. A., P. A. Luciw, and N. Duchange. 1988. Structural arrangements of transcription control domains within the 5'- untranslated leader regions of the HIV-1 and HIV-2 promoters. Genes Dev. 2:1101-1114.

92. Jones, K. A. and B. M. Peterlin. 1994. Control of RNA initiation and elongation at the HIV-1 promoter. Annu.Rev.Biochem. 63:717-743.

93. Joshi, V. V. and J. M. Oleske. 1985. Pathologic appraisal of the thymus gland in acquired immunodeficiency syndrome in children. A study of four cases and a review of the literature. Arch.Pathol.Lab Med. 109:142-146.

94. Kato, H., M. Horikoshi, and R. G. Roeder. 1991. Repression of HIV-1 transcription by a cellular protein. Science 251:1476-1479.

95. Kaufman, J. D., G. Valandra, G. Roderiquez, G. Bushar, C. Giri, and M. A. Norcross. 1987. Phorbol ester enhances human immunodeficiency virus-promoted gene expression and acts on a repeated 10-base-pair functional enhancer element. Mol.Cell Biol. 7:3759-3766.

96. Kim, J. Y., F. Gonzalez-Scarano, S. L. Zeichner, and J. C. Alwine. 1993. Replication of type 1 human immunodeficiency viruses containing linker substitution mutations in the -201 to -130 region of the long terminal repeat. J.Virol. 67:1658-1662.

97. Kinoshita, S., B. K. Chen, H. Kaneshima, and G. P. Nolan. 1998. Host control of HIV-1 parasitism in T cells by the nuclear factor of activated T cells. Cell 95:595-604.

98. Kinoshita, S., L. Su, M. Amano, L. A. Timmerman, H. Kaneshima, and G. P. Nolan. 1997. The T cell activation factor NF-ATc positively regulates HIV-1 replication and gene expression in T cells. Immunity. 6:235-244.

99. Kitchen, S. G. and J. A. Zack. 1997. CXCR4 expression during lymphopoiesis: implications for human immunodeficiency virus type 1 infection of the thymus. J.Virol. 71:6928-6934.

100. Klatt, E. C. 1988. Diagnostic findings in patients with acquired immune deficiency syndrome (AIDS). J.Acquir.Immune.Defic.Syndr. 1:459-465.

101. Koenig, S., H. E. Gendelman, J. M. Orenstein, M. C. Dal Canto, G. H. Pezeshkpour, M. Yungbluth, F. Janotta, A. Aksamit, M. A. Martin, and A. S. Fauci. 1986. Detection of AIDS virus in macrophages in brain tissue from AIDS patients with encephalopathy. Science 233:1089-1093.

102. Koken, S. E., J. L. van Wamel, J. Goudsmit, B. Berkhout, and J. L. Geelen. 1992. Natural variants of the HIV-1 long terminal repeat: analysis of promoters with duplicated DNA regulatory motifs. Virology 191:968-972.

103. Korber, B. T., K. J. Kunstman, B. K. Patterson, M. Furtado, M. M. McEvilly, R. Levy, and S. M. Wolinsky. 1994. Genetic differences between b. J.Virol. 68:7467-7481.

104. Kourtis, A. P., C. Ibegbu, A. J. Nahmias, F. K. Lee, W. S. Clark, M. K. Sawyer, and S. Nesheim. 1996. Early progression of disease in HIV-infected infants with thymus dysfunction [published erratum appears in N Engl J Med 1997 Feb 20;336(8):595]. N.Engl.J.Med. 335:1431-1436.

105. Kowalski, M., J. Potz, L. Basiripour, T. Dorfman, W. C. Goh, E. Terwilliger, A. Dayton, C. Rosen, W. Haseltine, and J. Sodroski. 1987. Functional regions of the envelope glycoprotein of human immunodeficiency virus type 1. Science 237:1351-1355.

106. Krebs, F. C., M. M. Goodenow, and B. Wigdahl. 1997. Neuroglial ATF/CREB factors interact with the human immunodeficiency virus type 1 long terminal repeat. J.Neurovirol. 3 Suppl 1:S28-S32.

107. Krebs, F. C., D. Mehrens, S. Pomeroy, M. M. Goodenow, and B. Wigdahl. 1998. Human immunodeficiency virus type 1 long terminal repeat quasispecies differ in basal transcription and nuclear factor recruitment in human glial cells and lymphocytes. J.Biomed.Sci. 5:31-44.

108. Kumar S., Tamura K., and Nei M. MEGA: Molecular Evolutionary Genetics Analysis, version 1.0. The Pennsylvania State University, University Park, Pa. 1993.

109. Kurth, J., J. M. Buzy, L. Lindstrom, and J. E. Clements. 1996. In vivo transcriptional regulation of the human immunodeficiency virus in the central nervous system in transgenic mice. J.Virol. 70:7686-7694.

110. Lamers, S. L., J. W. Sleasman, J. X. She, K. A. Barrie, S. M. Pomeroy, D. J. Barrett, and M. M. Goodenow. 1993. Independent variation and positive selection in env V1 and V2 domains within maternal-infant strains of human immunodeficiency virus type 1 in vivo. J.Virol. 67:3951-3960.

111. Langston, C., D. E. Lewis, H. A. Hammill, E. J. Popek, C. A. Kozinetz, M. W. Kline, I. C. Hanson, and W. T. Shearer. 1995. Excess intrauterine fetal demise associated with maternal human immunodeficiency virus infection. J.Infect.Dis. 172:1451-1460.

112. Lenardo, M. J., C. M. Fan, T. Maniatis, and D. Baltimore. 1989. The involvement of NF-kappa B in beta-interferon gene regulation reveals its role as widely inducible mediator of signal transduction. Cell 57:287-294.

113. Leonard, C. K., M. W. Spellman, L. Riddle, R. J. Harris, J. N. Thomas, and T. J. Gregory. 1990. Assignment of intrachain disulfide bonds and characterization of potential glycosylation sites of the type 1 recombinant human immunodeficiency virus envelope glycoprotein (gp120) expressed in Chinese hamster ovary cells. J.Biol.Chem. 265:10373-10382.

114. Leonard, J., C. Parrott, A. J. Buckler-White, W. Turner, E. K. Ross, M. A. Martin, and A. B. Rabson. 1989. The NF-kappa B binding sites in the human immunodeficiency virus type 1 long terminal repeat are not required for virus infectivity. J.Virol. 63:4919-4924.

115. Lifson, J. D., M. B. Feinberg, G. R. Reyes, L. Rabin, B. Banapour, S. Chakrabarti, B. Moss, F. Wong-Staal, K. S. Steimer, and E. G. Engleman. 1986. Induction of CD4-dependent cell fusion by the HTLV-III/LAV envelope glycoprotein. Nature 323:725-728.

116. Lipshultz, S. E., C. H. Fox, A. R. Perez-Atayde, S. P. Sanders, S. D. Colan, K. McIntosh, and H. S. Winter. 1990. Identification of human immunodeficiency virus-1 RNA and DNA in the heart of a child with cardiovascular abnormalities and congenital acquired immune deficiency syndrome. Am.J.Cardiol. 66:246-250.

117. Lu, Y., M. Stenzel, J. G. Sodroski, and W. A. Haseltine. 1989. Effects of long terminal repeat mutations on human immunodeficiency virus type 1 replication. J.Virol. 63:4115-4119.

118. Lu, Y. C., N. Touzjian, M. Stenzel, T. Dorfman, J. G. Sodroski, and W. A. Haseltine. 1990. Identification of cis-acting repressive sequences within the negative regulatory element of human immunodeficiency virus type 1. J.Virol. 64:5226-5229.

119. Maddon, P. J., A. G. Dalgleish, J. S. McDougal, P. R. Clapham, R. A. Weiss, and R. Axel. 1986. The T4 gene encodes the AIDS virus receptor and is expressed in the immune system and the brain. Cell 47:333-348.

120. Maekawa, T., T. Sudo, M. Kurimoto, and S. Ishii. 1991. USF-related transcription factor, HIV-TF1, stimulates transcription of human immunodeficiency virus-1. Nucleic Acids Res. 19:4689-4694.

121. Mayaux, M. J., M. Burgard, J. P. Teglas, J. Cottalorda, A. Krivine, F. Simon, J. Puel, C. Tamalet, D. Dormont, B. Masquelier, A. Doussin, C. Rouzioux, and S. Blanche. 1996. Neonatal characteristics in rapidly progressive perinatally acquired HIV-1 disease. The French Pediatric HIV Infection Study Group. JAMA 275:606-610.

122. Medina, E., N. Borthwick, M. A. Johnson, S. Miller, and M. Bofill. 1994. Flow cytometric analysis of the stimulatory response of T cell subsets from normal and HIV-1+ individuals to various mitogenic stimuli in vitro. Clin.Exp.Immunol. 97:266-272.

123. Meisterernst, M., A. L. Roy, H. M. Lieu, and R. G. Roeder. 1991. Activation of class II gene transcription by regulatory factors is potentiated by a novel activity. Cell 66:981-993.

124. Meyer, T. E. and J. F. Habener. 1993. Cyclic adenosine 3',5'-monophosphate response element binding protein (CREB) and related transcription-activating deoxyribonucleic acid- binding proteins. Endocr.Rev. 14:269-290.

125. Michael, N. L., L. D'Arcy, P. K. Ehrenberg, and R. R. Redfield. 1994. Naturally occurring genotypes of the human immunodeficiency virus type 1 long terminal repeat display a wide range of basal and Tat-induced transcriptional activities. J.Virol. 68:3163-3174.

126. Millhouse, S., F. C. Krebs, J. Yao, J. J. McAllister, J. Conner, H. Ross, and B. Wigdahl. 1998. Sp1 and related factors fail to interact with the NF-kappaB-proximal G/C box in the LTR of a replication competent, brain-derived strain of HIV-1 (YU-2). J.Neurovirol. 4:312-323.

127. Molitor, J. A., W. H. Walker, S. Doerre, D. W. Ballard, and W. C. Greene. 1990. NF-kappa B: a family of inducible and differentially expressed enhancer- binding proteins in human T cells. Proc.Natl.Acad.Sci.U.S.A 87:10028-10032.

128. Moore, J. P., A. Trkola, and T. Dragic. 1997. Co-receptors for HIV-1 entry [see comments]. Curr.Opin.Immunol. 9:551-562.

129. Morris, A., M. Marsden, K. Halcrow, E. S. Hughes, R. P. Brettle, J. E. Bell, and P. Simmonds. 1999. Mosaic structure of the human immunodeficiency virus type 1 genome infecting lymphoid cells and the brain: evidence for frequent in vivo recombination events in the evolution of regional populations. J.Virol. 73:8720-8731.

130. Moses, A. V., C. Ibanez, R. Gaynor, P. Ghazal, and J. A. Nelson. 1994. Differential role of long terminal repeat control elements for the regulation of basal and Tat-mediated transcription of the human immunodeficiency virus in stimulated and unstimulated primary human macrophages. J.Virol. 68:298-307.

131. Nabel, G. and D. Baltimore. 1987. An inducible transcription factor activates expression of human immunodeficiency virus in T cells [published erratum appears in Nature 1990 Mar 8;344(6262):178]. Nature 326:711-713.

132. Natsuka, S., S. Akira, Y. Nishio, S. Hashimoto, T. Sugita, H. Isshiki, and T. Kishimoto. 1992. Macrophage differentiation-specific expression of NF-IL6, a transcription factor for interleukin-6. Blood 79:460-466.

133. Niedt, G. W. and R. A. Schinella. 1985. Acquired immunodeficiency syndrome. Clinicopathologic study of 56 autopsies. Arch.Pathol.Lab Med. 109:727-734.

134. Ometto, L., C. Zanotto, A. Maccabruni, D. Caselli, D. Truscia, C. Giaquinto, E. Ruga, L. Chieco-Bianchi, and A. De Rossi. 1995. Viral phenotype and host-cell susceptibility to HIV-1 infection as risk factors for mother-to-child HIV-1 transmission. AIDS 9:427-434.

135. Orchard, K., N. Perkins, C. Chapman, J. Harris, V. Emery, G. Goodwin, D. Latchman, and M. Collins. 1990. A novel T-cell protein which recognizes a palindromic sequence in the negative regulatory element of the human immunodeficiency virus long terminal repeat. J.Virol. 64:3234-3239.

136. Osborn, L., S. Kunkel, and G. J. Nabel. 1989. Tumor necrosis factor alpha and interleukin 1 stimulate the human immunodeficiency virus enhancer by activation of the nuclear factor kappa B. Proc.Natl.Acad.Sci.U.S.A 86:2336-2340.

137. Pang, S., H. V. Vinters, T. Akashi, W. A. O'Brien, and I. S. Chen. 1991. HIV-1 env sequence variation in brain tissue of patients with AIDS- related neurologic disease. J.Acquir.Immune.Defic.Syndr. 4:1082-1092.

138. Pantaleo, G., C. Graziosi, L. Butini, P. A. Pizzo, S. M. Schnittman, D. P. Kotler, and A. S. Fauci. 1991. Lymphoid organs function as major reservoirs for human immunodeficiency virus. Proc.Natl.Acad.Sci.U.S.A 88:9838-9842.

139. Pantaleo, G., C. Graziosi, J. F. Demarest, L. Butini, M. Montroni, C. H. Fox, J. M. Orenstein, D. P. Kotler, and A. S. Fauci. 1993. HIV infection is active and progressive in lymphoid tissue during the clinically latent stage of disease [see comments]. Nature 362:355-358.

140. Papiernik, M., Y. Brossard, N. Mulliez, J. Roume, C. Brechot, F. Barin, A. Goudeau, J. F. Bach, C. Griscelli, R. Henrion, and . 1992. Thymic abnormalities in fetuses aborted from human immunodeficiency virus type 1 seropositive women. Pediatrics 89:297-301.

141. Parrott, C., T. Seidner, E. Duh, J. Leonard, T. S. Theodore, A. Buckler-White, M. A. Martin, and A. B. Rabson . 1991. Variable role of the long terminal repeat Sp1-binding sites in human immunodeficiency virus replication in T lymphocytes. J.Virol. 65:1414-1419.

142. Pascal, E. and R. Tjian. 1991. Different activation domains of Sp1 govern formation of multimers and mediate transcriptional synergism. Genes Dev. 5:1646-1656.

143. Pedroza-Martins, L., K. B. Gurney, B. E. Torbett, and C. H. Uittenbogaart. 1998. Differential tropism and replication kinetics of human immunodeficiency virus type 1 isolates in thymocytes: coreceptor expression allows viral entry, but productive infection of distinct subsets is determined at the postentry level. J.Virol. 72:9441-9452.

144. Pereira, L. A., K. Bentley, A. Peeters, M. J. Churchill, and N. J. Deacon. 2000. A compilation of cellular transcription factor interactions with the HIV-1 LTR promoter. Nucleic Acids Res. 28:663-668.

145. Poli, G. and A. S. Fauci. 1992. The effect of cytokines and pharmacologic agents on chronic HIV infection. AIDS Res.Hum.Retroviruses 8:191-197.

146. Pomerantz, R. J., M. B. Feinberg, R. Andino, and D. Baltimore. 1991. The long terminal repeat is not a major determinant of the cellular tropism of human immunodeficiency virus type 1. J.Virol. 65:1041-1045.

147. Power, C., J. C. McArthur, R. T. Johnson, D. E. Griffin, J. D. Glass, S. Perryman, and B. Chesebro. 1994. Demented and nondemented patients with AIDS differ in brain-derived human immunodeficiency virus type 1 envelope sequences. J.Virol. 68:4643-4649.

148. Pugh, B. F. and R. Tjian. 1992. Diverse transcriptional functions of the multisubunit eukaryotic TFIID complex. J.Biol.Chem. 267:679-682.

149. Rao, A., C. Luo, and P. G. Hogan. 1997. Transcription factors of the NFAT family: regulation and function. Annu.Rev.Immunol. 15:707-747.

150. Reddy, R. T., C. L. Achim, D. A. Sirko, S. Tehranchi, F. G. Kraus, F. Wong-Staal, and C. A. Wiley. 1996. Sequence analysis of the V3 loop in brain and spleen of patients with HIV encephalitis. AIDS Res.Hum.Retroviruses 12:477-482.

151. Robey, W. G., B. Safai, S. Oroszlan, L. O. Arthur, M. A. Gonda, R. C. Gallo, and P. J. Fischinger. 1985. Characterization of envelope and core structural gene products of HTLV- III with sera from AIDS patients. Science 228:593-595.

152. Rohr, O., D. Aunis, and E. Schaeffer. 1997. COUP-TF and Sp1 interact and cooperate in the transcriptional activation of the human immunodeficiency virus type 1 long terminal repeat in human microglial cells. J.Biol.Chem. 272:31149-31155.

153. Rohr, O., C. Schwartz, C. Hery, D. Aunis, M. Tardieu, and E. Schaeffer. 2000. The nuclear receptor chicken ovalbumin upstream promoter transcription factor interacts with HIV-1 Tat and stimulates viral replication in human microglial cells. J.Biol.Chem. 275:2654-2660.

154. Rosenzweig, M., D. P. Clark, and G. N. Gaulton. 1993. Selective thymocyte depletion in neonatal HIV-1 thymic infection. AIDS 7:1601-1605.

155. Ross, E. K., A. J. Buckler-White, A. B. Rabson, G. Englund, and M. A. Martin. 1991. Contribution of NF-kappa B and Sp1 binding motifs to the replicative capacity of human immunodeficiency virus type 1: distinct patterns of viral growth are determined by T-cell types. J.Virol. 65:4350-4358.

156. Ross, H. L., M. R. Nonnemacher, T. H. Hogan, S. J. Quiterio, A. Henderson, J. J. McAllister, F. C. Krebs, and B. Wigdahl. 2001. Interaction between CCAAT/enhancer binding protein and cyclic AMP response element binding protein 1 regulates human immunodeficiency virus type 1 transcription in cells of the monocyte/macrophage lineage. J.Virol. 75:1842-1856.

157. Rousseau, C., E. Abrams, M. Lee, R. Urbano, and M. C. King. 1997. Long terminal repeat and nef gene variants of human immunodeficiency virus type 1 in perinatally infected long-term survivors and rapid progressors. AIDS Res.Hum.Retroviruses 13 :1611-1623.

158. Rubbert, A., C. Combadiere, M. Ostrowski, J. Arthos, M. Dybul, E. Machado, M. A. Cohn, J. A. Hoxie, P. M. Murphy, A. S. Fauci, and D. Weissman. 1998. Dendritic cells express multiple chemokine receptors used as coreceptors for HIV entry. J.Immunol. 160:3933-3941.

159. Ryder, K., A. Lanahan, E. Perez-Albuerne, and D. Nathans. 1989. jun-D: a third member of the jun gene family. Proc.Natl.Acad.Sci.U.S.A 86:1500-1503.

160. Sawadogo, M., M. W. Van Dyke, P. D. Gregor, and R. G. Roeder. 1988. Multiple forms of the human gene-specific transcription factor USF. I. Complete purification and identification of USF from HeLa cell nuclei. J.Biol.Chem. 263:11985-11993.

161. Sawaya, B. E., O. Rohr, D. Aunis, and E. Schaeffer. 1996. Chicken ovalbumin upstream promoter transcription factor, a transcriptional activator of HIV-1 gene expression in human brain cells. J.Biol.Chem. 271:23572-23576.

162. Sawaya, B. E., O. Rohr, D. Aunis, and E. Schaeffer. 1996. Regulation of human immunodeficiency virus type 1 gene transcription by nuclear receptors in human brain cells. J.Biol.Chem. 271:22895-22900.

163. Scarlatti, G., E. Tresoldi, A. Bjorndal, R. Fredriksson, C. Colognesi, H. K. Deng, M. S. Malnati, A. Plebani, A. G. Siccardi, D. R. Littman, E. M. Fenyo, and P. Lusso. 1997. In vivo evolution of HIV-1 co-receptor usage and sensitivity to chemokine-mediated suppression. Nat.Med. 3:1259-1265.

164. Scarlatti, G., E. Tresoldi, A. Bjorndal, R. Fredriksson, C. Colognesi, H. K. Deng, M. S. Malnati, A. Plebani, A. G. Siccardi, D. R. Littman, E. M. Fenyo, and P. Lusso. 1997. In vivo evolution of HIV-1 co-receptor usage and sensitivity to chemokine-mediated suppression. Nat.Med. 3:1259-1265.

165. Schnittman, S. M., H. C. Lane, J. Greenhouse, J. S. Justement, M. Baseler, and A. S. Fauci. 1990. Preferential infection of CD4+ memory T cells by human immunodeficiency virus type 1: evidence for a role in the selective T-cell functional defects observed in infected individuals. Proc.Natl.Acad.Sci.U.S.A 87:6058-6062.

166. Schuitemaker, H., M. Koot, N. A. Kootstra, M. W. Dercksen, R. E. de Goede, R. P. van Steenwijk, J. M. Lange, J. K. Schattenkerk, F. Miedema, and M. Tersmette. 1992. Biological phenotype of human immunodeficiency virus type 1 clones at different stages of infection: progression of disease is associated with a shift from monocytotropic to T-cell-tropic virus population. J.Virol. 66:1354-1360.

167. Sharpless, N. E., W. A. O'Brien, E. Verdin, C. V. Kufta, I. S. Chen, and M. Dubois-Dalcq. 1992. Human immunodeficiency virus type 1 tropism for brain microglial cells is determined by a region of the env glycoprotein that also controls macrophage tropism. J.Virol. 66:2588-2593.

168. Shaw, J. P., P. J. Utz, D. B. Durand, J. J. Toole, E. A. Emmel, and G. R. Crabtree. 1988. Identification of a putative regulator of early T cell activation genes. Science 241:202-205.

169. Sheehy, N., U. Desselberger, H. Whitwell, and J. K. Ball. 1996. Concurrent evolution of regions of the envelope and polymerase genes of human immunodeficiency virus type 1 during zidovudine (AZT) therapy. J.Gen.Virol. 77 (Pt 5):1071-1081.

170. Sheridan, P. L., C. T. Sheline, K. Cannon, M. L. Voz, M. J. Pazin, J. T. Kadonaga, and K. A. Jones. 1995. Activation of the HIV-1 enhancer by the LEF-1 HMG protein on nucleosome- assembled DNA in vitro. Genes Dev. 9:2090-2104.

171. Shioda, T., J. A. Levy, and C. Cheng-Mayer. 1992. Small amino acid changes in the V3 hypervariable region of gp120 can affect the T-cell-line and macrophage tropism of human immunodeficiency virus type 1. Proc.Natl.Acad.Sci.U.S.A 89:9434-9438.

172. Short, M. K., S. A. Okenquist, and J. Lenz. 1987. Correlation of leukemogenic potential of murine retroviruses with transcriptional tissue preference of the viral long terminal repeats. J.Virol. 61:1067-1072.

173. Siekevitz, M., S. F. Josephs, M. Dukovich, N. Peffer, F. Wong-Staal, and W. C. Greene. 1987. Activation of the HIV-1 LTR by T cell mitogens and the trans-activator protein of HTLV-I. Science 238:1575-1578.

174. Sieweke, M. H., H. Tekotte, U. Jarosch, and T. Graf. 1998. Cooperative interaction of ets-1 with USF-1 required for HIV-1 enhancer activity in T cells. EMBO J. 17:1728-1739.

175. Singh, A., G. Besson, A. Mobasher, and R. G. Collman. 1999. Patterns of chemokine receptor fusion cofactor utilization by human immunodeficiency virus type 1 variants from the lungs and blood. J.Virol. 73:6680-6690.

176. Smith, P. D., G. Meng, G. M. Shaw, and L. Li. 1997. Infection of gastrointestinal tract macrophages by HIV-1. J.Leukoc.Biol. 62:72-77.

177. Sodroski, J., R. Patarca, C. Rosen, F. Wong-Staal, and W. Haseltine. 1985. Location of the trans-activating region on the genome of human T-cell lymphotropic virus type III. Science 229:74-77.

178. Sodroski, J., C. Rosen, F. Wong-Staal, S. Z. Salahuddin, M. Popovic, S. Arya, R. C. Gallo, and W. A. Haseltine. 1985. Trans-acting transcriptional regulation of human T-cell leukemia virus type III long terminal repeat. Science 227:171-173.

179. Spear, G. T., C. Y. Ou, H. A. Kessler, J. L. Moore, G. Schochetman, and A. L. Landay. 1990. Analysis of lymphocytes, monocytes, and neutrophils from human immunodeficiency virus (HIV)-infected persons for HIV DNA. J.Infect.Dis. 162:1239-1244.

180. Speck, R. F., K. Wehrly, E. J. Platt, R. E. Atchison, I. F. Charo, D. Kabat, B. Chesebro, and M. A. Goldsmith . 1997. Selective employment of chemokine receptors as human immunodeficiency virus type 1 coreceptors determined by individual amino acids within the envelope V3 loop. J.Virol. 71:7136-7139.

181. Spina, C. A., H. E. Prince, and D. D. Richman. 1997. Preferential replication of HIV-1 in the CD45RO memory cell subset of primary CD4 lymphocytes in vitro. J.Clin.Invest 99:1774-1785.

182. Stewart, C. B. 1993. The powers and pitfalls of parsimony. Nature 361:603-607.

183. Stocking, C., R. Kollek, U. Bergholz, and W. Ostertag. 1986. Point mutations in the U3 region of the long terminal repeat of Moloney murine leukemia virus determine disease specificity of the myeloproliferative sarcoma virus. Virology 153:145-149.

184. Tanaka, T., S. Akira, K. Yoshida, M. Umemoto, Y. Yoneda, N. Shirafuji, H. Fujiwara, S. Suematsu, N. Yoshida, and T. Kishimoto. 1995. Targeted disruption of the NF-IL6 gene discloses its essential role in bacteria killing and tumor cytotoxicity by macrophages. Cell 80:353-361.

185. Teo, I., C. Veryard, H. Barnes, S. F. An, M. Jones, P. L. Lantos, P. Luthert, and S. Shaunak. 1997. Circular forms of unintegrated human immunodeficiency virus type 1 DNA and high levels of viral protein expression: association with dementia and multinucleated giant cells in the brains of patients with AIDS. J.Virol. 71:2928-2933.

186. Tersmette, M., R. E. de Goede, B. J. Al, I. N. Winkel, R. A. Gruters, H. T. Cuypers, H. G. Huisman, and F. Miedema. 1988. Differential syncytium-inducing capacity of human immunodeficiency virus isolates: frequent detection of syncytium-inducing isolates in patients with acquired immunodeficiency syndrome (AIDS) and AIDS-related complex. J.Virol. 62:2026-2032.

187. Tersmette, M., R. A. Gruters, F. de Wolf, R. E. de Goede, J. M. Lange, P. T. Schellekens, J. Goudsmit, H. G. Huisman, and F. Miedema. 1989. Evidence for a role of virulent human immunodeficiency virus (HIV) variants in the pathogenesis of acquired immunodeficiency syndrome: studies on sequential HIV isolates. J.Virol. 63:2118-2125.

188. Tesmer, V. M., A. Rajadhyaksha, J. Babin, and M. Bina. 1993. NF-IL6-mediated transcriptional activation of the long terminal repeat of the human immunodeficiency virus type 1. Proc.Natl.Acad.Sci.U.S.A 90:7298-7302.

189. Timmers, H. T., R. E. Meyers, and P. A. Sharp. 1992. Composition of transcription factor B-TFIID. Proc.Natl.Acad.Sci.U.S.A 89:8140-8144.

190. Toronto General Hospital. 2001. University Health Network. http://www.thehivcliniccom/lifecycle.htm.

191. van't Wout, A. B., N. A. Kootstra, G. A. Mulder-Kampinga, N. Albrecht-van Lent, H. J. Scherpbier, J. Veenstra, K. Boer, R. A. Coutinho, F. Miedema, and H. Schuitemaker. 1994. Macrophage-tropic variants initiate human immunodeficiency virus type 1 infection after sexual, parenteral, and vertical transmission. J.Clin.Invest 94:2060-2067.

192. van't Wout, A. B., L. J. Ran, C. L. Kuiken, N. A. Kootstra, S. T. Pals, and H. Schuitemaker. 1998. Analysis of the temporal relationship between human immunodeficiency virus type 1 quasispecies in sequential blood samples and various organs obtained at autopsy. J.Virol. 72:488-496.

193. Vazeux, R., N. Brousse, A. Jarry, D. Henin, C. Marche, C. Vedrenne, J. Mikol, M. Wolff, C. Michon, and W. Rozenbaum. 1987. AIDS subacute encephalitis. Identification of HIV-infected cells. Am.J.Pathol. 126:403-410.

194. Veronese, F. D., A. L. Devico, T. D. Copeland, S. Oroszlan, R. C. Gallo, and M. G. Sarngadharan. 1985. Characterization of gp41 as the transmembrane protein coded by the HTLV- III/LAV envelope gene. Science 229:1402-1405.

195. Wang, L. H., S. Y. Tsai, I. Sagami, M. J. Tsai, and B. W. O'Malley. 1987. Purification and characterization of chicken ovalbumin upstream promoter transcription factor from HeLa cells. J.Biol.Chem. 262:16080-16086.

196. Wiley, C. A., R. D. Schrier, J. A. Nelson, P. W. Lampert, and M. B. Oldstone. 1986. Cellular localization of human immunodeficiency virus infection within the brains of acquired immune deficiency syndrome patients. Proc.Natl.Acad.Sci.U.S.A 83:7089-7093.

197. Wu, F. K., J. A. Garcia, D. Harrich, and R. B. Gaynor. 1988. Purification of the human immunodeficiency virus type 1 enhancer and TAR binding proteins EBP-1 and UBP-1. EMBO J. 7:2117-2130.

198. Yang, Z. and J. D. Engel. 1993. Human T cell transcription factor GATA-3 stimulates HIV-1 expression. Nucleic Acids Res. 21:2831-2836.

199. Zaitseva, M. B., S. Lee, R. L. Rabin, H. L. Tiffany, J. M. Farber, K. W. Peden, P. M. Murphy, and H. Golding. 1998. CXCR4 and CCR5 on human thymocytes: biological function and role in HIV- 1 infection. J.Immunol. 161:3103-3113.

200. Zeichner, S. L., G. Hirka, P. W. Andrews, and J. C. Alwine. 1992. Differentiation-dependent human immunodeficiency virus long terminal repeat regulatory elements active in human teratocarcinoma cells. J.Virol. 66:2268-2273.

201. Zeichner, S. L., J. Y. Kim, and J. C. Alwine. 1991. Linker-scanning mutational analysis of the transcriptional activity of the human immunodeficiency virus type 1 long terminal repeat. J.Virol. 65:2436-2444.

202. Zhang, L., Y. Huang, H. Yuan, B. K. Chen, J. Ip, and D. D. Ho. 1997. Genotypic and phenotypic characterization of long terminal repeat sequences from long-term survivors of human immunodeficiency virus type 1 infection. J.Virol. 71:5608-5613.

203. Zhang, L., Y. Huang, H. Yuan, B. K. Chen, J. Ip, and D. D. Ho. 1997. Identification of a replication-competent pathogenic human immunodeficiency virus type 1 with a duplication in the TCF-1alpha region but lacking NF-kappaB binding sites. J.Virol. 71:1651-1656.

204. Zhu, T., N. Wang, A. Carr, D. S. Nam, R. Moor-Jankowski, D. A. Cooper, and D. D. Ho. 1996. Genetic characterization of human immunodeficiency virus type 1 in blood and genital secretions: evidence for viral compartmentalization and selection during sexual transmission. J.Virol. 70:3098-3107.

BIOGRAPHICAL SKETCH

Brant Roger Burkhardt Jr. was born in Mount Holly, New Jersey, in 1971 to Brant and Louis Burkhardt. He graduated from Florence Township Memorial High School, Florence, NJ, in 1989. He then received his Bachelor of Science degree majoring in biology with a minor in psychology from the College of New Jersey (formerly known as Trenton State College) in 1993. He briefly worked for the New Jersey Department of Health in 1993. He later received his Master of Science degree in microbiology from Clemson University in 1996. He then entered the University of Florida Interdisciplinary Program in Biomedical Sciences in 1996. After completion of his degree he will begin a post-doctoral position in the lab of Mark Atkinson focusing on diabetes.

I certify that I have read this study and that in my opinion it conforms to acceptable standards of scholarly presentation and is fully adequate, in scope and quality, as a dissertation for the degree of Doctor of Philosophy.

Maureen M. Goodenow, Chairperson
Professor of Pathology, Immunology, and
Laboratory Medicine

I certify that I have read this study and that in my opinion it conforms to acceptable standards of scholarly presentation and is fully adequate, in scope and quality, as a dissertation for the degree of Doctor of Philosophy.

John W. Sleasman,
Professor of Pathology, Immunology, and
Laboratory Medicine

I certify that I have read this study and that in my opinion it conforms to acceptable standards of scholarly presentation and is fully adequate, in scope and quality, as a dissertation for the degree of Doctor of Philosophy.

Steven S. Sugrue.
Professor of Anatomy and Cell Biology

I certify that I have read this study and that in my opinion it conforms to acceptable standards of scholarly presentation and is fully adequate, in scope and quality, as a dissertation for the degree of Doctor of Philosophy.

Ayalew Mergia
Associate Professor of Pathology,
Immunology, and Laboratory Medicine

This dissertation was submitted to the Graduate Faculty of the College of Medicine and to the Graduate School and was accepted as partial fulfillment of the requirements for the degree of Doctor of Philosophy.

December, 2001

Wayne J McCormack

Dean, College of Medicine

Winfred M Phillips

Dean, Graduate School

UNIVERSITY OF FLORIDA

3 1262 08554 3121